ANL-94/15

Chemical Technology Division

Annual Technical Report

1993

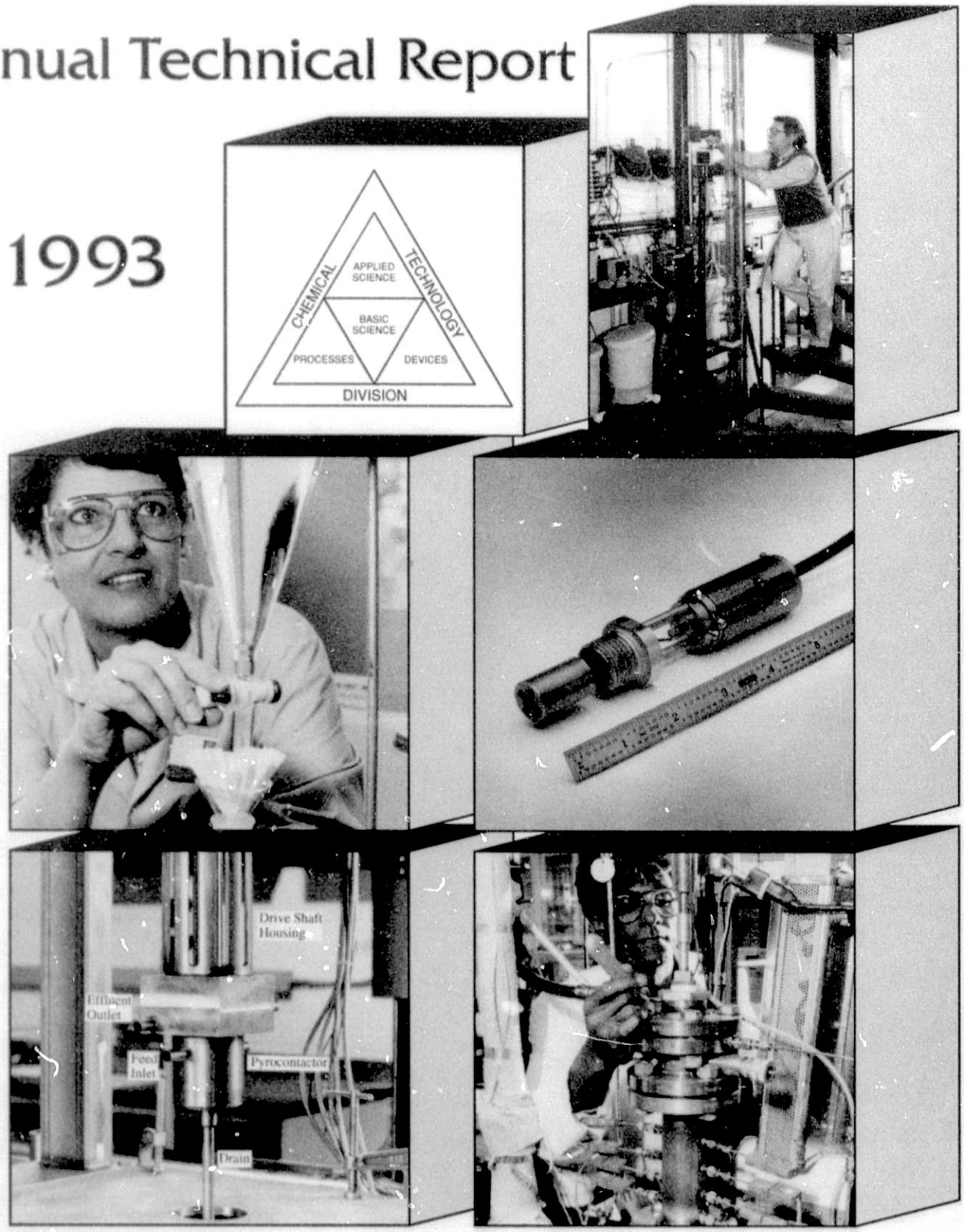

Argonne National Laboratory

Operated by The University of Chicago for the U.S. Department of Energy under Contract W-31-109-Eng-38

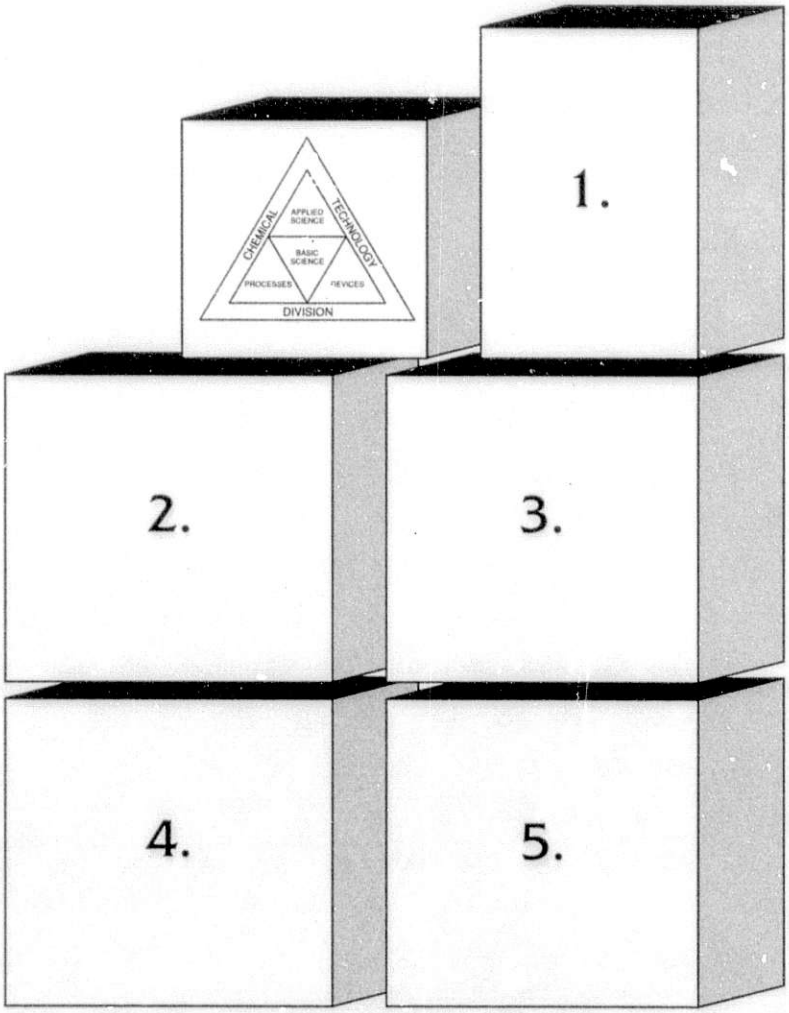

Cover Description

1. Pilot plant developed for cleaning uranium-contaminated soil by aqueous biphasic separation.
2. Chemist analyzing wastewater sample for oil and grease.
3. Toroid cavity imager developed for magnetic resonance imaging studies at high temperatures and pressures.
4. Pyrocontactor developed for extracting transuranics from the waste molten salt that will be produced in electrorefining Integral Fast Reactor spent fuel.
5. Fuel reformer developed for converting alcohols (e.g., methanol) to hydrogen for use in low temperature fuel cells.

Disclaimer

Printed in the United States of America

This report has been reproduced from the best available copy.

Available to DOE and DOE contractors from the Office of Scientific and Technical Information
P.O. Box 62
Oak Ridge, TN 37831
Prices available from (615) 576-8401,
FTS 626-8401

Available to the public from the National Technical Information Service
U.S. Department of Commerce
5285 Port Royal Road
Springfield, VA 22161

Distribution Category:
General Energy Research (UC-400)
General, Miscellaneous, and Progress
Reports (Nuclear) (UC-500)

ANL-94/15

ARGONNE NATIONAL LABORATORY
9700 South Cass Avenue
Argonne, IL 60439

CHEMICAL TECHNOLOGY DIVISION

ANNUAL TECHNICAL REPORT

1993

J. E. Battles	Division Director
K. M. Myles	Associate Division Director
J. J. Laidler	Associate Division Director
D. W. Green	Associate Division Director

April 1994

Previous reports in this series

ANL-93/17	January-December 1992
ANL-92/15	January-December 1991
ANL-91/18	January-December 1990
ANL-90/11	January-December 1989

TABLE OF CONTENTS

TABLE OF CONTENTS (contd)

TABLE OF CONTENTS (contd)

Page

TABLE OF CONTENTS (contd)

CHEMICAL TECHNOLOGY DIVISION
ANNUAL TECHNICAL REPORT
1993

ABSTRACT

Highlights of the Chemical Technology (CMT) Division's activities during 1993 are presented. In this period, CMT conducted research and development in the following areas: (1) electrochemical technology, including advanced batteries and fuel cells; (2) technology for fluidized-bed combustion and coal-fired magnetohydrodynamics; (3) methods for treatment of hazardous waste and mixed hazardous/radioactive waste; (4) the reaction of nuclear waste glass and spent fuel under conditions expected for an unsaturated repository; (5) processes for separating and recovering transuranic elements from nuclear waste streams, concentrating radioactive waste streams with advanced evaporator technology, and producing ^{99}Mo from low-enriched uranium; (6) processes for recovering actinides from the core and blanket fuel in the Integral Fast Reactor (IFR), removing fission products from the recycled fuel, and incorporating them into suitable waste forms for disposal; (7) processes for removal of actinides in spent fuel from commercial water-cooled nuclear reactors; and (8) physical chemistry of selected materials in environments simulating those of fission and fusion energy systems. The Division also conducts basic research in catalytic chemistry associated with molecular energy resources and novel ceramic precursors; materials chemistry of superconducting oxides, electrified metal/solution interfaces, molecular sieve structures, thin-film diamond surfaces, effluents from wood combustion, and molten silicates; and the geochemical processes involved in water-rock interactions. In addition, the Analytical Chemistry Laboratory in CMT provides a broad range of analytical chemistry support services to the technical programs at Argonne National Laboratory (ANL).

SUMMARY

Current programs within CMT are briefly summarized below. These programs are discussed in greater detail in the remainder of the report.

1. *Electrochemical Technology*

The CMT Division is engaged in a variety of activities related to the development of advanced batteries for vehicle propulsion, utility load-leveling, and other energy storage applications. These activities include research, performance and lifetime testing, post-test examinations, modeling, and technology transfer. Work is also being conducted on advanced fuel cells for power plant and transportation applications. The technical management of industrial contracts for the Department of Energy (DOE) is also carried out on the use of fuel cells for transportation applications.

The support that the CMT Electrochemical Technology Program receives from the U.S. Advanced Battery Consortium (USABC) continues to grow. The USABC is a partnership among DOE, the U.S. automobile industry, and the U.S. electric utility industry and was formed with the objective of accelerating the development of advanced batteries for electric vehicles. Early in 1993, CMT was awarded two contracts by the USABC: one for developing bipolar Li/FeS_2 batteries, the other for testing advanced batteries in CMT's Analysis and Diagnostics Laboratory. Additionally, CMT is negotiating a third contract with 3-M Company for developing lithium-polymer electrolyte batteries.

The in-house battery work during 1993 was devoted to three systems: lithium/iron sulfide, sodium/nickel chloride, and lithium-polymer electrolyte.

The work on the Li/FeS_2 system involved a collaborative effort with SAFT America to develop a bipolar battery that will meet the long-term goals of the USABC (performance of 300 Wh/L and 600 W/L, life of >1000 cycles, cost of <$100/kWh). During 1993, the following activities were conducted jointly with SAFT: transfer of the Li/FeS_2 battery technology from ANL to SAFT, development of a conceptual design for a first-generation battery stack/module, improvement of fabrication and testing facilities at CMT, and testing of chemical and electrochemical stability of cell materials.

Work also continued on the Na/$NiCl_2$ cell. In 1992, we had significantly improved the performance of the positive electrode, which had limited the performance of the Na/$NiCl_2$ cell. During 1993, this improved performance (three times that of any other nickel-containing battery system) was demonstrated in over 4000 cycles of testing with laboratory research cells. This substantial performance improvement was achieved by the use of additives and a modified morphology in the Ni/$NiCl_2$ electrode. These tests also showed that cells with this new electrode can operate at much lower temperature (153 vs. 300°C) and will recharge much faster (1-2.5 h vs. 10-15 h). This new technology is now being investigated by two industrial firms: Hughes Aircraft Co. and Eagle-Picher Industries, Inc.

In our work on the lithium-polymer electrolyte system, electrochemical experiments were conducted on a Li-Sn alloy, which may be suitable as a reference electrode of the first kind in studies of lithium-polymer batteries. Two types of electrodes were tested: lithiated tin foil and tin thin films deposited on a stainless steel substrate. The lithiated tin foil electrode demonstrated good voltage stability (average open-circuit voltage of 0.7336 V ± 0.17 mV) over months under open-circuit conditions. The tin thin-film electrodes also displayed excellent open-circuit voltage stability and reproducibility during the lithium loading reaction. Best results were obtained using ion-beam assisted deposition of the thin film (~1000 Å in thickness).

The Analysis and Diagnostics Laboratory in CMT includes a test laboratory to conduct battery evaluations under simulated application conditions. During 1993, performance and life evaluations were conducted for nickel/metal hydride, sodium/sulfur, advanced lead-acid, and nickel/cadmium systems fabricated by industrial firms. In addition, nickel/metal hydride cells were subjected to post-test analyses after life evaluations. The information gained from these evaluations and tests provides a measure of the technical progress made by the battery developers

and identifies specific areas where changes in design or the materials of construction would improve battery performance.

Three advanced fuel cells are under development at CMT: the solid oxide, molten carbonate, and polymer electrolyte fuel cells. The first two systems are targeted for utility applications, and the third for transportation vehicles.

For the solid oxide fuel cell, we are developing insulating sealants for sealing the edges and gas-supply and exhaust manifolds. These sealants must be compatible with the fuel cell materials under the aggressive fuel-cell operating conditions (including temperatures of 800-1000°C). We have developed a glass-ceramic sealant with the desired properties. This sealant was tested in an electrochemical cell in which yttria-stabilized zirconia was sealed to the end of a zirconia tube. The cell was thermally cycled once between room temperature and 1000°C with no evidence of cracking. The measured and theoretical emf's at 800-1000°C showed excellent agreement and indicated that the sealant had formed a gas-tight seal. Work is also underway on development of anodes that are tolerant to the sulfur in coal-derived fuels and natural gas. Tests have indicated that $La_{0.7}Mg_{0.3}CeO_{3.35}$ and $La_{0.8}Nb_{0.2}CeO_{3.7}$ have promise as a sulfur-tolerant anode.

In molten carbonate fuel cells, the present NiO cathodes have dissolution/precipitation problems that limit cell lifetime under pressurized operating conditions, and we are searching for alternative conductive materials that are stable in the high-temperature (650°C) cell environment. Tests of two alternative stable materials (double doped $LiFeO_2$ and $LiCoO_2$) showed them to have performance close to that of the state-of-the-art NiO cathode. We are also investigating ways to reduce the solubility of the NiO cathode by modifying the present 70 mol% Li_2CO_3-30 mol% K_2CO_3 electrolyte and are modeling a new molten carbonate fuel cell stack, which consists of numerous inlet and exit manifolds distributed throughout the plane of the fuel cell.

In the past year, research has been initiated on the polymer electrolyte fuel cell, which operates at lower temperature (<100°C) than the molten carbonate or solid oxide fuel cells. In the present polymer electrolyte fuel cell, the efficiency of the platinum-based anode is decreased by the presence of CO and CO_2 in the hydrogen fuel. We have identified a platinum alloy that shows promise as an improved anode material and will be testing it in a fuel cell using fuel contaminated with CO. We are also testing catalysts for use in the reforming of alcohols into hydrogen fuel and are conducting a systems analysis to design improved polymer electrolyte fuel cell systems, with particular emphasis on the engineering issues involved in integrating the fuel cell stack with the other system components.

In another effort, we are managing contracts by industrial firms developing fuel cell systems for transportation applications. The contractors include General Motors Corp., Arthur D. Little, and H-Power Corp.

2. *Fossil Fuel Research*

The Chemical Technology Division is the lead division for several projects in the ANL Fossil Fuel Program. These projects involve studies on pressurized fluidized-bed combustion (PFBC) and magnetohydrodynamic (MHD) power generation.

One of the potential applications of Illinois high-sulfur coal is as a fuel for a PFBC/gas-turbine combined-cycle system (GTCC) for power generation. In PFBC/GTCC, the entrained particulates in the PFBC off-gas need to be controlled to protect the gas turbine from corrosion and to meet the Environment Protection Agency's New Source Performance Standards for particulate emissions. We conducted tests to evaluate the FIBROSIC™ candle filter (developed by Industrial Filter and Pump Manufacturing Co.) as a hot-gas cleanup device. These 10-h laboratory tests with Illinois No. 6 high-sulfur coal under PFBC conditions showed that the FIBROSIC™ filter has acceptable particulate collection efficiency (>99.9%), permeability characteristics, and physical and mechanical strength. Longer term tests (minimum of 50 h) are planned.

Previous tests in a PFBC/alkali sorber with an Ames on-line alkali analyzer had shown that the sampling and analysis of the alkali vapor compounds were complicated by the interactions of these compounds with the stainless steel sampling line. Thus, experiments are in progress to identify metallic materials that will not adsorb alkali vapors and can be employed as alkali sampling lines and/or process components in advanced coal utilization systems, such as PFBC. In related work, we used the analytical alkali sorber bed technique developed in CMT to measure the alkali vapor/aerosol concentrations in PFBC exhaust gases downstream of a hot gas filter at the 15-MW Component Test Facility in Finspong, Sweden.

Open-cycle MHD has the potential to improve substantially the electrical efficiency of coal-fired power plants and to reduce their environmental impact. We are participating in materials evaluation studies to support development of the MHD bottoming cycle (heat and seed recovery). We examined deposits that formed on tubes of various heat exchanger materials during long-duration (2000 h) tests at the Coal Fired Flow Facility (operated by the University of Tennessee Space Institute). Among the materials tested, Type 310 stainless steel exhibited the least corrosion attack, while Types 304 and 316 exhibited severe degradation. The alloy 253MA exhibited intermediate corrosion.

3. *Hazardous Waste Research*

This research includes studies on methods for treating hazardous waste and mixed hazardous/radioactive waste.

One project in this area involves developing aqueous biphasic separation processes for solid waste treatment, soil remediation, high-level liquid waste treatment, and industrial waste treatment. For the treatment of solid radioactive wastes, we are investigating the wet grinding of radioactive solids to a particle size of 1 μm, followed by aqueous biphasic extraction to maximize plutonium recovery and minimize waste volume. The biphasic system combines aqueous solutions of polymers [e.g., polyethylene glycol (PEG)] with aqueous salt solutions [$(NH_4)_2SO_4$, Na_2SO_4,

or Na_2CO_3]. Promising results have been attained in test-tube-scale extraction studies using actual plutonium residues (incinerator ash and ash heels, metallurgical residues, and LECO crucibles). The partition coefficients for biphasic extraction of particulate plutonium were above 100. In test-tube-scale experiments with uranium-contaminated soil from the DOE Fernald site, the uranium concentrations were reduced from 500-600 mg/kg to about 90 mg/kg and, in some samples, 15 mg/kg. We are now installing a pilot-scale column to test aqueous biphasic extraction with Fernald soils.

In a collaborative effort with Northern Illinois University, we are developing aqueous biphasic systems for the selective extraction of long-lived radionuclides from caustic high-level liquid waste. Preliminary work has shown that aqueous biphasic systems are capable of extracting nearly all the technetium as TcO_4^- into the PEG-rich phase. Partition coefficients as high as 600 have been obtained for pertechnetate in carbonate/PEG biphasic systems. Work has recently begun on the biocatalytic destruction of nitrate in DOE waste streams by use of an aqueous biphasic system.

Use of silica gel barriers is being considered as a method to significantly reduce the migration of contaminants (radionuclides, heavy metals, and hazardous organic compounds) through soil subsurface. We are investigating the use of electrokinetic processing for injecting silica sol solutions into soil. Preliminary experiments were conducted using a bench-scale electrokinetic test cell in which 10 wt% of a commercial colloidal silica solution was placed in the cathode and NaCl solution in the anode. The cell was loaded with either a saturated sand or kaolinite soil sample. Test results showed that the permeability was greatly reduced for the sandy soil but increased for the kaolinite soil. Microscopic examination of soil samples showed evidence of cementing of the sand particles but not the kaolinite particles.

Efforts were continued to investigate the speciation of radionuclides under conditions relevant to subsurface groundwaters on DOE lands. The current focus is on the environmental chemistry of plutonium-organic mixtures in the presence of microbes, inorganic substrates, and metal cations. For example, the interaction of Pu(VI) with citric acid was investigated as a function of ligand-to-metal ratio (1:1 to 100:1) and pH (2 to 10) at room temperature. At low ligand-to-metal ratios (<10:1), citrate reduced Pu(VI) to form a stable Pu(IV) complex. The reaction became faster with increasing pH. At ligand-to-metal ratios of ~100:1, however, no reduction of Pu(VI) was evident even at near-neutral pH. This suggests that multi-ligand complexation of the Pu(VI) stabilized the oxidation state. We are also investigating the degradation of the plutonium-citrate complex by a *Pseudomonas* strain microbe and the interaction of plutonium with phosphate in subsurface aqueous solutions.

Work has continued to investigate the effects of ionizing radiation on gas production in environments similar to those expected in the Waste Isolation Pilot Plant (WIPP), which is DOE's proposed long-term transuranic waste storage facility. Our investigations into gas generation in plutonium-spiked WIPP brine indicated that oxygen is produced at high absorbed doses (>10 Mrad). Thus, low levels of oxygen will likely be sustained in the WIPP over long times and not completely depleted as previously thought. We also found that alpha irradiation of WIPP plastic and rubber materials caused them to degrade and react with the gas phase

present and generated hydrogen, carbon oxides, and volatile organic compounds. The extent to which this occurred depended on the material and the gas phase present.

The Office of Waste Management Programs in CMT is assisting DOE in maintaining a national program of applied R&D in environmental restoration and waste management. Effort in the past year focused on providing technical and management support to the Minimum Additive Waste Stabilization Program and the Hazardous Substance Research Center Program.

4. *Nuclear Waste Programs*

Work is being performed to support programs on the disposal of high-level nuclear waste and spent fuel in the candidate repository site at Yucca Mountain in southwestern Nevada.

During the past several years, the literature regarding the corrosion characteristics of borosilicate glasses developed worldwide for high-level waste disposal has been reviewed to evaluate the state of understanding of the glass corrosion process and the effect of testing parameters [e.g., temperature, glass composition, radiation, glass surface area to leachant volume (SA/V)] on glass corrosion. The findings have been summarized in a draft document entitled "High-Level Nuclear Waste Borosilicate Glass: A Compendium of Characteristics."

Several series of laboratory tests are being performed to determine the corrosion behavior of high-level waste glasses upon exposure to liquid water or water vapor. These tests are being conducted to determine the corrosion behavior of various high-level radioactive waste forms under the hydrologically unsaturated conditions anticipated at the proposed Yucca Mountain site. In one such series, static leach tests at SA/V ratios of 10-20,000 m^{-1} have been in progress using glass compositions representative of the waste forms (SRL 131 and SRL 202 glass) to be produced at the Defense Waste Processing Facility. The results indicate that a laboratory test with a single SA/V ratio cannot be used to assess the long-term glass corrosion. A suite of tests is being developed to better characterize the glass corrosion behavior for use in projecting the long-term glass durability.

Long-term tests are underway with radioactive sludge-based and simulated nuclear waste glasses having three compositions (SRL 131/11, 165, and 200). In tests up to 980 days at SA/V ratios of 340 or 2000 m^{-1}, little difference was found between the radioactive and simulated glasses. However, in tests with the SRL 200 glass at the SA/V ratio of 20,000 m^{-1}, the leach rate of the simulated glass after one year accelerated such that the boron release rate was 1000 times higher compared with the radioactive counterpart. This accelerated corrosion rate is associated with the formation of crystalline phases on the glass surface and a slight rise in solution pH.

A series of drip tests following the Unsaturated Test Method has been in progress for 27 months with 200-type radioactive glass. This glass was used as-cast or was pre-aged by reacting the glass in a water vapor environment before testing. The following observations have been made: the leachates from the pre-aged glass were concentrated in cations (mainly Li, Na, and B) and anions (SO_4^{2-}, PO_4^{3-}, and Cl^-) after 180 days, but then the concentrations decreased with time; the actinide release from the pre-aged glass was considerably greater than from the as-cast

glass but also decreased with time; for the pre-aged glass tests, a significant fraction of Pu and Cm was dissolved in solution, whereas in the as-cast glass tests, these actinides were associated with colloidal material; and many colloidal phases were identified in solution from tests of both glass types.

In addition to glass studies, long-term tests with unirradiated UO_2 pellets and simulated spent fuel are in progress to determine radionuclide release rates when these materials are exposed to repository-relevant conditions. Results from drip tests with UO_2 pellets and EJ-13 well water for 6.8 to 8.0 yr indicated an order of magnitude decrease in the uranium release rate compared with the initial 1.0 to 2.0 yr period. This decrease is thought to result from the formation of a dense surface mat of uranyl silicate phases that have entrapped particulate material in the UO_2 pellet surface. Tests have also been ongoing for one year with two types of spent fuel (ATM-103 and ATM-106) under drip and water vapor conditions. Preliminary results indicate a radiolysis effect on leachate composition, a difference in actinide release behavior for the two fuel types, and formation of colloidal material in the leachate.

Other work is being performed to investigate the use of vitrification for treating mixed and low-level wastes. Tests are in progress to develop and analyze glass and glass/ceramic vitrified waste forms for remediation of contaminated materials, including soils, industrial catalysts, and equipment. Vitrified waste forms which require a minimum amount of additives are being developed to lower treatment and disposal costs. Many of the testing and analytical techniques developed for high-level waste forms are being applied to the low-level waste form so that its long-term durability can be assessed during its development.

5. *Separation Science and Technology*

The Division's work in separation science and technology is concerned with developing methods for treating radioactive, mixed, and hazardous waste. The TRUEX (TRansUranic EXtraction) process continues to be developed for removing and concentrating actinides from acidic waste streams contaminated with transuranic elements. An important part of this effort is the development and application of the Generic TRUEX Model (GTM), which allows users to design multistage flowsheets for specific waste streams and estimate the cost and space requirements for implementing a site- and feed-specific TRUEX process. During this past year, new features were added to the GTM so that it could reroute an effluent from one section of the process to another section than the normal one, account for the effects of high solvent loading, account for the effects of temperature, handle extraction efficiencies of less than 100% at each stage, and automatically calculate the speciation and distribution ratios of aqueous-phase components for a wide variety of feed compositions. Also, experiments were conducted on the extraction behavior of bismuth (an important component in the Hanford nuclear waste storage tanks) and the reductive stripping of plutonium; these data will be incorporated into the data base generated for the GTM.

An effort was begun to demonstrate the new TRUEX-SREX process, which is a combination of the TRUEX process and a recently invented SREX (strontium extraction) process. Both these processes were invented in the ANL Chemistry Division. The GTM was used to develop a TRUEX-SREX flowsheet that will handle the expected range of feed compositions for

dissolved sludge waste from the Hanford site. A 20-stage centrifugal contactor has been set up to verify experimentally the operation of the TRUEX-SREX flowsheet. We also used the GTM to design a flowsheet for recovering TRU elements from aluminum-clad PuO_2 targets for Oak Ridge National Laboratory.

A multi-year project on using the TRUEX process for treating plutonium-containing waste from ANL and the New Brunswick Laboratory was completed. In the four batches processed to date (each containing 12-34 g of plutonium), the alpha activities for the feeds were reduced from 21,400-88,000 nCi/mL to below the target of 10 nCi/mL. The alpha-activity decontamination factors for the four batches ranged from 4,000 to 65,500. The test results have demonstrated the ability of the GTM to design workable flowsheets based on waste feed compositions and the use of the TRUEX process for treating real waste streams.

Magnetically assisted chemical separation (MACS) processes are being developed for removing contaminants (^{137}Cs, ^{90}Sr, transuranics) from waste solutions. The MACS process combines the selective and efficient separation afforded by chemical sorption with the high physical separation afforded by magnetic recovery of ferromagnetic beads. Studies during 1993 involved evaluating polymeric coatings for magnetic particles and measuring the hydrolytic and radiolytic damage to coated particles during processing. An in-field, portable, compact evaporator/concentrator is also under development for treating effluents from an ion exchange unit designed to remove cesium from Hanford tank supernatant.

A substantial effort during this past year involved support to ANL Waste Management Operations. Activities included assisting them in purchasing evaporators and concentrators for treating ANL waste waters; designing, fabricating, and testing a mixed-waste treatment facility; developing a method for treating spent scintillation cocktails; and designing a treatment facility for liquid transuranic waste.

Finally, efforts have been renewed to determine the feasibility of substituting low-enriched uranium for the high-enriched uranium used in the production of ^{99}Mo for medical applications.

6. *Integral Fast Reactor Pyrochemical Process*

The Integral Fast Reactor (IFR) is an advanced reactor concept proposed by, and under development at, Argonne National Laboratory. One of its distinguishing features is an "integral" fuel cycle in which the discharged reactor core and blanket materials are processed and fabricated into new fuel elements in an on-site facility. The CMT Division has the responsibility for developing the pyrochemical process for separating the valuable actinide elements present in the core and blanket materials from the fission products and for immobilizing the fission products in a high-level waste form suitable for disposal in a geologic repository.

Development of the IFR pyrochemical process is proceeding at both the laboratory scale and the engineering scale. Laboratory-scale experiments with plutonium and other transuranic elements have been focused on the development of a high-efficiency cathode for recovery of transuranic elements. The transuranics are collected at a liquid cadmium cathode

immersed in a molten electrolyte salt within an electrorefining vessel at 500°C; the formation of dendritic deposits that tend to grow out of the cathode crucible and produce electrical short circuits is a problem with conventional stirred cathodes, leading to collection efficiencies of the order of 50%. A new design for the liquid cadmium cathode has been developed that utilizes a reciprocating agitator, or "pounder," to force the growing dendrites back into the liquid cadmium. Experiments conducted with the pounder cathode have shown that product collection efficiencies of virtually 100% can be routinely achieved. In related work, a reference electrode based on a low-solubility zirconium salt has been developed and successfully tested. This electrode makes possible *in situ* voltammetric analysis of the electrorefiner salt phase, specifically the U^{3+} and Pu^{3+} concentrations. By simple cyclic voltammetry measurements, it is possible to estimate the relative concentrations of U and Pu in the salt phase. This is important not only to operational monitoring but to materials control and accountancy and facility surveillance for safeguards and non-proliferation purposes.

Engineering-scale process development has centered on demonstration of drawdown operations and on the development of zirconium recovery methods. In the pyrochemical processing of spent IFR fuel, a heavy metal drawdown operation is required for recovering the heavy metals present in the electrorefiner salt phase before removal of fission products from the salt phase. The drawdown process employs a source of electrons at the anode that does not increase the heavy metal loading of the salt; a Li-Cd alloy has been used in these experiments. The heavy metals in the salt are deposited at a solid cathode, ultimately reducing the heavy metal concentration in the salt to 0.01 wt% or less. Cathode deposits (~10 kg) were successfully produced and were found to have a much coarser dendritic structure than produced at normal heavy metal concentrations in the salt. Experiments were also conducted to develop procedures that permit the co-deposition of Zr and U in proportions equal to their respective concentrations in the fuel alloy to be recycled. The recovery of zirconium, which constitutes 10 wt% of the IFR fuel alloy, is important because this element tends to accumulate in the electrorefiner and complicates operations unless it is removed. A number of co-deposition runs were carried out in the engineering-scale electrorefiner, producing deposits with the proper U-to-Zr ratios. The work makes it possible to perform direct recycle of Zr with U and should result in improved efficiency of fuel recycle operations.

The development of waste treatment processes for the IFR pyrochemical process is continuing. The waste treatment operations are intended to remove any residual actinides from the spent salt electrolyte before the salt and metal phases are treated to concentrate the fission product elements and immobilize the fission products in high-level waste forms. Two of the key steps in spent salt treatment have been emphasized during the year: the salt extraction step, which removes actinides, and the salt stripping step, which removes rare earth fission products. The extraction step uses a centrifugal contactor ("pyrocontactor") operating at a temperature of 500°C and a rotational speed of 2700 rpm. Initial tests with the pyrocontactor were successfully completed, with the results indicating that the entire electrolyte salt content of a full-scale electrorefiner can be treated in a matter of only 4-6 h. Tests with the salt stripper, in which the extracted salt is reacted with a strong reductant (lithium), showed that the stripping reaction proceeds in accordance with predictions made by the XTRACT code developed in CMT.

High-level waste forms are being developed to accommodate the spent salt and metal phases from the IFR electrorefiner. Fission products from the salt phase are concentrated by infiltrating the stripped salt through a bed of zeolite, which absorbs the fission products by a combination of ion exchange and molecular occlusion. Two versions of a final waste form for the fission product-bearing zeolite are being investigated. One is a composite waste form using glass frit as a bonding agent to aggregate the loaded zeolite particles. The second version involves the pyrolysis of loaded zeolite into a mineral form, sodalite. Parametric studies of the sodalite synthesis process have been conducted, and the properties of the final waste form appear comparable to those of the glass-zeolite composite. Development of the metal waste form has focused on the use of stainless steel, derived from the spent fuel cladding hulls, as a matrix for the containment of the metallic fission products recovered from the anode baskets and from filters. The stainless steel waste form was selected in preference to a metal waste based on a Cu-Al alloy because of superior corrosion resistance anticipated for an unsaturated repository environment.

7. *Actinide Recovery*

Spent fuel from commercial light water reactors (LWRs) contains a considerable quantity of unreacted fissile uranium as well as transuranic elements (mainly Pu, Np, Am, and Cm). These actinides constitute a valuable energy resource, and the purpose of the current work is to develop pyrochemical processes for actinide recovery for use as fuel in the IFR. These processes are intended to be simple and efficient and to provide a cost-effective method for recovering actinides from LWR spent fuel.

Over the last several years, three processes employing calcium as reductant for LWR spent fuel have been investigated. During 1993, another alternative process was developed, this one employing lithium as the reductant. Based on the merits of all four process concepts, the lithium process was chosen as the reference for further development. The principal advantages of the lithium process over the calcium-based processes are: (1) the lithium process has a much less corrosive environment, allowing use of ordinary steel containment vessels for most steps, (2) the molten salt is similar to the IFR salt, allowing use of a common waste form for both systems, (3) the operating temperature is lower (650°C compared with 800°C for the calcium systems), allowing easier handling and control of the process, and (4) the uranium-transuranic element separation is accomplished by electrorefining, a well-developed process in the IFR fuel cycle.

Early experiments on reduction of spent fuel oxides with lithium reductant were not very successful. However, during this year 99.99% reduction of the actinide oxides was achieved in a single reduction step with lithium. The key to this success was the discovery that the temperature of the reduction reaction and the quantity of LiCl molten salt were critical parameters in achieving complete reduction. To minimize waste in the process, an electrochemical step is used to recover the lithium reductant and molten salt for recycle. Experiments were done to develop this lithium electrowinning process, and good performance of the electrochemical step was demonstrated.

Engineering-scale tests are planned to demonstrate the feasibility of each step of the processes developed in the laboratory. The test equipment is sized to handle up to 20-kg batch

sizes of simulated LWR spent fuel and is housed in a large argon-filled glovebox. The first experiment in this engineering-scale system was completed in October 1993. The experiment tested the lithium reduction step, and 4.4 kg of uranium oxide was completely reduced.

8. *Applied Physical Chemistry*

The program in applied physical chemistry involves studies of the thermodynamic, thermophysical, and transport behavior of selected materials in environments simulating those of fission and fusion energy systems.

Measurements and calculational analyses are being performed to provide needed information on the thermophysical properties of IFR fuel. One study is addressing the phase relations with fuel-cladding systems over a wide temperature range. To that end, improvements were made to the existing Pu-Zr phase diagram at temperatures ranging up to 1850°C. This work is an extension of previous assessments of the U-Zr, Fe-U, Pu-U, and Fe-Zr phase diagrams. The feasibility of examining IFR materials is also being explored by use of synchrotron radiation sources. The compositional and structural information obtained by such an analysis could help in understanding and predicting intermetallic compound formation, local melting, and fuel redistribution in IFR fuel. In other work, the data base on the properties of IFR materials is being updated by examining and analyzing literature data.

A critical element in the development of the fusion reactor is the blanket for breeding tritium fuel. Studies are underway with the objective of determining the feasibility of using lithium-containing ceramics as breeder material. During this period, experiments were conducted to evaluate tritium release from the candidate breeding material Li_2TiO_3. The results indicated that (1) tritium is released from lithium titanate at temperatures as low as 330°C, (2) this tritium release compares favorably with that of other candidate ceramics, (3) the tritium is released from several types of sites, and (4) hydrogen addition to the helium purge gas is detrimental to tritium recovery with this material. Investigations were also carried out to determine the tritium release characteristics from the beryllium discs used in the SIBELIUS experiment--a CMT/European collaborative effort designed to identify performance-limiting issues associated with the use of beryllium as a neutron multiplier in ceramic breeder blankets. The results showed that retained tritium in the beryllium discs was readily released when they were heated to 650°C and above. They also indicated that optimizing the density and operating temperature for the beryllium neutron multiplier in ceramic breeder blankets will facilitate ease of tritium release and avoid safety issues associated with tritium buildup.

9. *Basic Chemistry Research*

Fluid Catalysis. This program uses an array of *in situ* spectroscopic and kinetic techniques at high pressures and temperatures to explore new catalytic chemistry and catalytic reaction mechanisms for the transformation of simple precursor molecules that serve as raw materials for many industrial processes. Current activities include studies of (1) homogeneous catalytic chemistry in supercritical fluids, (2) catalytic and ceramic precursor processes associated with the production of advanced materials, and (3) catalytic processes for the selective functionalization of methane and other hydrocarbons.

Our activities in catalytic chemistry with supercritical fluids focused on measurement of the concentration of the tetracarbonylcobalt radical, $(CO)_4Co\bullet$, present under the high-pressure conditions of the commercial oxo reaction for the hydroformylation of olefins. (This oxo process is the largest scale industrial process for homogeneous catalysis.) Nuclear magnetic resonance (NMR) measurements of the magnetic susceptibilities of solutions of $Co_2(CO)_8$, the oxo catalyst, in supercritical CO_2 yielded the requisite enthalpy and entropy changes for the dissociation to produce radicals: 80 ± 8 kJ/mol and 121 ± 17 J/mol•K, respectively.

In the ceramic precursor research, we have recently developed a magnetic resonance imaging device that appears to have excellent potential for characterizing advanced materials and materials chemistry processes. The device uses the powerful radio-frequency field gradient present within a toroid cavity resonator to provide NMR spectral information as a function of distance on a micron scale.

Our current research in hydrocarbon activation explores the use of solubilized phthalocyanine (Pc) ligands bound to rhodium centers to achieve controlled reactions of methane in solution. In the past year, we prepared some new, extremely electrophilic complexes in which the phthalocyanine ligand is substituted with eight trifluoromethyl groups. A new methoxyrhodium complex, $(CF_3)_8PcRhOCH_3$, was found to react with H_2 under unusually mild conditions, suggesting that a parallel approach might be useful for CH_4.

Materials Chemistry. This effort involves work on high-critical-temperature (T_c) superconductors, interfacial electrochemistry that is relevant to aqueous corrosion and battery operation, and theoretical studies of technologically important materials. The emphasis of the high-T_c superconductor effort is on elucidating phase equilibria in the Bi-Pb-Sr-Ca-Cu-O system for compositions near the two high-T_c phases: $Bi_{1.8}Pb_{0.4}Sr_{2.0}Ca_{2.0}Cu_{3.0}O_x$ (Bi-2223) and $Bi_{1.8}Pb_{0.4}Sr_{2.0}Ca_{1.0}Cu_{2.0}O_y$ (Bi-2212). A technique based on electrochemical titration of oxygen through a doped zirconia electrolyte is being used to examine Bi-2223 and Bi-2212 phase stability as a function of oxygen partial pressure, temperature, and oxygen stoichiometry. Measurements on two separately prepared Bi-2223 samples (one from Ames Laboratory, the other from ANL) gave reproducible results that defined the stability region for single-phase Bi-2223 as lying between O_2 partial pressures of ~0.02 and ~0.20 atm at 815°C (a common processing temperature for Bi-2223 composite conductors). Paralleling differential thermal analysis and X-ray diffraction studies showed that the decomposition occurring at low O_2 pressures (starting at ≤0.001 atm) leads to formation of $(Bi,Pb)_2Sr_2CuO_x$, $(Ca,Sr)_2CuO_3$, and Cu_2O. A comparable study of Bi-2212 is in progress.

In the interfacial electrochemistry research, the passive films that form on iron in alkaline media have been characterized by a combination of surface-enhanced Raman spectroscopy and electrochemistry. We found that over the temperature range from ambient to 95°C, $Fe(OH)_2$ and Fe_3O_4 form in the prepassive region, while Fe_3O_4 and FeOOH predominate at passive potentials. All the films have highly disordered or amorphous structures. In a related activity, the Cu^{2+}/Cu^0 reduction reaction, a known contributor to stress corrosion cracking of steam generator piping in light water nuclear reactors, is being investigated by advanced electrochemical and theoretical techniques. In prior work, the Cu^{2+}/Cu^+ step was found to be rate

limiting but highly sensitive to certain common impurities, such as Cl^-. During the past year, we measured the impurity-free rate constant for the reaction at ambient temperature. Values obtained after scrupulous purification of the electrolyte solution were two orders of magnitude lower than any previous measurements. The various interaction terms in the $Cu^{2+}(H_2O)_m$ clusters used to model the solution environment have been studied by quantum mechanical methods and will be used in modeling the electron transfer reaction.

Synchrotron radiation in combination with electrochemistry is becoming a powerful tool for our *in situ* investigations of immersed electrochemical interfaces and corroding metal surfaces. Experimental studies of the oxidation of the Pt(111) surface in perchloric acid by X-ray scattering techniques have revealed that the progressive roughening of the surface at oxygen coverages beyond a monolayer is adequately represented by the generally accepted scaling law for interface growth. These same techniques have been used for the first time to explore the initial stages of the pitting corrosion of copper in bicarbonate solution. Adsorbed water clusters on the Pt(111) single-crystal surface have been detected and characterized by synchrotron-generated far infrared radiation.

Achievements in our theoretical studies of technologically important materials include the following: the Gaussian-2 theory was further refined and used to calculate molecular energies of diamond-like carbon clusters; the inorganic chemistry of wood combustion was elucidated using computer programs for thermodynamic analysis that employ some of our own fundamental molten salt theories; and a statistical-mechanical theory for molten silicate solutions of the type used in a variety of industrial processes was refined to broaden its utility.

Geochemistry. The geochemistry research program includes efforts in (1) experimental mineral-fluid interactions, (2) geochemistry and evolution of natural hydrothermal systems, and (3) compound-specific isotopic geochemistry of petroleum. In the first area, *in situ* X-ray scattering measurements of a calcite-fluid interface showed that the structure of the calcite cleavage surface during dissolution is determined by the near-ideal, atomic-scale termination of this surface and the long-range atomic order of the underlying bulk crystal. This surface was characterized by a multistep mathematical model. In the second area, chemical and isotopic studies of Egyptian thermal waters showed that they contain water from either the Nubian sandstone aquifer or the Nile River, derived their solutes from Tertiary marine sedimentary rocks, and were conductively heated at depths of 3 to 4 km under a normal regional geothermal gradient. In the third area, nitrogen isotopic analyses of petroleums from southern California showed significant variations, reflecting primary differences in source rock composition rather than secondary fractionation processes such as biodegradation or maturation.

10. *Analytical Chemistry Laboratory*

The Analytical Chemistry Laboratory (ACL) is administratively within CMT, its principal client, but collaborates as a full-cost-recovery service center with many technical divisions and programs at ANL. In addition, the ACL conducts research in analytical chemistry and provides analytical services for governmental, educational, and industrial organizations.

During the past year, the ACL was involved in a diverse array of activities, including the following: analyses in support of the engineering studies of the IFR pyrochemical processes, development of a Fourier transform infrared spectrometer for continuously monitoring the effluents of waste incinerators, development of analytical methods in support of the Waste Isolation Pilot Plant, development and implementation of a comprehensive program to provide DOE with information on data quality from laboratories analyzing environmental and waste samples, analysis of environmental samples (waters, soils, sediments, filters, air, etc.) and waste samples for ANL and other DOE sites, studies of analytical separations using extraction chromatography with applications in environmental and bioassay areas, development of improved methods for determining actinides in environmental samples, analyses in support of the development of high-temperature superconductors, development of a method for characterizing chlorofluorocarbons in polyurethane foam insulation from discarded appliances, analyses of glassy slags with high metal content and simulated nuclear-waste glasses, measurements for a study of metabolic uptake and incorporation of calcium isotopes into bone, development of automated methods for real-time analysis of chemical sensor data from environmental monitoring, characterization of products from recycling of automobile shredder "fluff," development of alternative methods for radiochemical analysis of environmental samples, analyses for a study developing methods to treat cesium-contaminated milk, and liquid chromatography/mass spectrometry analysis of soils for residual explosive materials.

I. ELECTROCHEMICAL TECHNOLOGY

The Electrochemical Technology Program in CMT undertakes (1) in-house research, development, testing, post-test analysis, and technical evaluation studies of advanced battery and fuel cell systems and (2) support research, technology transfer, and technical management for industrial R&D contracts to develop these systems. To date, in-house battery R&D has focused on three advanced technologies: lithium/iron disulfide, sodium/metal chloride, and lithium-polymer. The testing, evaluation, and post-test analysis of a variety of advanced batteries (e.g., lead-acid, nickel/metal hydride, lithium/sulfide, sodium/sulfur) fabricated by industrial firms are performed in CMT's Analysis and Diagnostics Laboratory. Potential uses of these battery systems include vehicle propulsion, utility load-leveling, and other energy storage applications. In-house R&D is also being conducted on fuel cells, where the CMT Division continues to be the premier DOE laboratory in fuel-cell technology development. We are engaged in R&D on the solid oxide fuel cell and the molten carbonate fuel cell, which are targeted for utility applications, and we are becoming increasingly involved with R&D on the polymer electrolyte fuel cell for transportation applications.

A. *Battery Research and Development*

1. U.S. Advanced Battery Consortium

The U.S. Advanced Battery Consortium (USABC) was formed in 1991 to accelerate the development and commercialization of advanced battery technologies for electric vehicle applications. The USABC is a government-industry partnership among the U.S. Department of Energy, the U.S. automobile industry (Chrysler Corp., Ford Motor Co., and General Motors Corp.), and the U.S. electric utility industry through the Electric Power Research Institute (EPRI). Early in 1993, CMT was awarded two contracts (in the form of Cooperative Research and Development Agreements or CRADAs) by the USABC. One of the CRADAs involves a 38-month project to develop bipolar Li-alloy/FeS_2 batteries (Sec. I.A.2) to meet the long-term performance targets of the USABC. These targets include performance of 300 Wh/L and 600 W/L, lifetime of >1000 cycles, and cost of <$100/kWh. The other CRADA provides for the independent evaluation of advanced batteries in CMT's Analysis and Diagnostics Laboratory (Sec. I.B). The value of this CRADA continues to increase as the USABC assigns more battery evaluation work to CMT. Also, this battery-evaluation CRADA provides funding support for ANL advisors to the USABC's Technical Advisory Committee. This participation included resolving issues regarding battery testing terminology, methodology, and reporting; conducting surveys of $Ni(OH_2)$ supplies and analyzing cost of the nickel electrode for the nickel/metal hydride system; and participating in battery readiness reviews to verify proper test planning, instrumentation, and data acquisition.

Additionally, CMT is in the final stages of negotiating a third CRADA in support of USABC-sponsored battery R&D. Under this new CRADA, CMT will provide R&D support to 3-M Company for the development of lithium-polymer batteries. This will be a 24-month project under which CMT will assist 3-M in optimizing the design, fabrication, and performance of lithium-polymer cells and batteries to meet the long-term performance targets of the USABC.

2. Bipolar Lithium/Sulfide System

In January 1993, SAFT America initiated a 36-month, cost-shared contract with the USABC to work jointly with ANL in the development of the bipolar lithium/sulfide system. The baseline technology for this system is shown in Fig. I-1.[1] It employs disk-shaped cells, assembled into a series-connected stack in which adjacent cells share a common current collector, denoted the bipolar plate. The cells employ lithium-alloy anodes, dense FeS_2 cathodes, LiCl-LiBr-KBr molten salt electrolyte, and MgO powder separators. Cells are sealed around their periphery using a chalcogenide-based material for ceramic-to-metal seals. Final assembly is accomplished with metal-to-metal peripheral welds. Cells are operated in the temperature range of 375-450°C to maintain the electrolyte molten. Cylindrical bipolar stacks will be housed inside thermal modules engineered to maintain acceptable operating temperature (see Fig. I-2). Vacuum multifoil thermal modules are being developed to achieve low thermal losses in lightweight, low-volume packages. Another feature of the thermal management system will be a means of selectively increasing heat removal during periods of battery recharge. The system shown employs a thermally controlled hydrogen gas getter that controls heat transfer rates through the walls of the thermal enclosure. Another more-conventional approach under consideration is to use a forced-air heat exchanger, located inside the thermal enclosure, to remove excess heat on demand.

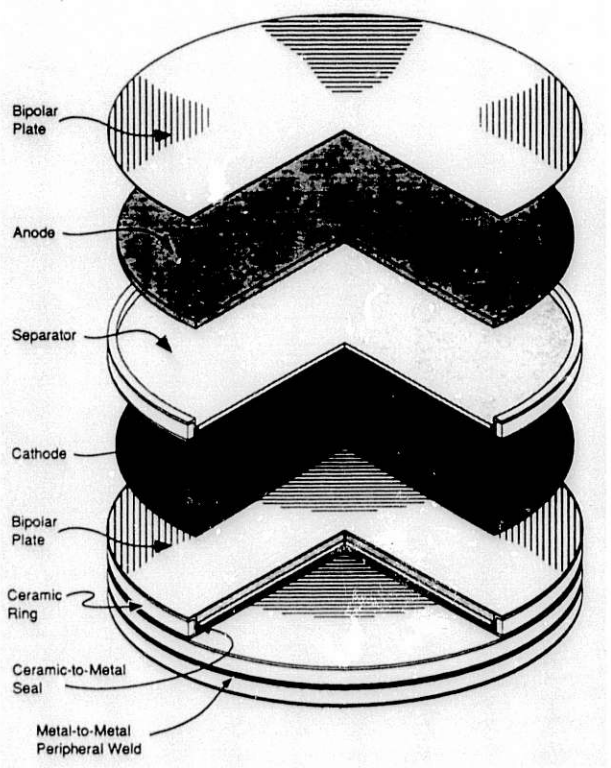

Fig. I-1.

Exploded View of Li-Alloy/FeS_2 Bipolar Stack

[1] T. D. Kaun, P. A. Nelson, L. Redey, D. R. Vissers, and G. L. Henriksen, *Electrochim. Acta* **38**, 1269-1287 (1993).

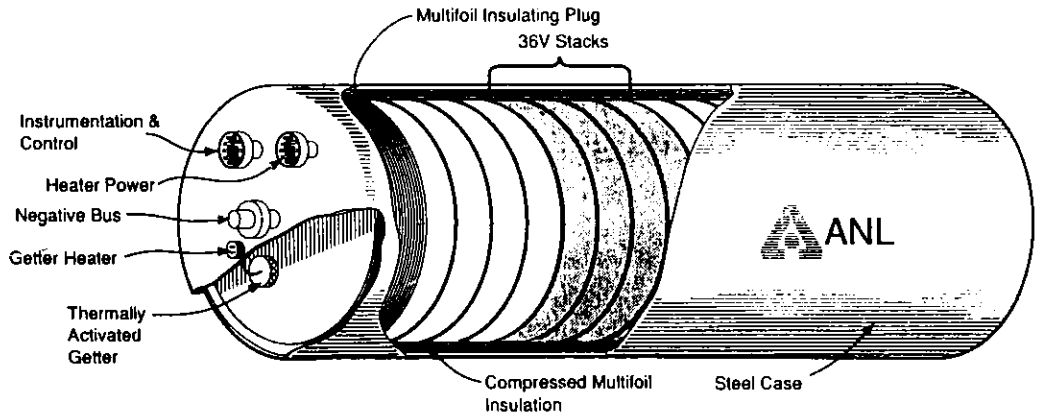

Fig. I-2. Cutaway View of Thermally Controlled Module for Bipolar Lithium/Sulfide Battery

During 1993, five major activities were conducted jointly with SAFT: transfer of baseline technology from ANL to SAFT, refinement of baseline cell and stack technology, development of a design for a first-generation battery stack/module, improvement of ANL's fabrication and testing facilities, and testing of the chemical and electrochemical stability of cell materials. Technology transfer was performed in a variety of ways: conducting technology transfer and technical exchange meetings, establishing and maintaining a chemical and physical properties data base on ANL's baseline cell and stack technology, developing detailed descriptions of fabrication processes, demonstrating component fabrication processes at ANL, and assisting SAFT in hardware fabrication. During 1994, ANL will assist SAFT in the development of first-generation stacks and second-generation components.

3. Sodium/Metal Chloride System

The objective of this research is to (1) generate the scientific and technical base needed for development of sodium/metal chloride (Na/MCl_2) batteries for electric-vehicle propulsion and (2) transfer the technology to industry.

Of the possible metals for the positive electrode, nickel offers the technically most promising choice. The high voltage (2.58 V at 300°C) and the high theoretical specific energy (790 Wh/kg) make the cell with the nickel-containing positive electrode especially attractive. The cell system can be represented as

$$- \; Na/\beta''\text{-alumina}/NaAlCl_4/NiCl_2/Ni \; +$$

The cell uses a solid β"-alumina electrolyte that conducts sodium ions. Moreover, $NaAlCl_4$ is added to the porous $Ni/NiCl_2$ positive electrode to transport sodium ions from the surface of the β"-alumina electrolyte to the reaction sites at the interior of the electrode. The $NaAlCl_4$ and sodium are molten at the operational temperature of the cell (typically, ~300°C), but the $NiCl_2$ of the positive electrode is solid.

In the past, cell performance was limited because $NiCl_2$ is sparingly soluble in the chloroaluminate electrolyte and forms a poorly conducting layer on the nickel in the positive electrode during charge. This layer hinders capacity uptake during charge and limits power during discharge.[2] As reported earlier,[3,4] we overcame this problem by developing a new type of $Ni/NiCl_2$ electrode, termed the "ANL-92 electrode." This electrode contains chemical additives (NaBr, NaI, and S) and has a dual-porosity morphology produced by a sintering process. In this reporting period, we further improved our $Na/NiCl_2$ cell and initiated technology transfer to industry, who were encouraged by the excellent performance results from our laboratory cell measurements.

The excellent performance of the new $Na/NiCl_2$ cells has been verified by electrochemical performance measurements in engineering research cells (unsealed) with 1- to 2-Ah capacity. To date, we have characterized 42 engineering research cells under a wide variety of experimental conditions and established a data base for more than 4000 cycles. These measurements demonstrated that $Na/NiCl_2$ cells fabricated with the ANL-92 electrode can be operated at temperatures as low as 153°C, which is only 5°C higher than the melting point of the electrolyte. Very high energy capacities have been demonstrated for the whole 153-360°C operational temperature range (Fig. I-3). This figure shows that 1 g of nickel produces 1.15 Wh specific energy in $Na/NiCl_2$ cells at 360°C. This specific energy is about three times more than

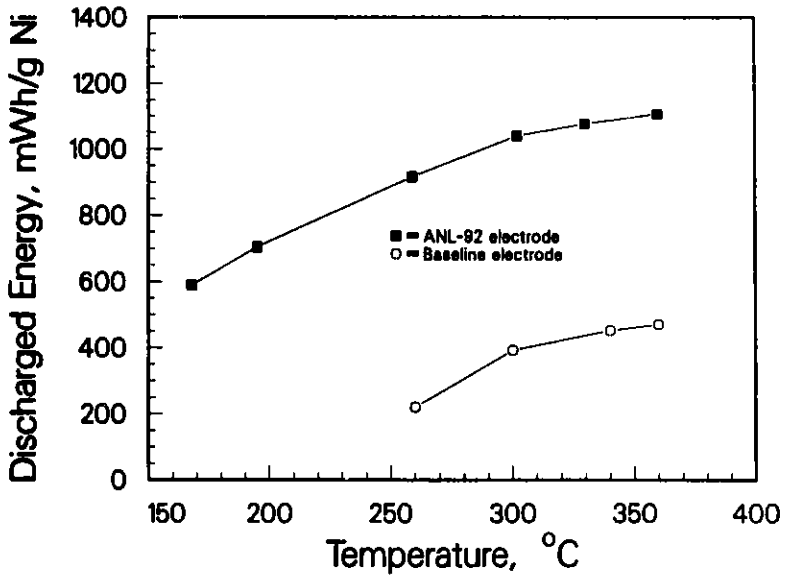

Fig. I-3. Discharged Energy of $Na/NiCl_2$ Cells with ANL-92 and Baseline Electrodes as Function of Temperature

---

[2] L. Redey and D. R. Vissers, "Investigations of $Ni/NiCl_2$ Electrodes in Basic Chloroaluminate Melt," Extended Abstracts, 176th Electrochem. Soc. Meeting, Hollywood, FL, October 15-20, 1989, Vol. 89-2, p. 143 (1990).

[3] L. Redey, J. Prakash, D. R. Vissers, and K. M. Myles, "Development of $Na/NiCl_2$ Cells," Proc. of the IEEE 32nd Power Sources Symp., Cherry Hill, NJ, June 22-28, 1992, p. 343 (1992).

[4] J. Prakash, L. Redey, R. Skocypec, and D. R. Vissers, "High-Performance Nickel Chloride Electrode Studies," Extended Abstracts, 182nd Electrochem. Soc. Meeting, Toronto, Canada, October 11-16, 1992, Vol. 92-2, p. 108 (1992).

that achievable in Ni/Cd or other nickel cells under development and is due to the high cell voltage and the two-electron cell reaction. Moreover, the excellent kinetics of the ANL-92 electrode permits fast recharge of the cell at high current density. The charge times have been reduced to about one hour, from 10-15 hours, with relatively little penalty in the capacity.

Our engineering research cell measurements have been used in calculations that we have performed to project the performance of full-size batteries.[5,6] These calculations indicate that a $Na/NiCl_2$ electric-vehicle battery with tubular cells can surpass the mid-term performance requirements of the USABC (135 Wh/L and 250 W/L), while the same battery with bipolar cells could approach the long-term requirements (300 Wh/L and 600 W/L).

From the performance measurements with the engineering research cells and other investigations, we have concluded that the $Na/NiCl_2$ cell system has several attractive features for its development as a high-performance battery. First, the wide temperature range and advantageously low minimum temperature permit the use of a simple, energy-efficient system for controlling temperature. Second, the current efficiency of the cell is 100% at all times because the ceramic electrolyte prevents self-discharge. Third, the cell is extremely tolerant to overcharge and overdischarge; this tolerance is a very favorable feature for long cycle life of the full-size battery. In batteries with serially connected cells, both overcharge and overdischarge normally develop during extended use because of capacity inequalities among the cells. The $Na/NiCl_2$ battery, however, has experimentally proven electrochemical mechanisms that allow about 30% of the cell capacity to be overcharged or overdischarged without damaging the cell. Fourth, the cell chemistry necessitates that the cells fail in the short-circuited mode, which is a prerequisite for reliable and simple construction of a high-voltage battery with long cycle life. Fifth, the low solubility of $NiCl_2$ in the cell electrolyte[7] and the very limited corrosion of the current collectors[8] are additional features of this system that extends cycle life. Finally, our $Na/NiCl_2$ cell can produce about three times more energy per weight of nickel than the other nickel cells under development (Ni/Cd, Ni/metal hydride, Ni/H_2, Ni/Zn, and Ni/Fe).

The excellent performance, long life, and other attractive features of the $Na/NiCl_2$ cell encouraged us to seek industrial partner(s) for battery development. In 1993, technology transfer was initiated with two companies: Eagle-Picher Industries, Inc. and Hughes Aircraft Co. Both these companies have built sealed $Na/NiCl_2$ cells (4-12 Ah capacity) according to our composition and design recommendations. In this phase of collaboration, the primary purpose is

---

[5] P. A. Nelson and J. Prakash, "Modeling of Sodium/Nickel Chloride Batteries for Electric Vehicles," Proc. Symp. on Modeling Batteries and Fuel Cells, eds., R. E. White et al., 180th Electrochem. Soc. Meeting, Phoenix, AZ, October 13-18, 1991, Vol. 91-10, p. 122 (1991).

[6] L. Redey, T. Rauworth, J. Prakash, and D. R. Vissers, "Electric Vehicle Battery Performance Projections from Research Cell Measurements," Extended Abstracts, 184th Electrochem. Soc. Meeting, New Orleans, LA, October 10-15, 1993.

[7] L. Redey, C. Rose, and R. Lowrey, "Solubility of $NiCl_2$ in Sodium-Chloroaluminate Melts," Extended Abstracts, Electrochem. Soc. Meeting, Toronto, Canada, October 11-16, 1992, Vol. 92-2, p. 116 (1992).

[8] J. Prakash, L. Redey, R. Skocypec, L. Lowrey, and D. R. Vissers, "Dual Role of Nickel in Sodium/Nickel Chloride Batteries," Extended Abstracts, 182nd Electrochem. Soc. Meeting, Toronto, Canada, October 11-16, 1992, Vol. 92-2, p. 112 (1992).

to demonstrate the viability of sealed cells. Additional purposes are to search for expedient cell fabrication processes and establish quantitative relationships between performance data measured in engineering research cells and full-sized cells.

The two companies followed different fabrication routes. The Eagle-Picher cells (4-Ah capacity) have the ANL additives and a "powder" nickel electrode (no sintering) inside the β"-alumina electrolyte tube. For comparison, Eagle-Picher also fabricated similar cells without the ANL additives. The Hughes cells (12-Ah capacity) contain the ANL additives and a sintered nickel electrode outside the electrolyte tube. Testing of the Eagle-Picher and Hughes cells under constant-current cycling confirmed the feasibility of the ANL-design $Na/NiCl_2$ cell and also the cell fabrication capability of the respective companies. Although the cells have not been optimized, they have demonstrated performance consistent with the engineering research cell measurements at ANL. For example, Fig. I-4 shows the impedance and discharged energy of the additive-containing Eagle-Picher cell at three temperatures. As shown, this cell produced a specific energy of 0.8 Wh/g-Ni and an average impedance of 60 mohm at 345°C. Although this performance is not as good as measured for sintered $Ni/NiCl_2$ electrodes with additives (about 80% of the specific energy and twice the impedance), it shows the viability of the fabrication technology and is consistent with expectations for nonsintered electrodes. Moreover, as shown in Fig. I-4, a significant result is that the additives can extend the range of operation to lower temperatures for nonsintered electrodes, just as was the case for the sintered ones. In addition, the Eagle-Picher cells with and without additives have not shown signs of significant capacity degradation with cycling in tests at ANL. For example, after 850 charge/discharge cycles and several freeze-thaw cycles, one of the Eagle-Picher cells still shows 80% of the capacity attained during the early cycles.

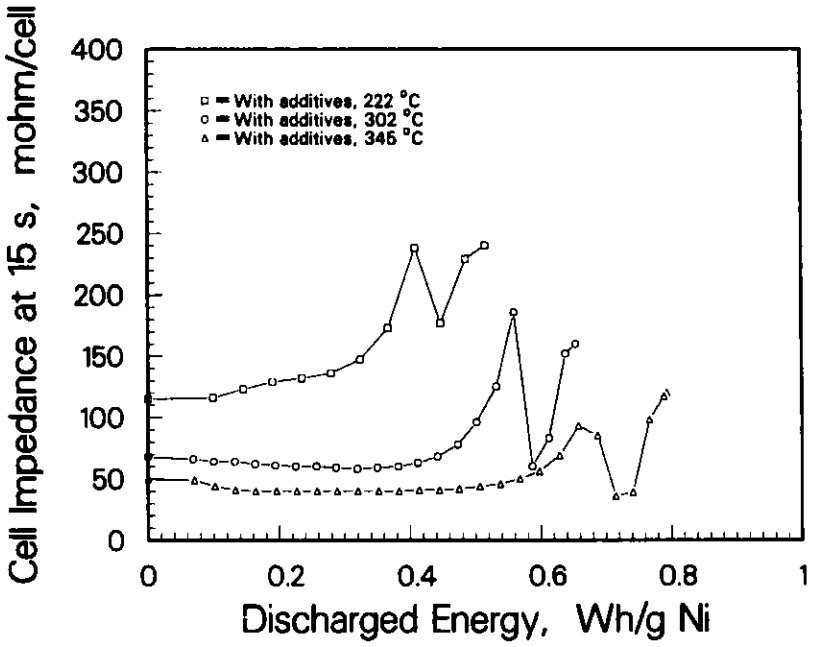

Fig. I-4. Performance of Sealed 4-Ah $Na/NiCl_2$ Cell with Nonsintered, Inside Positive Electrode as Function of Temperature

The Eagle-Picher cells with additives have also demonstrated good performance in the Dynamic Stress Test (DST) required by the USABC. The DST is a "powerdynamic" simulated-driving test in which the cell is discharged and the cumulative energy is measured in repeated 6-min-long standard DST power profiles until the cell voltage drops to a specified value. The DST-power performances indicate that the Eagle-Picher cell with additives has three times higher power capability and produces two times more energy from a discharge half-cycle than the same cell without additives. In the next year, Eagle-Picher plans on fabricating engineering cells with additives and sintered, outside positive electrodes for testing.

Our future efforts will concentrate on optimizing our new design of nickel chloride electrode and transferring the technology to an industrial contractor and the USABC.

4. Lithium-Polymer Electrolyte System

Work this past year continued toward the development of a reference electrode to use in lithium-polymer electrolyte (LIPE) batteries. The LIPE batteries are all-solid-state electrochemical devices that operate at or near ambient temperature and consist of ultra-thin (<100 μm) layers laminated together. The primary objective is to fabricate a micro-reference electrode capable of operation inside the very thin polymer electrolyte gap common to LIPE cells and batteries. Careful, controlled placement of the reference electrode is essential because the positive and negative electrodes are typically separated by less than 100 μm. Electrochemical experiments were conducted on a lithium binary alloy, Li_xSn, as a possible candidate electrode. We have advanced our study of this material from the preliminary electrochemical examination of bulk (thick) tin foil samples to thin-film specimens.

Tin-thin-film specimens were fabricated into electrodes and tested at 100°C in polymer electrolyte cells. Using vacuum evaporation-deposition techniques, we prepared these specimens as ultra-thin tin layers (50-1000 Å) deposited *ex situ* onto stainless steel foil substrates. For comparison, two deposition techniques were employed: ion-beam assisted deposition (IBAD) and physical vapor deposition (PVD). The processes differ only in that the argon ion gun (500 eV) is left on after cleaning the substrate for IBAD and turned off for PVD. The IBAD technique is known to improve the adhesion between the depositing vapor and the support.[9] Electrodes were cut or punched from the foil; each had an area of approximately 5 cm^2. Electrochemical test cells consisted of a tin thin film and metallic lithium as electrodes. The polymer electrolyte material was polyethylene oxide (PEO) that contained the dissolved lithium trifluoromethane sulfonate ($LiCF_3SO_3$) salt. The cell designation is Li/PEO_y-$LiCF_3SO_3$/Sn, where y = 8 or 10.

Figure I-5 shows a representative coulometric titration curve for an IBAD electrode (tin film thickness ~ 1000 Å) in the Li/PEO_{10}-$LiCF_3SO_3$/Li_xSn cell. Similar results were obtained for an IBAD electrode with a 500-Å tin film. The results indicate three different, two-phase compositions, which maintain flat voltage regions at approximately 0.73 V (plateau I), 0.63 V (plateau II), and 0.53 V (plateau III) vs. lithium metal. We intend to exploit such a two-phase

---

[9] F. A. Smidt, *Int. Mater. Rev.* **35**, 61 (1990).

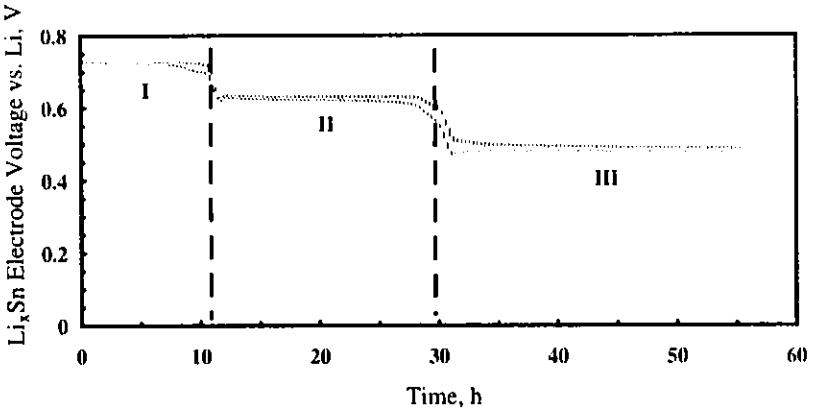

Fig. I-5. Coulometric Titration Curve for Tin-Thin-Film Electrode in Li/PEO_{10}-$LiCF_3SO_3$/Li_xSn Cell (film thickness of ~ 1000 Å)

compositional range and to use its associated emf as the reference electrode potential in the LIPE cells at temperatures of 60-100°C. For instance, the 0.53-V phase (plateau III) showed excellent stability, remaining fairly constant (±1 mV) at open circuit during two weeks of monitoring.

The shape of the voltage curve and the average voltage (0.734 V) for plateau I in Fig. I-5 closely match those obtained in previous experiments using bulk tin foil electrodes.[10] This result verifies that the bulk-tin-foil electrode and the tin-thin-film electrode electrochemically function in a similar way. The verification is significant because it enables us to project the electrochemical performance of thin-film reference electrodes in polymer electrolyte environments. A second observation involves the appearance of multiple voltage plateaus for the tin-thin-film electrodes. This result stands in contrast to the electrode experiments with bulk tin foil, which displayed only the first voltage plateau (at 0.7336 V).[10] The data suggest that lithium diffusion is limited by the molecular scale layer of the lithium-tin thin film. As a consequence, the increased concentration of mobile yet confined lithium atoms causes the stoichiometric ratio (Li/Sn) within the layer to grow. This results in the formation of additional lithium-rich, biphasic alloys of Li_xSn. In the bulk tin foil, the lithium is not confined to a thin tin layer but is free to migrate to lower regions of lithium activity (i.e., the larger mass). As a result, the surface concentration of lithium cannot grow to the larger proportions that are necessary to produce additional phases of Li_xSn.

In further electrochemical experiments, the composition of the phases in IBAD and PVD electrodes (i.e., x in Li_xSn) was coulometrically varied by repeatedly reversing the current, and electrodes made from IBAD tin deposits performed more reversibly, with little or no degradation, as compared to the PVD-type electrodes. The PVD electrodes appear to be more unstable.

---

[10] J. E. Battles et al., *Chemical Technology Division Annual Technical Report, 1992*, Argonne National Laboratory Report ANL-93/17, p. 24 (1993).

We have concluded that lithiated tin-thin-film deposits (IBAD) greater than 1000 Å thick should provide the best stability and reproducibility as micro-reference electrodes in lithium-polymer laboratory cells. We have recently used the IBAD technique to coat stainless steel dissecting needles with tin to a thickness of 1000-3000 Å. Our next goal is to incorporate the coated needles in real lithium-polymer laboratory cells and to examine the electrochemical properties of the needles as micro-reference electrodes.

B. *Analysis and Diagnostics Laboratory*

The Analysis and Diagnostics Laboratory (ADL) was established at ANL to study advanced battery systems for applications such as electric vehicles and utility load-leveling. The facilities include a test laboratory to conduct battery experimental evaluations under simulated application conditions and a post-test analysis laboratory to determine, in a protected atmosphere if needed, component compositional changes and failure mechanisms. Evaluations are performed for DOE, EPRI, and others to provide insight into those factors that limit the performance and life of advanced battery systems. The results of these evaluations help identify the most-promising R&D approaches for overcoming these limitations and provide battery users, developers, and program managers with a measure of the progress being made in battery R&D programs, a comparison of battery technologies, and basic data for modeling.

1. Performance and Life Evaluations

During 1993, performance and life evaluations were conducted on two electric-vehicle battery systems under a CRADA with the USABC (Sec. I.A.1): (1) nickel/metal hydride (Ni/MH) cells and multi-cell modules from Ovonic Battery Co., manufactured under a contract with USABC, and (2) a Na/S multi-cell module from Silent Power Ltd. (England), fabricated as part of the DOE ETX-II Program. In early 1993, ANL activities under the CRADA were expanded to include evaluation of a Ni/MH battery system from Eagle-Picher. Testing of the Ovonic and Silent Power systems is continuing; evaluation of the Eagle-Picher system has been completed. The results of these tests will be released by the USABC at a later date.

Two advanced lead-acid battery systems are being evaluated for EPRI. One battery system, assembled by Bell Computer, Inc., features a unique lightweight package. The other system is a quasi-bipolar design from Electrosource, Inc. These evaluations are continuing, and the performance and life data on both systems will be available in mid-1994.

Two Ni/Cd batteries from SAFT (France) are being tested for the fuel cell/battery bus project (Sec. I.C.4). One battery (model STM5-200) is rated at 200 Ah, and the second (STH-800) at 80 Ah. Life testing is performed with a load that simulates operation in a hybrid bus on an urban route. The STM5-200 system has been on test for almost two years and has accumulated 9084 cycles, which is equivalent to >75,000 fuel-cell bus miles (>120,000 km). The STH-800 system has accumulated 4104 cycles (~35,000 simulated bus miles or 56,000 km) in almost one year of testing. Both batteries continue to perform well and have shown no sign of capacity loss to date.

2. Post-Test Analysis

A number of Ovonic Ni/MH cells have undergone post-test analysis after life evaluation in the ADL. This activity is being sponsored by the USABC to assist Ovonic in identifying and focusing their resources on critical issues facing their technology. Many of these post-test analyses have been a joint effort between ANL and Ovonic.

The USABC also chartered ANL to draft a procedural outline for the standardization of post-test procedures. The ANL procedural guideline includes a review of all battery documentation, the performance of diagnostic and non-destructive tests to select specific cells for full examination, a teardown inspection, and specific analyses of key components within the cells. The level of analyses is guided by the preliminary diagnostic and teardown findings.

In 1994, post-test analyses, as well as performance and life evaluations, will be continued on cells, modules, and batteries for the USABC and EPRI.

C. *Fuel Cell Research and Development*

The CMT Division continues to conduct R&D on the solid oxide fuel cell (SOFC) and the molten carbonate fuel cell (MCFC), which are targeted for utility applications, and on the polymer electrolyte fuel cell (PEFC) for transportation applications. All fuel cells convert the chemical energy of fuels such as hydrogen, methane, methanol, or ethanol to electricity with little or no pollution and with greater efficiency than heat engines. In the low-temperature fuel cell (PEFC), only hydrogen can be used directly, and hydrocarbons need to be reformed in separate reforming reactors. In the high-temperature fuel cells (SOFC and MCFC), the reforming can be internal to the fuel cell.

1. Solid Oxide Fuel Cells

The present design for the solid oxide fuel cell (SOFC) has an oxide-ion-conducting electrolyte material, yttria-stabilized zirconia; a cathode of strontium-doped lanthanum manganite; an anode of nickel/yttria-stabilized zirconia; and a cell interconnect material of strontium-doped lanthanum chromite. The cell operating temperature is 800-1000°C. The objectives of our R&D on the SOFC are to develop (1) electronically insulating sealants for use in state-of-the-art fuel cells and (2) anodes tolerant to sulfur in the fuel gas.

a. Sealants

The objective of this effort is to develop insulating sealants for sealing the edges and gas-supply and exhaust manifolds in solid oxide fuel cells and stacks. These sealants must be compatible with the fuel cell materials under the aggressive fuel-cell operating conditions. In addition to forming a good bond, the sealant must have a coefficient of thermal expansion that closely matches the coefficients of thermal expansion of the SOFC and the manifold materials. Since all of these materials do not have identical coefficients of thermal expansion, the sealant is required to possess a degree of compliance to tolerate the thermal expansion mismatches without unduly stressing the fuel cell stack or manifold components.

For this purpose, we have developed a glass-ceramic sealant with a glass transition temperature of 780°C and a coefficient of thermal expansion of 11.5×10^{-6}/°C (from room temperature to 650°C). The sealant's viscosity was measured by the bending-beam method[11] to vary from 10^{10} Pa·s at 800°C to $10^{6.5}$ Pa·s at 1000°C. A viscosity less than 10^{12} Pa·s is needed to afford some degree of compliance[12]; thus, this sealant has the right viscosity range for the SOFC application.

In a compatibility and compliance test, a tape of the glass-ceramic material was bonded to a monolithic SOFC stack and an alumina disk. The composite structure was then cycled twice between room temperature and 1000°C. Even though there was an estimated mismatch in the coefficients of thermal expansion of the stack materials and alumina of at least 20%, the bonds formed with the sealant were strong and dense. Examination by optical microscopy showed some isolated large pores in the sealant, which were attributed to removal of the binder used for making the sealant tape. The sealant/alumina and sealant/stack interfaces were sharp and showed no signs of reaction or delamination. Examination by scanning electron microscopy showed that the bonding phase at all interfaces consisted of glass. Energy dispersive X-ray spectroscopy of the alumina/seal interface indicated diffusion of aluminum into the glassy component of the sealant, producing a composition gradient. Hence, a seal with a graded profile for the coefficient of thermal expansion may have been formed at this interface, thus reducing the interfacial stresses.

Next, the sealing ability of the glass-ceramic sealant was tested in an electrochemical cell consisting of a 500-μm-thick disk of yttria-stabilized zirconia sealed to the end of a zirconia tube. The sealant formed an O-ring gasket with 1-mm thickness. Platinum screen electrodes were bonded to either side of the YSZ disk to make up the cell. Flowing humidified 5% H_2-95% He was used as the fuel gas and stagnant furnace air as the oxidant. The bonded cell was thermally cycled once between room temperature and 1000°C with no evidence of any cracking. Leakage and/or gas permeation through the seal was determined by measuring the electrochemical performance of the cell. The measured open-circuit emf's are given in Table I-1, along with the theoretical emf's at 800, 900, and 1000°C. The theoretical and measured values show excellent agreement and indicate that the sealant formed a gas-tight seal.

While the cell was operating, the fuel gas flow was periodically shut off. The resulting rate of decay in cell emf was used to calculate the permeation constant for oxygen through the sealant material at the different temperatures (Table I-1). The published permeation constant for oxygen permeating through fused SiO_2 at 700°C is less than 10^{-15} (in the units shown in Table I-1).[13] Since permeation through crystalline solids is about 10^7 slower than in glasses,[13] the permeation constant for oxygen diffusing through quartz was expected to be about 10^{-22}. Thus, the data in Table I-1 are consistent with the fact that the sealant is an elastic, rigid solid

---

[11] H. E. Hagy, *J. Am. Ceram. Soc.* **46**, 93 (1963).

[12] H. Rawson, *Properties and Applications of Glass*, Glass Science and Technology Series, Vol. 3, Elsevier, Netherlands, pp. 74-82 (1980).

[13] W. H. Kohl, *Handbook of Materials and Techniques for Vacuum Devices*, Reinhold Publishing Co., New York, pp. 10-13 (1967).

Table I-1. Measured and Theoretical Electromotive Force and Calculated Permeation Constant from Electrochemical Cell Sealed with Compliant Sealant

Temp., °C	Electromotive Force, mV		Permeation Constant, mm·cm³(STP)/(s·cm²·cm Hg)
	Measured	Theoretical	
800	967 ± 3	968	2.19×10^{-23}
900	938 ± 2	939	6.91×10^{-20}
1000	911 ± 2	911	5.46×10^{-17}

composed primarily of crystalline material at 800°C. The higher permeation rates at 900 and 1000°C are very likely due to the small but significant amounts of the glassy component. Future work on sealants will focus on conducting materials interactions studies and on customizing the sealant composition for specific applications.

b. Sulfur-Tolerant Anodes

The purpose of this effort is to develop sulfur-tolerant anode materials for use in SOFCs in the temperature range 800-1000°C. Such anodes are necessary for long-term operation of these cells on sulfur-containing, coal-derived fuels or natural gas. In the current SOFC technology, a nickel/yttria-stabilized-zirconia (30-40 vol% Ni) cermet is used as the anode. The yttria-stabilized zirconia supplies all the ionic conductivity, and the nickel provides the electronic conductivity. An intimate mixture of nickel and yttria-stabilized-zirconia particles is required to spread the reaction sites throughout the porous anode. Over prolonged use at high temperatures, especially 1000°C, sintering of nickel particles in contact with each other takes place, thereby reducing the number of reaction sites. The second main drawback of this anode is the reaction of nickel with sulfur or sulfide-containing fuel gases, which degrades fuel cell performance over time. We are, therefore, searching for alternative materials to be used in the SOFC anode.

To facilitate the electrochemical reactions at the anode, the candidate anode material should have ionic conductivity at least equal to yttria-stabilized zirconia and electronic conductivity at least comparable to the ionic conductivity. Pure CeO_2 has several attractive properties as a candidate anode. It possesses a high ionic conductivity, more than twice that of yttria-stabilized zirconia, and in fuel-cell anode conditions, it has a high electronic conductivity as well (about 10 S/cm). However, this oxide suffers from large lattice distortions due to changes in nonstoichiometry as a result of changes in the oxygen content of the surrounding gas. The lattice distortions cause the material to flake off.[14] To minimize lattice distortions in reducing environments, we explored two doped cerium-containing compounds: $La_{0.7}Mg_{0.3}CeO_{3.35}$ and $La_{0.8}Nb_{0.2}CeO_{3.7}$. Owing to the doping, nonstoichiometry is inherent and not as such altered in reducing environments.

[14] I. S. Metcalfe, P. H. Middleton, P. Petrolekas, and C. C. H. Steele, *Solid State Ionics* **57**, 259-264 (1992).

The nonstoichiometry per cation of $La_{0.7}Mg_{0.3}CeO_{3.35}$ was found to be half that for pure CeO_2. Furthermore, since a large nonstoichiometry is built in by the La_2O_3 and MgO additions (as evidenced by an oxygen content of 3.35 instead of 4.0, which amounts to 16.25% oxygen vacancies per O^{2-} ion), further small nonstoichiometry changes, such as those associated with changes in oxygen partial pressure, will not cause significant lattice distortion. Thus, this candidate anode has a significant advantage over CeO_2.

The ionic transference number was measured for $La_{0.7}Mg_{0.3}CeO_{3.35}$ and $La_{0.8}Nb_{0.2}CeO_{3.7}$ in oxidizing (O_2) and reducing (humidified 6% H_2 + 94% He) conditions at 800-1000°C. The results are given in Table I-2. The ionic transference number represents the ionic conductivity (δ_i) part of the total conductivity (δ_t):

$$t_i = \frac{\delta_i}{\delta_t} \qquad (1)$$

For a good anode material, the value of t_i should be ≤0.5 under reducing conditions, indicating approximately equal ionic and electronic conductivity. As shown in Table I-2, $La_{0.7}Mg_{0.3}CeO_{3.35}$ at low oxygen partial pressure (reducing environment) exhibits a t_i of ~0.5 at 900-1000°C, which is ideal for the SOFC anode application. For $La_{0.8}Nb_{0.2}CeO_{3.7}$ under reducing conditions at 800-1000°C, the t_i values are less than 0.5 but above 0.25; thus, it also shows promise as the anode material. For both materials under oxidizing conditions (1 atm), t_i is close to 1.0, indicating an ionic conductor. Both these materials will be studied further.

Table I-2. Ionic Transference Numbers for Candidate Anode Materials as Function of Temperature and Oxygen Partial Pressure

O_2 Partial Pressure, atm (Pa)	Temp., °C	Ionic Transference Number	
		$La_{0.7}Mg_{0.3}CeO_{3.35}$	$La_{0.8}Nb_{0.2}CeO_{3.7}$
7.3×10^{-20} (7.4×10^{-15})	800	0.63	0.36
8×10^{-18} (8×10^{-13})	900	0.55	0.31
4.2×10^{-16} (4.2×10^{-4})	1000	0.54	0.26
1 (10^5)	800	1.00	0.99
1 (10^5)	900	1.00	0.97
1 (10^5)	1000	1.01	0.94

2. Molten Carbonate Fuel Cells

The present molten carbonate fuel cell (MCFC) comprises a porous (chromium-stabilized) nickel anode, a porous nickel oxide cathode, a liquid electrolyte of lithium and potassium carbonates retained by a ceramic matrix of $LiAlO_2$, and appropriate metal separators.

The cell operates at an average temperature of about 650°C. The objectives of our work on this fuel cell are to develop new, electronically conductive ceramic oxides that are chemically stable in the fuel cell environments as electrodes and to improve state-of-the-art components.

a. Cathodes

Commercial MCFCs are being operated near ambient pressure, but their operation at pressures of up to ten times ambient is desired because of their greater power capabilities at higher pressures. However, pressurization significantly shortens the life of an MCFC because of accelerated dissolution of the nickel oxide cathode in the molten carbonate electrolyte and subsequent deposition of metallic nickel near the anode.[15] Alternatives to the NiO cathode are, therefore, under investigation at ANL; these alternatives are lithium ferrate ($LiFeO_2$) and lithium cobaltate ($LiCoO_2$). The $LiCoO_2$ cathode is also being investigated at the Netherlands Energy Research Foundation (ECN).[16] Both $LiFeO_2$ and $LiCoO_2$ exhibit lower rates of transport to the anode than NiO. In fact, we find that $LiFeO_2$ transports to the cathode if placed in the anode.

The resistivities of $LiFeO_2$, $LiCoO_2$, and NiO at 650°C are about 300, 1, and 0.1 Ω·cm, respectively. The higher resistivities of the $LiFeO_2$ and $LiCoO_2$ would lead to decreased MCFC performance if they were merely substituted for NiO. Consequently, the objective of our studies has been to improve the properties of the alternative cathodes by decreasing their resistivities with dopants and by modifying their microstructures.

Half-cell measurements of the effects of individual dopants such as Mn, Co, Ni, and Cu on the performance of $LiFeO_2$ cathodes in various cathode-gas mixtures at 650°C were presented in previous reports.[17,18] Although each of these dopants decreased the resistivity of $LiFeO_2$, no single dopant produced the needed improvement in cathode performance. The best of the single dopants, cobalt, reduced the resistivity of $LiFeO_2$ from 300 to 3 Ω·cm. However, this Co-doped $LiFeO_2$ cathode only performed well with cathode-gas mixtures having CO_2-to-O_2 ratios at or below 1 to 5. This restriction was unacceptable because commercial MCFCs would generally be operated at higher ratios of CO_2 to O_2.

Consequently, we began an investigation of doubly doped $LiFeO_2$ cathodes (the composition of the doubly doped $LiFeO_2$ is to be patented, and, therefore, cannot be disclosed at this time). Double doping reduced the resistivity of $LiFeO_2$ from 300 to 0.3 Ω·cm

---

[15] W. M. Vogel, L. J. Bregoli, H. R. Kung, and S. W. Smith, "Stability of NiO Cathodes in Molten Carbonate Fuel Cells," Proc. of 166th Electrochem. Soc. Meeting, New Orleans, LA, October 7-12, 1984, Vol. 84-12, pp. 443-451 (1984).

[16] L. Plomp, E. F. Sitters, J. B. J. Veldhuis, R. C. Makkus, and S. B. van der Molen, "Performance and Dissolution of Molten Carbonate Fuel Cell Cathodes," Proc. of 3rd Int. Symp. on Carbonate Fuel Cell Technology, 183rd Electrochem. Soc. Meeting, Honolulu, HI, May 16-21, 1993, Vol. 93-3, pp. 171-185 (1993).

[17] J. E. Battles et al., *Chemical Technology Division Annual Technical Report, 1992*, Argonne National Laboratory Report ANL-93/17, pp. 34-39 (1993).

[18] M. J. Steindler et al., *Chemical Technology Division Annual Technical Report, 1991*, Argonne National Laboratory Report ANL-92/15, p. 42 (1992).

and improved the performance of the cathode for a broad range of cathode-gas compositions. Figure I-6 shows the polarization curves of the doubly doped $LiFeO_2$ cathode, the $LiCoO_2$ cathode, and the state-of-the-art NiO cathode in a cathode gas containing 58% O_2-42% CO_2. Although the $LiFeO_2$ and $LiCoO_2$ curves are slightly below the NiO curve, we expect that they will ultimately match NiO with further optimization of the $LiFeO_2$ and $LiCoO_2$ cathode microstructures and thicknesses. For all three cathodes, the polarization was independent of cathode-gas composition over the range 85% O_2-15% CO_2 to 40% O_2-60% CO_2.

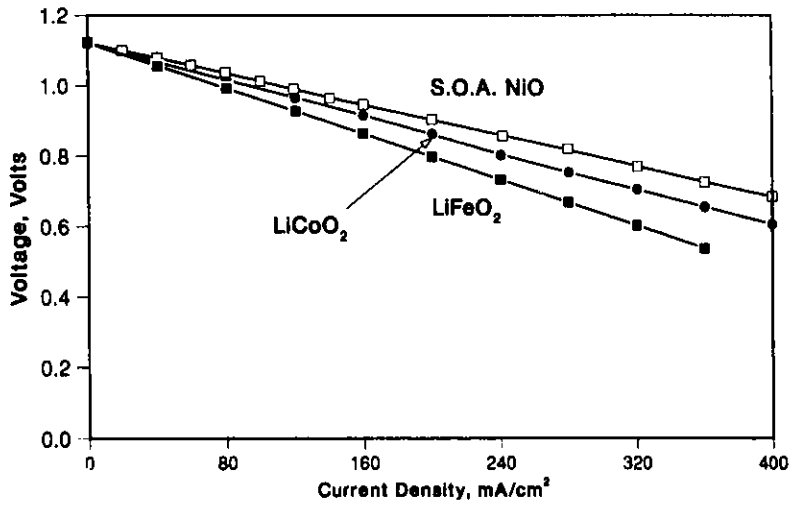

Fig. I-6. Polarization of Molten Carbonate Fuel Cells with Doubly Doped $LiFeO_2$ and $LiCoO_2$ Cathodes Employing 58% O_2-42% CO_2 Cathode Gas at 650°C. Performance of state-of-the-art (S.O.A.) cathode shown for comparison.

Despite its good performance, there remains an issue concerning the use of $LiCoO_2$ as a cathode material: the dissolution and deposition of metallic cobalt in or near the anode. Investigators at ECN[16] report a transport rate that is significantly lower than the rate of NiO, but our post-test examinations show some migration of cobalt from the cathode into the electrolyte structure. Future tests of $LiCoO_2$ cathodes will focus on quantifying the rate of cobalt transport.

b. Alternative Electrolytes

In addition to developing cathode materials with lower solubility than the standard NiO cathode, we are examining ways to reduce the solubility of NiO by modifying the electrolyte. In our previous work,[17] we showed that the addition of $CaCO_3$ to Li_2CO_3-K_2CO_3 and Li_2CO_3-Na_2CO_3 melts reduced the solubility of NiO by a factor of three and five, respectively. Because other components are affected by the properties of these ternary electrolytes, one of these electrolytes (55 mol% Li_2CO_3-24 mol% K_2CO_3-21 mol% $CaCO_3$) was evaluated with regard to hardware corrosion, electrode performance, and relative cation migration.

The material of choice for the bipolar-plate separator in a MCFC is stainless steel (SS), typically, Types 316L and 310. The anodic side of this plate is nickel clad to protect it from corrosion by the molten salts and anode gas (80% H_2-20% CO_2), but the cathodic side cannot be protected in this manner. Corrosion tests were conducted at 650°C for 1500 h on coupons of Types 316L and 310 SS in two electrolytes: 70 mol% Li_2CO-30 mol% K_2CO_3 and 55 mol% Li_2CO_3-24 mol% K_2CO_3-21 mol% $CaCO_3$. Humidified cathode gas (14% O-28% CO-58% N_2) was bubbled into the molten salts while the coupons were submerged in them.

The corrosion of Type 316L SS was significantly lower in the $CaCO_3$-containing electrolyte. Scanning electron microscopy showed the corrosion layer to be 60-μm thick in the 70 mol% Li_2CO_3-30 mol% K_2CO_3 electrolyte and 30-μm thick in the 55 mol% Li_2CO_3-24 mol% K_2CO_3-21 mol% $CaCO_3$ electrolyte. A similar electrolyte-dependent reduction in corrosion-layer thickness was observed for the Type 310 SS. In addition, the thickness of the corrosion layer on Type 310 SS was significantly lower than that for Type 316L SS. The corrosion-layer thickness on the Type 310 SS coupon was 40 μm for the 70 mol% Li_2CO_3-30 mol% K_2CO_3 electrolyte and about half that thickness for the $CaCO_3$-containing electrolyte.

A cell employing a standard NiO cathode was operated using the alternative electrolyte. The initial performance was only slightly inferior to that of the standard cell with 70 mol% Li_2CO_3-30 mol% K_2CO_3. However, the cell with the $CaCO_3$-containing electrolyte was unable to support current densities above 40 mA/cm^2 for extended periods of time. Measurements of the cell voltage vs. time at various current densities (80 to 200 mA/cm^2) suggested that concentration polarization may have affected both the cathode and the anode. The cell was terminated by rapid cooling while being polarized at a current density of 160 mA/cm^2. This procedure locked in concentration polarization effects. A post-test examination of the components showed that about half of the $CaCO_3$ had segregated to the anode. This suggests that, to avoid calcium-ion segregation, much lower $CaCO_3$ concentrations would be required. However, a lower concentration would not result in the desired reduction in the NiO solubility. Consequently, $CaCO_3$ additions are not considered to be practical. We will be testing other mixtures of alkali and alkaline earth carbonates in future work.

c. Modeling of Distributed Manifold Concept

A new MCFC stack design consisting of numerous inlet and exit manifolds distributed throughout the plane of the fuel cell has been proposed by M. A. Cobb & Co. This new design concept was claimed to be less expensive to fabricate and to be capable of higher power density. To more rigorously analyze the features of the design, we modeled it using thermodynamic and hydraulic principles and the overpotential relations developed by Wilemski et al.[19]

---

[19] G. Wilemski, N. H. Kemp, and A. Gelb, *Molten Carbonate Fuel Cell Performance Update, Final Report*, Department of Energy Report DOE/FE/15078-1742 (1985).

The model, as developed, was versatile enough to handle the complex flow patterns in the distributed-manifold concept as well as those in the more conventional designs where the anode and cathode flows run either parallel, counter, or cross (at right angles) to each other. This permitted the performance of MCFCs having either the conventional design or the new design to be evaluated on an equivalent basis.

The initial study focused on validating the model. For this purpose, a large fuel cell (1 x 1 m) with a cross-flow pattern of fuel and oxidant gases was analyzed using the new model and the cell parameters available from Wilemski et al.[19] The results of our study showed that the new model predicts the same general profiles of temperature and current densities as the previously used model.[19]

With this successful validation, it is now possible to use our model to calculate the various parameters of MCFCs operating with co-flow, cross flow, counter flow, and corner flow. The output of this modeling effort will be used to guide our research efforts associated with the distributed-manifold concept.

3. Polymer Electrolyte Fuel Cells

The goal of this effort is to advance the technology of power systems based on the polymer electrolyte fuel cell (PEFC). State-of-the-art PEFCs consist of a carbon-supported platinum anode for oxidation of the hydrogen fuel, an identical cathode for reduction of oxygen, and a polymer membrane for transport of hydrogen ions from the anode to the cathode. They are targeted for transportation applications where the hydrogen fuel would be produced by the reforming of alcohols.

a. Anode Development

The reforming process with state-of-the-art PEFCs leads to fuel containing substantial quantities of CO_2 and traces of CO impurity. Carbon dioxide and carbon monoxide both decrease the efficiency of the current platinum-based anode, causing degradation of the fuel cell's power output. We are addressing this problem by investigating alternative anode electrocatalysts to find an economical material that is less susceptible to poisoning by fuel impurities.

Platinum-based metal alloys are being evaluated for their potential use as PEFC anodes. The principle behind using a platinum alloy is to retain the high catalytic activity of platinum for the hydrogen oxidation reaction yet make the anode less conducive to the adsorption of impurities. Candidate alloys were first screened for catalytic activity in an environment which simulates the operating conditions of the PEFC. In these experiments, the alloys are exposed to CO-containing electrolyte only long enough to reach a platinum surface poisoning which is approximately equivalent to that experienced by a platinum anode operating on reformer output. The promising alloys are then incorporated into an actual PEFC. Next, a current pulse is applied to the anode material, and the resulting potential is measured as a function of time. This electrochemical technique allows separation of the reaction kinetics from other effects contributing to the measured potential. An Allen-Hickling plot can be constructed

by measuring the potential due to the reaction kinetics for a series of current pulses with differing magnitudes. The y-intercept of this plot yields the exchange current density or "kinetic facility" of the anode material for the hydrogen oxidation reaction. The material with a higher y-intercept (i.e., higher exchange current density) in the Allen-Hickling plot is the better catalyst for the reaction.

Figure I-7 shows the results of experiments comparing platinum and a platinum-based alloy for the kinetics of the hydrogen oxidation reaction with and without CO contamination. Comparing the y-intercepts of the plots, we see that platinum alone is a better anode material for a PEFC operating on pure hydrogen; however, with CO in the fuel stream, the alloy is a better material than platinum for the anode. This promising alloy is being incorporated into a PEFC, where its performance will be tested with hydrogen fuel and hydrogen contaminated with various amounts of CO.

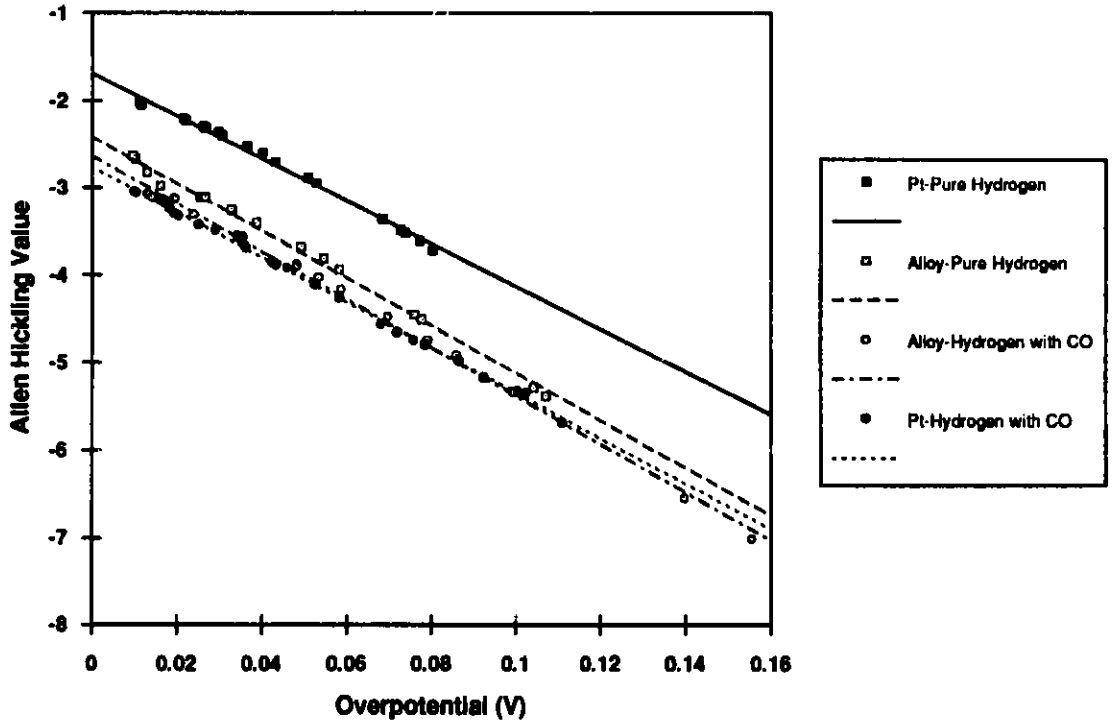

Fig. I-7. Allen-Hickling Plots for Hydrogen Oxidation on Platinum and Platinum-Based Alloy with and without Carbon Monoxide Impurity

b. Reformer Development

The objective of this work is to develop a reformer for the production of hydrogen from alcohols for PEFCs. Because of the weight and volume limitations for the transportation application, the reformer needs to use a highly active catalyst. Other desirable characteristics for the catalyst include high selectivity for hydrogen (little or no byproducts) and mechanical and thermal ruggedness. Hydrogen may be produced from alcohols by one of two

major processes: steam reforming, which is endothermic, and partial oxidation reforming, which is exothermic.

For the steam reforming of ethanol, we are investigating catalysts for the overall reaction:

$$C_2H_5OH + 3H_2O \rightarrow 2CO_2 + 6H_2 \quad (2)$$

Potential catalyst materials were screened using 200–500 mg of the material in a tubular reactor (6-mm OD) placed in a controlled-temperature furnace. The ethanol/water feed (water-to-ethanol molar ratio = 4:1) was first vaporized by passing it through a heated coiled tube, and then over the catalyst. The products were analyzed for H_2, CH_4, CO, CO_2, and CH_4 with a gas chromatograph.

A nickel-based catalyst was investigated in a low-temperature (250–450°C) and a high-temperature range (600–800°C). The reformate compositions obtained in the lower temperature range are shown in Fig. I-8a. Here, the reaction was dominated by ethanol dissociating into H_2, CO, and CH_4. With increasing temperatures, some of the CO was converted via the water gas shift reaction to H_2 and CO_2. The percentage of CH_4 in the product was quite high (20–35%). At temperatures above 600°C (Fig. I-8b), the H_2 concentration approached the theoretical 75%, and the CH_4 concentration dropped to <0.5%. A considerable amount of CO was formed, however. If this catalyst is used for steam-reforming ethanol, a water-gas shift converter will be needed after the reformer.

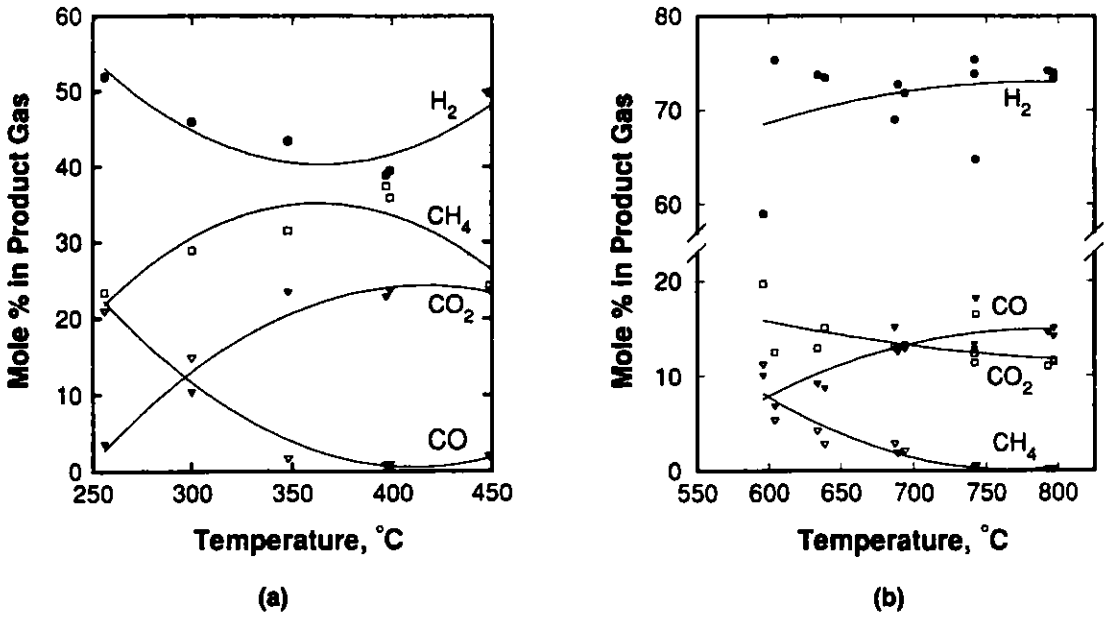

Fig. I-8. Product Gas Compositions Obtained with Nickel-Based Catalyst at (a) 250-450°C and (b) 600-800°C

For the partial oxidation of methanol, we are preparing to test a copper-based catalyst in a bench-scale reformer sized to provide sufficient hydrogen for a 10-kW(e) fuel cell. The catalyst was earlier tested in a microreactor and was found to provide the desired activity and selectivity for the overall reaction:

$$CH_3OH + \tfrac{1}{2}O_2 \rightarrow CO_2 + 2H_2 \qquad (3)$$

The reformer consists of a 5-cm-dia pipe packed with the catalyst pellets. In this down-flow reactor, a fine mist of methanol and water is sprayed at the top of the bed. A proportionate amount of air is also introduced into the reactor and carries the mist into the bed. An electrically heated ignition coil is located above the bed for startup purposes. The exothermic reaction provides the energy to vaporize the liquids and raise the catalyst to the 300–450°C reaction temperature for self-sustaining operation. Shake-down tests of the reformer are underway.

c. Systems Analysis

Propulsion systems based on the PEFC are being developed in the U.S. and other countries. We have conducted a system analysis to design improved PEFC systems, with particular emphasis on the engineering issues involved in integrating the fuel cell stack with the other system components. Systems design and analysis software developed at ANL was used to set up a reference system design and some variants for a methanol-fueled PEFC propulsion system. The reference system operates at an anode pressure of 2 atm and a cathode pressure of 3 atm; is based on published polarization curves; and includes a steam reformer for methanol, a two-stage air compressor, and an expansion turbine. A boost compressor raises the spent fuel gas from the anode pressure to the cathode pressure prior to burning with the spent air and expansion through the turbine.

Results of the simulation for the reference system showed that the system efficiency increases from 38.4% to 44.1% (expressed in terms of the lower heating value of methanol) as the cell current density is reduced from 750 to 450 mA/cm^2. The higher efficiency at the lower current density decreases the design loads for the main heat rejection radiator and the turbine exhaust cooler/condenser. However, to provide the same net power output of 80 kW(e), the active fuel cell area must increase from 18.8 to 27.3 m^2, with a proportional cost increase for the fuel cell stack.

In addition to the system design studies, some parametric studies were conducted to analyze the off-design performance of the reference system. In one such study, the air-moving equipment was assumed to maintain a constant efficiency of 75% as the net power output was decreased from 80 to 35 kW(e). The anode and cathode pressures were held constant at 2 and 3 atm, respectively, and the fuel and oxidant utilizations were held constant at 85% and 50%, respectively. With these assumptions, the average cell current density decreased from 750 to 300 mA/cm^2; the fuel cell efficiency increased from 52.6 to 64.7%; and the net system efficiency increased from 38.4 to 47.0%.

In another off-design study, considered more realistic, the anode and cathode pressures were permitted to float as the net system power was decreased from 80 to 11 kW(e). The fuel and oxidant utilizations were maintained constant at 85% and 50%, respectively. Under these conditions, the average cell current density decreased from 0.75 to 0.15 A/cm^2; the cathode pressure decreased from 3.0 to 2.0 atm; the anode pressure decreased from 2.0 to 1.0 atm; and the turbine inlet pressure decreased from 3.0 to 1.3 atm. In addition, the main air compressor efficiency decreased from 75.0 to 24.2%; the anode exit gas compressor efficiency decreased from 75.0 to 62.6%; and the turbine efficiency decreased from 75.0 to 51.0%. Figure I-9 shows the fuel cell stack and total system efficiencies for this simulation. While the fuel cell efficiency increased from 52.6 to 61.0% as the system power was decreased from 80 to 11 MW(e), the efficiency of the total system first increased from 38.4 to 39.6% down to a net system power of about 58 kW(e), and then decreased gradually to 26.8% at 11 kW(e). Future systems analysis will investigate use of hydrogen on board PEFC systems.

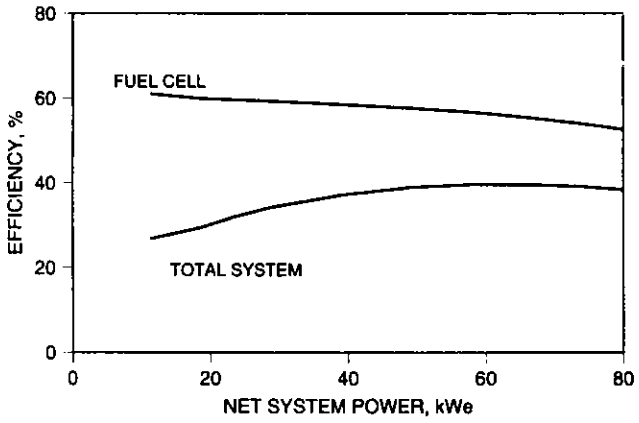

Fig. I-9.

Off-Design Efficiencies vs. Net System Power for Fuel Cell Stack and Total System

4. Management of Industrial Contracts

The CMT Division manages a DOE contract with General Motors Corp. (Allison Gas Turbine Division) for development of PEFCs. In 1993, General Motors completed the first phase of a three-year contract. Accomplishments included the following: showed proof-of-feasibility for methanol-fueled PEFCs as an electrochemical engine for automotive applications; built and tested a 10-kW PEFC system that integrated the fuel cell stacks, fuel processor system, and the system controls; and improved the PEFC membranes and electrodes, as well as the methanol fuel processing and control technologies. General Motors also completed a vehicle conceptual design study, which selected the minivan for initial demonstration. The projected performance for this vehicle was comparable to the internal combustion engine version but with twice the energy efficiency and nearly zero emissions. The Phase I success lays the groundwork for future scaleup and integration of a PEFC propulsion system into a vehicle. Phase II work toward this end is scheduled to begin in 1994.

The CMT Division also manages a DOE contract with Arthur D. Little (ADL) for developing systems that will reform ethanol and natural gas into hydrogen for use in transportation fuel cells and can be used for hydrogen storage on vehicles. This 30-month project is intended to provide fuel flexibility for fuel-cell powered vehicles, to reduce fuel processor size

and startup time, and to increase transient response capability. The outcome of this project, to be completed by November 1994, will be a prototype 10-kW reformer and a 1-kg hydrogen storage system for proof-of-concept.

The CMT Division, together with Georgetown University, manages the Fuel Cell Bus Project funded by DOE, the U.S. Department of Transportation, and California's South Coast Air Quality Management District. The objective of this project is to develop an urban transit bus powered by a methanol-fueled, phosphoric acid fuel cell. During 1993, H-Power Corp., the prime contractor, fabricated the structure and most major subsystems for the first bus, including the 50-kW phosphoric acid fuel cell. Component integration into the bus is well underway, with completion of the bus anticipated in early 1994. This bus will provide seating for 25 passengers, meet all of the performance requirements of the transit industry, provide air conditioning, and have a range of 240-320 km per tank of methanol. The bus will also meet the requirements of the Americans with Disabilities Act by providing a wheelchair lift and on-board accommodations for two wheelchairs. Two additional fuel cell buses will be built and tested during 1994.

On the fuel cell bus, batteries will be used to store energy recovered during bus braking and to provide short-duration power assist during acceleration. In support of the fuel cell bus project, we carried out testing at ANL on several lead-acid and Ni/Cd batteries identified as potential candidates for the fuel cell bus. The test results indicated that the Ni/Cd batteries met the bus requirements at lower battery weight and offered much greater life than lead/acid batteries. By the end of 1993, tests in the Analysis and Diagnostics Laboratory (Sec. I.B) had simulated over 9,000 h of fuel cell bus operation (equivalent to approximately 120,000 km) for the Ni/Cd battery, with little or no battery degradation.

In other related activities, we assisted DOE in preparing a ten-year plan for developing fuel cell vehicles (automobiles, vans, trucks, locomotives, and buses) and participated in the Fuel Cell Locomotive Task Force convened by California's South Coast Air Quality Management District. For the latter, we identified several viable options for a fuel-cell-powered locomotive using various types of fuel cells and fuels, and we formulated preliminary plans for a DOE program to build and demonstrate a fuel-cell powered locomotive.

II. FOSSIL FUEL RESEARCH

The Chemical Technology Division is the lead division for several projects in the ANL Fossil Fuel Program. These projects involve studies on fluidized-bed combustion and heat and seed recovery for open-cycle, coal-fired magnetohydrodynamic power generation.

A. *Fluidized-Bed Combustion Studies*

Fluidized-bed combustion involves a process in which coal is burned under atmospheric or pressurized conditions in a fluidized bed of limestone or dolomite, which reacts with most of the SO_2 released during combustion. The fluidized-bed combustion projects at CMT include (1) the evaluation of ceramic candle filters for the control of particulate emissions in the off-gas from a pressurized fluidized-bed combustor (PFBC), (2) the measurement of alkali vapor emissions in the off-gas from PFBC, and (3) the selection of non-alkali-adsorbing materials for high temperature service in PFBC and coal gasification systems.

1. Evaluation of Ceramic Candle Filters for Controlling PFBC Particulate Emissions

The Illinois Clean Coal Institute sponsored this study to promote the use of Illinois high-sulfur (3-5 wt%) coals. One of the potential applications of Illinois high-sulfur coal is as a fuel for a PFBC/gas-turbine combined-cycle system (GTCCS) for power generation. In PFBC/GTCCS, the entrained particulates in the PFBC off-gas need to be controlled to protect the gas turbine from corrosion and to meet the Environmental Protection Agency's New Source Performance Standards for particulate emissions. The objective of this effort was to evaluate the FIBROSIC™ candle filter (developed by Industrial Filter and Pump Manufacturing Co., Cicero, IL) as a hot-gas cleanup device for the PFBC/GTCCS. Compared with the more widely studied SiC ceramic candle filter, the FIBROSIC™ filter is lighter, less prone to thermal shock breakage, and less expensive, but has yet to be tested under PFBC off-gas conditions.

An Illinois No. 6 high-sulfur coal was combusted in our laboratory-scale (15.2-cm dia) PFBC facility to test the FIBROSIC™ candle filter for its particulate collection efficiency, permeability characteristics, and physical and mechanical strength. A SiC candle filter was also tested under the same PFBC conditions to obtain data for comparison. Results of this study showed that both filter types achieved particulate collection efficiencies >99.9% and exhibited comparable permeability characteristics. The latter finding is illustrated by Fig. II-1, which shows the pressure drop across the candle filters as a function of test duration. (The fluctuations in the curves are due to the sudden increase in pressure caused by reverse N_2-pulse cleaning of the filter.) Also, although the FIBROSIC™ filter has lower bursting and bending strengths than the SiC filter, these strengths are high enough to maintain the integrity of the FIBROSIC™ filter under PFBC conditions.

Because of the technical and economical benefits of the FIBROSIC™ filter over the SiC filter, longer duration (minimum of 50 h) testing at PFBC conditions is being pursued. This long-term testing will further evaluate the permeability characteristics and physical integrity of the filter element, determine the effect of dust loading in the PFBC off-gas on the filtration

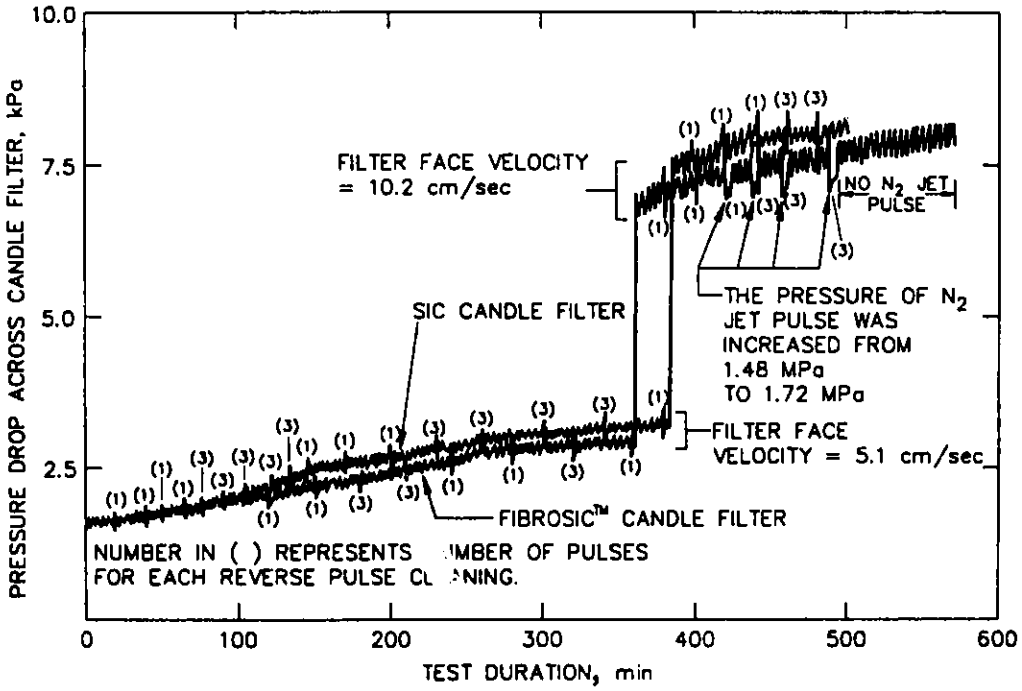

Fig. II-1. Pressure Drop for SiC and FIBROSIC™ Candle Filters during PFBC Testing

performance, and optimize filter operating parameters (such as jet pulse frequency, pressure, and duration) needed to achieve the maximum filtration performance.

2. Measurement of Alkali Vapor/Aerosol in PFBC Exhaust Gases

At the request of ABB Carbon, Sweden, we were contracted to measure the alkali vapor/aerosol in PFBC exhaust gases downstream of a hot gas filter assembly at the 15-MW(t) Component Test Facility (CTF) in Finspong, Sweden. The measurements were made as part of an International Energy Agency (IEA) project in which hot gas filters were tested and evaluated for commercial PFBC application.

The Na and K concentrations in the PFBC exhaust were measured by use of (1) the analytical alkali sorber bed (AASB) technique, which was developed in CMT,[1] and (2) an alkali and particulate sampling train (APST), which is a batch-type, grab-sampling condensation device. As part of this effort, we (1) designed and fabricated an AASB pressure vessel to interface with the exhaust ducts in the CTF, (2) purchased, assembled, and calibrated two downstream gas-conditioning and flow-control trains for use with the AASB and the APST sampling systems, and (3) measured alkalis in the CTF exhaust gas during two test campaign

[1] M. J. Steindler et al., *Chemical Technology Division Annual Technical Report, 1988*, Argonne National Laboratory Report ANL-89/15, pp. 44-46 (1988).

periods. The measurements were successfully completed, and the results analyzed and reported to ABB Carbon. (Because of the contractual agreement between ABB Carbon and ANL, the results of this work are ABB Carbon's proprietary data and, therefore, are not presented here.)

3. Selection of Non-Alkali-Adsorbing Materials for PFBC Components

The alkali metal compounds present in coal combustion off-gas are known to cause corrosion of fire-side boiler tubes at high temperature and pressure. They also have deleterious effects on many process components, such as valves, piping, filters, and separation membranes. Our earlier work[2] demonstrated that the accuracy of the real-time, on-line analyzers used for alkali measurements in PFBC off-gas is distorted because of the significant capture of alkali vapor by the stainless steel sampling line. A reliable measurement of alkalis (mainly Na and K) in PFBC off-gas is needed to evaluate the corrosivity of PFBC off-gas and the effectiveness of alkali control devices.

The objective of this work, which also involves the Energy Technology Division of ANL, is to identify metallic materials, if any, that do not adsorb alkali vapors and can be employed as alkali sampling lines and/or in process components in advanced coal utilization systems, e.g., direct coal-fired turbines, PFBC systems, and integrated gasification combined-cycle systems. More specifically, Fe-, Ni-, and Co-based alloys, as well as noble-metal-coated and ceramic-lined alloys, are being evaluated in a thermogravimetric analysis (TGA) apparatus for their extent of alkali-vapor capture under a simulated PFBC environment. After testing, the TGA-tested candidate materials are analyzed by scanning electron microscopy (SEM) coupled with energy-dispersive X-ray analysis (EDAX) and Auger electron spectroscopy (AES) to obtain a better understanding of the alkali adsorption mechanisms and behavior of the materials.

In the first phase of this study, TGA testing was completed to evaluate the following candidate materials: Type 304 stainless steel (304SS); Pt-, Au-, and Ag-coated 304SS; aluminized 304SS; Hastelloy C-276; Hastelloy X; and Haynes No. 188. Coupon specimens of candidate materials were exposed at 870-875°C and atmospheric pressure for 100 h in a simulated PFBC off-gas containing 3.1% O_2, 14.7% CO_2, 2.0% H_2O vapor, 880 ppm (by volume) SO_2, and the balance N_2. No alkali vapor was added in these baseline tests. During the test period, the weight change of the coupon specimens was continuously recorded. Except for the silver-coated 304SS, all coupon specimens showed a total weight gain caused by an oxide scale forming on the surface. The total weight loss observed for the silver-coated 304SS specimen was probably due to the oxide scale spalling off the surface during the test period.

The SEM/EDAX analyses of the tested coupon specimens showed that a fairly uniform 2-3 μm thickness of chromium oxide scale had formed on the surfaces of 304SS, Hastelloy X, and Haynes No. 188. The scale on the Hastelloy C-276 exhibited a ragged surface morphology with a number of cracks and voids. The oxide scale (thickness of 8-10 μm) contained

---

[2] S. H. D. Lee and E. L. Carls, *Measurement of Alkali Metal Vapors and Their Removal from a Pressurized Fluidized-Bed Combustion Process Stream, Annual Report for October 1986-September 1987*, Argonne National Laboratory Report ANL/FE-88-4 (1989).

Cr, Fe, and Ni. Apparently, the low concentration of chromium (15.5 wt%) in this alloy is not sufficient to form pure chromium oxide scale.

The noble-metal coating of 304SS was accomplished by sputter deposition of Pt, Au, or Ag to a thickness of ~1 μm. We found that the sputter deposition of the noble metals did not prevent outward diffusion of the substrate elements (Cr and/or Fe) in the base metal of 304SS and subsequent oxidation of these elements. The oxide scale (thickness of 2-3 μm) in the platinum-coated sample was almost pure chromium oxide, that in the gold-coated sample was (Cr, Fe) oxide, and that in the silver-coated sample was iron oxide.

The addition of aluminum to all grades of steel and stainless steel is known to improve their resistance to high-temperature sulfidation, oxidation, and carburization. A commonly known method to achieve this is an aluminizing technique. In this aluminizing technique, the steel or stainless steel is enclosed in a pack that contains Fe-Al powder, inert refractory powder, and a halide activator; the pack is heated to an elevated temperature (950-1000°C) for a length of time sufficient to allow the aluminum element to diffuse into the surface of the steel substrate (average depth of diffusion zone, 150-200 μm), producing an aluminum-rich alloy (not an aluminum coating) on the surface. In this study, the aluminized 304SS coupon specimen was pre-oxidized in a muffle furnace at 1000°C for 50 h in an air environment, forming an Al_2O_3 scale (>40 μm thickness) on the surface. This scale was intact after the 100-h exposure in the baseline PFBC environment.

For all candidate materials tested, no sulfur was detected in the scale or the substrate alloy after exposure to the baseline PFBC off-gas. Results of this study indicate that all candidate materials were subjected to only high-temperature oxidation, not sulfidation. The TGA testing of these candidate materials in a simulated PFBC off-gas containing 80 ppm (by weight) NaCl vapor is in progress. The extent of NaCl-vapor capture by these candidate materials will be evaluated by comparison with the baseline test results, and the most promising candidate material(s) will be recommended for further testing in an actual PFBC environment.

B. *Magnetohydrodynamic (MHD) Studies*

Open-cycle MHD is an advanced technology with the potential to improve substantially the electrical efficiency of coal-fired power plants and to reduce their environmental impact. In the coal-fired concept of MHD, an easily ionized seed material (usually a potassium salt) is injected into a high-temperature, slag-rejecting coal combustor. The resulting electrically conductive combustion gas then flows through a high-velocity channel in the presence of a strong magnetic field. An electrical potential develops across electrodes in contact with the gas stream in the channel walls and produces an electrical current. The fuel-rich combustion gas leaves the MHD topping cycle at approximately 2027°C (2300 K) and enters a bottoming cycle that is similar in function to the steam bottoming cycle of a conventional coal-fired power plant. However, the MHD steam plant must not only extract heat from the combustion gas to produce high-pressure steam, but also recover the seed material separately from the ash for reuse, preheat the primary combustion air to at least 727°C (1000 K), lower nitrous oxide emissions to acceptable levels, and inject secondary air to complete combustion of the fuel. The Chemical Technology Division is the lead ANL division in a multidivisional project that is directed toward

developing the technology required for the heat and seed recovery in an MHD plant. Other divisions working on the program are the Energy Technology Division (materials studies) and the Energy Systems Division (modeling and systems analysis).

Materials evaluation studies continued this past year in support of the MHD bottoming cycle. Candidate heat exchanger materials were tested in the Coal-Fired Flow Facility (CFFF), which simulates the MHD bottoming cycle and is operated for DOE by the University of Tennessee Space Institute. For these tests, tube specimens of candidate heat exchanger materials were exposed to a flowing MHD combustion gas after secondary air injection at metal temperatures of 370-720°C. The specimens were placed at 30.5-cm (1-ft) intervals along 4.3-m (14-ft) lengths of U-bend tubes. After these specimens had undergone testing for up to 2000 h, we examined them by X-ray diffraction and wet chemical analyses to evaluate their corrosion performance (as determined by corrosion-scale morphologies and scale thicknesses). Among the materials tested, Type 310 stainless steel exhibited the least corrosion attack (Fig. II-2), while Types 304 and 316 stainless steel exhibited severe degradation (Fig. II-3). (In these figures, the "leading edge" refers to the surface of the tube that the flowing combustion gas first contacts; the "trailing edge" refers to the surface that this gas contacts last.) The alloy 253MA exhibited intermediate corrosion performance. The corrosion-product layers were porous and offered little protection to the underlying alloy. As a result, selection of an alloy for long-term application in MHD balance-of-plant service will be dictated by the extent of grain-boundary oxidation/sulfidation of the base alloy.

The DOE MHD program is scheduled to be closed out in 1994. The ANL work will conclude with the publication of a topical report on the materials evaluation work discussed above.

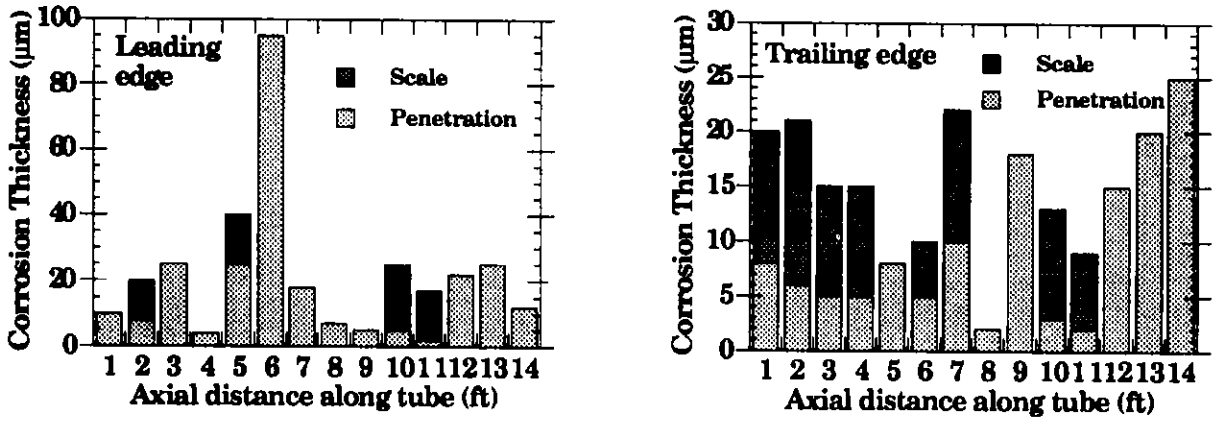

Fig. II-2. Corrosion Thicknesses for Leading and Trailing Edge of Type 310 Stainless Steel Tube after 2000-h Exposure in Superheater Test Section of CFFF (average specimen metal temperatures ~ 370 to 670°C)

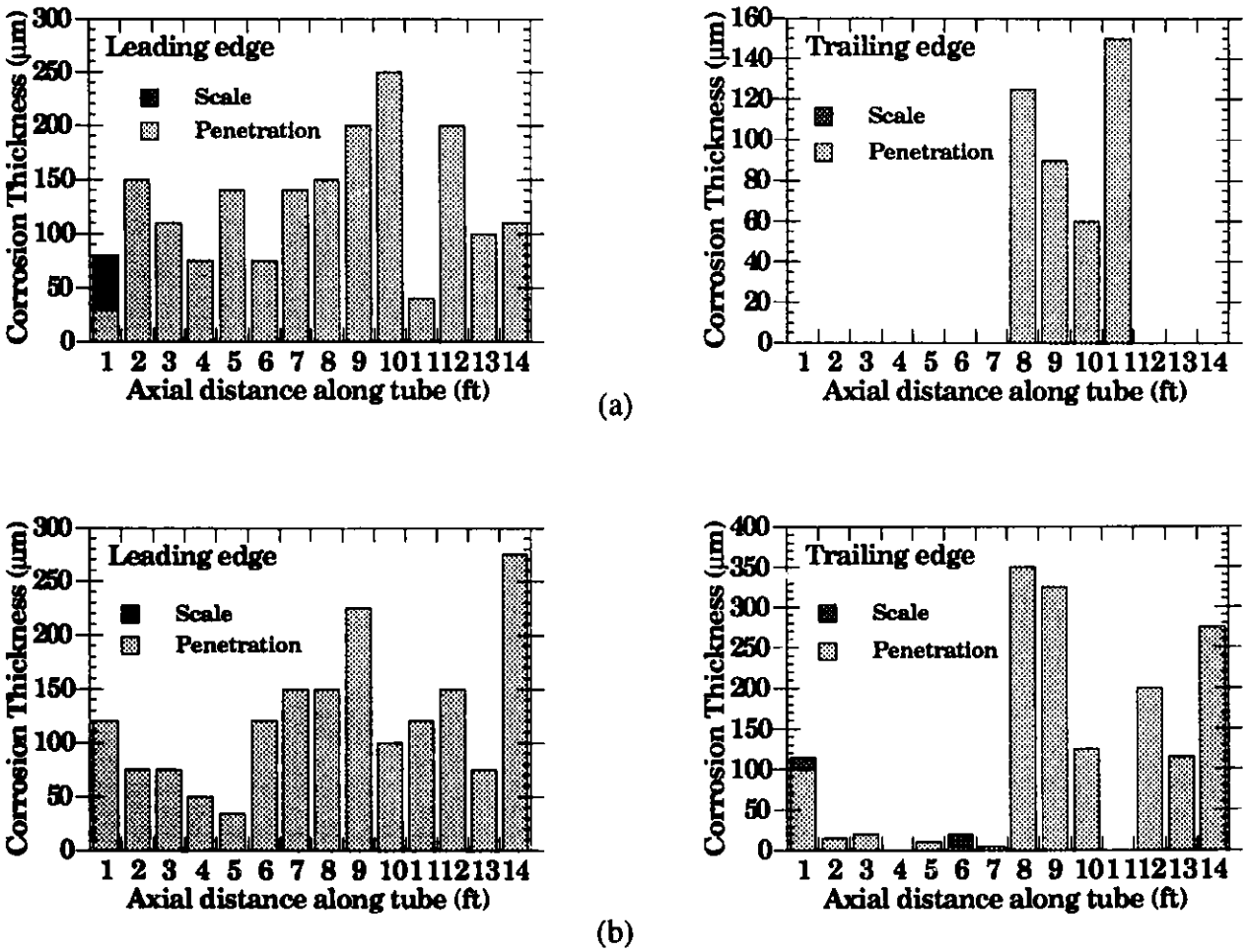

Fig. II-3. Corrosion Thicknesses of Leading and Trailing Edge for Tubes of (a) Type 304 and (b) Type 316 Stainless Steel after 2000-h Exposure in Superheater Test Section of CFFF (average specimen metal temperatures ≈ 440 to 720°C)

III. HAZARDOUS WASTE RESEARCH

Over 40 years of nuclear-defense production and other activities at DOE sites such as Hanford, Oak Ridge, and Savannah River have produced a massive quantity of hazardous and mixed hazardous/radioactive waste. This waste contains radionuclides, heavy metals, organic compounds, and many other regulated hazardous compounds. It is in a variety of forms, including soils, solid radioactive waste, supernatant liquids, slurries, salt cakes, and sludges. One of the current missions of DOE is the cleanup of these wastes. It is anticipated that this mission will last over 30 years and will cost hundreds of billions of dollars. To help accomplish this mission, we are participating in a variety of projects aimed at developing new or advanced technologies for treating and disposing of this waste. We are also experimentally investigating actinide speciation in groundwater-relevant systems and radiolytic gas generation from transuranic-containing waste buried underground.

A. *Aqueous Biphasic Separation Process*

The aqueous biphasic separation (ABS) process involves the selective partitioning of ultrafine particles or solutes between two immiscible aqueous phases.[1,2] We are examining a number of possible applications for this separation technology, including solid waste treatment, soil remediation, high-level liquid waste treatment, and industrial waste treatment.

1. Actinide Recovery from Solid Wastes

The objective of this project is to develop the ABS process for selectively separating submicron-size particles and to explore its possible application to the treatment of solid radioactive wastes being stored throughout the DOE sites. A flowsheet for treating these solid wastes would include wet grinding of the solids to an average particle size of about 1 μm to liberate refractory PuO_2 and selective partitioning of the particles between two immiscible aqueous phases, followed by solid/liquid separation and recycle of the aqueous phases. The goal is to recover the majority of the actinides in a concentrate that is only 1-5% of the initial waste volume.

The biphase systems that we have been working with are generated by combining aqueous solutions of low-molecular-weight polyethylene glycol (PEG) or polypropylene glycol (PPG) and aqueous salt solutions, such as $(NH_4)_2SO_4$, Na_2SO_4, or Na_2CO_3. We also use water-soluble metal complexants to selectively extract the actinide-bearing particles to the polymer-containing phase. Our earlier tests with model systems using parts-per-million concentrations of the complexant chlorophosphonazo III demonstrated that the ABS process is capable of extracting monomeric Pu(IV), polymeric Pu(IV), and micron-size PuO_2 into the PEG-rich phase with high partition coefficients (>100).[2]

---

[1] D. J. Chaiko, R. Mensah-Biney, C. J. Mertz, and A. N. Rollins, *Actinide Recovery Using Aqueous Biphase Extraction: Initial Development Studies*, Argonne National Laboratory Report ANL-92/36 (1992).

[2] D. J. Chaiko, R. Mensah-Biney, C. J. Mertz, and A. N. Rollins, *Sep. Sci. Technol.* **28**, 765 (1993).

During 1993, we conducted test-tube-scale extraction studies using actual plutonium residues. We obtained samples of incinerator ash and ash heels from Rocky Flats Plant and Los Alamos National Laboratory, SSC (sand, slag, and crucible) metallurgical residues from the Hanford site, and LECO crucibles from Savannah River Laboratory. Aqueous slurries of the residues were ground in a vibratory mill to an average particle size of less than 1 μm. Representative partition coefficients for particulate plutonium in the residue samples are shown in Fig. III-1 as a function of extractant concentration. Increasing the extractant concentration leads to an increased adsorption density of chlorophosphonazo III at the plutonium/water interface. This causes the particle surfaces to become increasingly hydrophobic, which, in turn, increases particle partitioning to the PEG-rich phase. With selective extractant adsorption, plutonium-containing particles can be recovered in the PEG phase, while non-plutonium-containing particles remain in the salt phase. The data in Fig. III-1 reflect partitioning of particulate plutonium species only. There were negligible amounts of dissolved plutonium, as determined by analyzing the aqueous phases after filtration at 0.02 μm.

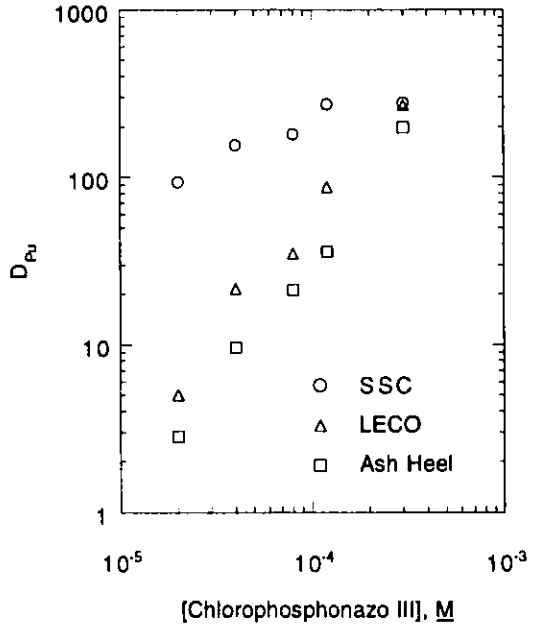

Fig. III-1.

Extraction of Plutonium from Various Waste Residues Using a PEG/$(NH_4)_2SO_4$ Biphasic System (D_{Pu} = partition coefficient for particulate plutonium)

Other studies involved the optimization of biphase composition. Extraction studies revealed that the choice of salt used in forming the biphase had a strong influence on plutonium partition coefficients. The best extraction behavior was obtained with biphase systems containing $(NH_4)_2SO_4$, as opposed to Na_2SO_4 or Na_2CO_3. We also initiated plutonium liberation studies, in which plutonium residues were ground and analyzed by scanning electron microscopy (SEM). Difficulties with immobilizing aqueous slurries in epoxy resins for SEM analysis have slowed progress. Nevertheless, we plan to complete particle liberation/characterization studies in 1994. We are also preparing to conduct continuous countercurrent extraction tests with ground plutonium residues and a Karr extraction column (1-m high).

2. Treatment of Uranium-Contaminated Soils

The ABS process is being evaluated for the removal of uranium from contaminated soil, such as that at the DOE Defense Production Facility in Fernald, Ohio. The goal is to selectively remove ultrafine particulate uranium from soil to below regulatory cleanup limits. The ABS process is an alternative to conventional soil-washing techniques that are based on physical separation methods, such as screening, classification, and flotation. Because of its ability to separate ultrafine particles, the ABS process is ideal for remediating high-clay-content soils. The upper limit on the size of soil particles that can be accommodated in the biphase system appears to be about 50 μm.

The laboratory tests that we have conducted to date used two soil samples provided by DOE's Fernald Environmental Management Project. One of the samples was collected near a waste storage area of the Fernald site, and the other was collected near its waste incinerator. The large amount of silt (particle sizes of 3 to 53 μm) and clay (<2 μm) in the soil makes treatment by conventional soil-washing techniques difficult. On the other hand, the fact that over 80 wt% of the soil is <45 μm particles makes this soil a good candidate for biphasic extraction.

During 1993, we conducted test-tube-scale experiments that used up to 1 g of soil per test. All of the biphasic systems used PEG in combination with an inorganic salt phase (sodium carbonate, potassium carbonate, sodium sulfate, or sodium hexametaphosphate). Initial results showed that the ABS process is capable of selectively extracting and concentrating uranium from the soil collected near the incinerator at Fernald. Uranium concentrations were reduced from 500-600 mg/kg, to about 90 mg/kg, and in certain cases, the uranium concentration was reduced to about 15 mg/kg. However, the soil sample that was collected from around the storage area did not respond as well to biphasic extraction. With this sample, the uranium concentration was reduced to only ~200 mg/kg, and there was no evidence of selective uranium partitioning.

Selective flocculation of the soil particles occurred in all of the biphasic extraction systems that we studied. Work with model systems suggests that this is not a problem with regard to solid/solid separation, and even aids in solid/liquid separation. We have done extraction tests with particles as small as 20 nm and obtained good solid/liquid separation with only mild centrifugation.

During 1993, we also conducted some initial scaleup tests using uncontaminated clay feeds at the pilot-plant facilities of Otto H. York Co., in Houston, Texas. During those tests we fed ~70 g of clay per hour into a Karr column (2.54-cm ID and 3.6-m high) with countercurrent feed solutions of 30% PEG and 20% Na_2CO_3. The success of these tests was demonstrated by the ability of the column to handle feed slurry with less than 1 vol% of other-phase carryover in the overflow and underflow from the column. We anticipate that a full-scale column would achieve a solids throughput of ~600 to 1200 kg/h. Our estimate of operating costs for soil remediation using the ABS process is approximately $25 to $50 per ton, which is considerably less than the costs of $1,000 or more per ton for excavation and burial of contaminated soils in approved landfill sites. We are now installing a pilot-scale column at ANL and will be conducting scaleup tests with Fernald soil during 1994.

3. Partitioning Systems for Waste Pretreatment

In a collaborative effort with Northern Illinois University, we are developing aqueous biphasic systems for the selective extraction of long-lived radionuclides, such as ^{99}Tc, ^{129}I, and ^{75}Se, from caustic high-level liquid waste. During 1993, we began to examine the ability of PEGs to selectively extract iodide and pertechnetate (TcO_4^-) from simulated supernatants in the underground storage tanks at the DOE Hanford site. This effort is based on the observation that TcO_4^- and I^- are selectively extracted from aqueous caustic solutions into an immiscible aqueous PEG layer.

Because of the high ionic strengths of supernatant liquids in Hanford underground storage tanks, aqueous biphasic systems can be generated by simply adding aqueous PEG solutions directly to the waste solution. Preliminary work has shown that aqueous biphasic systems generated by salting out PEGs are capable of extracting nearly all of the technetium as TcO_4^- into the PEG-rich phase. Partition coefficients as high as 600 have been obtained for pertechnetate in carbonate/PEG biphasic systems. Our work with Hanford tank waste simulants has also shown that the partition coefficients for a wide range of inorganic cations and anions, such as sodium, potassium, aluminum, nitrate, nitrite, and carbonate, are all less than one.

In this effort, we have been working with three tank waste simulants: neutralized current acid waste, single-shell-tank supernatant, and Hanford 101-SY supernatant. For all these simulants, the extraction of pertechnetate using aqueous PEG solutions was rapid. Representative single-stage separation factors obtained for separating pertechnetate from various anions are given in Table III-1. In general, the separation factors between pertechnetate and multivalent anions are greater than those between pertechnetate and monovalent anions. The best separation is obtained between TcO_4^- and CO_3^{2-}. The separation factors for pertechnetate and nitrate/nitrite are substantially lower; nevertheless, with multistage, countercurrent extraction, it should be possible to achieve technetium decontamination factors well above 10^3.

Table III-1. Separation Factors Obtained for Pertechnetate Extracted from Synthetic Waste Solutions Using PEG-3400 at 50°C

Ionic Species	Separation Factor
F^-	171
NO_3^-	79
NO_2^-	147
SO_4^{2-}	600
CO_3^{2-}	26,500
PO_4^{3-}	>700

We have also collected pertechnetate partition data at 25 and 50°C with fresh PEG and with PEG solutions gamma irradiated at dose levels of 14-75 Mrad. (For example, a one-year equivalent dose for processing supernatant solutions from tank 101-SY wastes is estimated to be approximately 5 Mrad.) Neither irradiation dose nor temperature significantly affected the partition coefficients of the pertechnetate.

Work is now underway to measure the extraction behavior of iodine and selenium. We will also be evaluating various options for the back extraction of radionuclides from polymer phases. The most direct approach involves the use of electrodialysis for stripping all ions from the polymer phase. Another approach involves the use of immobilized PEGs.

4. Biocatalytic Destruction of Nitrate

Work has recently begun on biocatalytic destruction of nitrate in an aqueous biphasic system. The presence of high nitrate and nitrite concentrations, on the order of 4 M, in many DOE mixed-waste streams complicates decisions regarding final waste forms and disposal options. For low-level waste, it is anticipated that most of this waste will be disposed by near-surface grouting. Grout formulations must be developed to minimize the leachability of nitrate so that nitrate levels in the surrounding groundwater will not exceed regulatory standards. High-level waste will probably be vitrified in high-temperature processes to generate a ceramic-glass waste form. During the vitrification process, nitrate may be converted to volatile nitrogen oxide compounds, which will require off-gas treatment facilities. These issues can be resolved if the nitrate is destroyed before generation of the final waste form.

We have thus started a project to develop and demonstrate an enzyme-based technology for the reduction of nitrate and nitrite to elemental nitrogen and water. The reduction of nitrate is carried out using purified nitrate, nitrite, and nitrous oxide reductase enzymes. The use of enzymes enables very large specific catalytic activity to be obtained without the need for additional chemical reagents or the production of secondary waste streams. An aqueous biphasic system, consisting of a salt-rich aqueous phase and a PEG-rich aqueous phase, is used to protect the enzymes and to facilitate nitrate/nitrite separation from the primary waste stream. In this system, the enzyme will be restricted to the PEG phase, which protects the enzymes from denaturation owing to the lower ionic strength of this phase. Nitrate and nitrite anions will preferentially partition from the salt-rich phase to the PEG phase, whereas the radionuclides present will remain in the salt-rich phase. A schematic of a proposed reactor process is shown in Fig. III-2.

Currently, we are performing screening experiments to identify the best electron-transfer dye for shuttling reducing equivalents from the cathode to the enzyme. Subsequent research will be directed toward identifying the most appropriate method that will immobilize the enzyme, building a small bench-scale reactor, and demonstrating this technology on a surrogate mixed-waste sample.

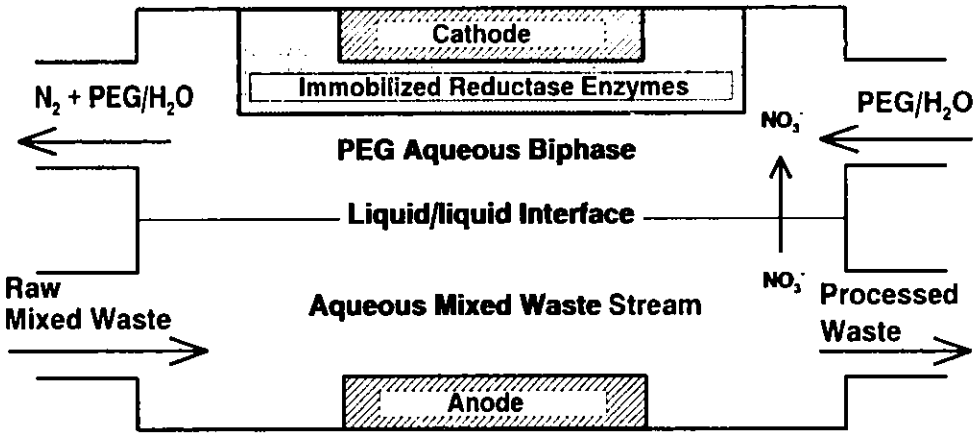

Fig. III-2. Schematic of Proposed Biocatalytic Reactor

B. *Electrokinetic Remediation of Soils*

The use of silica gel barriers to significantly reduce the migration of contaminants, such as radionuclides, heavy metals, and hazardous organic compounds, through soil subsurface has attracted much interest for environmental remediation and waste management operations. Among the attractive properties of silica gel barriers are: (1) the chemical reagents that yield the barrier are liquids, (2) once gelation occurs, the permeability of soils can be reduced by several orders of magnitude, and (3) the barriers are environmentally benign.

Silica gel barriers are formed by destabilizing a colloidal silica sol by two steps: lowering the pH and increasing the salt concentration. This process results in siloxane cross-linkage. Hydraulic pumping is the standard method used to inject the sol mixture into the soil. One potential disadvantage of hydraulic pumping is that the solution preferentially flows through the larger pore diameters since the hydraulic head is inversely proportional to the pore radius. As a result, use of hydraulic pumping may require a number of cycles of injecting the sol solution, allowing gelation to occur, then reinjecting the sol solution to seal pathways of successively smaller pore diameter. Another disadvantage of hydraulic pumping is that it is difficult to control the flow of the sol solutions in the soil.

We are investigating the use of electrokinetic processing as an alternative method of injecting the sol solutions into the soil. Electrokinetic processing for gel barrier emplacement involves taking advantage of the electromigration and electroosmosis that occur when an electric gradient is superimposed across electrodes placed in a soil-groundwater system. Unlike hydraulic pumping, the electroosmotic equivalent of the pressure head is independent of the pore radius; thus, electroosmotic flow occurs in all pores with equal probability.[3] By controlling the location and spacing of the electrodes, one can control the transport of both the charged silica colloids

[3] L. Casagrande, *Boston Soc. Civ. Eng.* **69**, 255-273 (1951).

and the cations through the soil. In electrokinetics processing, colloidal silica sol is loaded into the cathode reservoir and sodium chloride into the anode reservoir. The electric gradient causes the silica colloids and sodium cations to migrate in a countercurrent direction. In preliminary experiments using a bench-scale electrokinetics test cell designed by Lehigh University,[4] we used electrokinetics processing to transport the necessary chemical reagents for gel formation into saturated kaolinite or sandy soils. In a typical experiment, we placed 10 wt% of a commercial colloidal silica solution in the cathode reservoir and a 0.01 N NaCl solution in the anode. The cell was loaded with either a saturated sand or kaolinite soil sample. A 30-V potential was maintained across the cell at ambient temperature for various periods ranging up to 14 days. After processing, the volumetric flow of water across the soil sample was measured by hydraulic pumping at 14 and 35 kPa.

For the sandy soil, the permeability of the soil was greatly reduced after gelation using electrokinetic processing, as shown in Fig. III-3. Microscopic examination of these samples after

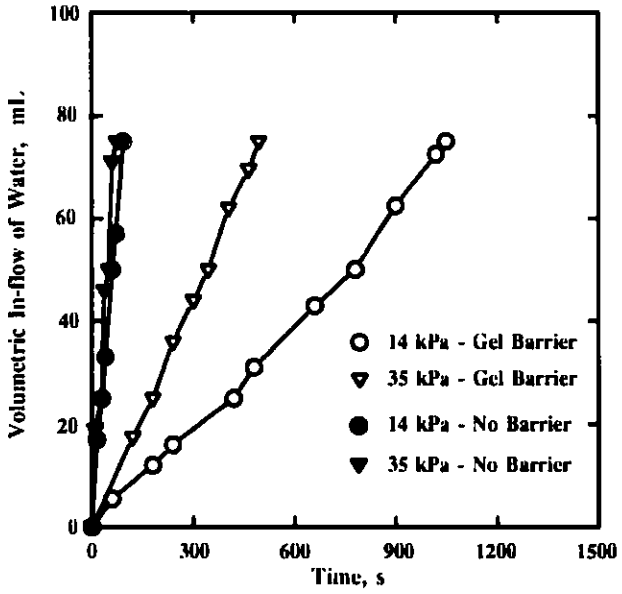

Fig. III-3.

Volumetric Flow of Water in Sandy Soil Samples before and after Gel Formation Using Electrokinetic Processing

hydraulic pumping showed evidence of cementing of the sand particles, confirming the formation of a gel barrier. For kaolinite soil, the permeability of the soil increased after electrokinetic processing, as shown in Fig. III-4. There was no evidence that the kaolinite particles were cemented, as was the case for the sandy soil. During the pumping, silica gel fibers were observed being extruded from the kaolinite sample, which formed low-resistance channels for groundwater flow. Further tests are underway to attempt to cement the kaolinite particles and thereby decrease the overall permeability of this soil. Future work also includes determining the optimal processing times and conditions for maximum reduction of soil permeability and constructing a larger test apparatus that simulates field conditions more closely than our present apparatus.

---

[4] J. E. Battles et al., *Chemical Technology Division Annual Technical Report, 1992*, Argonne National Laboratory Report ANL-93/17, p. 63 (1993).

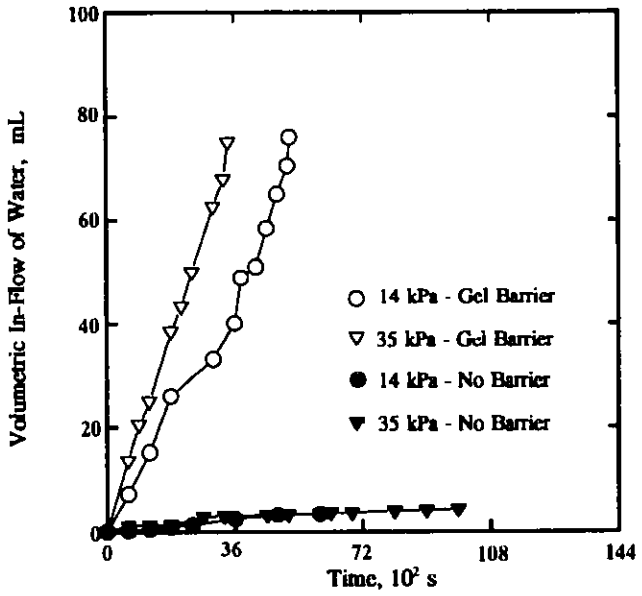

Fig. III-4.

Volumetric Flow of Water in Kaolinite Soil Samples before and after Gel Formation Using Electrokinetic Processing

C. *Actinide Speciation in Groundwater*

Efforts were continued to investigate the speciation (i.e., complexation, oxidation state, and aggregation) of radionuclides under conditions relevant to subsurface groundwaters on DOE lands. The current focus of the work is the environmental chemistry of plutonium-organic mixtures in the presence of microbes, inorganic substrates, and metal cations. Actinide speciation is determined by high-sensitivity laser spectroscopic methods, as well as more conventional methods (absorption spectrometry and alpha scintillation counting). In connection with this work, collaborations were initiated with Pacific Northwest Laboratory (PNL), Brookhaven National Laboratory (BNL), and Lawrence Berkeley Laboratory (LBL).

The interaction of Pu(VI) with citric acid was investigated as a function of ligand-to-metal ratio (from 1:1 to 100:1) and pH (2 to 10) at room temperature. At low ligand-to-metal ratios (<10:1), citrate reduced Pu(VI) to form a stable Pu(IV) complex. This reaction became faster with increasing pH. Typical results (for pH = 1.8) are shown in Fig. III-5. The reaction of citrate with the plutonium initially formed a Pu(VI)-citrate complex (absorption band at 638 nm). This complex was unstable. After about one month, only 10% of the Pu(VI) remained, with the plutonium distributed about equally between a Pu(V)-aquo/Pu(V)-citrate complex and a Pu(IV)-citrate complex. After about two months, only the Pu(IV)-citrate complex was present. In the absence of citrate under similar conditions, a Pu(V/VI) mixture with aquo species is evident after two months. At ligand-to-metal ratios of approximately 100:1, however, no reduction of Pu(VI) was evident even at near-neutral pH. This suggests that multi-ligand complexation of the Pu(VI) stabilized the oxidation state. Further work is planned to establish the nature of the reduction process and more clearly determine the tie between the complex formed and redox stability.

In the collaborative work with BNL, the degradation of the plutonium-citrate complex by a *Pseudomonas* strain microbe was studied (room temperature, ligand-to-metal ratio of 100:1,

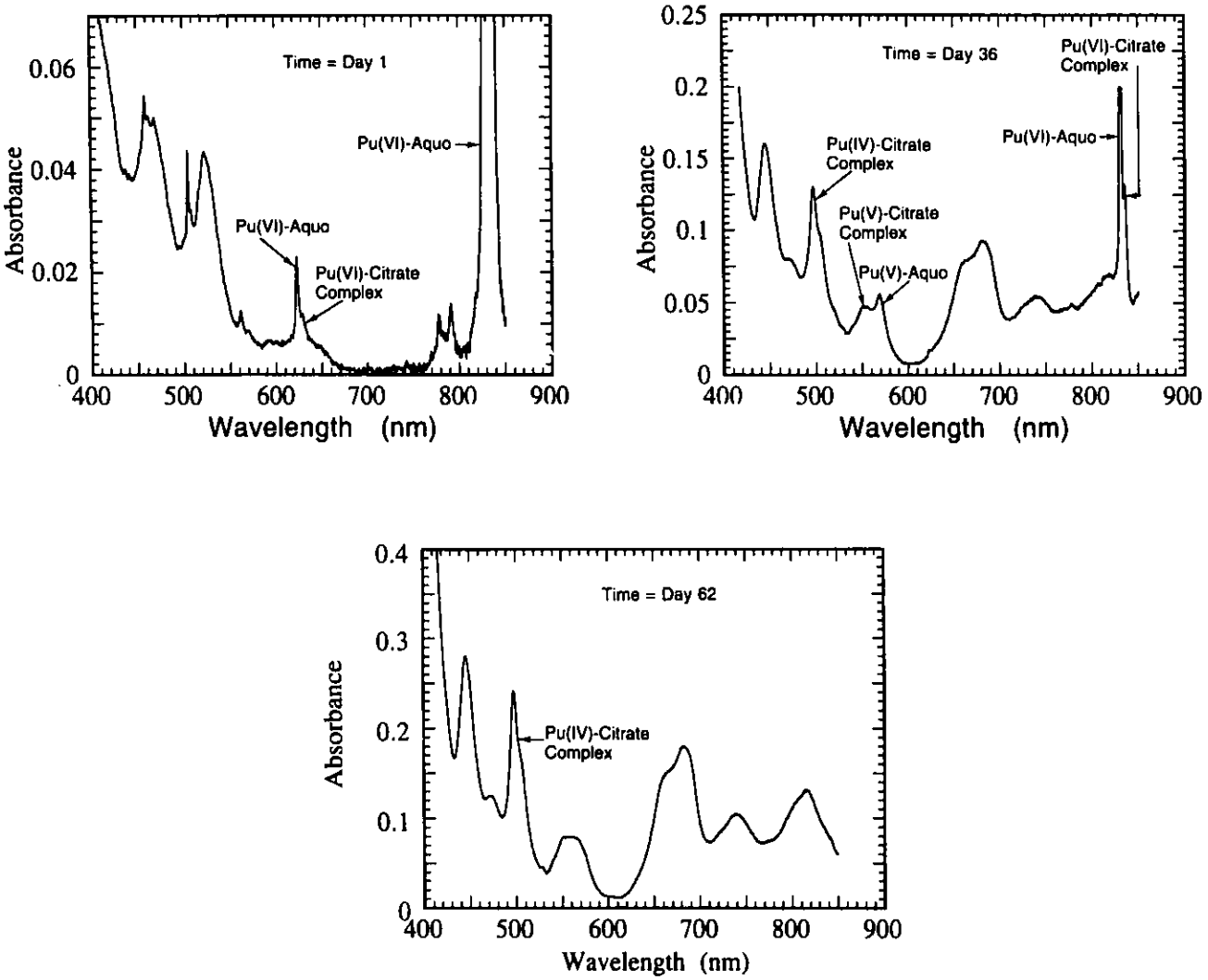

Fig. III-5. Absorption Spectra Showing Reduction of Pu(VI) by Citrate at pH = 1.8, Room Temperature, and Reaction Times of 1, 36, and 62 Days

and total plutonium concentration of 2 x 10^{-4} M in PIPES buffer* at pH = 6.2). Here, a stable Pu(IV)-citrate complex was observed that was not biotically reduced or oxidized over a period of two months. Approximately 20% of the plutonium initially present in solution was associated with the microbe. Degradation of the citrate was not extensive when plutonium was present.

In collaboration with PNL and LBL, we also investigated degradation of the Pu(IV)-nitrilotriacetic acid (NTA) complex by the *Pseudomonas* strain microbe. Experiments were done at very low Pu(IV) concentrations (<10^{-5} M) in the presence of 10^{-3} M NTA in PIPES buffer solution at pH = 6-7 and room temperature. The presence of a Pu-NTA complex did not prevent conversion of the NTA to carbon dioxide, but it did slightly lower (10-20%) the rate of

*PIPES buffer is 1,4-piperazinebis(ethane-sulfonic acid).

conversion. Because of promising preliminary results, more extensive work on this system is planned.

Solubility studies were also initiated to investigate the interaction of plutonium with phosphate in aqueous solutions (pH = 2-10) at 25°C. Samples were taken over a period of four months and passed through 50- and 200-nm filters. Alpha scintillation counting and spectroscopy were used to establish the speciation and plutonium concentration in solution. The solubilities of the Pu(VI)-phosphate species were found to be higher than expected, typically in the range of 10^{-5} to 10^{-6} M. We had some difficulty in interpreting the results because of the presence of easily solubilized colloidal material. Precipitation was also noted at pH > 3, and efforts are underway to determine the composition of the solids formed. Spectroscopically, four distinct absorption bands between 800 and 900 nm were associated with the presence of phosphate in solution. These are likely associated with the various conjugate acids of phosphate that are present as the pH is changed. These will be spectroscopically characterized to determine the formation constants for the various complexes.

D. *Radiolytic Effects Studies for Waste Isolation Pilot Plant*

Work has continued to investigate the effects of ionizing radiation on gas production in environments similar to those expected in the Waste Isolation Pilot Plant (WIPP), which is DOE's proposed long-term transuranic (TRU) waste storage facility. This work is part of an overall effort, coordinated through Sandia National Laboratories (SNL), to help evaluate the long-term performance of WIPP for the disposal of TRU waste. Ionizing radiation will be present in the WIPP primarily as alpha particles due to the radioactive decay of the transuranics present in the waste. The objective of this effort is to evaluate the effects of the interaction of these alpha particles with WIPP wastes and the anticipated environment on factors important in assessing the long-term performance of the WIPP.

Three technical issues, related to the presence of ionizing radiation, were identified as potentially important to WIPP performance assessment: (1) the generation of gases due to the interaction of alpha particles with WIPP wastes and brine, with particular emphasis on the speciation of dissolved transuranics, (2) the general effect of radiolysis on the redox conditions in the site, and (3) radiolytically induced conversion of presumably non-biodegradable plastics to those that are biodegradable. Current research emphasis is on the first two issues.

With regard to the first issue, our previous work on gas generation in plutonium-spiked WIPP brine had shown that hydrogen was the predominant radiolytic product at low absorbed dose (≤10 Mrad).[5] In experiments conducted during this report period, ^{238}Pu at a concentration of 10^{-4} M in WIPP brine was used to extend prior work to higher absorbed doses (up to 200 times greater). This was done to measure the yield of oxygen, which is predicted to be a significant product only at high absorbed dose. As expected, oxygen was produced at absorbed doses greater than 10 Mrad. The ratio of hydrogen to oxygen, however, remained approximately

---

[5] J. E. Battles et al., *Chemical Technology Division Annual Technical Report, 1992*, Argonne National Laboratory Report ANL-93/17, pp. 67-68 (1993).

4:1 rather than the 2:1 ratio expected at long times (4-8 months). The implication to the WIPP project is that low levels of oxygen will likely be sustained in the WIPP over long times and not completely depleted as previously thought.

In research related to the second issue, we are irradiating selected plastic (polyethylene and polyvinylchloride) and rubber materials (hypalon and neoprene) with alpha particles in environments important to the WIPP and characterizing the overall effect of alpha particle degradation on the materials. The plastic is typical of materials used in packaging TRU waste at Rocky Flats Plant, and the rubber is typical of glove material used in glovebox and radioactive waste cleanup operations. The biodegradation studies, using the plastics that we irradiated, will be performed at Brookhaven National Laboratory.

The alpha-irradiation experiments were conducted for two months with the plastic and rubber materials in either an air or nitrogen atmosphere at 30°C and an initial relative humidity of 70%. The dose rate to the sample surface was 2×10^5 rad/h. The gas phase was periodically sampled and analyzed by gas chromatography. The composition of the organic compounds generated, along with their yields, was determined to help evaluate the effect of ionizing radiation on the long-term WIPP performance.

The radiolytic degradation and alteration of various plastic and rubber materials have been extensively studied by others.[6,7] The predominant gaseous products are hydrogen, carbon oxides, and hydrogen chloride (chlorine-containing organics). Although it is generally recognized that organic species are being generated, the radiolytic production of volatile organic compounds (VOCs) has been largely ignored in past studies. Our irradiation of WIPP plastic and rubber materials caused the materials to degrade and react with the gas phase present and generated hydrogen, carbon oxides, and VOCs. The extent to which this occurred depended on the material and the gas phase present.

We found that hydrogen yields, expressed in terms of G values (molecules per 100 eV absorbed dose), were comparable to those observed in gamma- and beta-irradiation studies performed earlier.[8] Carbon dioxide was generated in the air and nitrogen atmospheres with all four materials. Yields were comparable to, but greater than, those of hydrogen for all but polyethylene in the nitrogen atmosphere. Total radiolytic yields observed for both hydrogen and carbon dioxide were low relative to the potential for gas generation in corrosion and microbial processes.

We also observed wide diversity of VOCs, including alkenes, alkanes, alcohols, ketones, benzene derivatives, and nitro compounds. These VOCs were generated by a combination of direct interactions of ionizing radiation with the materials being irradiated and secondary reactions in the gas phase once the VOCs had been generated. In general, the presence of oxygen

---

[6] M. Dole and D. M. Dodily, *Adv. Chem. Series* **66**, 31 (1967).

[7] S. T. Kosiewicz, *Nucl. Tech.* **54**, 92 (1981).

[8] D. T. Reed, J. C. Hoh, J. W. Emery, and D. Hobbs, "Radiolytic Gas Production in the Alpha Particle Degradation of Plastics," Proc. of Waste Management '92 Conf., Tucson, AZ, March 1-5, 1992, pp. 1081-1086 (1992).

greatly increased the extent and diversity of the VOC products observed. This follows given the importance of oxygen in the free radical and ionic reactions that define net radiolytic degradation in both the material matrix and the gas phase.

The generation of VOCs does not appear to be important from the perspective of the total gas generation in the WIPP. Total yields were lower than those observed for hydrogen and carbon oxides. Volatile organics may, however, remain of interest to the WIPP in attaining regulatory compliance since a number of them that we detected are compounds listed as hazardous in the Resource Conservation and Recovery Act. These include halogenated hydrocarbons (chorine-containing organics), ketones, aldehydes, benzene, and some nitro compounds. Further evaluation of these results relative to WIPP is the subject of ongoing studies.

E. *Office of Waste Management*

The Office of Waste Management in CMT is assisting DOE in maintaining a national program of applied R&D in environmental restoration and waste management. The objective of the applied R&D is to improve the efficiency, safety, and timeliness of environmental cleanup activities so that DOE can meet the 30-year environmental compliance and cleanup goals for its facilities.

Effort in the past year focused on providing technical and management support to the Minimum Additive Waste Stabilization (MAWS) Program and the Hazardous Substance Research Center (HSRC) Program. The latter is co-funded by DOE and the Environmental Protection Agency (EPA).

1. Minimum Additive Waste Stabilization (MAWS) Program

The objective of the MAWS Program is to develop a process for separating hazardous from non-hazardous components of waste and thereby minimize the amount required for vitrification. This program also strives for integration of unit processes, where the effluent stream from one process is the resource for the next. For example, the contaminated fraction from washing of contaminated soil would contain both the waste that must be encapsulated and the silica needed to make glass in the vitrification step.

Vitrification is the center of the MAWS technology, which is applicable for a large variety of DOE wastes, such as soils, tank wastes, sludge pits, ashes, asbestos, and transite. Preliminary surveys have indicated that such DOE sites as Hanford, Savannah River, Rocky Flats, Oak Ridge, and Fernald are potential candidates for this technology. Indeed, there is growing interest in the MAWS concept because of waste minimization, reduced costs, and the stable nature of glass waste forms.

We support the MAWS Program in several areas: (1) contract administration and monitoring, (2) evaluation of waste form performance and test development, and (3) evaluation of the efficacy of extending the desirable vitrified waste forms to include glassy slag for waste streams with high metal content. Key accomplishments in the MAWS Program to date include the following:

- Radioactive wastes (uranium-contaminated soils) have been vitrified in a 10-kg/day melter. High levels of hydrogen fluoride in the off-gas have been effectively treated, with up to a fivefold volume reduction. The radioactive glass produced in the 10-kg/day melter passed a standard leaching test (Toxicity Characteristic Leaching Protocol) and compared favorably with the high-level waste glass from an initial glass characterization. Long-term durability testing of the radioactive glass has been initiated, and preliminary results appear favorable.

- A 100-kg/day melter and off-gas system have been constructed at the Catholic University of America, Vitreous State Laboratory, and successfully operated with both simulated and radioactive wastes.

- A laboratory-scale water treatment system has been installed and successfully operated in washing tests with uranium-contaminated soil. Results from these tests indicated a reduction in uranium concentration from an average of 600 pCi/g to less than 35 pCi/g and a volume reduction of greater than 80%. These tests produced radioactive soil concentrates for vitrification. A soil washing demonstration unit has been installed and tested by Lockheed Environmental under subcontract to GTS Duratek Corp. In the next year, 76 m^3 of contaminated soil will be processed in this unit.

- A 300-kg/day MAWS demonstration system has been installed and tested at the DOE Fernald site. All components (melter, feed system, gem maker, and off-gas system) have been fine-tuned and are working well. The "hot" startup, operation, and demonstration of this system are planned for next year.

2. Hazardous Substance Research Center (HSRC) Program

Through a memorandum of understanding, DOE and EPA are co-sponsoring research at five HSRCs. These centers are located in different regions of the country, with each center covering two federal EPA regions. Each center is located at a main participant university but consists of a consortium of several universities in the region. These centers are the Northeast (NE) HSRC, Great Lakes and Mid-Atlantic (GLMA) HSRC, South/Southwest (S/SW) HSRC, the Great Plains/Rocky Mountain (GPRM) HSRC, and the Western Region (WR) HSRC. The basic mission of the HSRCs is to study all aspects of the management of hazardous substances and waste.

Currently, DOE is co-funding 21 research projects (6 in NE, 4 in GLMA, 2 in S/SW, 4 in GPRM, and 5 in WR). Several projects involve study of microbial degradation of contaminants. Other projects involve use of a radon-222 method for locating non-aqueous liquids in the subsurface, modeling of contaminant plumes in the subsurface, use of electric purging for removing heavy metals and mixed wastes from soil, development of hollow-fiber membranes for metal recovery in waste, and development of nano-scale metal oxides as reagents for destruction and immobilization of hazardous substances. During 1993, the NE HSRC received 16 new research proposals and the GPRM HSRC, 24 new proposals. These have been reviewed by an

Argonne Review Panel to determine which ones should be recommended to DOE Headquarters for funding.

A number of technologies developed through the HSRC Program are in the demonstration stage or close to it. A brief description of two technologies is given here as illustrative examples.

One project co-funded by DOE over the past three years, at the New Jersey Institute of Technology, has developed pneumatic fracturing technology for removing volatile organic compounds from clay, siltstone, and sandstone formations. Several demonstrations of the technology have been completed in New Jersey under EPA programs for the removal of trichloroethylene, and the removal was enhanced by a factor of six over remediation efforts in the pre-fracture environment. The DOE funded a major demonstration of the technology in 1993 at Tinker Air Force Base in Oklahoma. Enhanced recovery of fuel oil and chlorinated solvents was confirmed, and DOE is evaluating an application of the technology at the Portsmouth Gaseous Diffusion Plant.

In another HSRC project, Tufts University is developing an electrochemical sensor for heavy metals in groundwater. The objective is to develop a sensor for real-time, *in situ* measurement of environmentally significant heavy metals in surface or groundwater at concentrations ranging from high parts per million to low parts per billion. In Phase I (1991-92) of this project, the researchers successfully constructed and tested the electroanalytical component of the sensor, an iridium-based ultramicroelectrode, and showed that it was capable of measuring heavy metal ions such as lead and cadmium, over a wide concentration range, in various model and natural water systems. In collaboration with Stanford University's Integrated Systems Center, workers at Tufts University then designed and fabricated a prototype sensor and showed it to have the required analytical sensitivity, reproducibility, and stability. During the past year (first half of Phase II), the researchers assembled a prototype instrument that consisted of an array sensor operating with an external potentiostat and extensively evaluated its electroanalytical operation and its quantitative analytical capabilities with natural water samples. The performance results appear very promising, and only minor modifications will be required for the final version of the sensor. The final sensor will be thoroughly tested in the laboratory, and the results compared with conventional methods. Field testing is expected to follow soon after that.

IV. NUCLEAR WASTE PROGRAMS

Work is being performed to support the development of a high-level nuclear waste (HLW) repository located in an unsaturated environment, similar to that expected for the candidate site at Yucca Mountain in southwestern Nevada. The performances of HLW glass and spent fuel under typical repository conditions are being determined in long-term laboratory tests. In a new program area, the technology of HLW glass is being extended to the immobilization of low-level wastes, including the incorporation of high-metal-content wastes in two-phase (glass and crystalline) slags. Our work to characterize the radioactive phases in uranium-contaminated soils is continuing.

A. *Preparation of Review Documents*

During the past year, a final draft of "High-Level Nuclear Waste Borosilicate Glass: A Compendium of Characteristics" was completed. It is intended to be a concise presentation of the worldwide information on the alteration of nuclear glass waste forms during storage and geologic disposal. A key objective of this document is to gain a scientifically sound understanding of waste-glass alteration processes and radionuclide release mechanisms over very long time periods. This document was prepared by assembling and integrating contributions from authors at ANL, Westinghouse Savannah River Co., Lawrence Livermore National Laboratory, and Battelle Pacific Northwest Laboratory. The document has undergone extensive internal reviews and formal external reviews by representatives from the University of New Mexico, Catholic University of America, and Battelle Pacific Northwest Laboratory.

As an outgrowth of this effort, critical reviews of the literature on nuclear waste glass performance are being prepared and will be issued in 1994. These include reports on the effects of radiation, the ratio of glass surface area to solution volume (SA/V), glass composition, and unsaturated conditions; testing of radioactive vs. nonradioactive glass; and modeling of glass performance. Summaries of the data obtained at ANL on each of these topics will be included with the critical reviews. Together with the Compendium, these documents will provide a sound data base to support the qualification of nuclear waste glass for geologic disposal.

B. *Testing of High-Level Waste Glass and Spent Fuel*

Tests are being performed to determine the behavior of HLW glass and spent oxide fuel upon exposure to liquid water or water vapor. Laboratory test conditions simulate alterations in the repository environment caused by the emplaced wastes, such as the effects of elevated temperature and radiation. A battery of sophisticated techniques is used to analyze the corrosion layers formed on the waste forms. The tests are designed to provide data for validating models being developed to predict long-term performance of nuclear waste forms. The work on glass performance supports DOE's Environmental Restoration and Waste Management in evaluating the glasses expected to be produced by the Defense Waste Processing Facility (DWPF) and West Valley Demonstration Project (WVDP). The spent fuel tests, as well as the glass tests, are being done to support the Yucca Mountain Site Characterization Project (YMP) in evaluating the suitability of these waste forms.

1. Effect of SA/V Ratio

Static leach tests, such as the standard test of the Materials Characterization Center and the Product Consistency Test, are being used by researchers to measure the durabilities of borosilicate glasses that may be employed in the vitrification of high-level waste. An important test variable in these static leach tests is the SA/V ratio, which mainly affects the glass reaction through dilution of the reaction products. Since the glass reaction rate depends on the solution chemistry (particularly the silicic acid concentration and the pH),[1] the response of a glass may differ in tests at different SA/V ratios because of the difference in dilution; both the dominant reaction step and the measured rate of glass reaction may change as the SA/V ratio is varied.

The objective of this CMT effort is to assess the effects of the SA/V ratio used in static leach testing on the mechanism and rate of the glass reaction. Tests are designed to monitor changes in both the leachate composition and the reacted glass surface as a function of the SA/V ratio, the reaction time, and the initial leachant composition. The results of these tests will provide insight regarding how tests performed at different SA/V ratios are related, if the SA/V ratio can be used as an accelerating parameter for static leach tests, how the SA/V ratio influences the secondary phase assemblage, and what the long-term glass reaction rate is.

Static leaching tests at SA/V = 10, 340, 2000, and 20,000 m^{-1} and T = 90°C have been in progress for up to 1000 days. The simulated (nonradioactive) HLW glass compositions are representative of the waste forms to be produced by the DWPF and were prepared from SRL 131 and SRL 202 glass provided by Westinghouse Savannah River Company (WSRC). The leachate solutions and reacted glasses are periodically analyzed during testing to compare the mechanisms and kinetics of the glass reaction at the different SA/V ratios.

The glass corrosion process can be illustrated by the evolution of the leachate concentrations of major glass components, including uranium, alkali metals, boron, and silicon, as the corrosion proceeds. These data are plotted in Fig. IV-1 for tests conducted with the SRL 202 glass at 2000 m^{-1}. The concentrations have been normalized to the amount of each element in the original glass. These results show the alkali metals and boron to be released from the glass to a greater extent than silicon and uranium through about 100 days, but the release of all elements occurs at a similar rate beyond about 100 days. The initial difference in release rates is due to differences in the hydrolysis rates of the different bonds. As the solution chemistry evolves, the release rates of all glass components become controlled by the release of silicic acid. These tests reflect the first two stages of the glass corrosion process: during the initial stage, corrosion is not affected by the solution chemistry, and during the next stage, the corrosion becomes controlled by the effect of the solution chemistry on the release of silicic acid. As the solution concentration of silicic acid increases, the glass corrosion rate decreases.

---

[1] B. Grambow, "Geochemical Approach to Glass Dissolution," in *Corrosion of Glass, Ceramics and Ceramic Superconductors. Principles, Testing, Characterization and Applications*, eds., D. E. Clark and B. K. Zoitos, Noyes Publications, Park Ridge, NJ, pp. 124-152 (1992).

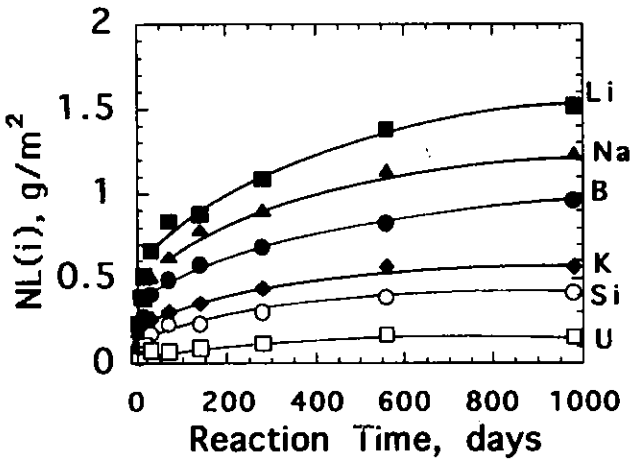

Fig. IV-1.

Normalized Elemental Mass Loss [NL(i)] vs. Reaction Time for Tests with SRL 202 Glass at SA/V = 2000 m^{-1}

For the same glass in tests at 20,000 m^{-1}, the glass corrosion is similar to that in tests at 2000 m^{-1} for the first 180 days in that the release rate of all species is initially high but decreases with the reaction time. However, as shown in Fig. IV-2, beyond 180 days, the boron and alkali metal release is significantly greater than the silicon and uranium release. The increased release rate for the boron and alkali metals occurs simultaneously with the formation of various secondary phases, including zeolites and other silicate phases. Because silicon is incorporated into secondary phases, the silicon solution concentration increases only slightly beyond 180 days. The increased release rate for the boron and alkalis is interpreted to signify a third stage in the corrosion process, where secondary phase formation affects the solution chemistry, which then affects the glass corrosion rate. For SRL 202 glass reacted at 20,000 m^{-1}, the initial rate (after three days) is about 0.04 g/(m^2·day), based on the boron release. The rate decreases to about 0.0025 g/(m^2·day) after 180 days, and then increases to about 0.03 g/(m^2·day) beyond 180 days. Thus, tests run for less than about 180 days underestimate the long-term corrosion rate by a factor of about 10. Our test results have been successfully simulated using a reaction affinity model, which accounts for the influence of the silicic acid solution concentration and the pH on the glass corrosion rate.[2] Work is in progress to better understand the relevance of fitting parameters used in the model.

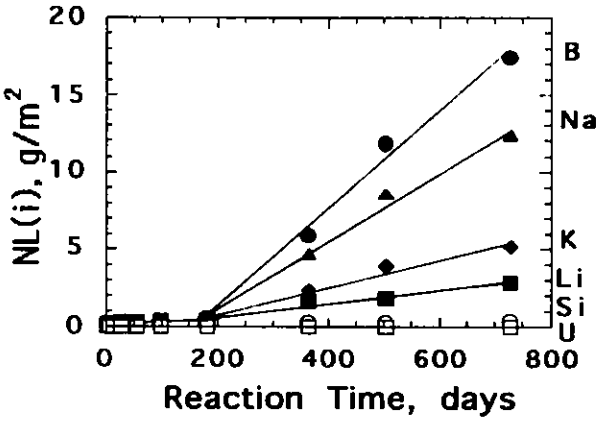

Fig. IV-2.

Normalized Elemental Mass Loss [NL(i)] vs. Reaction Time for Tests with SRL 202 Glass at SA/V = 20,000 m^{-1}

[2] W. L. Bourcier, W. L. Ebert, and X. Feng, *Mat. Res. Soc. Symp. Proc.* **294**, 577-582 (1993).

In summary, these tests clearly show that a laboratory test with a single SA/V ratio cannot be used to assess the long-term corrosion behavior of HLW glasses. Instead, a suite of tests is being developed to better characterize the glass corrosion behavior for use in projecting the long-term glass durabilities. Also, the observed increase in the corrosion rate has important consequences regarding the long-term stability of HLW glasses and must be better understood. Work is in progress to identify the secondary phases that control the solution chemistry and the mechanism through which the corrosion rate is increased. The major objective is to determine if the accelerated corrosion is common to all waste glasses, if it is a transient phenomenon, and how the glass composition affects the long-term stability.

2. Effect of Radioactive Glass

Most testing to evaluate the performance of HLW glasses has been done using simulated nonradioactive analogues of the same general composition as the radioactive glass. To apply the knowledge gained in those studies to a fully radioactive production glass, we have to demonstrate that the simulated glass experiments yield results equivalent to experiments with fully radioactive glasses. Thus, long-term tests on fully radioactive glasses are being performed to compare the reaction of simulated and fully radioactive glasses and to collect long-term data on glass performance under conditions that may exist in an unsaturated environment. Because an unsaturated repository environment has a range of glass/water contact scenarios, three different types of tests are being performed: static immersion tests using three compositions of waste glass, drip tests using as-cast and pre-aged glass, and a laboratory analogue test (that simulates reactions in a tuff-rock environment) using as-cast and pre-aged glass.

a. Static Tests

The difference in the reactivity of simulated nonradioactive (S) and fully radioactive (R) glasses is being investigated as part of a long-term testing program with three nuclear waste glass compositions (SRL 131, 165, and 200).[3] Results to date indicate little difference in leach trends for both simulated and radioactive glasses in 90°C static tests at SA/V of 340 and 2000 m^{-1} for time periods up to 980 days. The basis for these observations was given in last year's report,[4] and the data trends have remained the same. The data suggest that both radioactive and simulated glasses of the same base composition generally follow the same reaction-controlling processes. The relative glass durability observed for the simulated glasses is 165S > 131S > 200S; the same order of glass durability is preserved for the fully radioactive glasses. The solution pH's are usually lower for the tests with the fully radioactive glass than the simulated glass because of the radiolysis-induced formation of nitrogen-related acids and other acids in the leachates. This reduction in the solution pH's of the radioactive glasses, combined with the rate-controlling processes, can explain the observed minor differences in leach behavior between radioactive and simulated glasses at 340 and 2000 m^{-1}, where the radioactive glass reacts

---

[3] J. K. Bates, W. L. Ebert, X. Feng, and W. L. Bourcier, *J. Nucl. Mater.* **190**, 198-227 (1992).

[4] J. E. Battles et al., *Chemical Technology Division Annual Technical Report, 1992*, Argonne National Laboratory Report ANL-93/17, pp. 73-76 (1993).

slightly less than the corresponding simulated glass for both 131- and 200-type glasses but slightly more for 165-type glasses.

For tests with SA/V = 20,000 m^{-1}, we observed a large difference in reactivity (up to a factor of 1000 in the corrosion rate of boron) between 200R and 200S within one year (Fig. IV-3). Particularly noteworthy is that the 200S glass exhibits a high corrosion rate between 182 and 360 days [1145 mg/(m^2·day) for boron], which is associated with the formation of crystalline phases, such as a clinoptilolite, and a slight rise in pH (Fig. IV-3e). Corrosion beyond 360 days occurs at a lower rate. The fully radioactive glass does not show this behavior. The radiation field generated by the fully radioactive glass maintains a lower solution pH, which prevents secondary phase formation and the resulting increase in the reaction rate. These results suggest that 200-type radioactive glass may be more durable than the corresponding simulated glass if the leachate pH of the former remains lower than that of the latter. In modeling the performances of glass, all factors that influence glass reaction (such as the radiation-induced pH reduction in the leachate) must be accounted for to make adequate long-term predictions. Thus, meaningful comparison of tests between radioactive and simulated nuclear waste glasses should include long-term and high-SA/V tests.

b. Drip Tests

It is likely that, in an unsaturated environment, the initial contact between glass and liquid water will be through slow ingress of dripping water. The Unsaturated Test Method[5] has been developed to evaluate glass performance under this condition, and this test method has been applied to 200R glass that is as-cast or pre-aged by reacting the glass in a water vapor environment. During the pre-aging process, the glass is reacted, but since no flowing liquid water is present, the reaction products remain associated with the glass. This pre-aged glass is then contacted by dripping water to evaluate whether the aging process will affect the radionuclide release response.

A series of drip tests has been ongoing for about 27 months. The tests are performed in a continuous mode, where every six months the test vessel is opened, the glass sample transferred to a new vessel, and the test is continued. The leachate in the original test vessel is then analyzed to evaluate the extent of glass reaction and the distribution of radionuclides in solution. Some tests are also performed in a batch mode whereby, after a one-year period, the test is terminated, and both the solution and glass samples are examined.

To date, the following observations have been made from the test results: (1) the leachates from the pre-aged radioactive glass (see Table IV-1) are concentrated in cations (mainly Li, Na, and B) and anions (SO_4^{2-}, PO_4^{3-}, and Cl^-) after 180 days, but then the concentrations decrease with time; (2) the release of actinides from the pre-aged glass is considerably greater than from the as-cast glass but has also been decreasing with time; (3) for the pre-aged glass tests, a significant fraction of the Pu and Cm is dissolved in solution, whereas in the as-cast

---

[5] J. K. Bates and T. J. Gerding, *One-Year Results of the NNWSI Unsaturated Test Procedure: SRL 165 Glass Application*, Argonne National Laboratory Report ANL-85-41 (1986).

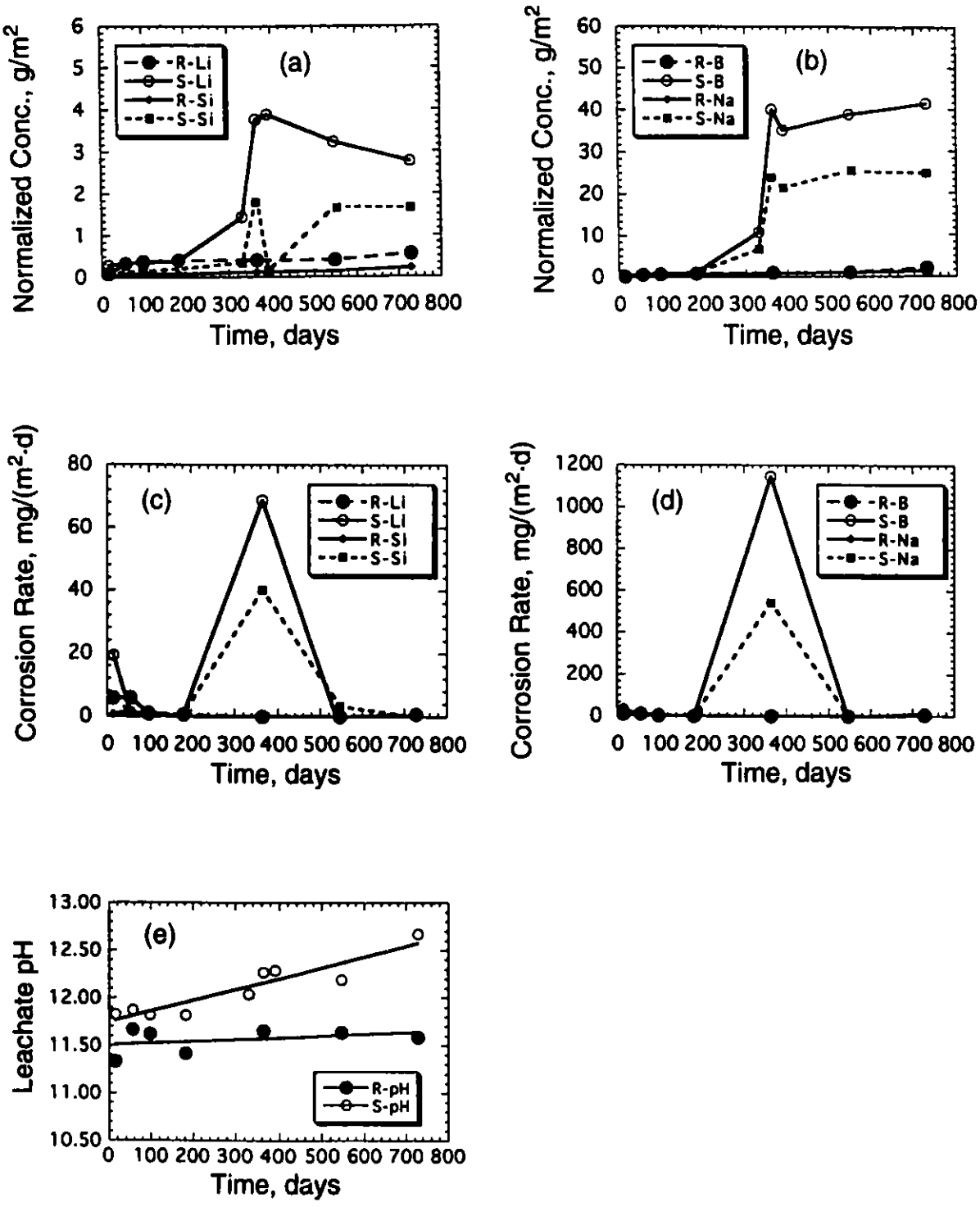

Fig. IV-3. Corrosion Behavior of SRL 200R and SRL 200S Glasses at SA/V of 20,000 m^{-1}: (a) Normalized Concentrations of Li and Si, (b) Normalized Concentrations of B and Na, (c) Normalized Corrosion Rates of Li and Si, (d) Normalized Corrosion Rates of B and Na, and (e) Leachate pH. In these figures, R = fully radioactive and S = simulated (nonradioactive) glass.

glass tests, these actinides are associated with colloidal material; and (4) many colloidal phases have been identified in solution from tests of both glass types. The increased solubility inferred from the results for the pre-aged glass is due to the high anion concentrations (between 200 and 8000 ppm), which promote the formation of stable actinide-bearing complexes. This test series is still in progress, and more specific release trends will become available after several more sampling periods.

Table IV-1. Solution Composition from Drip Tests Done with Fully Radioactive SRL 200R Glass after 180 days. Test conditions were 90°C with a water contact rate of 0.075 mL every 3.5 days.

	Concentration, ppm	
Elements	As-Cast Glass	Aged Glass
Li	10	1000
B	10	20,000
Na	100	40,000
Si	50	1500
Cl^-	9	200
SO_4^{2-}	100	8000
PO_4^{2-}	0	400

c. Laboratory Analogue Tests

In the laboratory analogue test that simulates reactions in a tuff-rock environment,[6] monoliths of as-cast and pre-aged glass (200R) are placed inside a hollowed-out tuff rock core, and very slow water flow is forced through the core. In these tests, an unsaturated environment is maintained, meaning that the hollowed-out section of tuff does not become filled with water, but instead a high-humidity dripping/condensation condition exists. The solution that passes through the tuff core is collected and analyzed for radioactivity. Two analogue tests have been ongoing for about 24 months. In both cases, no measurable radioactivity has been detected in the test solutions, indicating that any radioactivity released from the glass has not been transported through the rock.

[6] J. K. Bates, T. A. Abrajano, D. J. Wronkiewicz, T. J. Gerding, and C. A. Seils, *Strategy for Experimental Validation of Waste Package Performance Assessment*, Argonne National Laboratory Report ANL-90/21 (1990).

d. Future Progress

The static and drip tests will be continued, as tests are scheduled to last through eight years. Data generated from solution analyses will be combined with surface layer studies to compare more completely the reactivity of the radioactive and simulated waste glasses and to provide a data base for validation of glass performance models.

3. Glass Testing for an Unsaturated Repository

The current reference design[7] for the Yucca Mountain site calls for spent nuclear fuel from commercial reactors and HLW glass to be contained in an engineered barrier system that is surrounded by the natural host rock. Ideally, this multiple barrier system (waste form, engineered barrier system, rock) will limit radionuclide release from the waste material. In addition, radionuclide migration will be retarded due to chemical and physical interactions with the rock.

Long-term tests to simulate glass performance are in progress with actinide-doped glasses representative of the DWPF and WVDP. The test method[5] involves dripping water onto a cylindrically shaped glass-metal assemblage that is suspended in an enclosed test vessel at 90°C. The water that collects in the bottom of the test vessel provides information regarding (1) the identity of any radionuclides that are released from the glass and their release rates and (2) synergistic effects that occur in the glass-metal-water system. The tests have been ongoing 91 months for the DWPF glass and 72 months for the WVDP glass, and preliminary results have been given previously.[8] During the past year, we have continued these tests, but no new sampling or analysis of the solution has been performed. In the upcoming year, solutions from both tests will be sampled and analyzed, and we anticipate that enough extra solution will be available to conduct a test using tuff rock from the repository horizon to evaluate the performance of tuff as a backfill material.

4. Spent Fuel Testing

This multiple barrier system in the current reference design for the repository at the Yucca Mountain site limits the radionuclide release from spent nuclear fuel (irradiated UO_2). Long-term tests with both unirradiated UO_2 and spent fuel samples are in progress to determine the behavior and radionuclide release characteristics of spent fuel under the unsaturated conditions expected at the Yucca Mountain site.

---

[7] U.S. Department of Energy, *Site Characterization Plan: Yucca Mountain Site, Nevada Research and Development Area, Nevada*, DOE-RW-1099, 7 Vols., Office of Civilian Radioactive Waste Management, Washington, DC (1988).

[8] M. J. Steindler et al., *Chemical Technology Division Annual Technical Report, 1991*, Argonne National Laboratory Report ANL-92/17, pp. 82-85 (1992).

a. Unsaturated Tests with UO_2 Pellets

Experiments are continuing to investigate the reaction behavior of unirradiated Zircaloy clad-UO_2 pellets exposed to dripping EJ-13 water in an oxidizing environment within a stainless steel vessel at 90°C. (The EJ-13 water is prepared by equilibrating water obtained from well J-13 with tuff; the pH for different batches of EJ-13 is 8.3 ± 0.1.) These tests are being conducted with variable sample surface areas and water drip rates chosen to simulate a range of unsaturated conditions. To date, eight experiments have been initiated, five of which have been subsequently terminated at various times, while the remaining three have been in continuous operation for more than eight years. These experiments are designed to develop test procedures to be used with spent fuel, identify long-term trends in alteration of minerals that form on the sample surface, and identify parameters that control the release of uranium from the waste package assembly.

Analysis of leachates collected from a 6.8- to 8.0-yr test interval indicated a uranium release rate from the samples of 0.1 to 0.3 mg/(m^2·day), which represents a decrease from the ~3 mg/(m^2·day) release observed during the initial 1.0- to 2.0-yr period. Detailed analyses of the sample surfaces by scanning electron microscopy (SEM) combined with X-ray energy dispersive spectroscopy (EDS) indicated that the more rapid release period corresponds to the spallation of micron-sized fragments of uranium-rich material, apparently produced as corroded and dislodged UO_2 granules were washed from the sample surface during the biweekly leachant injection. The decrease in release rates after two years is thought to result from the formation of a dense surface mat of uranyl silicate phases that have entrapped particulate material on the UO_2 pellet surface. The SEM examinations of the post 2-yr samples revealed a notable decrease in the abundance of loosened particulate material. With the ongoing tests, it still appears that uranium release is being dominated by particulate material release, despite the reduction in total uranium loss and the disappearance of micron-sized particulate material from the sample surfaces. The particulates from these longer tests appear to be finer-grained than those from the 1.0- to 2.0-yr samples. A comparison of filtered and nonfiltered solution aliquots from the 8-yr tests indicated that only 2 to 6% of the uranium will pass through a 20 Å filter, with the remainder being released in particulate form or reprecipitated as secondary uranyl phases on the test vessel walls. Examinations of filtered residues from these long-term tests revealed the presence of elongated uranium silicate grains. These phases probably formed as crystalline alteration phases on the same surface and became dislodged by dripping water during the biweekly leachant injection.

Cation results from the 6.8- to 8.0-yr samples indicate continued depletion of Mg, Ca, K, and Si in the leachate relative to the starting EJ-13 composition. Our SEM/EDS analyses indicate that these elements became incorporated into uranyl-bearing phases that formed on the UO_2 pellet surfaces. Mineral trends indicate the following paragenetic sequence for the top UO_2 surfaces over the past eight years: uraninite → uranyl oxide hydrates → uranyl silicates → uranyl alkaline silicates. This trend is identical to the pattern of uraninite alteration observed in deposits of naturally occurring weathered uraninite. The top surface of samples after 8 yr of testing was dominated by the uranyl alkaline silicate phase, boltwoodite [$K(H_3O)UO_2(SiO_4)\cdot nH_2O$]. Also present were hollow-shaped Mg-Al-Si tubes believed to be

either the clay-mineral palygorskite (attapulgite) or amesite. This tube-shaped phase had not been observed on any previous samples.

Solution pH values after 8 yr ranged from 6.5 to 7.8, representing little change from last year's test results.[9] These values represent a slight decrease from the initial 8.3 ± 0.1 value of EJ-13 leachant. Testing of the unirradiated UO_2 will continue.

b. Unsaturated Tests with Spent Fuel Samples

The objective of this effort is to measure the reactivity of spent fuel under a range of potential repository conditions. Fragments of two types of irradiated fuel, ATM-103 and ATM-106, which represent the majority of spent fuel types, are being tested under drip and saturated-water-vapor conditions. The average burnup is 30 MW·day/kg U for ATM-103 and 43 MW·day/kg U for ATM-106. The tests examine the effects of EJ-13 water drip rate (0.075 or 0.75 mL every 3.5 days) and saturated water vapor on the radionuclide release behavior of the fuel types. The tests have been ongoing for one year. At the end of two successive 60-day test periods, the solutions in the test vessels were examined. There appeared to be a radiolysis effect on solution composition, a difference in actinide release behavior for the two fuel types, and colloidal material in the leachate. Each is addressed below.

The effect of radiolysis on solution composition was determined by monitoring the change in the pH, as well as the nitrate, nitrite, formate, and bicarbonate contents, of the EJ-13 water. After 120 days, the pH decreased from 8.3 ± 0.1 for the original EJ-13 water to 7.2 ± 0.2 for the vapor tests, 6.4 ± 0.1 for both drip tests with ATM-103, and 7.4 for the low-drip-rate test and 4.7 for the high-drip-rate test with ATM-106. Nitrate content in the EJ-13 decreased from 1 x 10^{-2} g/L to 2-8 x 10^{-3} g/L. The nitrite content increased from 1 x 10^{-4} g/L to 2-30 x 10^{-3} g/L. The formate ion increased from <2 x 10^{-4} g/L to 2-17 x 10^{-3} g/L, which paralleled both a bicarbonate decrease and the nitrite increase. A possible reaction to account for these changes is:

$$N_2 + 2H_2O + 2HCO_3^- \rightarrow 2NO_2^- + 2HCO_2^- + 2H^+ + H_2 \qquad (1)$$

The formation of formate and oxalate, as well as nitrate, during glass-waste leaching under external gamma irradiation was previously reported by Barkatt et al.[10] The presence of formate and oxalate could also result in the formation of highly stable actinide complexes. However, these complexes have not yet been identified in these leachates.

Actinide release with ATM-106 fuel differed from that with ATM-103 fuel. For both ATM-106 drip tests, actinide release was minimal at the end of the first 60-day test

---

[9] J. E. Battles et al., *Chemical Technology Division Annual Technical Report, 1992*, Argonne National Laboratory Report ANL-93/17, p. 86 (1993).

[10] A. Barkatt, A. Barkatt, and W. Sousanpour, *Nucl. Technol.* **60**, 218-227 (1983).

period, and was still two orders of magnitude less than that for the ATM-103 fuel at the end of the second test period.

The largest concentration of actinide species observed in the leachate was for the high-drip-rate test with ATM-103, and a major fraction of the actinides appeared to be in the form of colloids. The amount of colloidal material was several orders of magnitude greater than that found in earlier saturated tests with spent fuel.[11] This difference, if it persists, would indicate an enhanced source term for actinide transport.

Transmission electron microscopy of the leachate from a high-drip-rate test with ATM-103 fuel indicated two major, intermixed uranium phases containing rare earth elements. The two phases differed in that one contained silicon and the other did not. Partially crystalline uranium silicate colloids were identified as soddyite, a uranyl silicate with a U/Si ratio of 1:1. The second uranium-bearing phase, which consisted of 20-50 nm particles in agglomerates, was not crystalline. Its elemental composition suggested a schoepite phase (a uranyl hydrate species). The two uranium phases form part of the paragenic sequence found for unirradiated UO_2, as described in Sec. IV.B.4.a.

Sampling of the unsaturated tests will continue at intervals of 2 to 6 months to determine fission product and actinide release rates as functions of time. Additional tests with other irradiated UO_2 fuels are planned.

C. *Vitrification of Low-Level Waste*

Vitrification is being investigated as a treatment method for low-level radioactive and mixed waste streams. The emphasis is on techniques that minimize the volume of the resultant waste forms. We are investigating one such technique, called Minimum Additive Waste Stabilization (MAWS), in which vitrification is combined with washing and ion-exchange waste water treatment. With this technique, the multiple waste streams are blended together so that additives, such as fluxes, are not needed to produce a durable waste form.

1. Durability of Minimum Additive Waste Stabilization Glasses

We are developing test methodologies to determine the long-term performance, or durability, of low-level waste glasses produced by the MAWS process. The results will be used to compare the durability of glasses against other low-level waste forms, such as cement. The glasses to be tested are being supplied by the Catholic University of America as part of the program to remediate the Fernald (Ohio) site, where soil has been contaminated with radioactive and toxic wastes during defense-related processing operations. To date, five glasses produced in glass melters at the Catholic University of America have been received, and additional samples are expected in 1994. They contain up to 0.7 wt% U_3O_8, 0.1% ThO_2, and small amounts of transuranic and fission product elements.

---

[11] C. N. Wilson, *Results from NNWSI Series 3 Spent Fuel Dissolution Tests*, Pacific Northwest Laboratory Report PNL-7170 (1990).

Leach tests (Product Consistency Test[12]) of the glasses with deionized water have been performed at 90°C for times up to 128 days, and analyses of the resulting solutions are in progress. One glass is being tested in a fluidized-bed reactor to determine the maximum glass reaction rate. Leach testing with surrogate groundwater leachants and vapor hydration testing of MAWS glasses will be initiated in 1994. In the next phase of this program, glass produced by a 300 kg/day melter at Fernald from actual waste streams will be tested according to the procedures being developed in this initial phase.

To provide further evidence of the durability of waste glasses, the alteration layers on the surface of ancient glass artifacts are being examined by analytical electron microscopy. The objective is to identify similarities between the alteration layers formed on old glasses exposed to natural environments and the layers formed on waste glasses in short-term laboratory tests.

2. Development of Glassy Slags

Significant progress has been made in developing the MAWS concept to vitrify wastes. However, many DOE sites have large volumes of waste streams that are not amenable to disposal in glass waste forms. These wastes contain large amounts of metallic elements (such as Cr, Ni, Ti, Fe, Ca, and Mg) that have low solubilities in glass. (For example, over 22% of the buried wastes at the Radioactive Waste Management Complex of Idaho National Engineering Laboratory is scrap metals.) These waste streams may not be suitable for a glass waste form without use of large amounts of glass-forming additives during the vitrification process, which would significantly reduce waste loading. Moderate loadings of these waste streams will result in significant crystallization during vitrification, which can lead to difficulties in glass processing and uncertainties in glass durability. Low waste loadings and large amounts of additives will substantially limit volume reduction and cost savings during remediation and treatment of these waste streams.

Work is in progress to develop a glassy slag waste form that is composed of crystalline metal-oxide-containing phases embedded in a glass matrix. Such a waste form has the potential of extending MAWS technology to a much wider range of waste streams. To produce the glassy slag, waste metals are mixed with contaminated soil and melted in air at temperatures up to about 1500°C. Metal-oxide-containing phases crystallize as the melt cools. Elements not contained in crystalline phases become incorporated into the glass phase. By this method, we have achieved up to 74% metal loading in contaminated soil without needing any purchased glass-forming additives. Glassy slag formulations developed at ANL were successfully prepared by melting scrap metals, such as carbon steel and stainless steel, in a plasma centrifugal furnace.[13] Reported below is our evaluation of both unreacted and reacted glass slags.

---

[12] C. M. Jantzen, N. E. Bibler, D. C. Beam, W. R. Ramsey, and B. J. Waters, *Nuclear Waste Glass Product Consistency Test (PCT), Version 5.0*, Westinghouse Savannah River Co. Report WSRC-TR-90-539, Rev. 2 (1992).

[13] S. T. Kujawa and C. W. Whiteworth, *Plasma Centrifugal Furnace Development Program at the CDIF*, MSE, Inc., Butte, MT, Report No. 2DOE-PAFE-D010 (1993).

As-melted slags have composition ranges of (in wt%): Al_2O_3, 2-10; CaO, 1-7; CeO_2, 0-1.2; Cr_2O_3, 0-7; Fe_2O_3, 17-85; NiO, 0-3; PbO, 0-2.2; SiO_2, 11-55; alkalis, 1-3. These slags were examined using X-ray diffraction (XRD), scanning electron microscopy/energy dispersive spectroscopy (SEM/EDS), and transmission electron microscopy (TEM). These examinations indicated the presence of spinel group minerals, including magnetite (Fe_3O_4), trevorite ($NiFeO_4$), chromite ($FeCr_2O_4$), and maghemite (γ-Fe_2O_3). The types and amounts of crystalline phases present depended on the metal-waste loadings. Hazardous elements such as Cr and Ni were incorporated into crystalline phases. The glass phase consisted of silicates with small amounts of Fe, Ca, Pb, K, and Ce. The glass phase contained as much as 70% SiO_2 and Al_2O_3, but the composition depended on both the materials that were melted and on the phases that crystallized. The ability of the slags to retain Ce (which is a surrogate for actinides) and Pb depends on the durability of the glass phase, while the retention of hazardous elements such as Ni and Cr depends on the stability of the crystalline phases.

The chemical durability of these slags was evaluated using the Toxicity Characteristic Leaching Procedure (TCLP),[14] the Product Consistency Test,[12] and the ANL vapor hydration test.[15] The test solutions were analyzed for cations using inductively coupled plasma/mass spectroscopy, anions using ion chromatography, and pH using a combination electrode. The reacted solids were characterized with optical microscopy, SEM/EDS, and TEM. All the slags passed the TCLP test by at least a factor of 40 and also passed Land Disposal Limits. The Product Consistency Tests indicated that the slags with high metal loadings have chemical durabilities (as determined by the release of silicon, sodium, and potassium into solution) similar to or better than HLW glasses, such as SRL 165 and WVCM62.

The results of SEM/EDS examination of slags reacted for 7 days in Product Consistency Tests at 90°C indicated an absence of alteration phases and similar compositions of the slags before and after testing. This finding suggests that the extent of reaction is small. The slags reacted in saturated water vapor at 200°C for 7 and 28 days showed less secondary phase formation than HLW glasses reacted under identical conditions.

The Structural Bond Strength (SBS) Model[16,17] was used to examine the relationship between the slag composition and its chemical durability. Modeling enabled us to lower the number of slag compositions required for testing, thereby reducing cost and shortening development time. The SBS model calculated relative durabilities of the slag formulations in good agreement with the durabilities measured in the Product Consistency Tests.

Our work indicates that tailored slags are good waste forms for several reasons: (1) they have chemical durabilities similar to or better than HLW glasses, (2) can incorporate large amounts of metals that have low solubilities in glasses, (3) can incorporate waste streams

---

[14] U.S. Environmental Protection Agency, "Toxicity Characteristic Leaching Procedure," 40 CFR 268, Appendix I (1988).

[15] W. L. Ebert, J. K. Bates, and W. L. Bourcier, *Waste Mgmt.* **11**, 205-221 (1991).

[16] X. Feng and A. Barkatt, *Mat. Res. Soc. Symp. Proc.* **112**, 543 (1988).

[17] X. Feng, E. Saad, and I. L. Pegg, *Ceram. Trans.* **9**, 457 (1990).

having low contents of flux components (boron and alkalis), (4) have less stringent requirements on processing parameters compared to glass waste forms, and (5) can be produced using minimal amounts of purchased additives, thereby yielding greater waste volume reduction and treatment cost savings.

Work is in progress to fully characterize slags produced in a plasma centrifugal furnace as part of DOE's remediation program. Future work will involve characterization of products from vitrifying actual DOE wastes, including those that contain significant amounts of plutonium.

D. *Characterization of Contaminated Soils*

The soils from the Fernald processing plant became contaminated with uranium after decades of defense-related activities. The uranium-bearing solid phases that control the solubility of uranium in the Fernald environment must be identified both for remediation efforts and determination of the long-term behavior of uranium. We are characterizing the uranium-contaminated soil from Fernald by optical microscopy, scanning electron microscopy with back-scattered electron detection (SEM/BSE), and analytical electron microscopy (AEM). We have also developed a method for preparing TEM thin sections by ultramicrotomy, which has allowed direct comparison between SEM and TEM images.

The SEM/BSE investigations of the Fernald soil have shown that uranium is contained within particles typically 1 to 100 μm in diameter. Further analysis with AEM revealed that these uranium-rich regions are made up of discrete uranium-bearing phases. The distribution of these uranium phases was found to be inhomogeneous at the microscopic level. Our analysis results also indicated that uranium-bearing phases include uranium adsorbed onto iron oxides, uranium silicates, uranium phosphates (autunites), uranium oxides (UO_{2+x}), calcium uranium oxide, and uranium contained within a calcium fluorite phase. Results suggest that the majority of these phases contained uranium in the (VI) oxidation state, in agreement with results from X-ray absorption spectroscopy; however, particles of U(IV) phases have also been identified, including uranium metaphosphate [$U(PO_3)_4$], uranium silicide (USi_{2-x}), and uranium oxides (UO_2). No detectable uranium was associated with the major phyllosilicates (chlorite and mica) in the soil.

Our AEM and SEM/EDS analysis of Fernald soil samples after washing with a carbonate solution demonstrated that >65% of the residual uranium in the soils was uranium metaphosphate [$U(PO_3)_4$] and around 20% was uranium oxide. Examination of carbonate- and citrate-treated soil samples indicated that the washing process is unable to solubilize ceramic-like uranium phosphite phases and uranium oxide particles. The types of uranium-bearing phases observed in the Fernald soil, such as the amorphous uranium iron oxides phases, uranium calcium phosphates, and oxidized uraninite, are similar in many cases to those found in uranium deposits. We intend to perform further soil characterization work to help direct the remediation efforts at Fernald on a firm scientific basis.

V. SEPARATION SCIENCE AND TECHNOLOGY

The Division's work in separation science and technology is concerned with developing methods for treating radioactive, mixed, and hazardous waste. The TRUEX (TRansUranic EXtraction) solvent extraction process continues to be developed and demonstrated; an important part of this effort is the development and application of the Generic TRUEX Model (GTM). The GTM allows users to design flowsheets for transuranic-containing waste streams and estimate the cost and space requirements for implementing a site- and feed-specific TRUEX process. It will also be useful as a tool for plant operators to vary, monitor, and control the process once it is in place. Our other work in separation science and technology includes the development of (1) a process based on sorbing modified TRUEX solvent on magnetic beads to be used for separation of contaminants from radioactive and hazardous waste streams, (2) evaporation/concentration technology for processing supernatant solution removed from underground waste storage tanks, and (3) a process that uses low-enriched uranium targets for production of ^{99}Mo for nuclear medicine uses. We are also involved in several tasks designed to assist ANL Waste Management in treating radioactive and hazardous waste generated as a result of research activities at ANL.

A. *TRUEX Technology-Base Development*

The TRUEX process extracts, separates, and recovers TRU elements from solutions containing a wide range of nitric acid and nitrate salt concentrations. The extractant found most satisfactory for the TRUEX process is octyl(phenyl)-N,N-diisobutylcarbamoylmethylphosphine oxide, which is abbreviated CMPO. This extractant is combined with tributyl phosphate (TBP) and a diluent to formulate the TRUEX process solvent. The diluent is typically a normal paraffinic hydrocarbon (NPH), either a C_{12}-C_{14} mixture or n-dodecane. The TRUEX flowsheet includes multistage extraction/scrub sections that recover and purify the TRU elements from the waste streams and multistage strip sections that separate TRU elements from each other and solvent. Our current work is focused on facilitating the implementation of TRUEX processing of defense TRU-containing waste and high-level waste, where such processing offers financial and operational advantage to the DOE community.

1. The Generic TRUEX Model

The main function of the GTM is flowsheet calculations for user-specified waste streams to be treated by the TRUEX process. The two main files used in these calculations are SASPE (Spreadsheet Algorithms for Speciation and Partitioning Equilibria), which calculates the extraction behavior of each component in the feed waste, and SASSE (Spreadsheet Algorithm for Stagewise Solvent Extraction), which calculates mass balances. These two sections iterate to a unique solution for the compositions of each stage and effluent in a specific flowsheet. A new version of the Generic TRUEX Model, GTM version 2.7, was released during this year. Its new features are briefly described below.

Stage Efficiency. Stage efficiency has been added to the SASSE worksheet. Stage efficiency is the amount of mass transfer that will take place in a stage divided by the amount

that would take place if the stage were an equilibrium stage, i.e., if it has a fractional efficiency of 1.0 (100%).

Temperature Effect. Distribution ratios for various extracted species typically decrease as temperature increases. A temperature correction factor, applicable from 10 to 70°C, has been added for the following elements: La, Ce, Pr, Nd, Pm, Sm, Eu, Gd, Am, Pu(III), and Cm. The distribution ratio for Pu(IV) has no temperature effect built into the GTM. However, because this distribution ratio is not a strong function of temperature, this omission should not have much effect on the calculated GTM values. A temperature correction of other species will be added in the future.

User-Specified Distribution Ratios. By specifying initial distribution ratios for some of the feed components, the user can (1) speed up the GTM calculations and (2) achieve convergence for the distribution ratios of a component that would not otherwise converge because of interactions set up between adjacent stages during the GTM iterations.

Reroute of Section Effluent. In modeling solvent extraction processes, we have defined our flowsheet so that the aqueous phase flows from right to left, and the organic phase flows from left to right. As the GTM was previously set up, the aqueous and organic effluents from section "i" either continued on to the next section (aqueous to section i - 1, organic to i + 1), were taken as external effluents, or were split between the two options. A further option has been added to the GTM: section effluent can now be rerouted to a section other than its normal section.

Solvent Loading. The effect of solvent loading by metal salts on the extraction of species has not been accounted for in previous versions of the GTM. Since the TRUEX process is a waste treatment process, the effects of solvent loading will be small in most cases. However, in some special cases the solvent loading can be high. The GTM was upgraded so that TRUEX flowsheets can be generated where loading is extremely high (close to 100%).

Distribution Ratio Improvements. Based on our investigation of zirconium extraction behavior, we have changed the form of Zr(IV) that we treat in the GTM from Zr^{4+} to ZrO^{2+}. Also, the GTM equations for calculating the distribution ratio for $H_3PO_4^{3-}$, Cd(II), Zr(IV), and F^- were improved. Our own laboratory data were used to improve distribution ratio calculations for PO_4^{3-} and Cd^{2+}. Our own data and data collected at Pacific Northwest Laboratory on TRUEX processing of actual neutralized cladding removal waste were analyzed with respect to the high distribution ratios of Zr(IV) and F^- in concentrated solutions of both. These data were modeled based on the extractability of $ZrO(NO_3)_2$ and $ZrOF_2$. Analysis of these data is not complete, but an upgraded model, which will be further improved in the near future, is included in this GTM version.

Additional Diluent. Based on limited experimental data acquired in the ANL Chemistry Division, the extraction behaviors of Sr, Na, Mg, Al, Ca, Mn, Ni, Cu, and Cs have been modeled for the TRUEX/SREX process (Sec. V.A.3). In addition, the extraction behavior of nitric acid has been modeled when diamyl(amyl) phosphonate (DAAP) is used in place of TBP

in the TRUEX-SREX solvent. Because DAAP is a much stronger extractant than TBP, significantly more nitric acid is extracted into the solvent and must be taken into account.

Many of the new developments discussed above are only accessible to the experienced GTM user; they are currently being made more accessible through changes in the user-friendly front end of the GTM.

2. TRUEX Data-Base Generation

The data base generated for developing the GTM contains information (from the literature and our own laboratory measurements) on the solution and extraction behavior of important feed components over a wide range of possible waste-stream and processing conditions. Algorithms for the extraction behavior of important feed components continue to be improved by use of our own laboratory results and literature data and by interactions with experimenters at Oak Ridge National Laboratory, Pacific Northwest Laboratory, and the Power Reactor and Nuclear Fuel Development Corp. of Japan. Our recent efforts in this area have been concentrated on experimental and modeling work with Bi and Pu(III) species.

a. Bismuth Extraction

The behavior of bismuth in the TRUEX process is important in treating the nuclear wastes stored at the DOE Hanford site, since the initial method for separating plutonium from neutron-irradiated uranium used bismuth phosphate to coprecipitate Pu(IV) and Pu(III) and sodium bismuthate to convert the lower oxidation states to Pu(VI). Thus, many Hanford tanks contain large amounts (of the order of grams per liter) of bismuth. Distribution ratios for bismuth continue to be determined from both forward and back extractions with different compositions of the aqueous phase. Measurements have given variable distribution ratio results at less than 0.5 M H^+, even in the presence of high concentrations of nitrate ion. Distribution ratios measured by the back extraction are, in general, higher and more consistent than those from forward extraction. This problem could be caused by (1) the presence of variable amounts of a higher oxidation state of bismuth, Bi(V), rather than the normal Bi(III), (2) the presence of small particles to which atoms of ^{210}Bi attach themselves, or (3) the hydrolysis of Bi(III). Experiments that have been done so far eliminate the first two options, and hydrolysis of Bi(III) appears to be the reason for the odd extraction chemistry of bismuth.

b. Reductive Stripping of Plutonium

The transfer of Pu(IV) from the organic phase to the aqueous phase (subsequently referred to as "stripping") in the TRUEX process has usually been done with a soluble oxalate compound, since oxalate forms a strong complex with Pu(IV). An oxalate salt (e.g., ammonium oxalate) is considerably more effective than oxalic acid for this stripping, since the oxalate concentration in solution is considerably higher. However, reduction of the plutonium from the (IV) to the (III) oxidation state is sometimes preferable because Pu(III) may be stripped, as is Am(III), with dilute nitric acid. Reduction to Pu(III) is used in the PUREX process to remove plutonium from the TBP solvent, but in this case plutonium is not as strongly complexed, and Pu(III) extracts relatively poorly. With TRUEX solvent, the Pu(III) distribution ratio, the rate

of reduction, and the effectiveness of various reducing agents are not known. We thus measured distribution ratios for Pu(III) at 0.01 to 2 M HNO_3 by contacting the aqueous phases four successive times with pre-equilibrated TRUEX/NPH solvent. Ascorbic acid (with hydrazine hydrate present as a nitrite "getter") was used as the reducing agent. The results of the four extractions are shown in Fig. V-1. The distribution ratios of Pu(III) at the lower acidities (≤0.1 M HNO_3) are orders of magnitude less than Pu(IV) and close to those for Am(III). At the higher acidities, complete reduction is evidently not obtained since the distribution ratios become quite large. As a practical matter, reductive stripping is effective only at low HNO_3 concentrations, about 0.01 M. Future studies will be investigating the practicality of stripping plutonium as Pu(III) and of keeping plutonium in the (III) oxidation state in typical feed solutions, extracting it as Pu(III), and holding it in the TRUEX solvent.

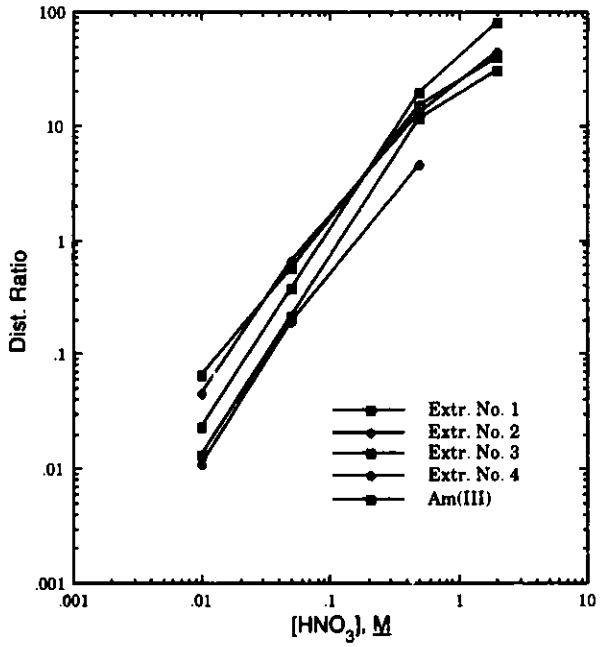

Fig. V-1.

Distribution Ratios for Four Extractions of Pu(III) between Nitric Acid and TRUEX/NPH as Function of HNO_3 Concentration at 25°C. Distribution ratio of Am(III) shown for comparison.

3. TRUEX/SREX Flowsheet Demonstration

A new project has been started, in collaboration with the ANL Chemistry (CHM) Division, to demonstrate the new TRUEX/SREX process, which combines the TRUEX process and the recently developed SREX (strontium extraction) process.[1,2] The TRUEX extractant, CMPO, selectively extracts and partitions Am, Pu, and U along with Si and the lanthanides. The SREX extractant, a crown ether called 4,4'(5')-di-t-butylcyclohexano-18-crown-6 (also referred to as CE), selectively extracts and partitions strontium and, to some extent, technetium. The combined process would be the first step in the pretreatment of dissolved sludge waste from Hanford single-shell tanks, so that the amount of nuclear waste that has to be vitrified is greatly reduced with an attendant major reduction in waste disposal costs. Our work includes detailed

---

[1] E. P. Horwitz, M. L. Dietz, and D. E. Fisher, *Solvent Extr. Ion Exch.* **9**, 1-25 (1991).

[2] E. P. Horwitz, R. Chiarizia, and M. L. Dietz, *Solvent Extr. Ion Exch.* **10**, 313 (1992).

flowsheet development, solvent evaluation, and process demonstration on a laboratory scale using an ANL-design centrifugal contactor.

Two cold (nonradioactive) tests using a 20-stage centrifugal contactor (i.e., 20 minicontactors with 2-cm dia rotors) were carried out for the TRUEX/SREX flowsheet shown in Fig. V-2. The composition of the combined TRUEX/SREX process solvent, called PS 12, is

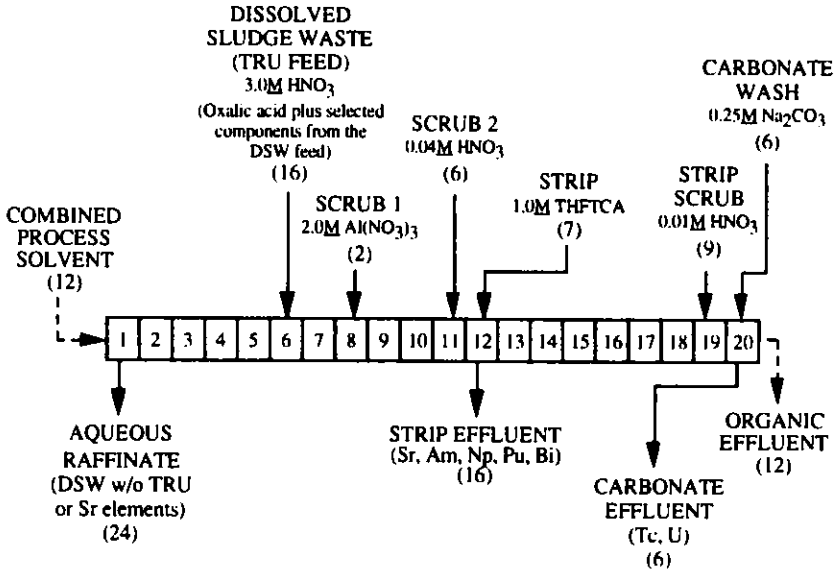

Fig. V-2. Combined TRUEX/SREX Flowsheet for 20-Stage Minicontactor Tests with Simulated Dissolved Sludge Waste (DSW). Relative flows are shown as numbers in parentheses.

0.2 M CMPO, 0.2 M CE, and 1.2 M DAAP in Isopar L. Note that tetrahydrofuran-2,3,4,5-tetracarboxylic acid (THFTCA) is used to strip Sr, Am, Np, Pu, Bi, and the lanthanides from the solvent. Recent data from the CHM Division indicate that THFTCA is more strongly extracted into the PS 12 solvent than was expected based on earlier data. As a result, THFTCA is now being added at the first strip stage (rather than the last, stage 14). Even doing this, we found that most of the THFTCA ends up in the carbonate wash. During the two cold tests, the solvent went through some vivid color changes. While the first cold test showed no operational problems, we observed significant other-phase carryover in the aqueous raffinate and strip effluents during the second cold test. These problems and potential problems will be resolved before we begin hot (radioactive) tests of the TRUEX/SREX process in a glovebox. After samples taken during the two cold tests are analyzed, the results will be compared with GTM calculations and, when appropriate, additional laboratory data specific to the TRUEX/SREX process.

In preparation for the cold tests, we extensively characterized the PS 12 solvent using our dispersion number test[3] and hydraulic tests in a single-stage minicontactor. As a part

[3] R. A. Leonard, G. J. Bernstein, R. H. Pelto, and A. A. Ziegler, *AIChE J.* 27(3), 495-503 (1981).

of this work, the dispersion number test was revised so that it could be used for more viscous solvents. These tests showed that, in many cases, which phase (aqueous or organic) is the continuous phase in a two-phase dispersion is important for contactor operation. In particular, if the more viscous organic phase is the continuous phase, maximum contactor throughput is decreased. For this reason, the minicontactor was started by introducing the aqueous phase before the organic phase for the first cold test. The operational problems with the minicontactor occurred during the second cold test, when the minicontactor was restarted with both phases in each stage. Such a start makes it likely that the organic phase will become the continuous phase.

Hot tests using simulated Hanford dissolved-sludge waste will be initiated in 1994. Other solvent compositions than PS 12 will also be tested.

4. Mark 42 Target Processing

Working in conjunction with Oak Ridge National Laboratory (ORNL), we applied the GTM to develop a TRUEX process flowsheet for recovering Pu, Am, and Cm from Mark 42 targets, which are aluminum-clad PuO_2 targets that were irradiated at the Savannah River Plant to very high burnup. These targets are being processed to recover plutonium (which now has high fractions of ^{238}Pu and ^{242}Pu) and valuable isotopes of Am and Cm. Flowsheet development (Fig. V-3) was guided by three process constraints: (1) the feed composition, (2) the available equipment, and (3) the desired effluent concentrations. The feed composition was set so that the target would be dissolved in the smallest volume possible. The flowsheet was designed for the three banks of 16-stage mixer settlers already in a shielded cell facility at ORNL. In addition, we assumed that stage extraction efficiency is as low as 80%, because there is no room or facilities to insert additional pumps or any centrifugal contactor stages in the cell. The effluent requirements are that the aqueous raffinate be a non-TRU waste, that is, less than 100 nCi/mL. The first strip effluent was to have less than 0.1% Pu with Am, Cm, and the rare earths; the second strip effluent was to have less than 0.1% Am and Cm with the Pu; and the zirconium is to be complexed so that it stays with the aqueous raffinate.

In developing the Mark 42 TRUEX flowsheet, we added new features to the GTM so that we could (1) reroute an effluent from one section to another section than the normal one, (2) account for the effects of high solvent loading, (3) account for the effect of temperature on the distribution ratios for the various feed components (since the temperature in the ORNL shielded cell is 45°C rather than the 25°C previously used in GTM calculations), (4) handle extraction efficiencies of less than 100% at each stage, and (5) automatically calculate the speciation and distribution ratios of aqueous-phase components for a wide variety of feed compositions.

The TRUEX Mark 42 flowsheet was tested four times at ORNL, one cold run and three hot runs. In all four tests, mechanical operation of the equipment and the process went reasonably well. In particular, all dispersions separated at or near expected process flow rates, and no significant amount of oxalate precipitate was formed. Rough measurements of effluent concentrations, based on their actinide-specific activity, indicate that the TRUEX Mark 42 flowsheet was performing about as expected. When detailed analytical data are available, we will determine exactly how well the GTM works at high solvent loadings. In particular, we will

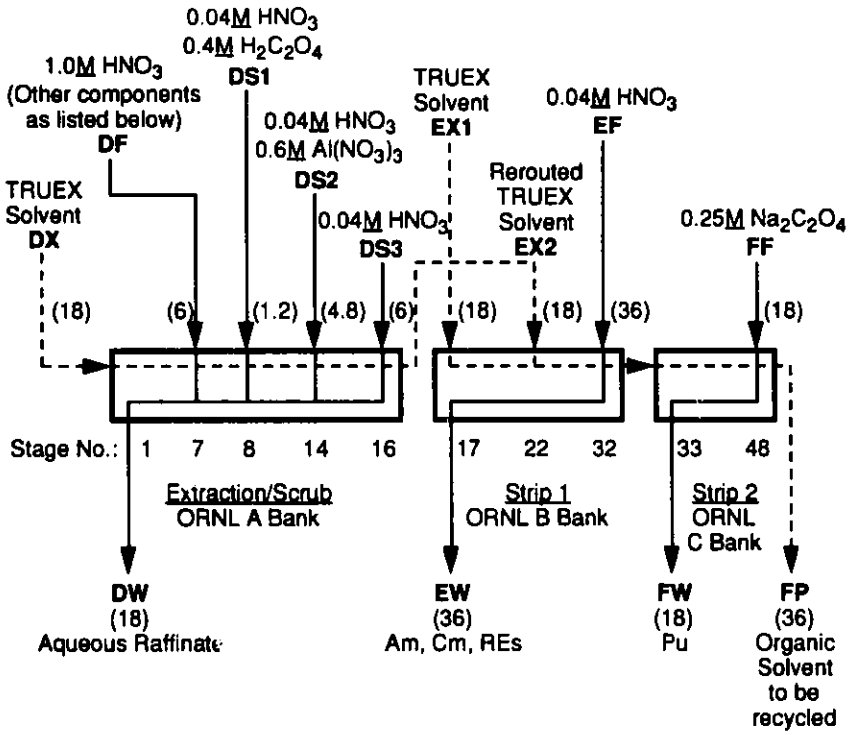

Flows, shown in ( ), have units of mL/min.
The TRUEX solvent (DX and EX1 feeds) is 0.2M CMPO and 1.4M TBP in NPH.
For one segment of Mark 42 target in 15 L of DF feed, expected concentations are:

0.016M Al	0.064M Mg	0.021M Ru	0.003M Am
0.003M Cd	0.048M Nd	0.019M Zr	0.003M Cm
0.004M Cu	0.024M Pd		0.011M Pu

Fig. V-3. Basic TRUEX Flowsheet for Processing Mark 42 Targets from Oak Ridge National Laboratory. The symbol REs represents rare earths.

evaluate recent model developments that should improve the GTM calculations at high solvent loadings (Sec. V.A.1).

5. Centrifugal Contactor Development

We have been modifying the basic design of the ANL centrifugal contactor as necessary to adapt it for specific solvent extraction processes. (See Ref. 4 for schematic of this contactor.) A key feature in these design efforts is the use of computational models for (1) the flow of the organic and aqueous phases through the contactor and (2) the vibrational parameters of the spinning motor/rotor combination. This past year we discussed contactor needs at Pacific Northwest Laboratory (PNL). As a result of the discussions, we are designing and building a laboratory-scale multistage contactor for use in a PNL shielded-cell facility. With this contactor,

---

[4] M. J. Steindler et al., *Chemical Technology Division Annual Technical Report, 1991*, Argonne National Laboratory Report ANL-92/15, p. 103 (1992).

PNL will be able to test various solvent extraction flowsheets for processing actual dissolved sludge waste from the Hanford underground storage tanks. As a part of this work, we demonstrated contactor operation at Argonne for PNL personnel.

6. Treatment of Plutonium-Containing Waste

Approximately 200 L of waste solution from the analysis of plutonium samples has accumulated over the past several years at New Brunswick Laboratory (NBL) and ANL. These residues contain varying concentrations of nitric, sulfuric, phosphoric, and hydrochloric acids, as well as U, Pu, Np, and Am. Originally destined for storage at Idaho National Engineering Laboratory and eventual disposal at the Waste Isolation Pilot Plant in New Mexico, these wastes now appear to have no place that will accept them. In this project, the TRUEX process was used to convert the bulk of this waste into a non-TRU (low-level) waste. The goal was to reduce the TRU elements to a concentration less than 10 nCi/mL. In the initial plan, the plutonium recovered by the TRUEX process was to be converted to a metal and returned to NBL for storage and subsequent transport to the DOE complex. However, because this material is no longer as critical in the defense complex, the recovered plutonium was returned to ANL Waste Management for disposal. This demonstration showed the applicability of using the TRUEX process for treating similar wastes at Rocky Flats Plant, Los Alamos National Laboratory, Hanford site, and Idaho Chemical Processing Plant.

The TRUEX solvent extraction process used to generate the non-TRU waste stream and recover the plutonium was designed with the GTM and carried out in a 20-stage centrifugal contactor (4-cm dia rotor) installed in a glovebox. A TRUEX solvent with n-dodecane diluent was used in this process. In 1991-1992, we processed two batches of NBL waste along with all of the resulting wastes generated during processing and the subsequent cleanups.[5,6] In 1993, two additional batches of NBL waste were processed. Table V-1 gives results from the processing of all four waste batches. As shown in the table, the feed activity varied from 21,400 to 88,000 nCi/mL. The alpha activity in the aqueous raffinate was always ≤10 nCi/mL, but greater than 1 nCi/mL. By comparing the feed versus the raffinate concentration, alpha decontamination factors were calculated to range from 65,500 for Batch 3 to 4,000 for Batch 4. One reason for this wide variation is due to the amount of TRU material in the feed. The higher the concentration in the feed, the more material that can be extracted, and the higher the resulting decontamination factor.

Major accomplishments in this program include the following: converted TRU waste to low-level waste, thereby greatly reducing the amount of TRU waste requiring disposal; demonstrated the robustness of the TRUEX process; and demonstrated the usefulness of the GTM in flowsheet development. The remaining plutonium waste being stored at ANL and NBL will

---

[5] M. J. Steindler et al., *Chemical Technology Division Annual Technical Report, 1991*, Argonne National Laboratory Report ANL-92/15, pp. 104-108 (1992).

[6] J. E. Battles et al., *Chemical Technology Division Annual Technical Report, 1992*, Argonne National Laboratory Report ANL-93/17, pp. 96-100 (1993).

Table V-1. Results from the TRUEX Processing of NBL Waste Solutions

Batch Number	Feed			Plutonium Product		Aqueous Raffinate	
	Pu, g	U, g	Alpha Activity, nCi/mL	Pu, g	U, g	Alpha Activity, nCi/mL	Alpha Decontamination Factor
1	12	0	40,000	8	0	1.8	22,400
2	13	16	21,400	13	10	4.4	4,900
3	28	7	88,000	30	5	1.3	65,500
4	34	3	40,000	33	3	10	4,000
Totals	87	26		84	18		

not be processed in this program. Other methods are being evaluated for processing this waste (see Sec. V.D.4).

B. *Magnetically Assisted Chemical Separations*

We are involved in developing magnetically assisted chemical separation (MACS) processes for the treatment of a variety of radioactive and hazardous waste streams, including Hanford waste tank sludges and supernatants in underground storage tanks. Transuranic-containing waste is of considerable concern because of the longevity of its potential hazard resulting from the long half-life of its radioactive components. For the remediation efforts at Hanford and other DOE sites, this project will develop compact, economic, in-tank or near-tank processes for the removal of contaminants (^{137}Cs, ^{90}Sr, TRU) from waste solution.

The MACS process combines the selective and efficient separation afforded by chemical sorption with the high physical separation afforded by magnetic recovery of ferromagnetic beads. For the Cs, Sr, or TRU removal, it uses magnetic particles coated with (1) either a selective ion exchange material (e.g., silicotitanates, resorcinol) or (2) an organic-complexant-containing solvent such as CMPO/TBP. By their chemical nature, these coatings selectively attract the contaminants onto the particles, which can be recovered from the waste solution by using a magnet. Once the removal is achieved, the contaminants can either (1) be left on the loaded particles and added to a glass feed slurry or (2) be stripped into a small volume of solution to regenerate the extracting particles. The studies in the process development effort during 1993 involved (1) evaluating polymeric coatings for magnetic particles and (2) measuring the hydrolytic and radiolytic damage to coated particles during processing.

1. Particle Coating Process

Many types of commercially available "microparticles" with magnetite and a wide range of polymeric coatings were tested to determine the suitability of the microparticles for the chemi-adsorption of CMPO/TBP solvent. Many types of polymeric coatings were eliminated as

suitable materials due to the poor adsorption of CMPO/TBP onto the polymeric surface. The polymeric coating showing the most promise was charcoal cross-linked with N,N-acrylamide.

One of the parameters to determine the effectiveness of contaminant adsorption is the partition coefficient (K_d):

$$K_d = \frac{\text{activity in the solid phase (cpm/g)}}{\text{activity in the liquid phase (cpm/mL)}} \quad (1)$$

The K_d values measured for TRU extraction in 2 M HNO_3 with polymer-coated particles (treated with CMPO/TBP solutions in ethanol and hexane carrier phase) are reported in Table V-2. Also given for comparison are experimentally determined distribution ratios for americium with traditional liquid/liquid extraction using similar solutions. These results indicate better extraction performance by the MACS process. Studies are underway to determine the loading capacity and stripping ability of the MACS particles under various conditions.

Table V-2. Partition Coefficients for TRU Extractions in 2 M HNO_3 with MACS Process Using Particles Coated with Charcoal Cross-Linked with N,N-Acrylamide. For comparison, experimentally determined distribution ratios are given for americium extraction by traditional solvent extraction for similar solutions.

Tracer	CMPO Conc., M	Expt. K_d, mL/g	Expt. D_{Am}, dimensionless
^{241}Am	0.25	141	40
^{241}Am	0.75	3000	240
^{238}Pu	0.75	5500	-
^{241}Am	1.0	2704	360
^{241}Am	1.2	1924	1700
^{241}Am	1.36	4000	-

2. Radiation Stability

We also determined the radiation stability under process conditions for micro-particles designed for TRU and ^{137}Cs removal. (Particles for cesium removal were prepared and evaluated by a commercial collaborator, Bradtec Inc.) The particles in various solutions (0.1-5.0 M HNO_3 with waste simulants) were sealed in quartz vials and rotated end over end while being irradiated in a ^{60}Co facility. In the irradiation solutions for TRU removal, the waste simulants were representative of acidic waste from the Plutonium Finishing Plant (operated by Westinghouse Hanford Co.) and dissolved sludge from the Hanford single-shell tanks. In the

irradiation solutions for ^{137}Cs removal, the waste simulants were alkaline single-shell tank supernatant. Upon completion of irradiations, the samples were recovered, and K_d values were determined as a function of nitric acid concentration and dose. The approximate doses to the particles were calculated based upon the composition of the waste solutions and the physical characteristics of the particles. The particles prepared for TRU removal receive most of their radiation dose from the alpha decay of Am and Pu, while the particles designed for ^{137}Cs removal receive their dose from beta and gamma decay. The dose is deposited through the ionization of target atoms when the emitted alpha or beta particles pass through them.[7,8] The particles received doses equivalent to 10, 100, and 2000 cycles of use. In general, the K_d values of the coated particles decreased as dose increased. We also found that the K_d values decreased as the HNO_3 concentration of the irradiation solutions increased from 0.1 to 5.0 M. For solutions with high nitric acid concentrations (>2 M), further studies are necessary to better resolve the contribution to the reduced K_d values from irradiation damage as opposed to magnetite dissolution.

C. *Advanced Evaporator Technology*

The purpose of this new program is to develop a mobile evaporator/concentrator unit for processing supernatant solution removed from underground storage tanks at Hanford and other DOE sites. Retrieval and initial processing of DOE underground storage tank wastes will likely result in the addition of significant amounts of water; further, approximately 30 wt% of the current waste inventory is water. Early estimates indicate that the volume of waste will increase by at least a factor of three through water addition. This additional water may have detrimental effects on proposed thermal processing for organic/nitrate destruction. A considerable amount of the energy in the thermal destruction process will need to go into boiling water, not destroying organics and nitrates.

For this program, we are developing a transportable, compact system to remove a majority of water from saturated $Na/NO_3/NO_2/OH$ solution. As envisioned, the system will consist of an evaporator followed by a concentrator. The bulk of the water will be removed by the evaporator; additional concentration (water removal) will be completed in a concentrator specially designed to handle high solids concentrations or slurries. The slurry discharged from the evaporator/concentrator system will be capable of being fed directly into the organic/nitrate destruction equipment.

The evaporator/concentrator system is being designed to test the feasibility of processing effluents from a compact ion exchange unit that will be removing cesium from Hanford tank supernatant. In addition to processing cesium-free salt solutions resulting from this equipment, we will also process a nitric acid stream. This unit will employ nitric acid for regeneration of the ion exchange resin. The regeneration operation will produce a cesium product stream containing ~0.3 M nitric acid. The recovered cesium product stream is slated for neutralization and return to the Hanford waste tanks. Our research is designed to reduce the volume of cesium waste that is returned to the waste tanks, to recover the nitric acid (the distillate), and to recycle this acid

---

[7] H. Cember, *Introduction to Health Physics*, Pergamon, New York, pp. 97-109 (1983).

[8] R. D. Evans, *The Atomic Nucleus*, Robert E. Krieger Publishing, Malabar, Florida, pp. 632-668 (1955).

to the ion exchange process. This nitric acid could then be used to remove additional cesium from the ion exchange columns. Removing and recovering nitric acid from this stream would greatly reduce neutralization requirements. Meeting these objectives demands achieving high decontamination factors, which have been demonstrated in evaporators designed by LICON, Inc. (Pensacola, FL). Although our 1994 goals are tightly tied to concentrating process streams from the cesium ion exchange process (both the cesium-free stream and the cesium-containing nitric acid stream), this work is viewed in the broader scope as proof of principle of the technology for concentrating radioactive waste streams at Hanford, Idaho, Savannah River, and Oak Ridge. Evaporator and concentrator testing will be completed and the data analyzed for use in conceptual design to be done in 1995.

D. *Technical Support to ANL Waste Management*

We are involved in several different tasks providing technical support for ANL Waste Management. The emphasis is on establishing a treatment scenario for all radioactive and hazardous liquids that have been, are, and will be generated at ANL. Our work during 1993 included designing, fabricating, and testing a mixed-waste treatment facility; assisting ANL Waste Management in purchasing two evaporators and two concentrators for treating on-site waste waters; developing a method for treating spent scintillation cocktails; and designing a liquid TRU waste treatment facility.

1. Mixed-Waste Treatment

Argonne as part of its ongoing research activities generates mixed wastes having the characteristic of corrosivity (pH <2 or >12.5) and toxicity caused by toxic metals (e.g., Pb, Cd, Cr, Ag, and Hg). These wastes are generated in small volumes with highly variable compositions. Treatment of these wastes is necessary before they will be accepted at a disposal site. Our goal is to create a process that will be applicable to 95 vol% of the aqueous, toxic-metal mixed waste generated at ANL.

The treatment process entails alkaline sulfide precipitation followed by filtration to remove the precipitated solids. The precipitation involves adding the acidic waste to a slurry of calcium hydroxide until a pH of 10 is achieved. This precipitates the majority of the toxic metals as hydroxides. The process is completed by metering a near saturated solution of sodium sulfide (1.9 M) into the treatment vessel until a concentration of 10 ppm total free sulfide is achieved. This sulfide addition converts the metal hydroxides into metal sulfides, which in general are much more insoluble than hydroxides. In addition to being less soluble, metal sulfides form a crystalline precipitate that is easier to filter than a gelatinous hydroxide sludge. The toxic-metal precipitates can then be removed by filtration, making the filtrate non-hazardous. In addition, metal sulfides will likely pass the Environmental Protection Agency's toxicity characteristic leaching procedure, indicating that the solids are also non-hazardous. Thus, the acidic mixed waste is converted into two low-level wastes.

To demonstrate this method, we treated a simulated waste solution containing Cd, Pb, and Ag. A solution of 0.1 M cadmium nitrate, lead nitrate, and silver nitrate in 4 M nitric acid was added to 50 mL of a 10 wt% calcium hydroxide slurry until a pH of 10 was achieved.

Then 1.9 M sodium sulfide was added until a total sulfide concentration of 10 ppm was obtained. The resulting slurry was passed through a 0.45 μm filter and analyzed by inductively coupled plasma/atomic emission spectroscopy (ICP/AES). The concentrations of the metals are reported in Table V-3. As can be seen, the alkaline sulfide precipitation process is effective at removing these metals from aqueous solution.

Table V-3. Concentrations of Cd, Pb, and Ag in the Filtrate

	Concentration, ppm		
	Initial	Filtrate	RCRA Limit[a]
Cd	11,200	<0.1	1.0
Pb	20,700	<1	5.0
Ag	10,800	<0.05	5.0

[a]Established by Resource Conservation and Recovery Act.

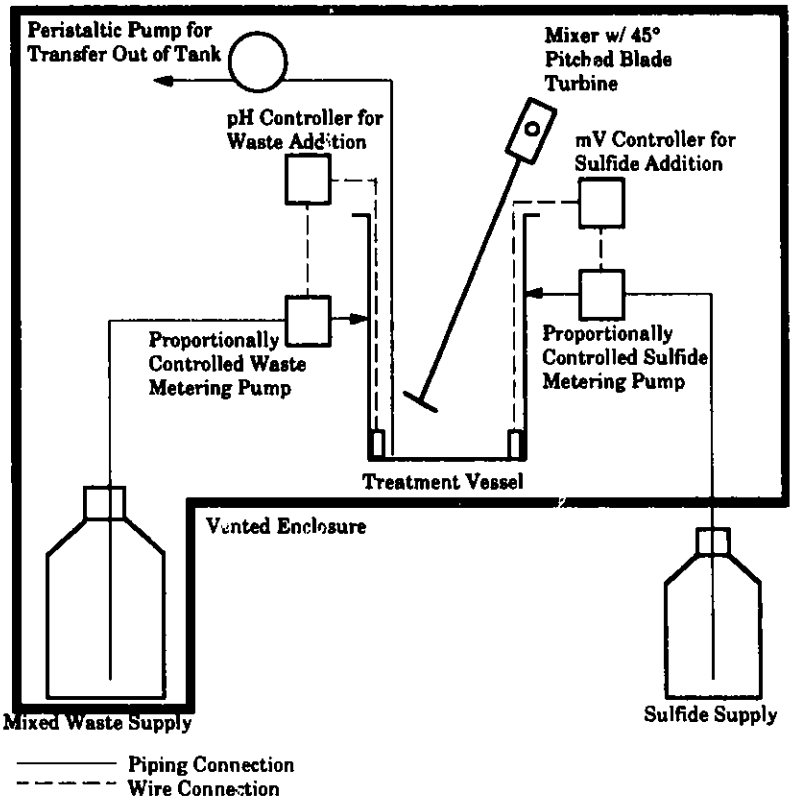

Fig. V-4. Schematic for Alkaline Sulfide Precipitation in Mixed-Waste Treatment

Following this demonstration, equipment for alkaline sulfide precipitation was designed (Fig. V-4) and installed in a Waste Management facility. The treatment equipment makes additions using pH and sulfide control loops; this allows semiautomated control of the treatment. Upon completion of the treatment, the waste is pumped into a transfer vessel via the peristaltic pump. This vessel is then moved to a filter skid for removal of the toxic metals.

A portable filtration system, incorporating a number of modules, has been designed for use in filtering a wide variety of mixed-waste streams, including the one generated in the alkaline sulfide precipitation process. The modular design allows the filtration scheme to be changed for treatment of a variety of influents. Each module can either be included in or isolated from the flow scheme, as desired.

The precipitation/filtration facility has been set up and will be demonstrated using much of the toxic-metal-containing mixed waste at ANL. We will remain in a consultation role for this operation and will develop treatment plans for mixed wastes that require special treatment.

2. Upgrade of Evaporator/Concentrator

Argonne's Waste Management organization presently has two low-level-waste (LLW) evaporators and one LLW concentrator that are more than 30 years old and in need of replacement. We are providing technical support in the specification, purchase, and documentation of two LLW evaporators and two concentrators, one for LLW and one for mixed waste.

Bid packages for LLW evaporators having a distillate production rate of 5.7 L/min (1.5 gal/min) were sent to six companies. The three bid responses were evaluated, and LICON was awarded the contract. The LICON evaporator, which operates under a vacuum, has a capacity of 340 L/h (90 gal/h) and is especially attractive because of its high decontamination factors, simplicity, low profile, and ability to handle solids.

Bid packages for the concentrators were sent to six companies, and two responded. The contract for two 34 L/h (9 gal/h) concentrators was awarded to Artisan Industries, Inc. (Waltham, MA). The main advantages of Artisan's Rototherm Concentrator are its ability to handle high solids feeds and its simplicity of design and operation.

To gather information regarding operating conditions and problems which ANL Waste Management may encounter in the new LICON evaporators, tests were completed using a LICON 12 L/h (3 gal/h) evaporator to treat a simulated typical feed (Table V-4). During the tests, the feed was evaporated down in a number of steps until a final concentration factor of 60 was attained. (The target concentration factor for the new evaporators is 20.) Important information regarding scale formation and dissolution, foaming in the evaporator shell, and solids buildup in the tanks and lines was gleaned from the tests. This information was communicated to LICON and used for design evaluation and modification.

Similar design tests were completed by Artisan with its Rototherm test unit. The feed for these tests was made 20 times more concentrated than the feed specified in Table V-4.

Table V-4. Ionic Composition of Simulated Evaporator Feed[a]

Cations		Anions	
Ion	mg/L	Ion	mg/L
Ca^{2+}	7.62	F^-	17
Cu^{2+}	0.27	Cl^-	204
K^+	21.8	SO_4^{2-}	362
Li^+	1.75	NO_2^-	130
Mg^{2+}	16.0	NO_3^-	129
Mn^{2+}	0.019	HCO_3^-	683
Na^+	630	SiO_3^{2-}	2.7
Ni^{2+}	0.574	$B_4O_7^{2-}$	2.5
		$H_2PO_4^-$	77

[a]Total solids = 2300 ppm.

No major problems were noted during the tests; concentration of the feed to a toothpaste consistency was attained by the Rototherm.

Both the evaporators and the concentrators will be delivered in early 1994. Besides filling Waste Management's needs for new equipment, the new units will also yield data important to our own evaporator program (Sec. V.C).

3. Treatment of Spent Scintillation Cocktail

A large volume of liquid scintillation cocktail wastes is in temporary storage at the ANL Waste Management facilities. The scintillation cocktail wastes are either mixed wastes or low-level radioactive waste, depending on the composition. Both types of wastes can be disposed through the use of commercial treatment, storage, and disposal (TSD) facilities, as long as they contain no radioactive nuclides with atomic number ≥88. However, a substantial part of the ANL wastes contains TRU nuclides, and commercial disposal facilities are not yet licensed to accept them.

We conducted a study to determine TSD options available for all types of scintillation cocktail wastes, and the results were reported in a document submitted to Waste Management. Wastes containing radionuclides with atomic number <88 may be sent to properly licensed commercial TSD facilities, such as Quadrex in Florida, and the wastes that contain TRU nuclides may be sent for storage at Hanford. The rules and regulations governing the packaging and shipping of the wastes to either of the two facilities were discussed in this document. Based on the information given in that document, Waste Management was able to commence shipping of the scintillation cocktail wastes to Hanford. Shipment to a commercial facility is still in negotiations.

We have begun a limited R&D program to remove actinide activity from the scintillation cocktail waste and make it acceptable to a commercial TSD facility. This program is being done in collaboration with the University of Illinois.

4. Transuranic-Waste Treatment

Aqueous wastes solutions containing TRU elements are in temporary storage at the ANL Waste Management facilities. This project involves the volume reduction of the aqueous TRU waste solutions and the shipment of the waste to a storage facility. The Waste Isolation Pilot Plant (WIPP) is the storage facility that is currently being considered. In work done during 1993, we identified (1) the waste form and packaging criteria that must be met in order to transport and place TRU waste at WIPP and (2) limits and criteria for treating TRU-containing wastes (low-level and TRU). Other tasks to be completed in 1994 include: (1) the literature will be reviewed to assess suitable methods available to treat the aqueous waste solutions; (2) a TRU-waste treatment process will be chosen in concert with Waste Management and will be developed and tested on the laboratory scale; (3) a full-scale process will be set up and demonstrated; and (4) training documents will be written, and Waste Management operators will be trained in using the facility.

E. *Production of ^{99}Mo from Low-Enriched Uranium (LEU)*

Molybdenum-99 ($t_{1/2}$ = 66.02 h) decays by beta emission to ^{99m}Tc ($t_{1/2}$ = 6.02 h). The latter nuclide is used in many nuclear medicine applications. For clinical use, it is prepared first in the form of pertechnetate ion (TcO_4^-) and then suitably changed to other chemical forms, depending upon the nature of the application. The TcO_4^- is washed from an alumina-column generator that contains the parent ^{99}Mo by elution with a saline solution. Much of the world's supply of ^{99}Mo is produced from fissioning of high enriched uranium (HEU).

The Reduced Enrichment for Research and Test Reactors (RERTR) program has been active for 16 years at ANL and many countries throughout the world. The objective is to modify reactor and fuel designs so that reactors could switch from HEU (a nuclear weapons material) to LEU (which is not) with no or little loss in flux. Many reactors have converted and many more are in the process. As conversions of reactor fuel proceeded, the amount of HEU being exported from the U.S. for ^{99}Mo production became an ever more visible proliferation concern. The LEU target program for ^{99}Mo production was begun at ANL in 1986 and was active through 1989. However, due to declining budgets for the RERTR program, no work has been done during the past four years. The program became active again in 1993 due to legislation severely limiting the export of HEU for both fuel and targets. An active U.S. program in LEU target and process development is part of that legislation.

As a part of this program, we are studying two LEU target designs. The LEU targets will contain either uranium-metal foil or uranium silicide (U_3Si_2). Either UO_2 or various UAl_x alloys are used in current HEU targets. The silicide fuel is being developed as a LEU substitute for UAl_x alloys, and the uranium metal foils are being developed as LEU substitute for UO_2.

At ANL, we have in storage an irradiated target of uranium silicide (LEU variety). This target was irradiated several years ago and therefore contains stable isotopes of molybdenum, as well as long-lived fission products (^{137}Cs, ^{90}Sr) and activation products (^{239}Pu). We want to separate the molybdenum contained in this target to demonstrate the efficiencies of the target dissolution and molybdenum separation steps proposed by Vandegrift et al.[9] Optimization studies of the dissolution and separation procedures for uranium silicide targets are in progress. Using the optimized procedure, we will complete the dissolution of the irradiated LEU target and recovery of the stable molybdenum in a hot cell. In addition, experiments will begin soon to characterize and optimize the dissolution of uranium metal foils.

[9] G. F. Vandegrift, J. D. Kwok, D. B. Chamberlain, J. C. Hoh, W. E. Streets, S. Vogler, H. R. Thresh, R. F. Domagala, T. C. Wiencek, and J. E. Matos, "Development of LEU Targets for ^{99}Mo Production and Their Chemical Processing--Status 1989," Proc. of the XIIth International Meeting, Reduced Enrichment for Research and Test Reactors, Berlin, September 10-14, 1989, pp. 421-433 (1989).

VI. INTEGRAL FAST REACTOR PYROCHEMICAL PROCESS

The Integral Fast Reactor (IFR) is an advanced reactor concept proposed by, and under development at, ANL. Its distinguishing features are that it is a sodium-cooled, pool-type reactor (all the major components, reactor core, pumps, and heat exchangers are in a large sodium-filled pot); it employs a metallic fuel (an alloy of U, Pu, and Zr clad with a stainless steel-type alloy); and it has an integral fuel cycle (discharged core and blanket materials can be processed and refabricated in an on-site facility). The advantages of this concept are (1) an exceptionally high degree of passive safety, resulting from the use of a metallic fuel with a sodium coolant, and (2) competitive economics, resulting from low costs for on-site fuel recycle and waste form preparation.

The CMT Division is responsible for developing the pyrochemical process for recovering Pu and U from spent core and blanket fuel, removing fission products from the recycled fuel, and incorporating them into suitable waste forms for disposal. To accomplish this, major efforts are directed toward laboratory experiments on process chemistry, engineering-scale demonstration of the process, and studies of IFR waste treatment and management. The process developed in this effort will be demonstrated in the Fuel Cycle Facility (FCF) for the Experimental Breeder Reactor-II (EBR-II) in Idaho. For this demonstration, reprocessed spent fuel will be used to refuel EBR-II for continued operation and to complete the fuel cycle.

A. *Process Development Studies*

The flowsheet developed for the IFR pyrochemical process will handle any mix of fuel from the IFR reactor; the process yields products from which fresh fuel can be fabricated and incorporates fission products and cladding hardware into waste forms suitable for long-term storage. Previous reports in this series have given details of the process flowsheet and chemistry, which we continue to refine. The current reference electrorefining process may be summarized as follows. Spent fuel in its stainless-steel cladding is chopped into approximately quarter-inch lengths and placed in an anode basket. The anode basket is introduced into an electrorefining vessel (Fig. VI-1) that contains an electrolyte of molten LiCl-KCl eutectic salt (an earlier design included a cadmium pool below this electrolyte). The operating temperature is 773 K (500°C). Sufficient oxidizing agent, such as $CdCl_2$, is added to oxidize chemically active fission-product metals (alkali, alkaline earth, and rare earth metals) to their chlorides; these remain in the salt. Enough additional oxidant is added to maintain 2 mol% of actinide chlorides in the salt. The basket is connected to a dc power supply and made anodic; nearly pure uranium is removed from the spent fuel by electrotransport to solid cathodes, then the transuranic (TRU) metals (Pu, Np, Am, and Cm) and some uranium are electrotransported to liquid cadmium cathodes. The cadmium-cathode product will be contaminated with small amounts of rare earths. Noble metal fission products remain in unoxidized form throughout the process; they are removed in the basket with the cladding hulls, although a fraction may fall to the electrorefiner bottom. Radiation levels and heat release that result from buildup of fission products require that fission product chlorides and accumulated noble metals be periodically removed from the salt. The fission product ions will be collected on a zeolite bed by ion exchange, and the noble metals will be removed by filtration.

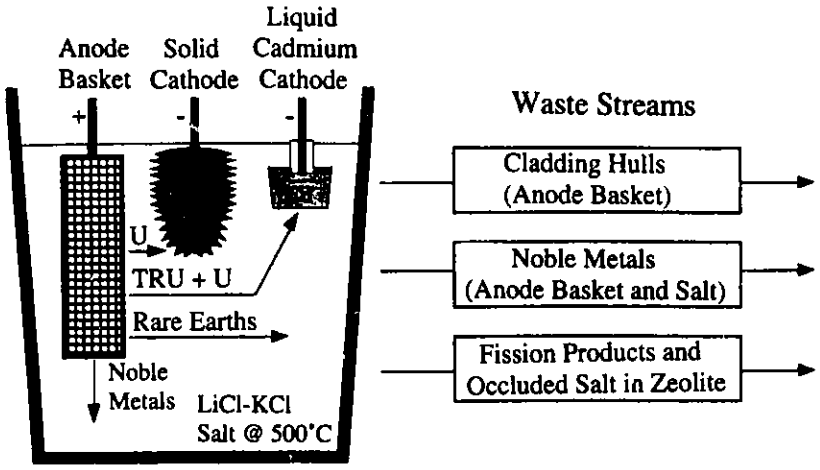

Fig. VI-1. Schematic Diagram of IFR Electrorefiner and Waste Streams

1. Electrotransport to Liquid Cadmium Cathode

During the past year, testing in our laboratory-scale (15-cm-dia) electrorefiner was continued with a new design of liquid cadmium cathode ("pounder"), which incorporates an axial and rotating motion agitator for collection of plutonium. Recent tests were focused on investigating variables which are important to scaleup from 5-cm to 18-cm dia for the cathode crucible. An 18-cm dia crucible is needed for plant-scale collection of non-critical batches of plutonium during electrorefining of spent IFR fuel. To achieve the goal, the Cd-Pu ingots produced at the cathode must contain at least 10 wt% plutonium.

As shown in Fig. VI-2, the pounder cathode is basically an insulated ceramic cylinder which moves up and down and rotates about the cathode current lead. The current lead

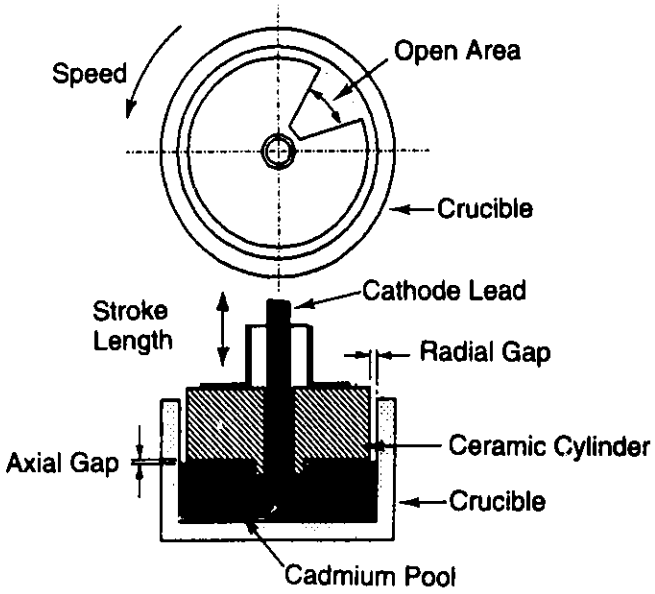

Fig. VI-2.

Schematic of Pounder Design for Liquid Cadmium Cathode

terminates in a cadmium liquid metal pool within a crucible. The cadmium liquid pool interfaces with the cell electrolyte. Access to the bulk electrolyte of the cell is provided through a notch in the ceramic cylinder. The vertical motion of the pounder produces downward forces at the cadmium-electrolyte interface, which cause cathode products to sink into the cadmium pool. Without this agitating motion at the interface, depositing metals tend to grow upward into the salt phase, rather than downward into the cadmium reservoir. The depositing dendrites overflow the crucible and tend to change cathode product composition and cause electrical short circuiting.

The results obtained from 12 experimental runs with the pounder cathode are summarized in Table VI-1. For Runs NE-11 and -12, deposit growth occurred outside the ingot because no pounder motion was applied. No such growth occurred with standard operation of the pounder cathode (Run NE-20: rotation speed, 35 rpm; stroke length, 0.94 cm; current, 1 A). Run NE-13 was carried out to measure the change in cell resistance with pounder position, and the results are given in Table VI-1. Increasing the current from 1 A to 2-3 A (Runs NE-14 and -15) at the cadmium surface or doubling the rotation speed (Run-17) did not have an adverse effect. However, when the rotation speed was lowered from 35 to 7.5 rpm (Run NE-16), product accumulated again outside the cadmium ingot.

The radial gap (see Fig. VI-2) was a concern since it is not practical to make a close fit between the pounder outer diameter and crucible inner diameter. Run NE-18 results indicate that increasing the radial gap from 0.08 to 0.3 cm did not lead to uncontrolled deposit growth up the crucible wall. For Run NE-19, the axial gap was increased from 0.58 to 0.96 cm. (The "axial gap" is defined as the spacing between the bottom surface of the pounder and the liquid cadmium pool surface when the pounder is at the bottom of its stroke.) In Run NE-19, cathode product buildup occurred on the rim of the crucible; this led to short circuiting. When the length of the stroke was shortened from 0.94 to 0.43 cm (Run NE-21), short circuits occurred because of product buildup on the lip of the crucible. This buildup can occur only when there is an electrical connection between the buildup and the cadmium pool. This condition can occur when a metallic (electrically conductive) path forms up the crucible wall. In Run NE-22 the short stroke was retained but the speed was doubled; this did not prevent product buildup on the crucible rim.

Except for those runs where short-circuiting occurred, the goal of loading the cathode to $\geq$ 10 wt% plutonium was achieved. Work is continuing with the pounder cathode to evaluate its performance at high U/Pu ratios and to determine the influence of the presence of rare earth fission products in the electrolyte salt.

2. Process Instrumentation

A new reference electrode for use in monitoring the IFR electrorefiner is under development. This electrode is based on a sparingly soluble zirconium salt and has several advantages over other reference electrodes for molten chloride applications, including rugged and simple construction and *in situ* regeneration. By simple voltammetric measurements with this electrode, it is possible to estimate the relative concentrations of U and Pu in the salt phase. This is important not only to operational monitoring but to materials control and accountancy and facility surveillance for safeguards and non-proliferation purposes.

The key element of the electrode is the sparingly soluble salt, K_xZrCl_{x+2} (where x = 1 or 2). This salt has a low solubility (<0.5 wt %) in potassium-containing melts such as the IFR salt, LiCl-KCl. Formation of a chloride salt with low solubility permits construction of a reference electrode of the second kind. A tight-fitting alumina plug (~10-mm long) is inserted into the bottom of an alumina tube. The tube serves as a sheath for a zirconium wire that is inserted into the tube along with some LiCl-KCl salt. The alumina is wetted by the salt, and the thin film of salt between the tube and the plug serves as a diffusion barrier/liquid junction. The electrode is charged by electrochemically oxidizing the zirconium wire, forming K_xZrCl_{x+2}. The goal in charging the electrode is to saturate the interior salt phase with K_xZrCl_{x+2}. This electrode has proved to be stable for several days if a sufficient concentration of K_xZrCl_{x+2} is formed.

Table VI-1. Results from Tests of Pounder Liquid Cadmium Cathode

Run No.	Variable Tested	Results
NE-11	No Pounder Motion	Material Growth Outside of Ingot
NE-12	No Pounder Motion	Material Growth Outside of Ingot
NE-13	Position vs. Cell Resistance	20% Increase (0.5 → 0.6 Ω) from Top of Stroke to Bottom 5% Change - Rotational Position of Pounder Gap
NE-14	Current Doubled 1 → 2 A	Same Favorable Result as at 1 A
NE-15	Current Tripled 1 → 3 A (current density 165 mA/cm^2)	Same Favorable Result as at 1 A
NE-16	Lowered Speed 35 → 7.5 rpm	Excess Growth Outside of Ingot
NE-17	Increased Speed 35 → 68 rpm	Same Favorable Result as at 35 rpm
NE-18	Increased Radial Gap 0.08 → 0.3 cm	Same Favorable Result as at 0.08 cm
NE-19	Increased Axial Gap 0.58 → 0.96 cm	Developing Short due to Buildup on Crucible Rim
NE-20	Standard Operations, Cadmium Pool Drawdown	Favorable Result
NE-21	Decreased Stroke 0.94 → 0.43 cm	Developing Short, Buildup on Rim
NE-22	Decreased Stroke 0.94 → 0.43 cm Increased Speed 35 → 68 rpm	Developing Short, Buildup on Rim

The presence of a reference electrode in the IFR electrorefiner makes several types of measurements possible. Primarily, it enables the operator to discern if a large change in voltage is primarily due to the cathode or the anode. However, a stable reference electrode also makes possible the *in situ* voltammetric analysis of the salt phase, specifically the U^{3+} and Pu^{3+} concentrations. With a technique as simple as cyclic voltammetry, one can estimate the relative

concentrations of U^{3+} and Pu^{3+} from the ratio of peak heights. Such a voltammogram of U and Pu reduction/oxidation is shown in Fig. VI-3. This voltammogram was taken in our laboratory-scale electrorefiner, containing the zirconium reference electrode described above and a steel wire cathode. There is obviously adequate separation between the uranium and plutonium peaks. By using more sophisticated techniques such as differential pulse voltammetry, anodic stripping voltammetry, or square-wave voltammetry, a more quantitative *in situ* analysis of the salt phase, and perhaps even the metal phase, should be possible.

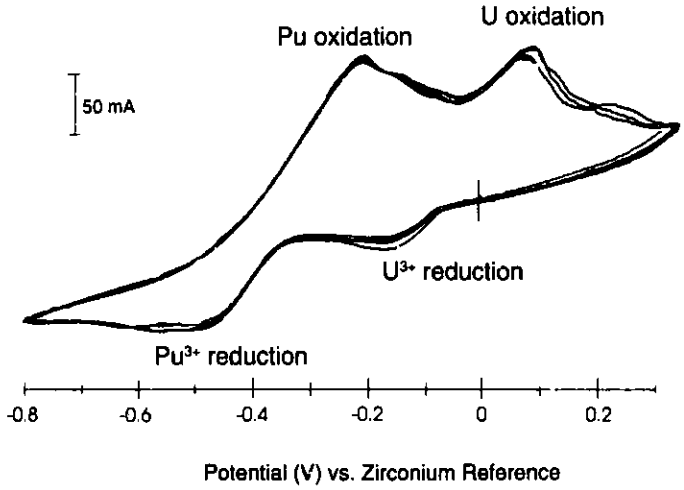

Fig. VI-3.

Cyclic Voltammogram Taken with a Working Electrode in Laboratory-Scale Electrorefiner. Scan rate, 100 mV/s; temperature, 708 K.

A single probe design that incorporates two reference electrodes as well as a working and a counter electrode is being developed. Such a design would allow these *in situ* measurements without requiring any additional penetrations of the electrorefiner cover.

B. *Engineering-Scale Process Development*

In the pyrochemical processing of spent IFR fuel, a heavy metal drawdown step (an operation to reduce the heavy metal concentration in the salt) is required before fission products are removed from the salt in the electrorefiner. At some point in the operation, fission products must be removed from the electrorefiner to reduce the amount of heat generated therein. Results from drawdown tests in an engineering-scale electrorefiner (capable of transporting 10 kg uranium to solid cathode) are presented below. Also reported are results from electrotransport tests to remove zirconium, a major constituent of IFR fuel, from the electrorefiner.

1. Electrorefiner Drawdown Operations

In a previous report,[1] engineering-scale drawdown operations were described in which the uranium concentration in the electrorefiner electrolyte was reduced from 6.68 to 0.015 wt% by using catch-bucket solid cathodes to collect the uranium product. During the

[1] J. E. Battles et al., *Chemical Technology Division Annual Technical Report, 1992*, Argonne National Laboratory Report ANL-93/17, pp. 116-117 (1993).

drawdown of the Fuel Cycle Facility electrorefiner, it may be necessary to remove large amounts of uranium from the electrolyte salt. In the early stages of this drawdown, it is convenient to use a normal solid cathode to collect uranium. Run 101 was completed to demonstrate the growth of a large uranium deposit on a solid cathode at the reduced uranium concentration in the electrolyte that will occur during the drawdown. For the test, Li-Cd alloy was added to the salt to reduce the uranium concentration from the nominal 7.7 wt% (2 mol% UCl_3) to 3.4 wt%; about 1.5 wt% rare earths was also in the electrolyte. The cadmium pool was then made the cell anode, and uranium was transported to the solid cathode. We obtained a deposit of 13.18 kg, containing 81.2 wt% U, 13.6 wt% salt, 2.7 wt% Zr, and 0.8 wt% Cd. The rare earth metals which were in the cathode-product salt were consistent with the amount of rare earths in the electrorefiner salt before the run, indicating no rare earth metal deposition, as expected. The uranium dendrites were much coarser than those normally found with 2 mol% UCl_3 in the salt. This test demonstrated that 10 kg of uranium can be transported to the normal solid cathode during the early stages of a drawdown run. Future work with the engineering-scale electrorefiner will involve tests of advanced electrode designs that are intended to lead to development of a high-throughput electrorefiner.

2. Zirconium Removal Studies

Zirconium is 10 wt% of normal IFR fuel. With repeated electrotransport cycles involving spent IFR fuel, the bulk of the zirconium accumulates in the electrorefiner (in the cadmium anode pool and on vessel and component surfaces). During 1992, removal of this zirconium by electrotransport to a solid cathode mandrel was demonstrated in our engineering-scale electrorefiner.[2] In this report period, experiments were conducted to investigate conditions which would co-transport U and Zr to the same cathode. This has the potential advantage of direct recycle of zirconium, one of the main constituents of the fuel, with the actinides to make new fuel.

For these experiments, an alloy containing 9.17 kg of uranium and 1.02 kg of zirconium was loaded into the baskets of the anodic dissolver. At startup, the cadmium pool in the electrorefiner contained 0.96 kg of zirconium. The first step (Run 95) in the operation was the direct electrotransport of U and Zr from the anodic dissolution baskets to the solid cathode mandrel. Only partial dissolution was attempted, then the cadmium pool in the electrorefiner was made the anode, and the U and Zr which passed into the cadmium pool (fallen dendrites from the solid cathode) were transported to the cathode. This two-step cycle was repeated, and then the dissolution was completed using the cadmium pool as the cathode. After this, we inspected the baskets and found no undissolved alloy. Low rotation speed for the anode baskets (0-20 rpm) and low mixing rates (0 rpm for the cadmium mixer and 0-50 rpm for the salt mixer) were employed, since our earlier tests had indicated that this condition was favorable for simultaneous transport. In normal dissolution, the anode-basket rotation speed is 75 rpm, and 664 Ah is required to dissolve each kilogram of uranium. Under a low rotating speed for the anode baskets (~20 rpm), about 20% more total current flow than normal was required to complete the alloy

---

[2] J. E. Battles et al., *Chemical Technology Division Annual Technical Report, 1992*, Argonne National Laboratory Report ANL-93/17, pp. 117-118 (1993).

dissolution. The cathode product from Run 95 contained 6.56 kg of uranium and 0.78 kg of zirconium.

After this initial run (No. 95), two more runs (Nos. 96 and 97) were conducted to remove the remaining U and Zr from the cadmium pool and complete the transport of the materials which were originally in the anode baskets. At the end of these runs, U and Zr concentrations in the cadmium pool were only 0.025 and 0.084 wt%, respectively. The estimated weights of U and Zr at startup were 9.17 and 1.98 kg, respectively; after the tests, the estimated weights were 9.40 kg and 1.94 kg. These results show a good mass balance and confirm the co-transport of U and Zr.

Figure VI-4 shows the zirconium-rich deposit along with a normal deposit. There is an obvious difference in the appearance of these products. Because of this difference, we carried out a cathode harvester test to ensure that the zirconium-rich product could be readily stripped from the cathode. This harvester device and its operation are described in earlier reports.[3,4] The deposit was harvested in about 3 min, which is not appreciably different from the time obtained with low-zirconium-content deposits.

C. *Development of Waste Treatment Processes*

Work continued on developing processes to recover TRU elements from the spent electrolyte salt and metal discharged from the electrorefiner and to separate the fission products so that the treated salt and metal can be recycled. A waste-treatment flowsheet that incorporates technology that is still in a relatively early stage of development was described in the previous report in this series.[5]

In the present flowsheet, the fission product elements from the spent fuel that accumulate in the electrolyte salt are periodically removed by temporarily reducing the actinide elements from the electrolyte salt into a circulating cadmium stream, extracting residual TRU halides with uranium in cadmium, then passing the salt through a bed of zeolite A. The fission product ions are removed almost completely by exchange with ions from the zeolite. The salt is then mixed with $CdCl_2$ and recontacted with the cadmium stream to oxidize the actinides back into the salt; the zeolite bed becomes the starting material for fabrication of a mineral waste form, which will be either glass-bonded zeolite or sodalite. A metal waste form will be used to dispose the cladding hull fragments that entered the process with the feedstock, unrecovered zirconium, noble metal fission products, and impurities that have been filtered out of the salt along with the steel filters.

---

[3] M. J. Steindler et al., *Chemical Technology Division Annual Technical Report, 1990*, Argonne National Laboratory Report ANL-91/18, p. 117 (1991).

[4] M. J. Steindler et al., *Chemical Technology Division Annual Technical Report, 1991*, Argonne National Laboratory Report ANL-92/15, p. 124 (1992).

[5] J. E. Battles et al., *Chemical Technology Divisior Annual Technical Report, 1992*, Argonne National Laboratory Report ANL-93/17, pp. 118-119 (1993).

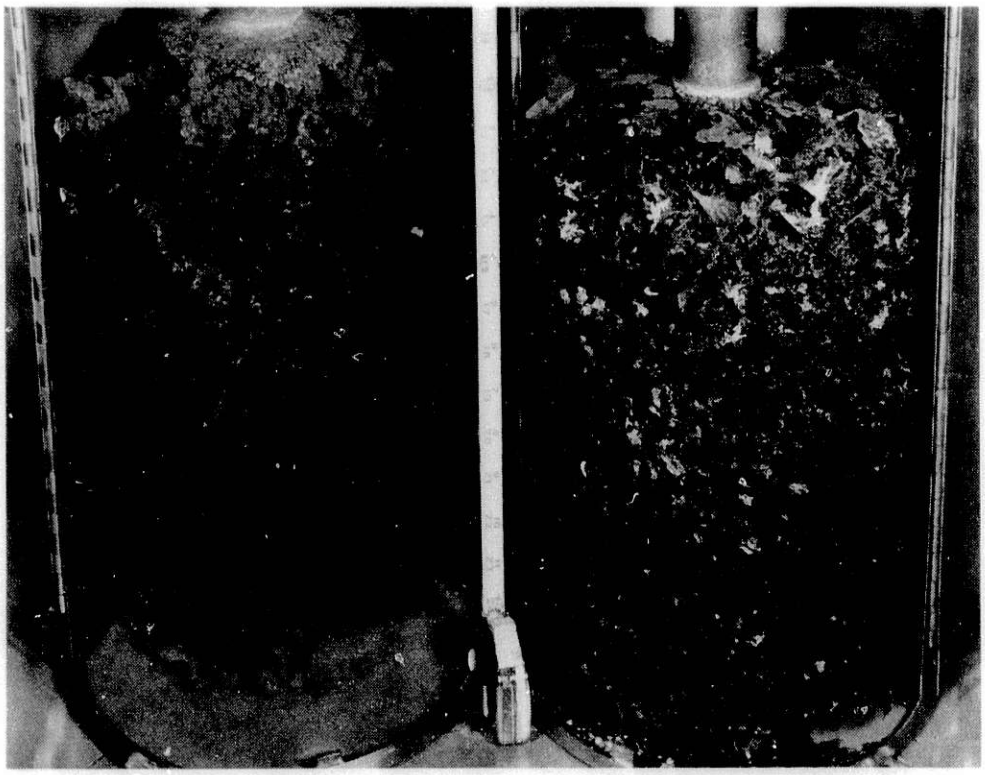

Fig. VI-4. Zirconium-Rich Uranium Deposit (left side) on a Solid Mandrel Cathode. Typical uranium deposit shown on right side for comparison.

1. Development of Pyrocontactor for Salt Extraction

Several steps in the IFR salt purification process employ the use of high-temperature centrifugal contactors ("pyrocontactors") to carry out salt/metal extractions. One of the goals of this work is to develop a continuous metal-salt extraction process that uses multistage, countercurrent pyrocontactors to recover the TRU elements from the spent electrorefiner salt. To that end, a pyrocontactor test system has been built and is being tested with molten cadmium and salt at 773 K. The test system includes a single-stage pyrocontactor with 4-cm-dia rotor, tanks to feed salt and metal to the contactor, tanks to receive salt and metal from the contactor, tanks to clean and treat salt and metal, heated transfer lines, and a glovebox with an argon purification system.

The initial tests included (1) charging, melting, and mixing 74 kg cadmium in the metal treatment tank and 15 kg LiCl-KCl eutectic salt in the salt treatment tank, (2) transferring materials between the treatment tanks, the raffinate tanks, and the feed tanks, and (3) feeding liquid cadmium from the feed tank through the pyrocontactor to the treatment tank.

The first two operations were succcessfully carried out. The maximum gas pressure required for liquid transfer between tanks was 0.2 MPa (35 psi). During this testing, the

equipment furnaces and heaters operated satisfactorily. The agitators for the tanks were operated at up to their maximum speeds of 350 rpm.

The flow tests with liquid cadmium through the pyrocontactor were also satisfactorily completed using both a 0.5- and 0.3-cm dia orifice in the feed line. In tests at 773 K with the contactor rotor spinning at 1800-2700 rpm, the mechanical performance of the pyrocontactor was excellent--no rotor vibration or over-temperature of the motor bearings occurred.

Next, two tests were completed to assess the pyrocontactor operation while liquid cadmium and molten salt at 773 K were fed to the spinning contactor from the feed tanks. The effluents from the contactor flowed to the treatment tanks. The first test was terminated when flooding of the contactor was observed. The flooding was caused by plugging of the metal effluent line and salt feed and effluent lines. Metal and salt samples were collected from the feed and effluent lines after the test and were analyzed by inductively coupled plasma/atomic emission spectrometry. Results indicated essentially no phase crossover from the contactor, i.e., metal exited from the metal effluent line, while salt exited from the salt effluent line. The finding of little phase crossover is particularly encouraging because the metal-to-salt feed ratio was high, about 3:1. After this test, the transfer lines were modified to prevent plugging from occurring again. A second test was then performed with liquid cadmium and salt flowing through the spinning pyrocontactor at 773 K. The average feed rates were 1.0 and 0.67 L/min for cadmium and salt, respectively. During this flow test, the contactor operated very smoothly, no vibration was observed, and the contactor rotation speed was easily controlled. This test demonstrated that feed rates could be controlled and indicated that the entire contents of the electrorefiner can be treated in 4-6 h. A four-stage pyrocontactor is now being designed for further testing of salt extraction.

2. Tests of Salt Stripping

Another step in the salt purification process is salt stripping, in which salt from the extraction step (Sec. VI.C.1) is contacted with a Cd-Li alloy. The lithium reduces essentially all of the uranium and residual TRU elements from the salt, as well as most of the rare earths, but none of the alkali metals and alkaline earths. Tests have been carried out using a salt stripper system which previously had been installed in an argon-filled glovebox adjacent to the engineering-scale electrorefiner.

Before the stripping experiments, a submersible centrifugal pump and transfer line designed for high-temperature service were inserted into the electrorefiner. The pump and transfer line were connected with freeze joints in which silver solder formed a seal. Some difficulties were encountered during the initial attempts to pump the salt. However, after some modifications, 90 kg of LiCl-KCl eutectic salt (containing U, Nd, Ce, and Y as chlorides) was pumped from the electrorefiner at a flow rate of about 4.5 L/min and an impeller speed of 800 rpm. The freeze seals held up extremely well, and the seals were easily made and disassembled. The pump will be modified further to increase its capability for more extended operation. After the salt was transferred, the pump and transfer line were removed, and 150 kg of cadmium was then charged from the electrorefiner to the stripper vessel, equivalent to a depth of about 18 cm.

During the stripping experiments, an inverted cup device was used to charge a 85 wt% Cd-15 wt% Li alloy into the cadmium layer at the bottom of the stripper vessel (Fig. VI-5). The charging device consisted of an inverted cup on a rod. The cup contained the Cd-Li alloy which had been cast into it. The Cd-Li alloy is a liquid at the 773 K temperature of the stripper contents and is lighter than cadmium. When the cup was immersed into the cadmium, the Cd-Li alloy melted, and the lithium reductant was released slowly into the cadmium layer and then came into contact with the salt at the salt-cadmium interface. After insertion of the cup with

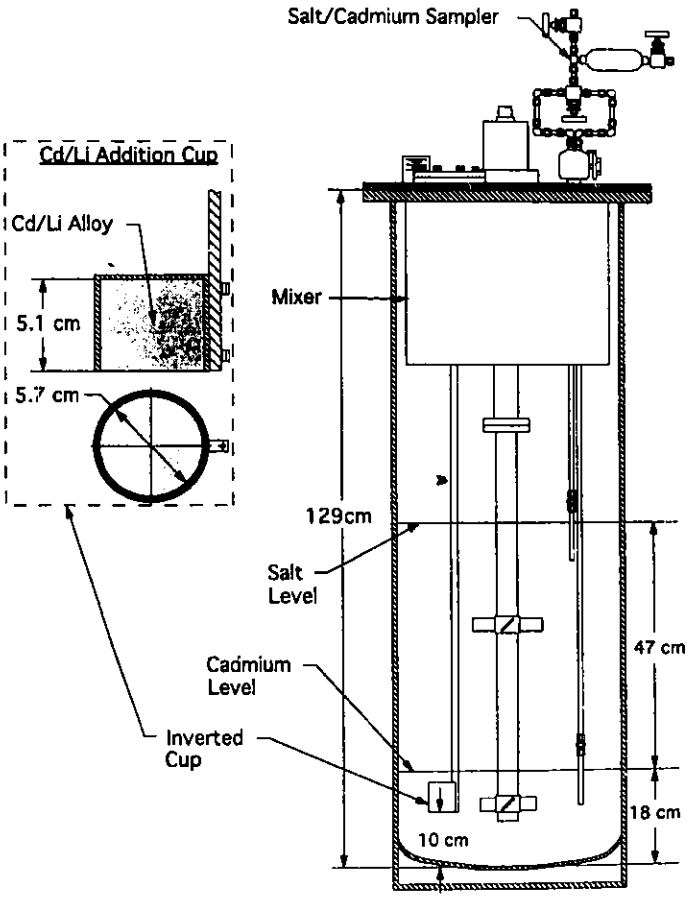

Fig. VI-5.

Schematic of Salt Stripping Apparatus

the alloy, the mixer was turned on, and samples of cadmium and salt were taken at various times. In certain tests, cadmium chloride was added to the stripper vessel. The transfer of uranium and rare earths between the salt and cadmium is dictated by the amount of reductant (Li) or oxidant ($CdCl_2$) added and by the equilibrium between uranium and the rare earths.

Figure VI-6 illustrates the typical behavior of uranium and the rare earths (Nd, Ce, and Y) during these tests (Nos. S4 to S9). Uranium initially transferred from the salt to the cadmium pool as the Cd-Li alloy reductant was added. Further additions of alloy caused Nd and Ce to also transfer from the salt, and finally yttrium began to transfer after several more additions of the reductant alloy. The experimental data agree quite well with the values predicted by our XTRACT computer code, which was based on earlier laboratory-scale experimental determina-

tions of separation factors.[6] During the tests, we monitored the voltage output of an Ag-AgCl reference electrode in the salt. The results show that this electrode can be used to indicate the uranium concentration in the salt. It also can be used to aid in determining the approach to steady-state conditions.

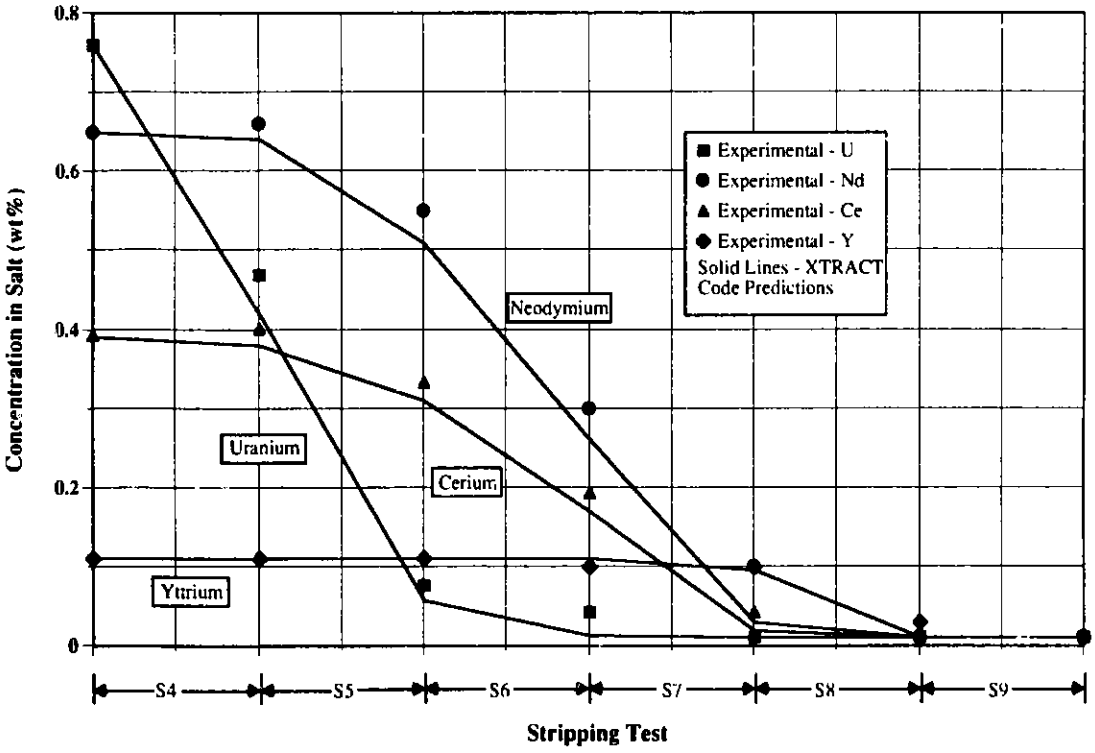

Fig. VI-6. Measured Concentrations of Uranium and Rare Earths in Electrolyte Salt during Stripping Tests S4 to S9. Curves show predicted behavior from our XTRACT computer code.

After the stripping experiments, the stripper vessel and centrifugal pump will be used for tests of our pumped filtration process for removal of insolubles from the electrorefiner salt and cadmium phases.

3. Flowsheet Development for Metal Waste Treatment

The hulls and filters that constitute the stainless steel waste form (along with zirconium and noble metal fission products) will be heavily contaminated with actinide-bearing salt; there may also be actinide oxides and carbides in the salt filters. We are investigating two flowsheets for handling these wastes. In the first flowsheet, these waste constituents are melted under a salt flux containing an oxidant. Actinides in the melt are oxidized into the flux, from which they are removed (by reduction) and returned to the pyroprocess. The resulting stainless

---

[6] J. E. Battles et al., *Chemical Technology Division Annual Technical Report, 1992*, Argonne National Laboratory Report ANL-93/17, pp. 110-111 (1993).

steel ingot has relatively high levels of zirconium and noble metal fission products, but little actinide content.

In the second flowsheet, the rare earths that accumulate in the pyroprocess salt are reduced into a cadmium stream, then extracted into a Cu-Al alloy. Additional copper is added to the alloy, which is then used to encapsulate the hulls, filters, zirconium, and noble metal fission products. Most, but not all, of the cadmium is distilled and returned to the salt purification process; the still bottoms are returned to the Cd/Cu-Al extractor. This relatively low-temperature (<1100 K) method avoids the prolonged high-temperature distillation of cadmium from a matrix of other metals that is required to meet toxicity limits set by the Resource Conservation and Recovery Act. High-temperature distillations have previously been shown to be impractically slow.[7]

Both metal waste treatment processes appear feasible. The relative merits of the resulting waste forms will be evaluated experimentally (see Sec. VI.D.2).

D. *Development of High-Level Waste Forms*

Several techniques are being explored for converting the waste salt and metal into high-level waste forms. To treat the waste salt, it will be sorbed into a zeolite, and the salt-zeolite compound will be hot-pressed into a solid waste form; a sodalite waste form is also being considered. The metal wastes will be combined with a matrix metal or alloy to produce a final waste form.

1. Mineral Waste Form

Use of Zeolite A, $M_{12}(AlO_2{\cdot}SiO_2)_{12}$, is being considered for immobilizing the waste salt. Zeolite A exposed to molten salt contains up to 24 equivalents of cations and 12 equivalents of halide ions per nominal unit cell, $M_{24}(AlO_2{\cdot}SiO_2)_{12}Cl_{12}$. When zeolite exposed to pure LiCl-KCl is used to treat the spent IFR salt, the cations and, to a lesser extent, the anions exchange with the fission products, removing them from the salt. The resulting zeolite bed contains "surface" salt that wets the zeolite particles. Blending the bed with "anhydrous" zeolite that has never been exposed to molten salt, i.e., $Na_{12}(AlO_2{\cdot}SiO_2)_{12}{\cdot}mH_2O$, where m is 3 or 4, removes the surface salt by absorption or "occlusion" in cages within lattices of the zeolite. The amount of salt in the lattice depends on the ratio of zeolite to salt in the blended material; we believe that the salt will be uniformly distributed in the zeolite. This blended material is the starting material for preparing the mineral waste form.

We are evaluating two approaches to the mineral waste form. In the first, the blended material is made to have 6-12 equivalents of halide per unit cell of zeolite; then, it is fabricated into a "monolithic" waste structure that is macroscopically homogeneous by mixing with a glass frit binder and treating with heat and pressure. Small waste form samples made this

---

[7] J. E. Battles et al., *Chemical Technology Division Annual Technical Report, 1992*, Argonne National Laboratory Report ANL-93/17, p. 120 (1993).

way appear promising. In a second, less-developed, approach, the blended material is made to have two equivalents of halide per nominal unit cell of zeolite. It is pyrolyzed to form sodalite. We have found that the pyrolysis process yields sodalite that contains no other mineral phases, as shown by X-ray diffraction; fabrication of monolithic sodalite samples is being investigated. In both approaches, leaching with water according to a method based on the Materials Characterization Center protocol (MCC-1) is used to evaluate the samples. A release rate (normalized to initial concentration) of 1 g/(m^2·day) for all leachable elements is used as a screening criterion.

We have tested 15 glass-bonded zeolite samples (2.5-cm dia, 3-mm thick) prepared from several glass and zeolite compositions. The samples that met the screening criterion had zeolite concentrations from 50 to 75 wt%, although some samples having 75% zeolite showed levels of potassium leaching higher than the screening criterion. Reproducibility of leaching results was good among samples prepared in a similar manner. We also measured mechanical properties for these samples, including Young's modulus (~60 GPa), Vickers hardness (~4.4 GPa), density (2.3 to 2.4 g/cm^3), and Poisson's ratio (0.15); only density varied significantly with glass/zeolite ratio. Initial values of all properties were satisfactory, but testing of larger samples is required before systematic studies of mechanical properties are undertaken.

Also under investigation is a sodalite waste form. Work this year showed that satisfactory conversion to sodalite was possible starting with (1) zeolite having a very high concentration of fission products and (2) zeolite formed into pellets with a clay-mineral binder, although product crystallinity was reduced in the latter. Parametric synthesis studies showed that pyrolysis temperatures of 1000 K are satisfactory, but that temperatures of 1150 K resulted in extensive cesium evaporation from the salt. Leach resistance of the sodalite samples was comparable to that of the zeolite samples. Further work may show the expected improved leach resistance for the sodalite waste form or improvement in some other property, such as ease of fabrication of homogeneous monoliths, that would justify the additional fabrication step. At present, it appears that either waste form could be developed to a satisfactory state.

2. Metal Waste Form

Two forms were under consideration for the metal waste at the beginning of this period. A form based on Cu-Al alloys was investigated to seek a satisfactory alloy composition with regard to corrosion resistance and mechanical properties. We found that most Cu-Al compositions involve intermetallic compounds and are too brittle for use. Although pure copper is adequately corrosion-resistant, aluminum is needed for fission product extraction from cadmium metal. Testing has shown that Cu-Al compositions rich in aluminum undergo rapid corrosion. Testing of copper-rich (>93 wt% Cu) compositions is near completion.

Stainless steel, type HT-9, is the major constituent of the metal waste; melting and fluxing the mixture of stainless steel, zirconium, and noble metal fission products that constitutes the metal waste should give a satisfactory waste form with excellent homogeneity and corrosion resistance. Initial melting and corrosion tests of several mixtures containing HT-9, zirconium, and fission products have been encouraging; a facility for melting and fluxing such mixtures (20-g capacity) is being designed.

3. Waste Qualification

The challenging work of qualifying salt and metal waste forms for repository disposal lies ahead. An IFR Waste Technical Review Group has been formed, with representation from national laboratories (ANL, Oak Ridge National Laboratory, Lawrence Livermore National Laboratory), other DOE sites (Idaho National Engineering Laboratory and Savannah River Plant), and DOE Headquarters (Nuclear Energy, Environmental Restoration and Waste Management, Defense Programs). The group is chartered to function as an advisory body on the merits of various technical approaches to waste qualification, to interact with researchers from other high-level waste programs, and to establish a basis for developing a consensus on waste form requirements and criteria as well as for establishing a national consensus on standard methods for evaluating IFR waste-form performance. The Technical Review Group is committed to establishing a set of IFR waste form requirements and criteria by the end of FY 1994 and to evaluating appropriate waste form performance tests by FY 1995.

VII. ACTINIDE RECYCLE PROCESS

Recovery of actinide elements, particularly the transuranic (TRU) elements, from light water reactor (LWR) spent fuel for use in the Integral Fast Reactor (IFR) offers several benefits for future energy resource conservation and waste management. The TRU elements (primarily Np, Pu, Am, and Cm) are toxic radioactive materials, with long half-lives, that constitute the primary hazard in disposal of spent LWR fuel, and they also act as "poisons" in the low-energy (thermal) neutron environment of LWRs. They render the LWR fuel inefficient after a fairly low burnup because they tend to absorb neutrons rather than generate energy by fissioning. In the high-energy (fast) neutron environment of the IFR, these same TRU elements function efficiently as fuel by fissioning rather than absorbing neutrons. Pyrochemical processes are being developed in CMT for recovery of these TRU elements from LWR spent fuel for use in an IFR. Such a process would offer an attractive alternative to direct repository disposal of LWR spent fuel.

Recent work has narrowed the choices of pyrochemical processes from four to two: the salt transport process and the lithium process. The salt transport process uses calcium in a Cu-Mg-Ca liquid alloy to reduce the spent fuel oxides to metals, and the lithium process uses lithium metal reductant. Work this year has concentrated on development of the lithium process flowsheet, laboratory-scale testing of the salt transport and lithium processes, experiments to determine whether the reductant oxides in the lithium process can be electrolyzed to allow salt recycle, and design and fabrication of an engineering-scale system for testing the actinide recycle process at larger scale.

A. *Process Chemistry and Flowsheet Development*

Over the last several years, we have been investigating three processes employing calcium as reductant for LWR fuel (salt transport process, magnesium extraction process, and the zinc-magnesium process).[1] During this year, another alternative, which employs lithium as the reductant, was also studied. An additional change made during this year eliminated fluoride ions from the reduction salts ($CaCl_2$-CaF_2 and LiCl-LiF) previously under investigation. This latter change was made because of potential deleterious interaction of these ions with proposed mineral waste forms for the spent reduction salt. Successful reductions were made with both the calcium and lithium systems using fluoride-free salt.

The principal steps in the lithium process are as follows. (1) The oxide fuel is reduced with lithium in the presence of LiCl-KCl salt at 500°C. (2) The spent reduction salt is processed electrochemically to decompose the Li_2O reduction product and recover lithium and LiCl-KCl. (3) A small portion of the recovered salt is removed to limit the accumulation of unreduced fission products (e.g., Cs, Sr, I, and rare earths), and the bulk of the salt and the recovered lithium are recycled. (4) The removed salt is processed for disposal by techniques under development for waste salt from the IFR process (Sec. VI.D). (5) After separation from the

---

[1] J. E. Battles et al., *Chemical Technology Division Annual Technical Report, 1992*, Argonne National Laboratory Report ANL-93/17, pp. 128-129 (1993).

reduction salt, reduced fuel and less reactive fission products (e.g., Zr, Mo, and Pd), which precipitate during the reduction step, are processed in an electrorefiner to recover purified uranium on a solid cathode while the transuranic (TRU) elements are recovered in a liquid cadmium cathode. (6) The uranium is stripped from the cathode and melted to separate it from the occluded electrorefining salt, which is recycled; the uranium is recovered as an ingot. (7) The TRU product is recovered as an ingot after distilling away cadmium for recycle. (8) The uranium is placed in long-term storage for future use as reactor blanket material, and the TRU product is fed into the IFR fuel cycle as a fuel resource.

The lithium process has been selected as the reference process for further development and engineering demonstration. The lithium-based process has the following advantages over calcium-based processes: the waste salt would be similar to that generated by the IFR electrorefiner and would not require development of an additional form for salt disposal; the lithium-based reduction conditions, which are less corrosive than those for the calcium systems, can be conducted in steel vessels rather than more expensive materials such as tungsten; reaction temperatures may be as low as 500°C as opposed to a minimum of 800°C for calcium systems; and the solid metal products of reduction are compatible with the IFR electrorefiner, which has a well-developed U-TRU separation technology. The potential problems with the lithium process are lower reduction rates, difficult separation of reduced fuel from reduction salt, and dependence on electrorefining, which may be slow. Development of a high-throughput electrorefiner will be a major program objective. The salt transport process, which is the most attractive of the calcium-based processes, is being retained as a back-up.

The mass-balance flowsheet for the lithium process will continue to be refined as the process evolves. Data from the laboratory-scale experiments, discussed below, will assist in this task. Also, a computer model will be developed to simulate the process and to assist in future work on designing a large-scale system.

B. *Laboratory-Scale Testing*

In the salt transport process, the TRUs and rare earths from the spent LWR fuel are extracted from a Cu-Mg reduction (donor) alloy with $MgCl_2$, leaving the noble metal fission products and uranium behind. They are subsequently stripped from the $MgCl_2$, using a Zn-Mg (acceptor) alloy. Experiments in support of the salt-transport process have been directed toward conducting reductions of simulated spent fuel (25-100 g) using fluoride-free salts and determining the chemistry of curium (a difficult TRU element to study because of its high specific radioactivity) in the reduction and transport steps. Successful reductions of UO_2 and simulated fuel have been conducted at 800°C using $CaCl_2$ as the salt phase. In fact, this simulated fuel experiment gave the best reduction of any of the experiments ever conducted. (Previous experiments gave 99.8% to 99.9% reduction. This experiment resulted in >99.99% reduction, and the salt was clean enough to be classified as "non-TRU.") The chemistry of curium in this process was determined using a ^{243}Cm tracer. The tracer was added to the simulated fuel as CmO_2, and it was followed through the reduction and salt transport steps. The distribution ratios for ^{243}Cm in the donor and acceptor stages were determined to be 0.48 and 0.028, respectively. These data indicate that curium will be reduced into the metal phase along with the other TRU elements and readily transported to the Zn-Mg phase during salt transport.

As mentioned earlier, the lithium process has replaced the salt transport process as the reference process for actinide recycle. Successful reductions of UO_2 and simulated fuel have been demonstrated using the lithium process with LiCl and LiCl-KCl salts. Analysis of the results from the simulated fuel reductions showed that, under our experimental conditions, the TRU elements were more completely reduced at 500°C than at higher temperatures (Table VII-1). We also measured the solubility of the Li_2O reduction product in these salts because it affects the quantity of salt that must be used in the process. The solubility of Li_2O in LiCl was determined to be 8.7 wt% at 650°C and 11.9 wt% at 750°C, while that in 60 wt% LiCl-40 wt% KCl was found to be significantly lower, 1.5 wt% at 500°C and 2.1 wt% at 600°C. On the basis of these results, the current lithium process employs an operating temperature of 500°C and reduction salt of 60 wt% LiCl-40 wt% KCl.

Table VII-1. Average Percent Reduction of TRU Elements Achieved with Lithium Process

Reduction Temp., °C	Percent Reduction Achieved
500	99.98
600	97.3
650	91.2
700	86.2
750	75.7

A laboratory-scale retort consisting of a bell jar, bell-jar lift, and internal components (e.g., induction coil and feedthrough) is being built to distill and separate materials generated during testing of the actinide recycle process. These materials will consist of process metals and salts containing residual uranium and the TRU product. This laboratory-scale retort has been installed in a glovebox. The work done this year includes the design and fabrication of the retort's induction coil, the induction feedthrough, and the ceramic crucible and graphite components used to contain the process melts. During testing of the retort, the temperature at the ceramic crucible was raised from room temperature to 850°C in 57 min. After the temperature was held at 850°C for 27 min, it was raised to 1050°C (temperature recorder limit), and the induction coil was de-energized. During the test, the induction power supply output was varied from 10 to 20% of full power. The coil reached its maximum temperature of 250°C when the crucible was at 1050°C. The testing of the retort was very encouraging and indicates that it will be capable of distilling cadmium and Zn-Mg (at ~850°C) and melting uranium (at 1100 to 1200°C). The next step is to test the retort operation in the presence of the appropriate metal melts and vapors. This test will be done by conducting zinc distillations under nonradioactive conditions.

C. *Electrolysis of Lithium Oxides*

The initial step in the lithium process uses lithium metal to reduce the oxide fuel in a molten salt. The Li_2O reduction product dissolves in the molten salt. To minimize waste, an

electrochemical step is proposed to recover the salt and lithium for recycle by converting the Li_2O back to lithium metal.

The standard free energies of formation and corresponding decomposition potentials of relevant compounds at 650°C are listed in Table VII-2. These data indicate the possibility for selective decomposition of Li_2O in the presence of chloride and fluoride salt. The selectivity is enhanced by the use of a consumable carbon anode which, because of the free energy of formation of CO and CO_2, reduces the decomposition potential of Li_2O.

Table VII-2. Standard Free Energies of Reaction and Decomposition Potentials at 650°C

Reaction	Standard Free Energy, kcal/mol	Decomp. Potential, V
$Li_2O(c) \rightarrow 2\ Li(l) + 1/2\ O_2(g)$	113.8[a]	2.47
$Li_2O(c) + C(c) \rightarrow 2\ Li(l) + CO(g)$	67.6[a]	1.47
$LiCl(l) \rightarrow Li(l) + 1/2\ Cl_2(g)$	79.9[b]	3.46
$LiF(c) \rightarrow Li(l) + 1/2\ F_2(g)$	125.9[b]	5.46
$LiF(c) + 1/4C(c) \rightarrow Li(l) + 1/4\ CF_4(g)$	78.5[c]	3.40

[a]From Ref. 2.
[b]From Ref. 3.
[c]From Ref. 4.

Six experiments in a specially designed electrochemical cell were performed to investigate electrowinning of lithium metal from Li_2O in molten LiCl (or $CaCl_2$-LiCl) salt. To successfully regenerate the reduction salt and lithium metal by electrowinning of the metal from Li_2O, anode performance is one of the key factors that has to be improved. A major problem encountered in our early experiments was carbon contamination of the electrolyte salt from the consumable carbon anode. This set of six experiments allowed us to evaluate different anode materials (gold, graphite, glassy carbon, and Zircaloy). Table VII-3 summarizes the experimental conditions and results. The results from EW-22 indicate that gold metal is unstable as an oxygen-evolving anode for Li_2O electrolysis in $CaCl_2$-LiCl salt. Good performance was achieved when a graphite rod anode (EW-24) was employed for the Li_2O electrolysis in molten LiCl salt at 644°C. Equally good performance was obtained with a glassy carbon anode (EW-30). A comparable amount of

---

[2] L. B. Pankratz, "Thermodynamic Properties of Elements and Oxides," U.S. Department of the Interior, Bureau of Mines, Bulletin No. 672 (1982).

[3] L. B. Pankratz, "Thermodynamic Properties of Halides," U.S. Department of the Interior, Bureau of Mines, Bulletin No. 674 (1984).

[4] M. W. Chase, Jr., et al., "JANAF Thermochemical Tables," Part 1, Vol. 14, Supplement No. 1, National Bureau of Standards (1985).

carbon dust was produced in the electrolyte during electrolysis with either a glassy carbon anode or a graphite anode. The average carbon particle size formed from the glassy carbon anode (14.9 μm) was smaller than that formed from a graphite anode (22.5 μm).

Table VII-3. Conditions and Results for Lithium Electrowinning Experiments

Expt. No.	Cathode	Anode	Salt	Temp., °C	Cell Voltage, V	Cell Current, A
EW-22	Cylindrical Steel	Gold Wire	$CaCl_2$-LiCl	605-607	3.0	0.01-1.75
EW-24	Steel Rod	Graphite Rod	LiCl	644-648	3.0	0.07-16.2
EW-25	Steel Rod	Zircaloy 4 Tube	LiCl	641-645	0.1-3.0	0-19.3
EW-27	Steel Rod	Zircaloy 4 Tube	LiCl	644	3.0	0.04-23
EW-28	Steel Rod	Zircaloy 4 Tube	LiCl	644	3.0	9-32
EW-30	Steel Rod	Glassy Carbon Rod	LiCl	647-648	3.0	0.5-4.6

Zircaloy tubes (EW-25, -27, and -28) were also tested as consumable metal anodes for Li_2O electrolysis in molten LiCl salt. If anodes could be made from the Zircaloy cladding of the LWR fuel, there would be no addition to the total waste stream of the actinide recovery process. On the basis of standard free energies of formation at unit activities and 1173°C, the decomposition potentials for Li_2O and LiCl with an active zirconium metal anode are -0.06 and 1.16 V, respectively. The negative potential indicates that the electrolysis cell should pass current spontaneously, i.e., it should function as a battery, reacting Li_2O with zirconium and forming ZrO_2. The LiCl decomposition potential is lower than those shown in Table VII-2 because of reaction of LiCl with zirconium to form $ZrCl_4$. The electrolysis experiment EW-25 did not function as expected, however. The initial open-circuit cell voltage was found to be -0.195 V. The electrolysis was started at an applied cell voltage of 0.1 V, but the cell showed no observable current. Then, the voltage was increased at increments of 0.1 V. The cell showed no observable current in the voltage range of 0.1 to 1.6 V, and it only showed significant current when the applied cell voltage reached 1.7 V and higher (Fig. VII-1). The maximum current of 19.3 A for experiment EW-25 (limited by the capacity of the power supply) was obtained at 3.0 V. (The corresponding maximum current density is 635 mA/cm^2.) Post-test examination showed that particles of both ZrO_2 and oxygen-saturated zirconium metal had settled to the bottom of the crucible below the Zircaloy anode. These performance data and post-test observations indicate that, under these operating conditions, Li_2O was not electrolyzed directly. However, equilibrium thermodynamic data suggest electrolysis of LiCl salt and reaction of chlorine with zirconium. The $ZrCl_4$ produced could react chemically with Li_2O in the salt to produce ZrO_2 and LiCl. The results are somewhat uncertain concerning the conversion of Zircaloy to ZrO_2. The reaction mechanism is not well understood, and more work is planned.

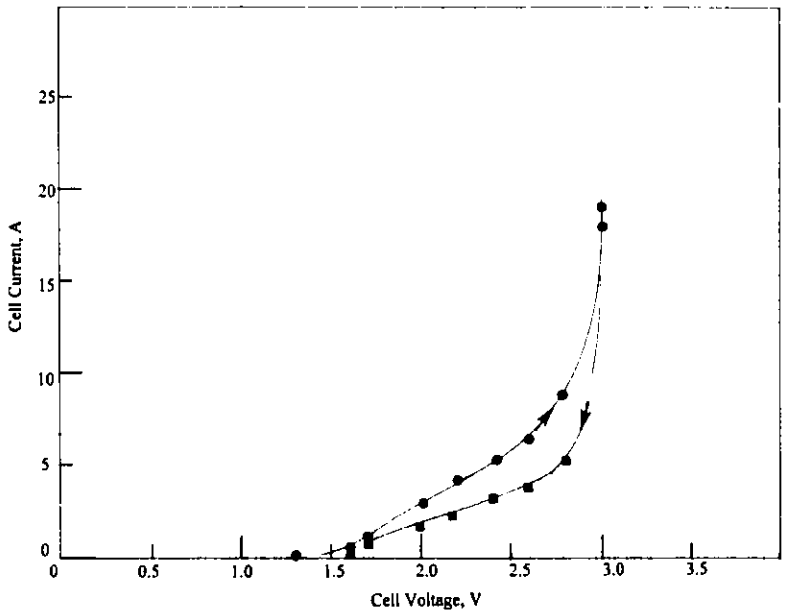

Fig. VII-1. Cell Voltage vs. Current for Experiment EW-25

The results of electrolysis experiments EW-25, -27, and -28 were surprising in that very high currents were achieved (Table VII-3), and rapid corrosion of the zirconium was observed. The former is advantageous in that rapid electrolysis of Li_2O was attained, but the latter finding is even more interesting in that it offers a possible method for removing Zircaloy cladding from spent fuel. The mechanism of corrosion and the rate of Zircaloy removal will be studied further in light of this new decladding possibility.

Our future work will also focus on improving the consumable carbon anode by fast removal of anode gases, better containment and removal of carbon dust from the anode region, and optimization of the anode shroud porosity, pore size, and material. We will also continue selection and evaluation of alternative anodes, such as non-consumable anodes (e.g., ferrites and ceramic/metal composites), and consumable metal anodes that are compatible with the lithium process.

D. *Engineering-Scale Testing*

Engineering-scale tests are planned to demonstrate the feasibility of each step in the lithium and salt transport processes being developed in the laboratory. The test equipment is configured for use of up to 20 kg of simulated spent LWR fuel as feed. The tests will be run in an enclosure consisting of a large (7.6 x 2.4 x 2.6 m) argon-filled glovebox and a smaller nitrogen-filled glovebox with an interconnecting transfer lock. The argon glovebox contains five vessels that will support the demonstration of the reduction, extraction, retorting, casting, electrowinning, and electrorefining process steps. Sufficient argon glovebox construction, process equipment fabrication, safety analyses and reviews, and safety tests have been completed this year to initiate the first run in October 1993. The first run tested the lithium-reduction process

step using a UO_2 fuel containing representative LWR simulated fission products but no TRU elements. Approximately 4.4 kg of simulated fuel was reduced using the reduction vessel shown schematically in Fig. VII-2. The product uranium (and fission product metal) will be analyzed and stored until an electrorefiner capable of processing the product is available. Future tests will employ a simulated LWR fuel containing TRU elements.

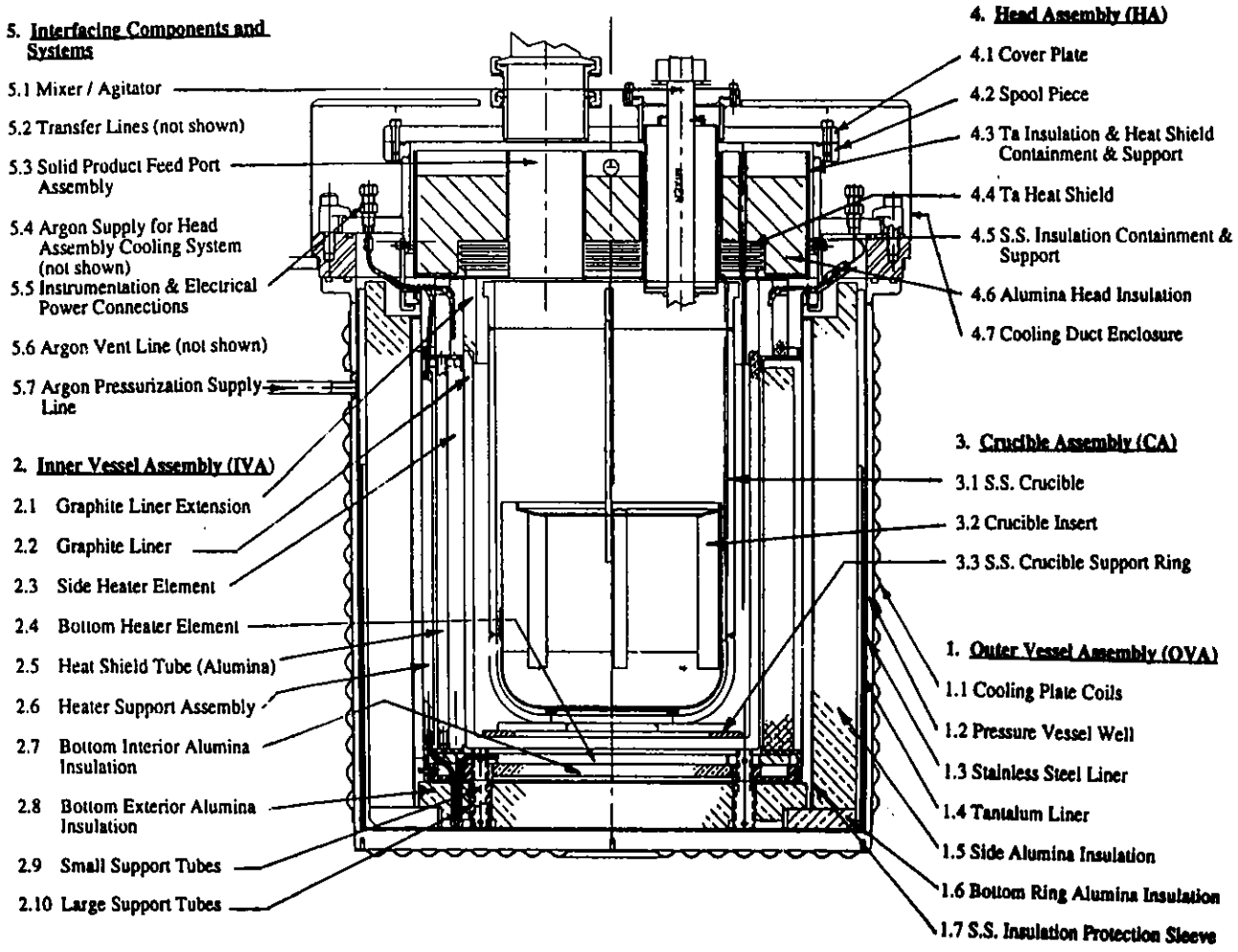

Fig. VII-2. Schematic of Reduction Vessel

VIII. APPLIED PHYSICAL CHEMISTRY

The program in applied physical chemistry involves studies of the thermodynamic, thermophysical, and transport behavior of selected materials in environments simulating those of fission and fusion energy systems.

A. *Thermophysical Properties Studies of Integral Fast Reactor Fuel*

We are performing measurements and analyses to provide needed information on the thermophysical properties of Integral Fast Reactor (IFR) fuel (see Sec. VI). In 1993, this effort was focused on determining the Pu-Zr phase diagram, examining fuel/cladding chemical interactions by use of synchrotron sources, and updating the IFR data base on materials properties. This information will be used to evaluate reactor performance during normal and off-normal operation.

1. Plutonium-Zirconium Phase Diagram

The IFR design employs a U-Pu-Zr alloy fuel clad in stainless steel. We are, therefore, interested in phase diagrams of fuel and stainless steel components, especially at high temperatures. In previous work done in collaboration with researchers at École Polytechnique (Montreal, Canada),[1-4] we presented our assessments of the U-Zr, Fe-U, Pu-U, and Fe-Zr phase diagrams, and this effort is continued here with our assessment of the Pu-Zr system.

Phase diagrams for the Pu-Zr system have appeared in several compilations but are based predominantly on the 1960 report of Marples.[5] We optimized the liquidus and solidus for the Pu-Zr system in a previous publication.[6] Our assessment of this phase diagram is based principally on the work of Marples,[5] Taylor,[7] and Ellinger and Land.[8]

---

[1] L. Leibowitz, R. A. Blomquist, and A. D. Pelton, *J. Nucl. Mater.* **167**, 76 (1989).

[2] L. Leibowitz and R. A. Blomquist, *J. Nucl. Mater.* **184**, 47 (1991).

[3] L. Leibowitz, R. A. Blomquist, and A. D. Pelton, *J. Nucl. Mater.* **184**, 59 (1991).

[4] L. Leibowitz, R. A. Blomquist, and A. D. Pelton, *J. Nucl. Mater.* **201**, 218 (1993).

[5] J. A. C. Marples, *J. Less-Common Metals* **2**, 331 (1960).

[6] L. Leibowitz, E. Veleckis, R. A. Blomquist, and A. D. Pelton, *J. Nucl. Mater.* **154**, 145 (1989).

[7] J. M. Taylor, *J. Nucl. Mater.* **30**, 346 (1969).

[8] F. H. Ellinger and C. C. Land, "On the Plutonium-Zirconium Phase Diagram," in *Proceedings of the Fourth International Conference on Plutonium and Other Actinides*, Ed., W. N. Miner, Vol. 17, Nuclear Metallurgy, New York, pp. 686-698 (1970).

The general methods used in our analysis have been described elsewhere.[9-11] The calculations are performed with programs of the FACT (Facility for the Analysis of Chemical Thermodynamics) computer system and involve determining equations for the Gibbs free energies of all phases existing in an alloy system as functions of temperature and composition. Phase diagrams are derived by calculating the lowest common tangents to the Gibbs energy-composition curves. This procedure ensures thermodynamic consistency of the resulting phase diagram and provides a powerful means for assessing conflicting data.

Figure VIII-1 shows our optimized Pu-Zr phase diagram. In deriving this phase diagram, we took the liquid solution to be ideal, as was done in our previous assessments. The Pu(ε)/Zr(β), Pu(δ), and Zr(α) phases were optimized simultaneously. All other phases were then optimized with respect to these phases. Three fixed points on the phase diagram were used in the optimization: the Pu(ε)/Zr(β) + Pu(δ) azeotrope; the eutectoid formed by these two phases with Zr(α); and the Pu(δ) + Zr(α) + θ eutectoid.

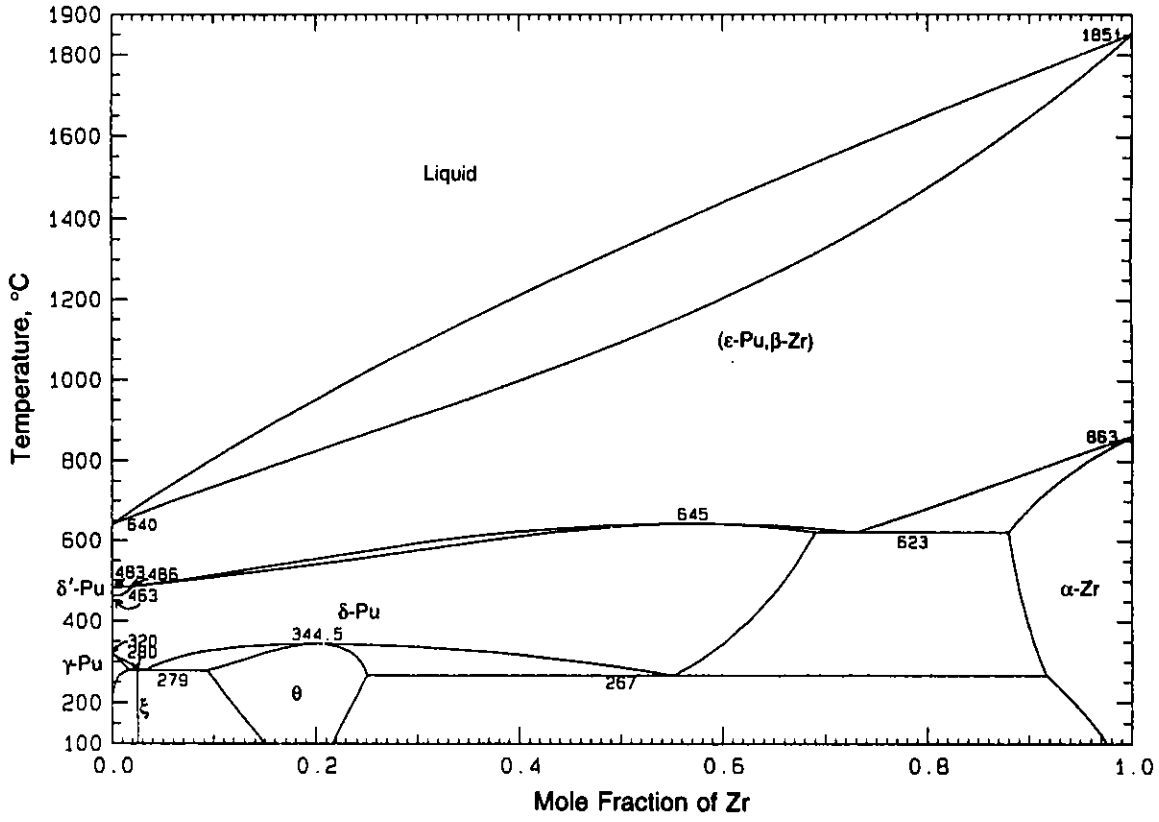

Fig. VIII-1. Optimized Pu-Zr Phase Diagram

---

[9] C. W. Bale, A. D. Pelton, and W. T. Thompson, *F*A*C*T Guide to Operations*, McGill University/École Polytechnique, Montreal (1985).

[10] A. D. Pelton, in *Physical Metallurgy*, 3rd ed., Eds., R. W. Cahn and P. Haasen, North-Holland Publishing, New York, p. 328 (1983).

[11] A. D. Pelton, in *Materials Science and Technology*, Vol. 5, Eds., R. W. Cahn, P. Haasen, and E. J. Kramer, VCH Weinheim, Germany, p. 1 (1991).

The Pu(δ') Henrian solution was optimized from the invariant with Pu(ε)/Zr(β) and Pu(δ). This is generally depicted as a peritectoid reaction, with only two sources[7,12] reporting a eutectoid. Most sources agree that the solubility of Zr in Pu(δ') lies between 1 and 2 at.%, and the peritectoid temperature is 485°C. Our calculated peritectoid temperature of 486°C is well within the experimental temperature limits. The calculated solubility of Zr is 1.8 at.% at the peritectoid. The corresponding equilibrium compositions of the Pu(ε)/Zr(β) and Pu(δ) phases are 1.5 and 2.0 at.% Zr, respectively.

The thermodynamic properties of the θ phase were optimized from two fixed points: the eutectoid with Pu(δ) and Zr(α) and the congruent transformation point to Pu(δ). In both cases we used the temperatures reported by Marples[5] of 345°C for the transformation point and 267°C for the eutectoid. We also tried to accommodate as many of the single-phase X-ray data points attributed to this phase as possible on the plutonium side. We have taken the nominal stoichiometry of this phase to be Pu_4Zr. The phase was studied with a general defect model for nonstoichiometric phases.[13] The congruent transformation point of the θ phase was calculated as 344.5°C at 20 at.% Zr, and the eutectoid formed by this phase with Pu(δ) and Zr(α) was calculated to be 267°C.

The ξ phase has been found to exist over the approximate composition range from 2.5 to 3.0 at.% Zr.[14] The unit cell has been determined,[15] and the ideal composition is probably $Pu_{28}Zr$ (3.4 at.% Zr). In the present assessment, the composition 2.55 at.% Zr used by Sandenaw and Harbur[14] in their measurements of the heat capacity has been employed as the stoichiometric composition. We have optimized the ξ phase to decompose peritectoidally to Pu(γ) and Pu(δ) at 280°C. According to our calculations, the ξ phase forms a eutectoid with the Pu(δ) and θ phases at 279°C. The eutectoid composition is 3.3 at.% Zr, and the corresponding composition of the θ phase is 9.4 at.% Zr. The optimization of the Pu(γ) phase was based on the same peritectoid as for the ξ phase. The calculated solubility of Zr in the Pu(γ) phase is 1.5 at.% at the peritectoid, and the corresponding composition in the Pu(δ) phase is 3 at.% Zr.

All the available literature data are generally well correlated by our optimization analysis (Fig. VIII-1), which yields reasonable and simple thermodynamic expressions for all phases. The calculated phase boundaries for most of the phase diagram are probably within ± 5°C or ± 3 at.% of the true values. The only part of the optimized phase diagram which may prove questionable is the high plutonium region at low temperature. Some further experimental measurements are necessary to clarify this area.

---

[12] A. A. Bochvar, S. T. Konobeevsky, V. I. Kutaitsev, T. S. Menishikova, and N. T. Chebotarev, "Interaction Between Plutonium and Other Metals in Connection with Their Arrangement in Mendeleev's Periodic Table," in *Proceedings of the Second United Nations International Conference on the Peaceful Uses of Atomic Energy*, Vol. 6, United Nations, Geneva, Switzerland, pp. 186-190 (1958).

[13] L. Li and A. D. Pelton, École Polytechnique, Montreal, private communication (1992).

[14] T. A. Sandenaw and D. R. Harbur, *J. Chem. Thermodyn.* **5**, 459 (1973).

[15] W. H. Zachariasen and F. H. Ellinger, *Unit Cell of the Zeta Phase of the Plutonium-Zirconium and the Plutonium-Hafnium Systems*, Los Alamos Scientific Laboratory Report LA-4367 (1970).

2. Phase Identification in U-Zr Fuel Diffusion Couples

In a collaborative effort with researchers at the ANL Intense Pulsed Neutron Source and the Fuels and Engineering Division, we are conducting synchrotron radiation studies to investigate the compatibility of metallic nuclear fuel and stainless steel cladding. During IFR operation, interdiffusion of fuel and cladding components could degrade the cladding over time, in part by forming brittle intermetallic phases or phases with relatively low melting temperatures. To better understand fuel/cladding chemical interactions, Keiser and Dayananda[16] performed isothermal interdiffusion experiments. In these studies, scanning electron microscopy (SEM) combined with energy-dispersive X-ray (EDX) analyses was used to measure composition profiles across the diffusion zones, from which kinetic information was calculated. Intermetallic phase identification was not possible, however, because crystal structures cannot be determined by SEM. Conventional crystallographic techniques (such as standard X-ray diffractometry) could not resolve the micron-sized phase layers in the diffusion zones. Transmission electron microscopy was not considered because that would involve formidable sample preparation difficulties with these easily oxidized, radioactive samples.

The high X-ray fluxes associated with synchrotron radiation sources, on the other hand, make them ideally suited for studying small phases because X-ray intensities are still significant even after substantial beam collimation. Unlike SEM, synchrotron radiation can reveal both composition (via fluorescence) and structure (via diffraction). We performed X-ray diffractometry of an IFR fuel/cladding diffusion couple at the National Synchrotron Light Source (NSLS) at Brookhaven National Laboratory. The techniques developed to study IFR materials can be extended to other material systems in which the characterization of microscopic structures is important.

We prepared a diffusion couple between a U-Zr fuel alloy and a Ni-Cr alloy as detailed in Ref. 16. The diffusion zone in the Ni-Cr/U-Zr couple was approximately 100 μm thick with nine distinct layers (Table VIII-1). Five of these layers consisted of mixtures of two phases; four of the regions were less than 10 μm wide. X-ray diffraction scans of this couple were performed at the NSLS. For each phase, we considered the following: (1) a qualitative matching of the diffraction line positions, (2) the effects of solubility of other elements that could produce shifts in the lattice parameters, (3) preferred orientation ("texture"), and (4) the volume fraction of the phases.

The U-Ni and Zr-Ni binary systems have many stable intermetallic phases. It was necessary to systematically examine published diffraction and structural data to verify the existence of each possible phase. Often there were no more than one to three uniquely defining diffraction peaks for a given phase. Despite the complicated morphology of the diffusion zone, the combination of a small beam (i.e., a small scattering volume) and excellent instrument resolution was sufficient to confirm the existence of the primary phases expected from the SEM results (Table VIII-1). It is interesting to note that, although nickel diffuses readily, chromium does not and appears to be hindered from diffusion by the UNi_5 layer. A possibility for the future

---

[16] D. D. Keiser, Jr., and M. A. Dayananda, *J. Nucl. Mater.* **200**, 229 (1993).

Table VIII-1. Phase Layers in the Ni-Cr/U-Zr Diffusion Couple

Layer	Presumed Phases	Thickness, μm
1	Cr + UNi_5	5
2	UNi_5	5
3	$UNi_{3.5}$ (δ, ε)	3
4	U_5Ni_7	4
5	(U, Zr)Ni_2	16
6	(U, Zr)Ni_2 + U_6Ni	14
7	U_6Ni + (Zr, U)$_7Ni_{10}$	15
8	(Zr, U)$_7Ni_{10}$ + U	20
9	(Zr, U)$_2Ni$ + U	25

is use of synchrotron instrumentation that provides X-ray fluorescence, X-ray diffraction, and extended X-ray absorption fine structure (EXAFS) analysis simultaneously for a given sampling region.

3. IFR Materials Data Base

In 1988, a data base on the properties of IFR materials was assembled. In collaboration with the Fuels and Engineering Division, we are updating this materials data base. Our initial effort was focused on the thermodynamic and transport properties of sodium (the IFR coolant) as a function of temperature. Data on vapor pressure, heat capacity, density, compressibility, surface tension, thermal conductivity, viscosity, and related properties of sodium have been added to the data base. Recommended values are given, as are estimated uncertainties. In addition to recommended equations for these properties, equations of the form required by the reactor accident modeling code, SASS, have been derived.

Examination of literature data showed significant differences for both the phase-transition enthalpies and the transition temperatures of fuel and fission-product elements. We have thus initiated efforts to provide updated properties data dealing with the IFR fuel. The data on the plutonium phase transitions were updated during the past year. We also examined the available data on the thermal conductivity and thermal diffusivity of U, Pu, Zr, and alloys of these elements and found that data on Pu and Pu-containing alloys are very limited. New measurements on relevant alloys containing plutonium are greatly needed to provide reliable data for reactor code calculations and accident risk assessment.

B. *Fusion-Related Research*

A critical element in the development of a fusion reactor is the blanket for breeding tritium fuel. We are conducting experimental and calculational studies with the objective of determining the feasibility of using lithium-containing ceramics (e.g., Li_2O, $LiAlO_2$, Li_4SiO_4, and

Li_2TiO_3) as breeder materials. During this report period, experiments were conducted to evaluate tritium release from the candidate breeding material Li_2TiO_3 and to assess the tritium release characteristics from beryllium neutron multiplier.

1. Tritium Release from Ceramic Breeders

The goals for fusion power are to produce energy in as safe, economical, and environmentally benign a manner as possible. To ensure environmentally sound operation, low activation materials should be used where feasible. The ARIES Tokamak Reactor Study has based reactor designs on the concept of using low activation materials throughout the fusion reactor.[17] For the tritium breeding blanket, the choices for tritium breeding materials are limited. Lithium titanate is an alternative low activation ceramic material for use in the tritium breeding blanket. To date, very little work has been done on characterizing the tritium release from lithium titanate and developing the requisite properties data base. Finn et al.[18] performed some early work which showed that lithium titanate has some attractive breeder blanket properties, including excellent tritium release. To extend the data base on Li_2TiO_3, we have performed several tritium release tests with this ceramic material.

Lithium titanate spheres were prepared by two methods: cold pressing of commercially available Li_2TiO_3 powder (Alfa Products) or extrusion/tumbling of a Li_2TiO_3-binder-water mixture. The latter were sintered at either 1225 or 1400°C. The samples were then irradiated, and the tritium release examined in post-irradiation annealing tests, following procedures described previously.[19,20] Anneals were carried out under a purge gas flow (pure He, He-0.1% H_2, pure Ar, or Ar-0.1% H_2) in Temperature Programmed Desorption (TPD) experiments at a constant heating rate (1, 2, or 5°C/min) and in constant-temperature experiments covering 330-950°C. The tritium release was monitored on-line by either an ionization chamber or a proportional counter. In addition, integrated values for the tritium released during an anneal were obtained by oxidizing the tritium and collecting it in ethylene glycol traps for later analysis. Anneals generally lasted 24 h at each temperature, with the ethylene glycol traps removed for tritium analysis just prior to a temperature increase.

Constant-temperature anneals under a purge gas of He-0.1% H_2 or Ar-0.1% H_2 were performed on extruded material sintered at 1400°C. A typical set of tritium release curves is shown in Fig. VIII-2. A large majority of the tritium in the sample is released at a relatively low anneal temperature, in this case 330°C. This release compares favorably with other candidate ceramics.[21] However, it appears that a small amount of tritium remains in the sample and will

---

[17] F. Najmabadi et al., *The Aries Tokamak Reactor Study*, University of California at Los Angeles Report UCLA-PPG-1323 (1991).

[18] P. A. Finn, T. Kurasawa, S. Nasu, K. Noda, T. Takahashi, H. Takeshita, T. Tanifugi, and H. Watanabe, in *Proceedings of the 9th Symposium on Engineering Problems of Fusion Research*, IEEE, New York, p. 1200 (1981).

[19] J. P. Kopasz, C. A. Seils, and C. E. Johnson, *J. Nucl. Mater.* **191-194**, 231 (1992).

[20] J. M. Miller, S. R. Bokwa, D. S. MacDonald, and R. A. Verrall, *Fusion Technol.* **19**, 996 (1991).

[21] J. M. Miller and R. A. Verral, "Performance of a Li_2ZrO_3 Sphere Pac Assembly in the CRITIC-II Irradiation Experiment," Proc. of the Sixth Int. Conf. on Fusion Reactor Materials, Stresa, Italy (1993).

not be released at this temperature, no matter how long the anneal continues. Similar behavior has been reported for tritium release from lithium aluminate.[22] This behavior suggests that tritium is being released from several different types of sites. For all the samples subjected to constant-temperature anneals, the percentage of the tritium released during the first anneal at temperatures between 330 and 450°C varied from 72 to 90% of the total tritium in the sample, with the percentage released not strictly dependent on the anneal temperature. The majority of the remaining tritium was released during a second anneal at temperatures between 533 and 653°C. The fraction of the total released at these temperatures varied from 24% to about 5%. The fraction still present in the sample after this second 24-h anneal was less than 11% of the total amount released during all the anneals (final anneal at > 827°C). The tritium release during the first anneal was fit to a first-order desorption equation. The slope obtained from a plot of the natural log of the desorption rate constant versus the inverse temperature gave an activation energy of 40 kJ/mol. Following the same procedure for the second anneal yielded an activation energy of 128 kJ/mol.

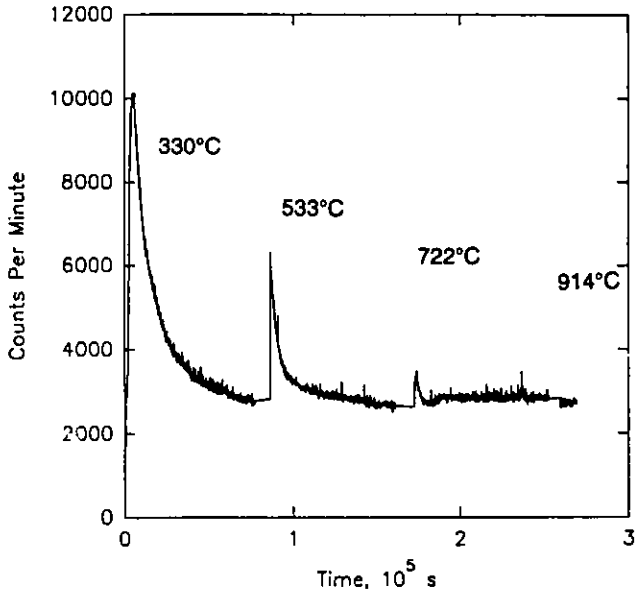

Fig. VIII-2.

Tritium Release from Li_2TiO_3 for Successive Step Anneals at 330°C, 533°C, 722°C, and 914°C

The TPD experiments were performed at ANL and Atomic Energy of Canada, Ltd. Assuming a first-order desorption mechanism, one can calculate an activation energy for a single peak in a TPD plot by using the following equation:

$$\ln (T_m^2/H) = (E/R)(1/T^2) + C \qquad (1)$$

where T_m is the temperature at which the peak maximum occurs, E is the activation energy, H is the heating rate, R is the gas constant, and C is a constant. For overlapping peaks, it is difficult

[22] J. P. Kopasz, S. Tistchenko, and F. Botter, in *Fabrication and Properties of Lithium Ceramics III*, eds., I. J. Hastings and G. W. Hollenberg, American Ceramic Society, Westerville, Ohio, p. 315 (1992).

to determine the location of the maximum for each peak. Thus, we fit the complete TPD curve to the first-order desorption equation for a linear temperature increase.[23] Equation 1 was then used as a check for consistency between runs at different heating rates.

Figure VIII-3 presents a typical TPD spectrum obtained in a pure helium purge gas for the ceramic sintered at 1225°C, which exhibited the best tritium release of the samples tested. Deconvolution of the TPD curve assuming first-order desorption yields five desorption peaks, also shown in Fig. VIII-3. The activation energies, maximum temperatures, and relative areas calculated for these five peaks are given in Table VIII-2. All of the activation energies, except the 48 kJ/mol for the second peak, are in good agreement with the activation energies calculated from Eq. 1. For the second peak, an activation energy was obtained by starting with an activation energy of 40 kJ/mol (determined from isothermal anneals) and then optimizing the fit to the overall TPD curve.

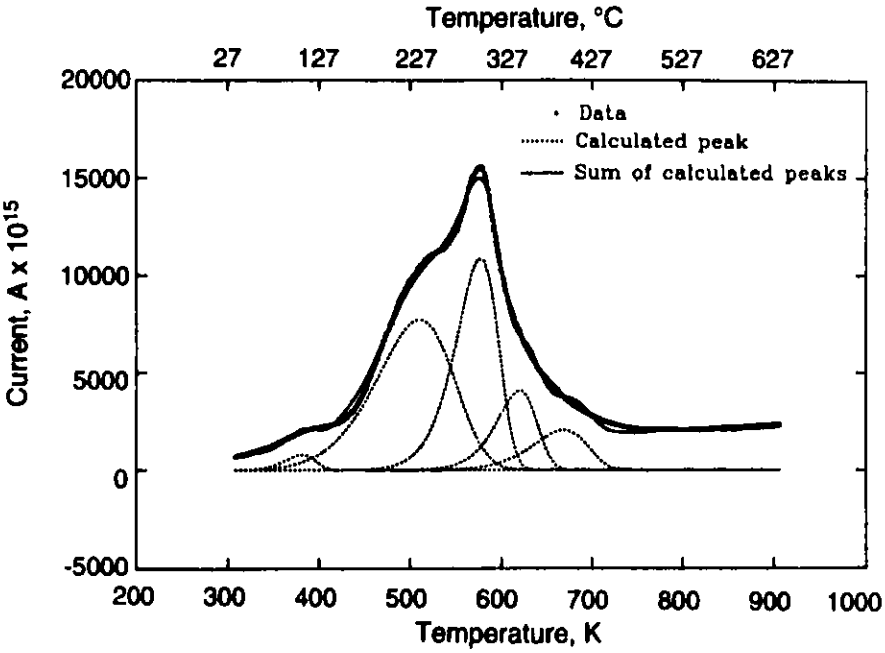

Fig. VIII-3. Spectra from Temperature Programmed Desorption for Li_2TiO_3 Sintered at 1225°C (purge gas, pure helium; heating rate, 2°C/min)

The data can also be analyzed using second-order desorption. In this approach, the data are best fit to three second-order curves and one first-order curve. The activation energies determined are 42, 75, 99, and 117 kJ/mol. For desorption into a pure purge gas, it is expected that tritium desorption would follow a second-order mechanism. The activation energies calculated here are in very good agreement with those reported for desorption of water from

[23] A. W. Smith and S. Aranoff, *J. Phys. Chem.* **62**, 684 (1958).

Table VIII-2. Calculated Activation Energies, Maximum Peak Temperatures, and Areas from Deconvolution of TPD Curve for Li_2TiO_3 Ceramic Sintered at 1225°C. (First-order desorption assumed.)

E_a, kJ/mol	T_m, °C (K)	Area, %
71	108 (381)	1.8
48	237 (510)	43.4
117	303 (576)	34.3
143	347 (620)	12.2
121	395 (668)	8.3

anatase and rutile of 36 kJ/mol, 55-69 kJ/mol, and 104 kJ/mol.[24] This suggests that the main mechanisms for desorption from Li_2TiO_3 involve dissociation of Ti-OH species.

The TPD spectra for the cold-pressed sample of Li_2TiO_3 in pure helium or pure argon consisted of a single narrow peak centered at about 422°C. The exact position of the peak varied from sample to sample, with the range covering about 20°C. This variation made it impossible to use Eq. 1 to obtain an activation energy for this peak. However, the peak position is comparable to that for the peak with an activation energy of 121 kJ/mol calculated for the material sintered at 1225°C.

The TPD spectra of tritium desorption from lithium titanate were compared for the cases of pure He and He-0.1% H_2 (heating rate of 2°C/min and titanate sintered at 1225°C). When hydrogen is added to the purge gas, the peaks centered at 108 and 395°C in the TPD curve for pure helium (see Fig. VIII-3 and Table VIII-2) disappear, while the peak centered at 237°C shifts to higher temperature, 285°C, and decreases in relative intensity from 43% of the total area under the curve to 10%. The peak at 303°C in pure helium shifts to slightly lower temperature, 294°C, and increases in intensity from 34 to 54%, while the peak at 347°C shifts to 373°C. There also appears to be new peaks centered at about 527°C, which account for about 25% of the tritium released in He-0.1% H_2. The overall result for hydrogen addition to the purge gas is a shift in the tritium release to higher temperature. This finding is unusual since hydrogen addition has been shown to be beneficial to tritium release in other lithium ceramic systems. The mechanism involved in the shift of tritium release to higher temperature with hydrogen addition to the purge gas is not yet known. Future efforts on development of the tritium breeder blanket will focus on tritium recovery issues, especially those related to surface release mechanisms and the role that hydrogen plays in the release process.

[24] M. Egashira, S. Kawasumi, S. Kagawa, and T. Seiyama, *Bull. Chem. Soc. Japan* **51**, 3144 (1978).

2. Tritium Release from Beryllium Neutron Multiplier

The SIBELIUS experiment is a Chemical Technology Division (U.S.)/European Community collaborative test[25] designed to identify performance-limiting issues associated with the use of beryllium as a neutron multiplier in ceramic breeder blankets. Small quantities of tritium are generated in the beryllium via a ^{9}Be-neutron reaction producing tritium and helium. Because the buildup of the tritium could become a safety issue, there is strong interest in tritium removal. Prior tritium release studies on beryllium have been on materials that have served as a reflector in a nuclear reactor. Generally, these reflector materials have remained in place for several years at low temperature, e.g., less than 100°C. When these reflector materials have been examined under isothermal anneal conditions, they have exhibited burst release of tritium at high temperatures. The objective of our current studies was to critically examine the tritium release characteristics of the beryllium discs and to characterize any differences in tritium behavior from beryllium discs located adjacent to steel and beryllium discs located adjacent to ceramic.

The experiment was conducted in the Siloe reactor (Grenoble, France). The irradiation vehicle consisted of eight capsules, seven of which were independently purged with a He-0.1% H_2 gas mixture. One capsule was not purged and contained beryllium pellets to obtain data on lifetime void swelling. Of the purged capsules, four were used to examine beryllium/ceramic (Li_2O, $LiAlO_2$, Li_4SiO_4, Li_2ZrO_3) and beryllium/steel (Types 316L and 1.4914) compacts; two contained only ceramic (Li_2O and $LiAlO_2$); and one contained 0.5-mm Li_4SiO_4 pebbles in contact with beryllium discs. The capsule containing the Li_4SiO_4 pebbles was operated at 450°C, while the other seven capsules were operated at 550°C.

Stepped-temperature anneal experiments were run on the beryllium and ceramic discs in five of the purged capsules (see Table VIII-3). The anneals covered temperatures of 550, 650, 750, and 850°C for 24 h at each temperature. A He-0.1% H_2 gas mixture flowing at 100 cm^3/min purged the sample contained in a quartz apparatus. Two independent tritium release curves were obtained, one from an on-line ion-chamber measurement and one from a gas-collection/bubbler system followed by liquid scintillation counting.

Table VIII-3 lists, in summary form, all the available data for tritium release from the beryllium discs in the five SIBELIUS capsules. Each capsule contained a stack of 17 discs. The discs were arranged so that beryllium-steel and beryllium-ceramic discs alternated in the stack, with the first disc in each stack being a beryllium disc. The German data are taken from a recent publication by Dienst et al.[26]

The ratios of tritium measured to tritium calculated for the beryllium discs adjacent to steel (namely, samples 2-1, 3-1, 5-1, and 6-1) are close to unity and thus suggest that the

---

[25] N. Roux, M. Briec, M. Bruet, T. Flament, C. Johnson, M. Masson, A. Terlain, and F. Tournebize, *J. Nucl. Mater.* **179-181**, 827 (1991).

[26] W. Dienst, D. Schild, and H. Werle, *Tritium Release of Li_4SiO_4, Li_2O, and Beryllium and Chemical Compatibility of Beryllium with Li_4SiO_4, Li_2O, and Steel (SIBELIUS Irradiation)*, Kernforschungszentrum Karlsruhe Report KfK-5109 (December 1992).

Table VIII-3. Tritium Content in Beryllium Discs from the SIBELIUS Experiment

Sample Number[a]	Origin	Pellet Weight, g	MBq Tritium Released	Tritium Retained, 10^8 Bq/g		Meas./Calc. Ratio for Retained Tritium
				Meas.	Calc.	
1-1	Ger	0.1890	191	10.10	3.84	2.63
1-6	Ger	0.1771	719	40.60	3.84	10.57
2-1	USA	0.1829	112	6.12	5.57	1.10
2-7	USA	1.1891	190	10.04	5.57	1.80
2-9	Ger	0.1877	238	12.67	5.57	2.27
2-15	Ger	0.1761	244	13.85	5.57	2.49
3-1	USA	0.1882	136	7.23	7.71	0.94
3-7	USA	0.1874	236	12.59	7.71	1.63
5-1	USA	0.1865	130	6.97	8.12	0.8
5-7	USA	0.1861	218	11.71	8.12	1.44
5-9	Ger	0.1868	229	12.26	8.12	1.51
5-15	Ger	0.1720	271	15.75	8.12	1.94
6-1	USA	0.1858	105	5.67	6.67	0.85
6-7	USA	0.1846	187	10.15	6.67	1.52

[a]First digit in sample number indicates the following: 1 = Li_4SiO_4 pebbles, 2 = Li_4SiO_4 pellets, 3 = $LiAlO_2$ pellets, 5 = Li_2O pellets, and 6 = Li_2ZrO_3 pellets. The second indicates the location of the sample in the stack.

neutronic calculations for tritium generation are satisfactory. These results also indicate that very little tritium has left the beryllium at 550°C, at least for this fluence level. However, beryllium sample 1-1, which is from the capsule containing the Li_4SiO_4 pebbles operated at 450°C, shows an abnormally high tritium content for a beryllium disc adjacent to steel. It is unlikely that the high tritium content is due solely to the lower temperature operation.

For the remainder of the beryllium discs within the body of the stack, where beryllium was in contact with a ceramic pellet, the measured-to-calculated tritium ratio is significantly greater than unity, ranging from 1.44 to 2.49. In fact, the ratio reaches 10.57 if one includes the capsule with Li_4SiO_4 pebbles (sample 1-6) at 450°C. In examining the data further, we identified two numerical groupings for the measured-to-calculated tritium ratio. The Li_4SiO_4 samples form one group, where the ratio ranges from 1.80 to 2.49 (10.57 if the pebbles are included), while the other ceramics form another group, where the ratio ranges from 1.44 to 1.94. There are also some differences in the measured-to-calculated ratio between laboratories and between materials. For the Li_4SiO_4, the USA value (1.80 for disc 2-7) is somewhat lower than

that of the German value (2.27 for disc 2-9). The comparison for Li_2O is mixed; the measured-to-calculated ratios for discs 5-7 and 5-9 are quite similar, while the value for disc 5-15 is high at 1.94. This latter ratio is the only outlier in this data set.

As a first approximation, we assumed that the "excess" tritium in the beryllium discs was caused by recoil of tritium from the higher tritium-generating ceramic disc. This assumption may have some merit. However, the relative loading of tritium in the adjacent beryllium discs does not rigorously correspond to the relative tritium generation rates for each ceramic. Our further analysis indicated that it does not appear to be simply tritium recoil that sets the tritium concentration in the beryllium disc, but tritium recoil plus additional material characteristics that ensures tritium retention.

A typical tritium release curve for the beryllium discs was found to be similar to that of previous isothermal anneal experiments on lithium ceramics.[27] That is, the tritium release generally showed a sharp increase with each increasing temperature increment. This increased release reached a maximum, which quickly settled down with time. There did not appear to be any "burst" release with increasing temperature as observed with the beryllium reflector materials; indeed, the amount of tritium available for release decreased significantly once the temperature had been increased above 650°C.

Figure VIII-4 presents data on tritium release from four different investigations covering different beryllium samples and temperatures of 300-900°C. As arranged in the figure,

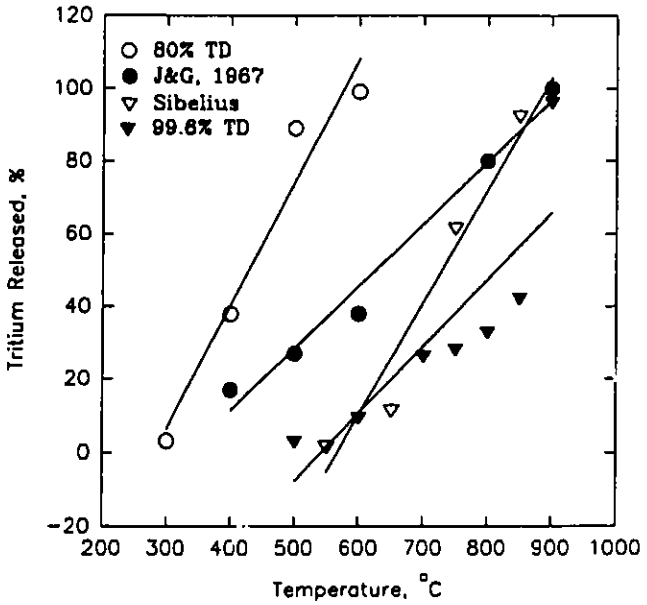

Fig. VIII-4.

Tritium Release as Function of Temperature from Different Beryllium Samples. See text for further explanation.

[27] C. E. Johnson, T. Kondo, N. Roux, S. Tanaka, and D. Vollath, *Fusion Eng. Des.* **16**, 127 (1991).

these materials are a low-density material (80% TD), a high-density arc-cast material analyzed by Jones and Gibson,[28] a high-density arc-cast disc containing <300 ppm BeO from the SIBELIUS experiment, and a high-density (99.6% TD) beryllium sample analyzed by Billone and Baldwin.[29] The 80% TD material exhibits the best release characteristics, with significant tritium being released at 400°C. The tritium release from the SIBELIUS beryllium discs is not as high as the Jones and Gibson data, at least at temperatures below 800°C, but is higher than the 99.6% TD data at temperatures above 600°C. Because of the many variables covered in these four experiments, it is difficult to develop a firm picture of the optimum material. What does appear to be attractive is to select a lower density beryllium and ensure that blanket designs include beryllium temperatures of 500°C or above. Optimizing the density and temperature parameters is certain to provide conditions that facilitate ease of tritium release.

---

[28] P. M. S. Jones and R. Gibson, *J. Nucl. Mater.* **21**, 353 (1967).

[29] M. Billone and D. Baldwin, "Tritium and Helium Behavior in Porous Beryllium," Proc. of Int. Workshop on Ceramic Breeder Blanket Interactions, Tokyo, Japan, October 26-29, 1992, 267 (1992).

IX. BASIC CHEMISTRY RESEARCH

Basic chemistry research is being pursued in three areas: (1) catalytic chemistry associated with molecular energy resources and novel pre-ceramic polymers; (2) materials chemistry of high-temperature superconducting oxides, electrified metal/solution interfaces, molecular sieves, thin-film diamond surfaces, effluents from wood combustion, and molten silicates; and (3) geochemical processes involved at mineral/fluid interfaces and in water/rock interactions occurring in active hydrothermal systems.

A. *Fluid Catalysis*

This program uses an array of *in situ* high-pressure spectroscopic and kinetic techniques to explore new catalytic chemistry and catalytic reaction mechanisms for the transformation of simple precursor molecules that serve as raw materials for many industrial processes. Precursors of interest include those of the C_1 chemical industry, e.g., CH_4, CO, CO_2, and CH_3OH; the ammonia synthesis precursors, i.e., N_2 and H_2; and the ceramic precursors, e.g., $(CH_3)_4Si$, $(CH_3)_3B$, and $Al_2(CH_3)_6$. Current activities encompass research into homogeneous catalytic chemistry in supercritical fluids, catalytic and stoichiometric organometallic processes associated with the production of advanced materials, and catalytic processes for the selective functionalization of methane and other hydrocarbons.

1. Catalytic Chemistry in Supercritical Fluids

The oxo process for the hydroformylation of olefins is the largest scale industrial homogeneous catalysis process. It is used to generate alcohols and aldehydes that are used as industrial solvents (e.g., plasticizers), detergents, and agricultural chemicals. World oxo-process capacity exceeds 5 million tons of product per year.[1]

The oxo process converts olefins ($RCHCH_2$) to the next higher homologous aldehyde [$RCH_2CH_2C(O)H$] and/or alcohol ($RCH_2CH_2CH_2OH$) by the reactions

$$RCHCH_2 + H_2 + CO \rightharpoonup RCH_2CH_2C(O)H \quad (1)$$

$$RCH_2CH_2C(O)H + H_2 \rightharpoonup RCH_2CH_2CH_2OH \quad (2)$$

Selectivity to produce alcohols and aldehydes is a key issue in oxo catalysis, and the most commonly used cobalt carbonyl catalyst, $Co_2(CO)_8$, is gradually being replaced with a more selective, albeit more expensive, rhodium catalyst, $HRh(CO)[P(C_6H_5)_3]_3$. We have been studying

---

[1] I. Kirshenbaum and E. J. Inchalik, "Oxo Process," in *Encyclopedia of Chemical Technology*, 3rd ed., Vol. 16, John Wiley & Sons, New York, pp. 637-653 (1981).

the $Co_2(CO)_8$ catalyzed process in supercritical fluid solvents in high-pressure NMR probes[2-4] and have recently determined that the selectivity for linear products using this catalyst is greatly improved with use of a supercritical CO_2 fluid.[5,6] Also, we have measured the thermodynamic properties for a key hydrogen activation step in this process, namely,

$$Co_2(CO)_8 + H_2 \rightleftharpoons 2\ HCo(CO)_4 \qquad (3)$$

Our thermodynamic results for the enthalpy (ΔH = 19.7 ± 0.8 kJ/mol) and entropy [ΔS = 18 ± 2 J/(mol•K)] are close to those measured by Ungváry[7] for the reaction in a conventional liquid medium, n-heptane, which is of the type commonly used in oxo catalysis. The results indicate that, at least in terms of the important equilibrium in Eq. 3, the reaction in CO_2 is well behaved, and that the improved selectivity and other benefits (such as eliminating gas/liquid mixing problems and providing a more energy-efficient pathway for product separation) that are anticipated to occur with the use of the supercritical medium might be realized without suffering other penalties in reaction performance.[8,9]

These same thermodynamic measurements, however, highlight an inconsistency in bond energies that occurs with the $Co_2(CO)_8$-derived species of the oxo reaction. The bond energy for the Co-Co bond in $Co_2(CO_8)$ medium can be calculated from

$$BDE(Co\text{-}Co) = 2\ BDE(H\text{-}Co) + \Delta H(Eq.\ 3) - BDE(H\text{-}H) \qquad (4)$$

The value for BDE(H-Co) in $HCo(CO)_4$ has recently been determined to be 280 kJ/mol by electrochemical measurements.[10,11] This value, combined with the enthalpy change for the reaction in Eq. 3 and the known BDE for the H-H bond in H_2 (435 kJ/mol), yields a value of 145 kJ/mol for BDE(Co-Co). However, this BDE(Co-Co) is much higher (>80 kJ/mol) than the 63 kJ/mol determined by mass spectral measurements of the equilibrium constants for the following dissociation[12]:

---

[2] J. W. Rathke, *J. Magn. Reson.* **85**, 150-155 (1989).

[3] R. J. Klingler and J. W. Rathke, *Prog. Inorg. Chem.* **39**, 113-180 (1991).

[4] J. W. Rathke, "Toroids as NMR Detectors in Metal Pressure Probes and in Flow Systems," U.S. Patent No. 5,045,793, issued September 3, 1991.

[5] J. W. Rathke, R. J. Klingler, and T. R. Krause, *Organometallics* **11**, 585-588 (1992).

[6] J. W. Rathke and R. J. Klingler, "Cobalt Carbonyl Catalyzed Olefin Hydroformylation in Supercritical Carbon Dioxide," U.S. Patent No. 5,198,589, issued March 30, 1993.

[7] F. Ungváry, *J. Organomet. Chem.* **36**, 363-370 (1972).

[8] M. J. Steindler et al., *Chemical Technology Division Annual Technical Report, 1991*, Argonne National Laboratory Report ANL-92/15, pp. 162-168 (1992).

[9] M. McHugh and U. Krukonis, *Supercritical Fluid Extraction*, Butterworths, Stoneham, MA (1986).

[10] M. Tilset and V. D. Parker, *J. Am. Chem. Soc.* **111**, 6711-6717 (1989).

[11] M. Tilset and V. D. Parker, *J. Am. Chem. Soc.* **112**, 2843 (1990).

[12] D. R. Bidinosti and N. S. McIntyre, *Can. J. Chem.* **48**, 593-597 (1970).

$$Co_2(CO)_8 \rightleftharpoons 2\ (CO)_4Co\bullet \qquad (5)$$

Because much of our current work on the oxo reaction has been involved with the radical product of Eq. 5, namely, the tetracarbonylcobalt radical, we decided to independently determine the enthalpy change for Eq. 5, which would provide a direct measurement of the Co-Co bond energy in $Co_2(CO)_8$. Since the tetracarbonylcobalt radical is paramagnetic, high-pressure NMR measurements of the magnetic susceptibilities of solutions containing $Co_2(CO)_8$ at elevated temperatures would provide the requisite data. We reasoned that a qualitative result would be immediately apparent with this approach, namely, if the Co-Co bond were as strong as 145 kJ/mol, virtually no dissociation would occur, and no paramagnetism would be measurable under any conditions achievable in our pressure probes, while if the bond were as weak as 63 kJ/mol, strongly paramagnetic solutions would be obtained even at relatively low temperatures.

Thermolysis of the Co-Co bond in $Co_2(CO)_8$ via Eq. 5 changes the magnetic susceptibility of its solutions due to the production of $(CO)_4Co\bullet$ radicals. The extent of the dissociation in Eq. 5 was measured by determining the temperature dependence (120-225°C) of the volumetric susceptibility for a gas phase solution of $Co_2(CO)_8$ in compressed carbon monoxide (concentration of 9.95 M). As might be expected based on the results for supercritical CO_2 fluid, $Co_2(CO)_8$ is also reasonably soluble in CO when it is compressed to a relatively high density. Using methane in a small cylindrical glass capillary within the probe as reference, we measured the requisite volumetric susceptibilities by a modification of Evan's method.[13] The susceptibilities were calculated from the chemical shift difference between the ^1H NMR signals of methane inside of, and exterior to, the capillary. Note that our gas phase measurements are advantageous in that unlike measurements in liquids, corrections for temperature-dependent gas-liquid partitioning and liquid expansion are not necessary. We calculated the concentrations of the radical, along with the equilibrium constants for Eq. 5, from the magnetic susceptibilities by using Curie's law and the spin-only magnetic moment of 1.73 Bohr magnetons for $(CO)_4Co\bullet$.[14] The van't Hoff plot (equilibrium constant vs. reciprocal temperature) for data measured in the temperature range 120 to 225°C is linear, and the enthalpy and entropy changes calculated from this plot are 80 ± 8 kJ/mol and 121 ± 17 J/(mol•K), respectively. While the new value for the Co-Co bond of 80 ± 8 kJ/mol is not much higher than the mass spectrally determined 63 kJ/mol value, it at least allows a measurable concentration of radicals to exist, while the 145 kJ/mol does not. The 80 kJ/mol value is also in excellent agreement with an independent determination of the bond energy, which we obtained by analysis of the ^{13}C NMR contact shift that occurs with the CO ligand in a mesitylene solution containing $Co_2(CO)_8$. The contact shifts stem from exchange of free CO with coordinated CO in the $(CO)_4Co\bullet$. The shifts were used to calculate the mole fraction of the radical at various temperatures, leading to the value of 80 ± 8 kJ/mol for the bond energy, in perfect agreement with the magnetic susceptibility result.

Equation 4 can be rearranged to determine the H-Co bond energy in $HCo(CO)_4$. In that case, using 80 ± 8 kJ/mol for the Co-Co bond energy in $Co_2(CO)_8$, 20 ± 0.8 kJ/mol for

---

[13] S. K. Sur, *J. Magn. Reson.* **82**, 169-173 (1989).

[14] T. H. Crawford and J. Swanson, *J. Chem. Educ.* **48**, 382-386 (1971).

the enthalpy change for the hydrogenation of $Co_2(CO)_8$ in Eq. 3, and 435 kJ/mol for the H-H bond energy in dihydrogen leads to a H-Co bond energy of 248 ± 4 kJ/mol. This value seems more reasonable than the 280 kJ/mol obtained from electrochemical measurements in that an upper limit of 264 kJ/mol for this bond energy was estimated from the activation parameters for the transfer of a hydrogen atom from $HCo(CO)_4$ to styrene.[15]

In future studies, we will begin high-pressure NMR studies of the Shell Oil process for the hydroformylation of olefins. The Shell catalyst, $Co_2(CO)_6(PBu_3)_2$, is obtained by phosphine modification of the cobalt carbonyl catalyst and has never been studied with an *in situ* spectroscopic technique at the high temperatures and pressures required for the commercial process. We intend to compare thermodynamic and kinetic parameters for the Shell and cobalt carbonyl catalysts under process conditions.

2. Ceramic Precursor Chemistry

In this activity, we have recently developed a magnetic resonance imaging (MRI) device[16] that appears to have great potential for characterizing advanced materials and materials chemistry processes. The toroid cavity in this device has the potential to achieve greater spacial resolution than previously attainable by conventional techniques and shows great promise to be useful in many areas of research. It seems noteworthy that the technique was developed for, and first used in, high-pressure probes.

Early in our research activities that involved the use of toroid detectors in high-pressure NMR spectroscopy, it became necessary to surmount difficulties in tuning to the very high frequencies required for protons. After all, toroids are the most efficient of inductors, and the inductance of even a very small three- or four-turn torus, when combined with the inductance and capacitance of the rf feedthrough in the pressure vessel, is too large to allow tuning to the 300 MHz proton frequency of our spectrometer. The tuning problem can be surmounted by the use of transmission lines; however, their use usually results in sensitivity losses. Because of its extremely low inductance, the toroid cavity detector in Fig. IX-1 can easily be tuned well above 300 MHz and is probably a preferable solution to the tuning problem in cases where a single nucleus probe for ^1H observation is required. As shown in Fig. IX-1, slots were machined into the detector to ensure complete filling or draining of the cavity when used with fluid media. Our cavity resonator differs from the gap reentrant cavity resonator reported by Alderman and Grant[17] in that the new cavity is tuned externally. Probe tuning is accomplished with use of a capacitor box mounted close to the pressure vessel in the same fashion as used for toroid coils. Compared with coils, the cavities possess the additional advantages of being more rugged and more reproducible in design. In our experience, they also achieve better resolution on protons (about 0.7 Hz for the best-performing cavities vs. 2.5 Hz for the best coils in measurements with $CHCl_3$).

---

[15] D. C. Eisengerg and J. Norton, *Isr. J. Chem.* **31**, 55-56 (1991).

[16] K. Woelk, J. W. Rathke, and R. J. Klingler, *J. Magn. Reson.* **105**(1), 113-116 (1993).

[17] D. W. Alderman and D. M. Grant, "A Cavity Technique for Use in High Field Superconducting NMR Probes," Program and Abstracts of the 21st Experimental NMR Conf., March 16-20, 1980, Tallahassee, FL (1980).

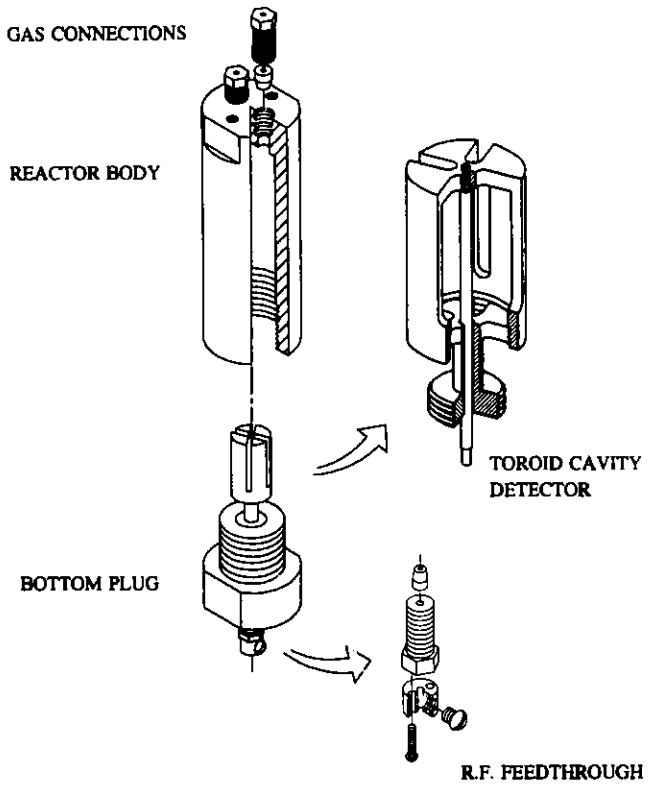

Fig. IX-1.

High-Pressure NMR Probe with a Toroid Cavity Resonator

When we began to consider the possibility of exploiting the rf field gradient (i.e., B_1) within toroids for imaging purposes, cavities were the obvious choice because they can be machined to high precision, and their smooth surfaces (so long as the aforementioned slots are not cut into the walls of cavities designed for imaging purposes) do not contribute irregularities in the field, as is known to occur with coils because of spaces between individual turns. In developing the toroid cavity imaging technique, we used the two-dimensional Fourier transform method devised by Hoult[18] for rotating-frame imaging. With use of the rotating-frame technique, the toroid cavity provides NMR spectral information while simultaneously resolving distance (i.e., radial displace from the central axis of the torus) on the micron scale. Early experiments using ^{19}F NMR successfully resolved and accurately measured Teflon layers to a spacial resolution of 20 μm near the surface of the toroid's central conductor. Moreover, calculations indicate that the device is probably capable of achieving a resolution of 1.0 μm for ^{1}H nuclei on the surface of a fine-wire copper conductor.

In contrast with conventional MRI, chemical shift information is not used to resolve distances with the toroid cavity method. Hence, unlike MRI, the spacial resolution of the torus does not depend on the width of the NMR lines used in the measurements. This feature is particularly advantageous in investigating solid films since solids frequently have extremely broad NMR signals. For example, the ^{19}F NMR signals from Teflon used in the experiment described above are about 7000 Hz wide, yet the wide lines were of no significant consequence in the resolution tests.

---

[18] D. I. Hoult, *J. Magn. Reson.* **33**, 183 (1979).

The experimental setup used to test the toroid cavity imaging method is shown in Fig. IX-2. As shown here, five capillaries (1.0-mm OD), each spaced by 0.8-mm radial increments from the center, were aligned parallel to the central conductor of the torus. Each capillary contained one of three test reagents: water, isopropanol, or acetone. The resultant three-dimensional plot of the NMR signal intensity versus chemical shift and radial displacement is shown in Fig. IX-3. This figure indicates that the chemical shift information for the samples is accurately reproduced (although the ppm axis in the figure is an arbitrary one and needs to be scaled to an internal reference). In addition, the data demonstrate accurate reproduction of the capillary diameters and spacing.

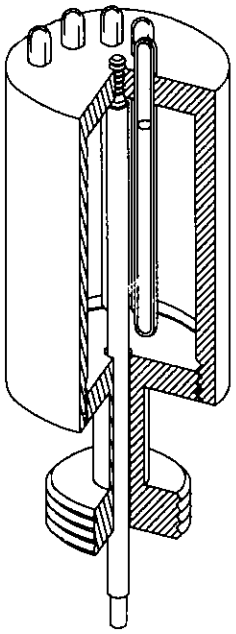

Fig. IX-2.

Experimental Setup to Test Rotating-Frame Imaging Method. Apparatus has five equally spaced capillaries containing one of three different liquids.

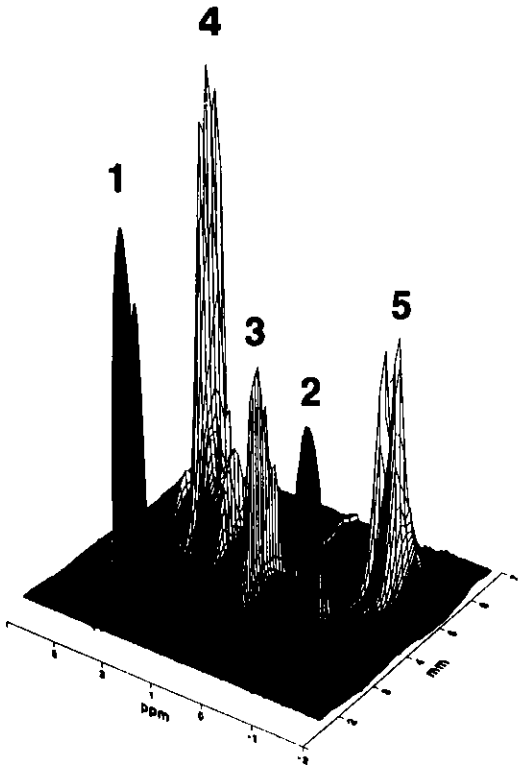

Fig. IX-3.

Three-Dimensional Mesh Plot of NMR Signal Intensity versus Chemical Shift and Radial Displacement for Apparatus of Fig. IX-2. Signals: 1, water; 2, isopropanol; 3, acetone; 4, water; and 5, isopropanol.

Our toroid cavity imager should be useful in obtaining (1) NMR spectra on the different regions of a flame, (2) structure or composition on the different layers of a thin film or coating, (3) the penetration depth or diffusion rate of a fluid into a porous substrate at high pressures, and (4) concentration gradients of various species near an electrode of an electrochemical cell. In future research, we intend to demonstrate a resolution of at least 1.0 μm for the device and to survey its applicability.

3. Hydrocarbon Activation Chemistry

Metallophthalocyanines have been used as catalysts for a variety of oxidation and reduction processes. Our own interest in them stems from their extreme thermal stabilities, as demonstrated by their ability to survive temperatures as high as 500°C. In terms of homogeneous catalytic activation of hydrocarbons, high temperature regions that are inaccessible to other organometallic complexes might be readily explored and utilized in commercial processes with metallophthalocyanine catalysts.

One approach that we have been exploring to activate methane in solution involves use of solubilized phthalocyanine (Pc) ligands bound to rhodium centers. In this approach, C-H bonds are activated by means of the rhodium center's ability to form reasonably strong, but still reactive, metal-carbon and metal-hydrogen bonds. We have recently activated methane and other hydrocarbons with a metal-metal bonded rhodium phthalocyanine dimer, $[(\text{n-pentyl})_8\text{PcRh}]_2$. This dimer reacts with methane in solution as follows:

$$[(\text{n-pentyl})_8\text{PcRh}]_2 + \text{CH}_4 \rightharpoonup (\text{n-pentyl})_8\text{PcRhCH}_3 + (\text{n-pentyl})_8\text{PcRhH} \qquad (6)$$

Both the methylrhodium and hydridorhodium products of Eq. 6 have interesting structural features, which we have recently characterized.[19,20] As might be expected, attractive sites for intermolecular C-H bond activation are the n-pentyl groups that are used in the rhodium phthalocyanine dimer both to solubilize it and serve as spacers to weaken and, thereby, activate the Rh-Rh bond. The presence of these sites limits the stability of the rhodium complexes, and early efforts were made to find suitable replacements. We have recently succeeded in synthesizing soluble rhodium complexes in which the n-pentyl groups are replaced with trifluoromethyl groups.

Figure IX-4 shows the calculated structure for a newly synthesized methoxyrhodium complex, $(\text{CF}_3)_8\text{PcRhOCH}_3$, including the location of the trifluoromethyl groups. This complex, like the related n-pentyl derivatives, is reasonably soluble in organic solvents but also displays some unusual reactivity. The complex reacts with hydrogen under unusually mild conditions, perhaps because of its high electrophilicity stemming from the presence of the electron-withdrawing inductive effects of the eight trifluoromethyl groups.

---

[19] M. J. Chen and J. W. Rathke, *J. Chem. Soc. Chem. Commun.* **4**, 308-309 (1992).
[20] M. J. Chen, J. W. Rathke, and J. C. Huffman, *Organometallics* **12**, 4673-4677 (1993).

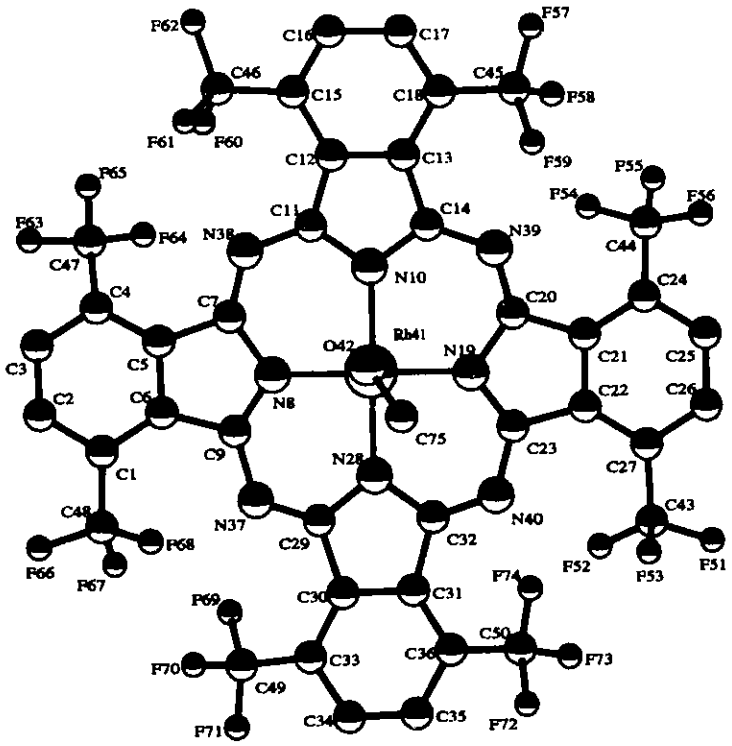

Fig. IX-4. Calculated Structure for $(CF_3)_8PcRhOCH_3$, Including the Location of Trifluoromethyl Groups

In future activities, we intend to exploit the highly electrophilic character of trifluoromethyl-substituted complexes in attempts to achieve electrophilic C-H bond activation. Complexes of interest include $(CF_3)_8PcRh$-X, where X = SO_4H, CF_3SO_4, or Cl.

B. *Materials Chemistry*

The materials chemistry program encompasses fundamental research on the phase chemistry of high-critical-temperature (T_c) superconducting oxides, the characterization of electrochemical metal/solution interfaces under conditions that are relevant to corrosion science and to electrochemical devices, the development of first-principle methods for computing molecular energies, and the study of materials properties by advanced computational methods.

1. Studies of High-T_c Superconducting Materials

The discovery of high-T_c superconducting oxides has spawned numerous efforts throughout the world to find practical fabrication methods for these novel materials. We are conducting electromotive force (emf) measurements of oxygen fugacity as a function of oxygen stoichiometry and temperature in the superconducting material $(Bi,Pb)_2Sr_2Ca_2Cu_3O_x$ (Bi-2223). A coulometric titration technique employing an yttria-doped zirconia electrolyte is being used to investigate the thermodynamic behavior of the Bi-2223 system as a function of oxygen partial pressure [$p(O_2)$ = ~10^{-4}-1 atm], oxygen stoichiometry (x = 9.5-10.5), and temperature

(T = 700-815°C). There are very few quantitative data concerning (1) the dependence of oxygen partial pressure and temperature on the nonstoichiometric behavior of Bi-2223 and the precursor powder $(Bi,Pb)_2Sr_2CaCu_2O_y$ (Bi-2212) or (2) the effect of oxygen stoichiometry variation on phase relationships and stability in these high T_c systems. Such data could prove useful in determining optimum processing conditions for producing silver-sheathed Bi-2223 wires capable of carrying high critical currents.

During this report period, we completed emf measurements on a lead-doped Bi-2223 sample prepared at ANL and another at Ames Laboratory. Prior to these measurements, X-ray diffraction analysis of the Ames sample showed only single-phase Bi-2223, whereas the ANL sample appeared to be a mixture of Bi-2212 and Bi-2223. Analysis by inductively coupled plasma/atomic emission spectroscopy (ICP/AES) combined with iodometric analysis gave oxygen coefficient (x) values of ~10.4 and 10.5 for the Ames and ANL samples, respectively. These oxygen coefficient values are tentative; a more rigorous analytical technique than ICP/AES analysis is required to define the metal content in these materials.

The results of our emf measurements at 815°C are shown in Fig. IX-5, where calculated oxygen partial pressures are plotted as a function of x in $(Bi,Pb)_2Sr_2Ca_2Cu_3O_x$. The shapes of the isotherms in Fig. IX-5 are similar for both the Ames and ANL samples, i.e., large changes in oxygen partial pressures occur as decreasing x approaches the plateau region [$p(O_2)$ ~3 x 10^{-3} atm]. Thermodynamic assessments of partial molar entropy and enthalpy of solution of oxygen in Bi-2223 from our emf measurements indicate that the plateau region can be represented by the diphasic CuO-Cu_2O system. It is also noteworthy that the oxygen partial pressure measurements as a function of x were reversible in the single-phase region [~1 atm < $p(O_2)$ > ~10^{-2} atm]; however, after the diphasic plateau region was achieved, they were irreversible in the sense that we could not return to the single-phase region by increasing x. Within the plateau region, nevertheless, oxygen partial pressure measurements were reversible.

Experiments employing thermogravimetric and differential thermal analysis equipment were also employed to check whether the shapes of the isotherms above the plateau truly represented single-phase Bi-2223. For these experiments, the Ames sample was heated in a flowing (100 cm^3/min) oxygen gas stream (balance nitrogen) at a rate of 5°C/min to a temperature of 815°C. The sample was held at this temperature for 10 h and then furnace cooled to room temperature. X-ray diffraction and ICP/AES analyses for metal constituents were performed on the residue. The results (horizontal dashed lines in Fig. IX-5) clearly indicate that the isotherms above the plateau regions for the Ames and ANL materials represent single-phase Bi-2223. The concentrations of the metal elements remain essentially constant in the single-phase region, except for a negligible loss of lead at 7.5% oxygen. It is apparent that decomposition of the Bi-2223 sample occurred in the presence of 0.1% oxygen. The decomposed product consisted of $(Bi,Pb)_2Sr_2CuO_x$ (major), $Ca_{1.8}Sr_{0.2}CuO_3$ (minor), and Cu_2O (trace).

The results of these and our earlier studies indicate that processing or annealing of Pb-doped Bi-2223 at 750-815°C and oxygen partial pressures of ~0.02 to 0.2 atm should preserve Bi-2223 as essentially single-phase material. The difference in the phase stability and thermodynamic behavior of lead-doped Bi-2212 and lead-doped Bi-2223 will be investigated.

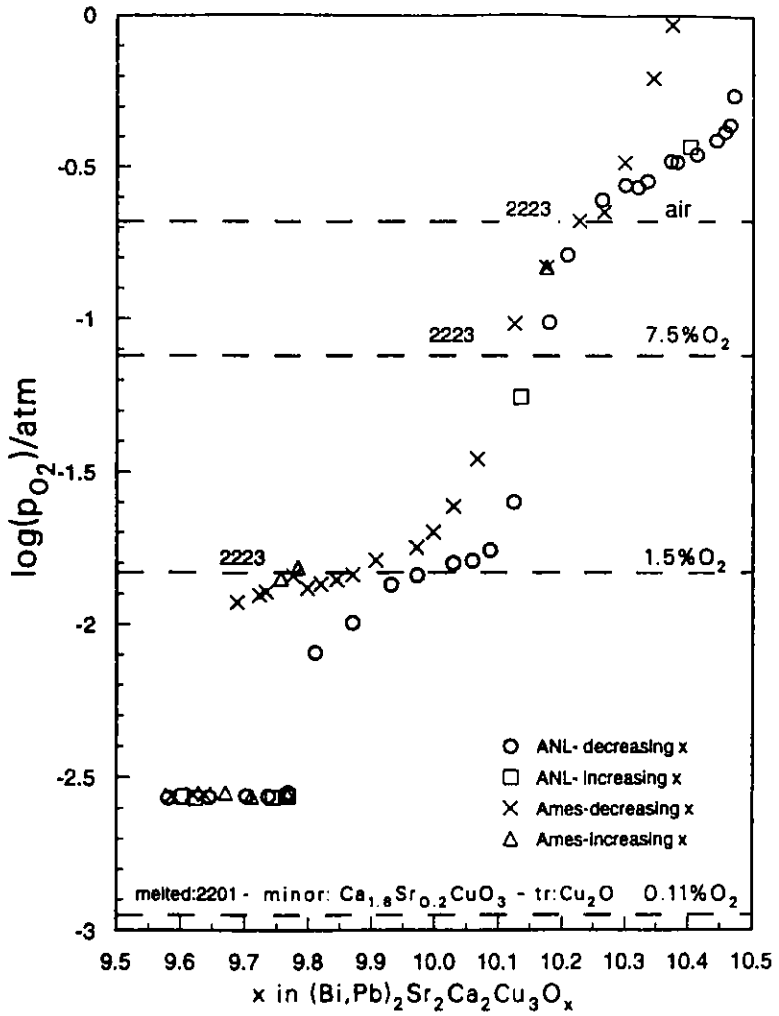

Fig. IX-5. Oxygen Partial Pressure vs. Oxygen Stoichiometry for $(Bi,Pb)_2Sr_2Ca_2Cu_3O_x$ at 815°C. Some data points were recorded in the direction of increasing x (back titration) to check for irreversibility effects. Horizontal dashed lines show composition of sample in gas streams with different oxygen contents at 815°C.

2. Electrochemical and Corrosion Studies

Electrochemical processes occurring in aqueous media are key steps in many established and emerging energy-related technologies. Two such technologies, high-performance batteries for electric vehicles and large-scale fuel cells for primary electric power generation, are on the verge of commercialization. Moreover, photoelectrochemical energy production and chemical processing (e.g., water splitting) are at an advanced stage of development. An electrochemical process cutting across practically all energy technologies is corrosion.

The goal of this research effort is to provide (1) experimental information on the structure and dynamics of metal/solution and metal oxide/solution interfaces as a function of temperature and (2) theoretical models against which the experimental results can be tested. The research program that we have established to reach this goal employs *in situ* surface-sensitive spectroscopic and synchrotron X-ray methods, transient and steady-state electrochemical

techniques, and theoretical modeling based on a combination of molecular dynamics and molecular orbital methods.

a. Spectroelectrochemical Studies

The objective of this research is to elucidate the relationship between the structural and transport properties of metal/solution interfaces and the mechanisms of interfacial reactions in aqueous solutions. Electrochemical, laser Raman, and infrared (IR) spectroscopic techniques are employed to make *in situ* determinations of the composition of surface films on metals, the structure of the interface region, and the rates and mechanism of the interfacial processes involved in the metal corrosion.

The composition and structure of the surface films on iron have been the subject of much debate for a long time but still remain largely unresolved. We have used *in situ* surface-enhanced Raman spectroscopy (SERS), facilitated through the use of an electrodeposited silver overlayer on an iron substrate, in an attempt to resolve important details of film composition. Results of our investigations to date have led to the following conclusions: (1) the pre-passive film at potentials below -0.8 V [vs. saturated calomel electrode (SCE)] in 5 M KOH solution consists of $Fe(OH)_2$ and Fe_3O_4, (2) the passive film (above -0.5 V vs. SCE) appears to be a bilayer of Fe_3O_4 and FeOOH, (3) α-FeOOH appears to always be present on the electrode surface, even at hydrogen evolution potentials (-1.4 V vs. SCE), and (4) the surface films are highly disordered or amorphous. Our SERS studies at temperatures up to 95°C have not shown any change in composition or structure of the films on iron.

In collaboration with researchers at the University of Poitiers (France) and the University of Auckland (New Zealand), we continue to carry out IR experiments on the U4IR beamline of the National Synchrotron Light Source (NSLS) at Brookhaven National Laboratory. Following studies on polycrystalline gold,[21] we examined the adsorption of water on single-crystal Pt(111). Water was found to adsorb molecularly and nondissociatively on this metal in ultra-high vacuum at low temperatures (less than -73°C or 200 K). Surprisingly, the far-IR spectrum of water on Pt(111) was very similar to that of polycrystalline gold. *In situ* infrared spectroscopic investigation of CO and SCN^- adsorbed on platinum was started, but spectra of rather poor quality have been obtained to date. Further measurements will be made following improvement in the optical setup and redesign of the spectroelectrochemical cell.

b. Electrode Kinetic Studies

This research concentrates on understanding the kinetic and mechanistic aspects of heterogeneous charge-transfer reactions over a wide temperature range (25 to 300°C). Heterogeneous charge-transfer reactions are the essential chemical reaction in many energy-related technologies, such as high-performance batteries for electric vehicles, large-scale fuel cells for primary electric power generation, and photoelectrochemical energy production. They are also involved in corrosion of these and other energy technologies. Clearly a fundamental understanding of the dynamics of charge-transfer reactions should spawn improvements in many energy

---

[21] J. E. Battles et al., *Chemical Technology Division Annual Technical Report, 1992*, Argonne National Laboratory Report ANL-93/17, p. 166 (1993).

technologies. Until now, advances have been hampered by poor agreement between measured and theoretically predicted kinetic parameters. One reason for these discrepancies is that many experimental results become questionable if the catalytic effect of trace impurities in aqueous solutions is not recognized. Whereas normally used "high-purity" solutions typically contain impurities in the part-per-million range, our results indicate that removal of impurities below the part-per-million range is needed to obtain a meaningful comparison with theory.

In a prior investigation of the ferrous/ferric reaction,[22] we obtained good agreement between the experimental kinetic parameters obtained in "chloride-free" solutions and theoretical values derived from molecular dynamics simulations. We are presently carrying out a similar comparison between experiment and theory for the Cu^{2+}/Cu^{0} reaction, a reaction that is one of the most troublesome cathodic corrosion reactions for cooling systems in light water nuclear reactors. Our electrode kinetic measurements are carried out with relaxation techniques, such as galvanostatic, coulostatic, or potentiostatic pulse transients; ac impedance measurements; and the rotating-disk-electrode technique. The measurement results are then analyzed with computerized data-evaluation methods.

In this report period, we continued our kinetic studies of the Cu^{2+}/Cu^{0} electrode reaction. Previously, we[23] found that the Cu^{2+}/Cu^{0} reaction in perchloric acid solution at room temperature is catalyzed by chloride ions, and that the rate of the Cu^{2+}/Cu^{+} step increased, while that of the Cu^{+}/Cu^{0} step remained virtually constant, as the chloride concentration was increased. This year we developed rigorous purification techniques for the perchloric solution and established that the "chloride-free" rate constant of this reaction at room temperature is two orders of magnitude smaller than the values reported previously, when the importance of the chloride catalytic effect was not recognized. It is essential that we measure the "chloride-free" rate constant at temperatures to 300°C and compare the results with theoretically predicted rate constants. A problem with such measurements, however, is that our perchloric acid purification procedure cannot be applied at high temperatures because it will decompose the perchlorate anion to chloride. Thus, to duplicate the conditions of the theoretical calculations, we are searching for a substitute electrolyte, the anion of which will not form complexes and will not adsorb on the electrode.

c. Theoretical Studies of Electrode/Electrolyte Interfaces

In collaboration with the Corrosion Research Center at the University of Minnesota, we are employing molecular dynamics and molecular orbital methods to study the electrolyte/electrode interface and reactions occurring thereat as they relate to aqueous corrosion. Electronic structure calculations using molecular orbital methods are employed to determine potentials that are utilized in the molecular dynamics calculations and to provide insights into contributions of electronic effects to electron transfer reactions. Molecular dynamics is used to simulate the structure of solvated ions and the water/electrode interface and to calculate electron transfer rates from the classical trajectories of the reactants. The focus of our current work is on

---

[22] M. J. Steindler et al., *Chemical Technology Division Annual Technical Report, 1990,* Argonne National Laboratory Report ANL-91/18, pp. 172-173 (1991).

[23] J. E. Battles et al., *Chemical Technology Division Annual Technical Report, 1992,* Argonne National Laboratory Report ANL-93/17, p. 167 (1993).

the Cu^{2+}/Cu^0 electrode reaction. Copper deposition is an important cathodic reaction occurring during stress corrosion cracking in light water reactors, but its mechanism is poorly understood (see also Sec. IX.B.2.b).

The simulations of multivalent transition metal ions in water play an important role in development of theoretical models of electron transfer at electrode/electrolyte interfaces, as well as other areas of solution chemistry. Ion-water pair potentials derived from *ab initio* molecular orbital theory have been used in molecular dynamics and Monte Carlo simulations of metal cations in water with varying degrees of success. The problems that arise from use of *ab initio* pair potentials are probably due to neglect of many-body interaction effects in the potentials. Various investigators have studied nonadditivity of pair interactions for numerous ion-water interactions, with most of this work concentrated on the magnitude of the three-body interaction. In general, the studies have shown that the three-body interaction terms are substantial. In addition, we previously studied the four-body interaction for hydrated Fe^{3+} clusters,[24] and the results indicated a slow convergence of the two-, three-, and four-body interaction energies to the full many-body result. During 1993, we investigated the many-body interactions in $Cu^{2+}(H_2O)_m$ clusters, where m = 4, 6, 8. (In previous work,[25] we studied two- and three-body interaction terms for these clusters.) The results indicated that the four-body interaction term is significant for the larger (n = 6, 8) clusters, and there is a slow convergence of the two-, three-, and four-body interaction terms to the full many-body result, similar to what was found in our previous study of $Fe^{3+}(H_2O)_m$ clusters. The results of this investigation will be incorporated into our studies of the $Cu^0 \rightarrow Cu^{2+} + 2e^-$ heterogeneous electron transfer reaction.

d. Synchrotron Radiation Studies

Adsorbed layers and surface films at metal/solution and oxide/solution interfaces can range in thickness from less than a monolayer to many hundreds of monolayers. In recent years, extensive research has been done on the development of methods to interrogate such interfaces. Among the most promising methods for determining structural properties are those based on the use of X-rays because of the ideal match of X-ray wavelengths to the desired dimensional information and the ability of X-rays to probe interfaces that are buried under or within condensed phases. As part of this effort, we have developed novel experimental techniques that permit direct *in situ* X-ray investigations of electrode surfaces and interfaces under uniform potential control. (See, for example, Ref. 26.) These techniques have been demonstrated in the NSLS. In the longer term, we expect to make extensive use of the unique capabilities afforded by the Advanced Photon Source (APS) currently under construction at ANL.

Using *in situ* X-ray scattering techniques, we continued the study of the electrochemical oxidation of the Pt(111) single-crystal face in perchloric acid. While our earlier studies were carried out at submonolayer coverage levels, this year we extended our studies to one-to-two monolayer film thickness, which causes irreversible roughening of the platinum surface upon repeated oxidation/reduction cycles. We have proven that progressive roughening

---

[24] L. A. Curtiss, J. W. Halley, and J. Hautman, Chem. Phys **133**, 89 (1989).

[25] L. A. Curtiss and R. Jurgens, J. Phys. Chem. **94**, 5509 (1990).

[26] Z. Nagy, R. M. Yonco, H. You, and C. A. Melendres, "X-ray/Electrochemical Cell," Patent No. 5,141,617, issued August 25, 1992.

of the surface can be well described by the scaling law from the generally accepted theory of interface growth.[27] We also carried out preliminary experiments to investigate electrochemical deposition of platinum on a Pt(111) surface in chloroplatinic acid. X-ray reflectivity measurements were carried out from submonolayer to a few monolayer level of deposition as a function of potential. Qualitative evaluation of the data indicated a progressive roughening of the deposits as the electrochemical potential became more negative.

In collaboration with Exxon Research and Engineering Co., we have also carried out *in situ* X-ray specular and diffuse scattering studies to determine the morphological changes in copper surfaces during both general and localized corrosion in aqueous solutions. Using reflectivity measurements, we found the oxide films on copper to be unstable in the presence of chloride in borate buffer solution. The passive state is stable in 0.01 M $NaHCO_3$, but the film breaks down at high positive potentials (> 0.4 V vs. SCE), leading to pitting corrosion. We have demonstrated for the first time that the technique of diffuse X-ray scattering can be used to study the initial stages of pitting corrosion *in situ*, as illustrated by Fig. IX-6. The pitted sample clearly exhibits a significant decrease in the specular component of the X-ray scattering (at theta = 0.6°) and an attendant increase in the diffuse component compared to the original sample held at -0.90 V vs. SCE (which although rough is not pitted). By theoretically fitting the experimental data, we expect to obtain information on the height-height correlation function for the pits formed as a function of applied electrical potential and solution conditions.

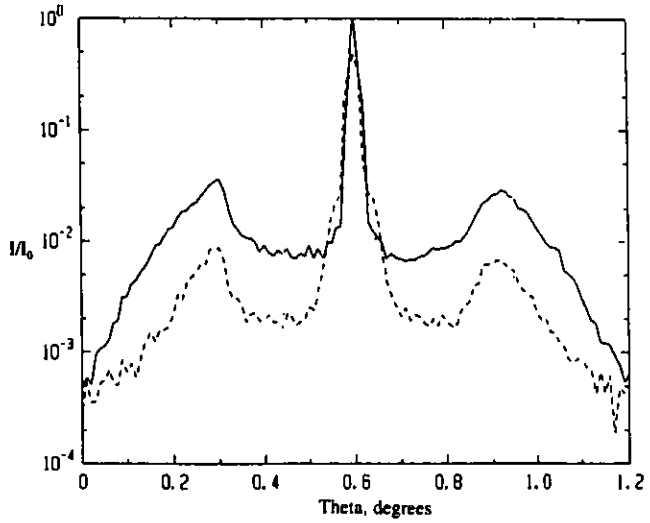

Fig. IX-6.

In Situ Diffuse X-ray Scattering Profile for Cu-on-Si Film Electrode: Clean Electrode at -0.90 V (bold line) and Pitted Electrode at + 0.60 V (broken line). The notation I/I_0 indicates the ratio of reflected beam intensity to incident beam intensity.

3. Theoretical Studies of Materials

We are performing theoretical calculations by various methods to determine the properties of the thin-film diamond surface, effluents from wood combustion for power production, and molten silicate solutions.

---

[27] F. Family and T. Vicsek, J. Phys. **A18**, L75 (1985).

a. Quantum Chemical Studies

The goal of this work is to develop new quantum mechanical methods and apply them, along with previously established ones, to the study of zeolites, metal halides, thin-film diamond growth mechanisms, and molecular cluster studies. One of the methods that has been developed, Gaussian-2 (G2) theory,[28] is now being widely used in universities and industry for the accurate calculation of thermochemical data. This method is based on *ab initio* molecular orbital theory and is accurate to ±2 kcal/mol for calculating reaction energies.

Our work in the past year was focused on modeling thin-film diamond growth mechanisms (based on carbon dimer as the growth species) by using *ab initio* molecular orbital methods. It is believed that the diamond surface structure is stabilized by the adsorption of atomic hydrogen, while the lattice structure is extended by adding carbon in the form of dimers, tilted at an angle to the surface.[29] As a preliminary attempt to model this process on an *ab initio* basis, we have used the methane molecule as an approximation to the hydrogen-terminated diamond surface and calculated the energy required to insert a carbon dimer.

The reaction

$$C_2 + CH_4 \rightarrow H_3CHCC \rightarrow H_3CCCH \qquad (7a)$$

can be considered to be a simple model for addition of C_2 to a diamond surface. The first step corresponds to insertion of singlet C_2 into the C-H bond. The second step corresponds to migration of the hydrogen to the terminal carbon. The energy for the overall reaction

$$C_2 + CH_4 \rightarrow H_3CCCH \qquad (7b)$$

was calculated by G2 theory to be -128.3 kcal/mol, indicating that formation of propyne, H_3CCCH, is very favorable compared to C_2 and CH_4. At the G2 level of theory, 1-propeneylidene, $H_3CHC{=}C{:}$, is 44.4 kcal/mol less stable than propyne. Calculations of the potential energy surface indicate a barrier of ~18 kcal/mol for the first step of Eq. 7a, i.e., insertion of C_2 into a CH bond of methane to form H_3CHCC. The barrier for isomerization of H_3CHCC to H_3CCCH, the second step in Eq. 7a, is about 8 kcal/mol. Hence, theoretical calculations on a simple model for addition of C_2 to a diamond surface suggests that the barrier to insertion will be relatively small. In future work, larger clusters will be used to represent the diamond surface.

b. Inorganic Chemistry of Wood Combustion for Power Production

Equilibrium calculations were used to investigate the inorganic chemistry of the combustion of aspen wood chips with a large excess of oxygen at pressures of 1, 4, and 10 atm. The calculations were made using a computer program that performs a free energy

---

[28] L. A. Curtiss, K. Raghavachari, G. W. Trucks, and J. A. Pople, *J. Chem. Phys.* **94**, 7221 (1991).

[29] D. Gruen, S. Liu, A. R. Knauss, and X. Pau, *J. Appl. Phys.* **75**, 1758 (1994).

minimization; has a thermodynamic data base for over 6000 solid, liquid, and gaseous compounds; and includes some of our own fundamental molten salt theories. The purpose was to calculate the complex equilibria of the combustion effluents with molten and solid sulfate-carbonate solutions. The results are summarized below.

At 1 atm, a potassium sulfate-rich liquid forms at high temperatures (>1000°C) and persists to a temperature between 975 and 1000°C, where it crystallizes to form solid alkali sulfates. At 4 and 10 atm, the liquid sulfate crystallizes above 1000°C. A large fraction of the alkali (largely potassium in wood) remains in the vapor as the KOH molecule at this temperature. Both KOH and CaO react with CO_2 in the vapor to form the solid carbonates $K_2Ca_2(CO_3)_2$ and $CaCO_3$ below 800°C at 1 atm. At 4 atm, a potentially corrosive molten carbonate forms at temperatures in the range 800-875°C. Below 800°C, all the carbonate crystallizes to the solid. At 10 atm, the liquid carbonate-rich solution forms to some extent above 900°C and crystallizes somewhat above 800°C to form solid carbonates.

These results were applied to analyzing combustion with a gravel-bed combustor combined with a gas turbine for power production as part of an effort sponsored by the DOE at the University of Wisconsin. Our calculations led to the suggestion to run the gravel bed at 900-1000°C rather than in the range of 800-900°C, where deposits degrade the combustor operation. This improved the bed performance considerably. In addition, the calculation led to a method for hot gas cleanup with additives that could, in principle, be effective enough to send the combustion effluents into a turbine system after treatment and solids separation.

c. Statistical Mechanical Theory for Molten Silicate Solutions

Our recent work on modeling the solution properties of molten silicates had been based on an *ad hoc* modification of quasichemical theory.[30] When silica is the only acid component, the solution properties of multicomponent silicates can be predicted from those of the subsidiary binaries. Because of the importance and wide use of our quasichemical model in industry and science, the capability of predicting molten silicate properties is needed for multicomponent silicate solutions containing alumina, borates, sulfides, sulfates, phosphates, carbonates, and other solutes. Such a capability requires, as a starting point, a realistic and flexible theory based on a structural model which takes into account the configuration dependence of the energy for breaking a bridging Si-O-Si bond in the silicate. All prior theories assume that the energies are independent of the local configuration.

Our structural model assumes that the energy for breaking bridging bonds in silicates by the addition of an oxide (e.g., CaO) is a function of the number of broken bonds already attached to the two silicons of the bridge. Thus, the energy for the reaction

$$Si-O-Si + O^{2-} = 2SiO^{-} \qquad (8)$$

[30] P. Wu, G. Eriksson, A. D. Pelton, and M. Blander, *Iron and Steel Inst. Japn. Int.* **33**(1), 26-35 (1993).

is a function of the numbers of broken bonds attached to each of the two silicons. A complicated partition function for this model was written, in which each silicon is surrounded by four bridging and non-bridging oxygens. Calculations of the thermodynamic activities of an oxide such as CaO and of silica led to physically meaningful results. For example, the activity of the oxide (a_{MO}) is given by

$$a_{MO} = X_{O^{2-}} = \frac{n_{O^{2-}}}{n_{O^{2-}} + n_{Si}} = 1 - X_{Si} \tag{9}$$

and that of silica by

$$a_{SiO_2} = X_{Si}\, X_{OO}^2 \tag{10}$$

where $X_{O^{2-}}$ is the concentation of free oxide ions that have not become part of a broken bridge given by $(n_{O^{2-}}/(n_{O^{2-}} + n_{Si}))$, $n_{O^{2-}}$ is the number of free oxide ions, n_{Si} is the number of silicons in the system, and X_{OO} is the fraction of the total number of bridges that are connected to silicons with no broken bridges. All these quantities are calculable in terms of the four equilibrium constants for breaking bonds (K_i) on the four types of silicons already having 0, 1, 2, and 3 broken bridge bonds. These constants are given by

$$K_i = \frac{X_{i+1}}{X_i\,(X_{O^{2-}})^{1/2}} \tag{11}$$

where X_i is the fraction of silicons that are connected to i broken bridges. These results should be significant for relating the thermodynamic properties of silicates to their structures, for performing realistic calculations of silicate properties, and for developing methods of predicting the properties of higher order solutions from those of the subsidiary binary solutions for many complex silicate solutions that are industrially and scientifically important.

C. *Geochemistry*

The geochemistry research program in CMT includes efforts in three areas: (1) experimental mineral-fluid interfaces, (2) geochemistry and evolution of natural hydrothermal systems, and (3) compound-specific carbon isotopic geochemistry of petroleum. The approach taken in the first area is to observe reacting mineral surfaces *in situ* by use of synchrotron X-ray radiation. In the other two areas, specific problems are investigated through detailed chemical and isotopic analyses of rock, mineral, water, gas, and oil sampled from appropriate, well-characterized field sites. Potential applications of these studies are in environmental restoration, waste management, and natural resource utilization.

1. Mineral-Fluid Interactions

The objective of this effort is to gain a better fundamental understanding of chemical processes occurring at mineral-fluid interfaces. Such processes control macroscopic

geochemical transport, including contaminant migration in groundwater aquifers, and are therefore of practical importance. We performed our second *in situ* experiment on beamline X10B at the NSLS in June 1993. Again, as in our first experiment,[31] we examined the evolution of the calcite cleavage surface during reaction at 25°C with dilute aqueous fluids having various pH values (4-8.5). This experiment differed from our first experiment, however, in that a flow-through X-ray cell was used, and the fluid pH was controlled by autotitration. Great care was taken to obtain optically flat cleavage surfaces, as indicated by the root-mean-square roughness of the initial surfaces being on the order of 1 Å. Our approach was to first contact the pristine calcite surface with a dilute Na-Ca-HCO_3-Cl solution that was approximately saturated with calcite at pH = 8.5. This surface was examined by synchrotron X-ray scattering while the pH was held at 8.5. No roughening was observed, confirming our expectation of limited reaction with the saturated solution. The pH was then reduced to 6 (or in another experiment, 4) for periods from 5 to 100 min, then raised to 8.5 again, while X-ray scans were taken to examine changes in the surface, through comparison with scans taken prior to reaction. The pH = 6 experiment lasted for roughly 70 h and involved 15 reaction steps. The pH = 4 experiment lasted about 35 h and involved 7 reaction steps. The total calcite removed from the surface in both experiments was calculated from chemical analyses of the solutions combined with data from the autotitrator. This amount was 7 to 8 μmol, which is equivalent to a mean etching depth of 11 to 12 μm. The surfaces were examined following the experiments by both scanning electron microscopy (SEM) and optical microscopy (reflected light). The main features observed on both surfaces were etch pits up to 70 μm across having shapes resembling inverted pyramids.

Structural changes normal to the calcite cleavage plane were determined by monitoring the intensity of the scattered X-ray beam as a function of the perpendicular momentum transfer, $Q_\perp$. In plane, structural changes were determined by monitoring the intensity of the scattered beam as a function of the momentum transfer parallel to the surface, $Q_\parallel$. The structural changes normal to the surface are evidenced by changes in the crystal truncation rod (CTR), which is a two-dimensional-like diffraction feature resulting from termination of a three-dimensional crystal lattice. The CTR intensity (I_{CTR}) for an ideally terminated single crystal is described by the following expression:

$$I_{CTR} = \left| A_0 \frac{e^2}{mc^2} \frac{1}{R_0} F(Q) N_1 N_2 \right|^2 \frac{1}{2\sin^2(Q_\perp a_3/2)} \qquad (12)$$

where A_0 is the amplitude of the incident plane wave, e is the charge of an electron, m is the mass of an electron, c is the speed of light, R_0 is the distance from sample to observer, F(Q) is the atomic form factor, N_1 and N_2 are the numbers of unit cells in the a_1 and a_2 directions, and a_3 is the lattice spacing in the direction $\perp$ to the diffraction plane. The CTR has monolayer sensitivity and provides information on interface topography and surface relaxation/reconstruction effects during our experiments. In the glancing incidence region (near the critical momentum

[31] R. P. Chiarello, R. A. Wogelius, and N. C. Sturchio, *Geochim. Cosmochim. Acta* **57**, 4103-4110 (1993).

transfer for total external reflection of X-rays), X-ray scans are sensitive to the average electron density profile near the interface (within about 10 to 1000 Å).

In Fig. IX-7, the open circles represent the measured CTR of the solid-liquid interface of calcite cleavage surface in contact with calcite-saturated aqueous fluid (pH = 8.5).

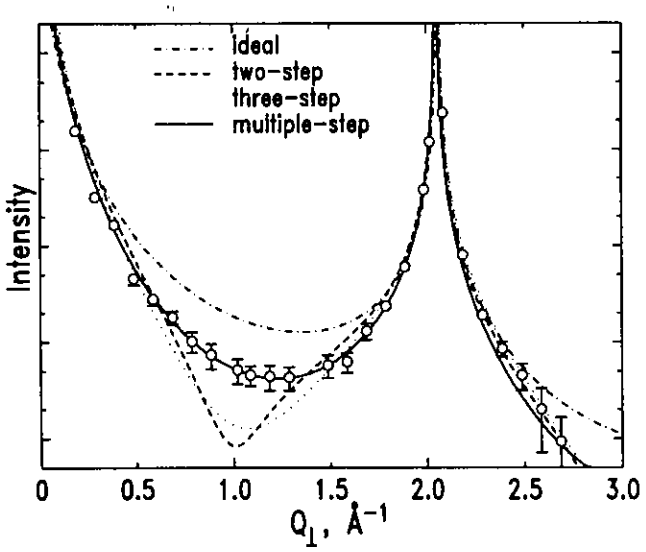

Fig. IX-7.

Normalized Intensity of Scattered X-ray Beam (log scale) vs. Perpendicular Momentum Transfer ($Q_\perp$). Data points for measurements conducted at the calcite cleavage surface in contact with calcite-saturated aqueous solution at pH = 8.5 are shown as open circles. Model curves calculated using Eq. 13 (N = 1, 2, 3, ∞) are also shown.

The CTR was measured as a function of $Q_\perp$ and found to be sensitive to solid-liquid interface topography in the direction perpendicular to the cleavage plane. Surface reconstruction/relaxation and statistical roughness models failed to adequately characterize the CTR data. However, a stepped-surface model for the calcite-fluid interface described all the CTR data. For a stepped surface/interface, the reflected intensity is

$$I_{step} = I_{CTR}\left|\sum_{j=1}^{N} \theta_j e^{iQ_\perp c}\right|^2 \qquad (13)$$

where θ_j is the coverage at the j^{th} step height. Equation 13 can be used to describe an ideal interface (N=1), as well as two-step (N = 2), three-step (N = 3), and multiple-step (N = ∞) interfaces. The best-fit results are shown in Fig. IX-7, and clearly, the multiple-step interface model best represents the CTR data. The only fit parameter was the average step height (σ_r), which was 2.44 Å. The multiple-step interface model also best described the CTR measured after reactions at pH = 6.0 and 4.0. At pH = 6.0, σ_r increased from 2.42 Å to 7.92 Å after 6.71 μmol of calcite was dissolved, and at pH = 4.0, σ_r increased from 2.44 Å to 5.93 Å after 6.95 μmol of calcite was dissolved. These results indicate that on the atomic-scale the calcite-fluid interface topography (in the direction perpendicular to the cleavage planes) does not undergo a dramatic transformation after reaction at pH = 4.0 or 6.0. However, SEM images taken of calcite surfaces

after completion of the X-ray experiments at both pH = 4.0 and 6.0 show etch pits up to 70 μm across having shapes resembling inverted pyramids.

Figure IX-8 is an example of time-dependent X-ray scattering data measured during a reaction cycle from pH = 8.5 to 4.0 and back again to pH = 8.5. As can be seen from the figure, the count rate decreases to a minimum intensity after approximately 700 s, then begins to gradually increase *during* reaction at pH = 4.0. This behavior is also observed in time-dependent data recorded during reaction at pH = 6.0 and may indicate that a dynamic, steady-state topography is achieved on this time scale under these conditions. This topography may be maintained by continuous nucleation, deepening, and lateral growth of etch pits.

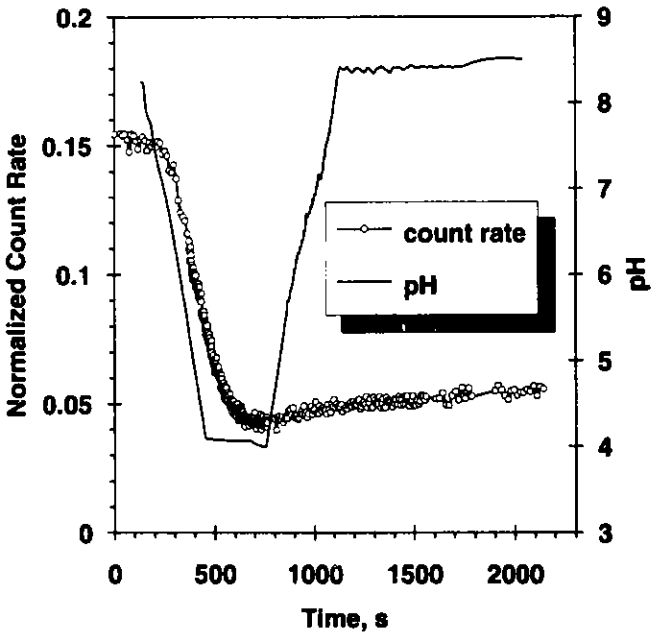

Fig. IX-8.

Normalized Count Rate of Scattered X-ray Beam (at $Q_{\perp}$= 0.1 $Å^{-1}$) and pH vs. Time for Reaction Step with pH = 4

From the above results, we conclude that the topography of the calcite cleavage surface during dissolution is determined by the near ideal atomic-scale termination of this surface and the long-range atomic order of the underlying bulk crystal. The angstrom-scale surface topography of etch pit bottoms and terraced sides and the intra-terrace areas between etch pits is essentially identical to that of the pristine calcite cleavage surface (in the direction perpendicular to the cleavage planes). Etch pit depth is determined during the initial stages of the reaction (≤ 700 s), after which etch pits grow faster laterally than longitudinally. Future studies will include time-resolved synchrotron measurements of surface reconstruction and adsorbed-layer structure during adsorption of heavy metals (Cd, Pb, Co) on mineral surfaces.

2. Chemical and Isotopic Composition of Egyptian Thermal Waters

Thermal springs along the shores of the Gulf of Suez (Ain Sokhna, Hammam Faraoun, and Hammam Musa) and along the Nile River at Helwan (just south of Cairo) were sampled for chemical and isotopic analysis. This was done in collaboration with Egyptian colleagues from Washington University and the Egyptian Geological Survey and Mining Authority for the purpose of determining the geothermal potential of these areas and better under-

standing their hydrogeochemistry. The results from determination of temperature, composition, $\delta^{18}O$, δD, and $^{87}Sr/^{86}Sr$ are summarized below.*

Thermal springs along the Gulf of Suez have temperatures of 32-70°C. The solutes are Na-Ca-Mg-Cl-SO_4-HCO_3, and total dissolved solids are 8-14 g/L. The $\delta^{18}O$ values of these waters range from -5.6 to -4.3 ‰, and their δD values from -44 to -36 ‰. These values correlate with those of "paleowaters" found widely in the Nubian sandstone aquifer throughout northeast Africa and in the Sinai Peninsula. The thermal water at Helwan has temperatures of 30-36°C. Solutes in Helwan thermal waters resemble those in the Gulf of Suez waters except for lower Cl/SO_4 ratios. The $\delta^{18}O$ and δD values of one Helwan sample were determined to be +2.1 and +10.6 ‰, respectively. These resemble values for Nile River water prior to construction of the Aswan High Dam.

The $^{87}Sr/^{86}Sr$ ratios for the thermal waters in the Gulf of Suez and Helwan areas range from 0.70795 to 0.70803; these are consistent with a mid-Tertiary rather than a Holocene seawater source for strontium. This rules out recent seawater mixing but supports derivation of most solutes from the extensive Tertiary marine sedimentary formations exposed around the Red Sea. Geothermometric analysis of these thermal waters indicates moderate subsurface temperatures, consistent with conductive heating under the normal regional geothermal gradients at depths of 3 to 4 km. Additional work next year will include sampling of more thermal springs and analysis of dissolved gases.

3. Nitrogen Isotope Geochemistry of Petroleums

The chemical and isotopic composition of hydrocarbon compounds (those containing only hydrogen and carbon) in petroleums has been well studied. These data have led to interpretations of the source-rock depositional environments and the history of specific petroleum occurrences. However, the geochemistry of nitrogen compounds in petroleums, in particular their nitrogen isotopic composition, is not well characterized. To better understand the nitrogen isotopic geochemistry of petroleums, we determined nitrogen isotope ratios for 25 well-characterized nitrogen-rich crude oils from southern California. Of this sample set, the sulfur-rich oils derived from marine-dominated organic matter have relatively low $\delta^{15}N$ values* (<6.4 ‰), while the sulfur-poor oils generated from organic matter containing some terrigenous material have relatively high $\delta^{15}N$ values (>6.4 ‰). Oils affected by biodegradation and those exhibiting maturation variations generally do not show effects related to these processes in their $\delta^{15}N$ values. We propose that variations in the nitrogen isotopic composition of southern California oils generally reflect changes in the depositional environment of the source rocks and are not produced by secondary processes. Nitrogen fixation, biological productivity, nitrate concentration, decomposition of organic matter, and assimilation of resultant ammonia are some of the factors which might be responsible for these variations. These results imply that geochemical interpretations based on the nitrogen isotopic composition of the source rocks and ancient nitrogen cycles can be made with confidence. Analyses in progress for oils from other fields will provide additional data to test these conclusions.

---

* Definition of δ notation for isotope ratios: $\delta = 1000[(R_{sample}/R_{standard}) - 1]$, where R = D/H, $^{18}O/^{16}O$, or $^{15}N/^{14}N$. The standard for D/H and $^{18}O/^{16}O$ analyses is Standard Mean Ocean Water, and that for $^{15}N/^{14}N$ is atmospheric nitrogen.

X. ANALYTICAL CHEMISTRY LABORATORY

A. *Introduction*

The Analytical Chemistry Laboratory (ACL) is a full-cost-recovery service center, with the primary mission of providing a broad range of analytical chemistry support services to the scientific and engineering programs at ANL. In addition, the ACL has a research program in analytical chemistry, conducts instrumental and methods development, and provides analytical services for governmental, educational, and industrial organizations. The ACL handles a wide range of analytical problems, from routine standard analyses to unique problems that require significant development of methods and techniques and analytical expertise.

The ACL is administratively within CMT, its principal ANL client, but provides technical support for many of the technical divisions and programs at ANL. The ACL has four technical groups--Chemical Analysis, Instrumental Analysis, Organic Analysis, and Environmental Analysis--which together include about 45 technical staff members.

The Chemical Analysis Group uses wet-chemical and instrumental methods for elemental, compositional, and isotopic determinations in solid, liquid, and gaseous samples and provides specialized analytical services. The Instrumental Analysis Group uses nuclear counting techniques in determining the radiochemical constituents in a wide range of sample types, from environmental samples with low radioactivity to samples with high radioactivity that require containment. The Organic Analysis Group uses a number of complementary techniques to separate, at the trace level, organic compounds and then perform qualitative and quantitative analyses. Samples that can be analyzed include complex organic mixtures and compounds, pesticides, potentially hazardous wastes, and drugs. Organic Analysis Group personnel also develop methods for such purposes as continuously monitoring incinerator emissions, detecting organic compounds remotely and performing rapid on-site determination of organic constituents, and analyzing headspace gas of DOE waste containers for volatile organic compounds. The Environmental Analysis Group performs analyses of environmental, hazardous waste, and coal samples for the inorganic constituents.

The ACL has a sample receiving system that allows efficient processing of environmental and hazardous and mixed waste samples, including chain-of-custody procedures. The ACL also has quality assurance and quality control systems in place to produce data packages that meet the rigorous reporting requirements of the DOE and the Environmental Protection Agency (EPA), as well as other similar organizations. New ACL capabilities established in 1993 include additional laboratory facilities for analysis of radioactive organic samples, a laboratory robotics system, a mercury analyzer, and a facility for sample preparation using microwave ovens.

B. *Technical Highlights*

The ACL provides analytical services to CMT, other ANL divisions and programs, other DOE sites, DOE's Chicago Operations Office, and DOE Headquarters. In addition, ACL conducts

research and development programs funded by DOE and other sponsors. Selected accomplishments for 1993 are summarized here.

1. Engineering Studies of Pyrochemical Processes for Integral Fast Reactor Fuels

In the electrorefining of spent fuels for the Integral Fast Reactor (IFR), metallic fuel pins (U, Pu, Zr) are chopped into small segments and placed into a basket that is introduced into molten salt (LiCl-KCl) at 500°C. Nearly pure uranium is removed from the spent fuel by electrotransport to solid cathodes, followed by electrotransport of the plutonium and any remaining uranium to liquid cadmium cathodes. Engineering-scale development of this electrorefining process are being conducted in CMT (Sec. VI). In this effort, process models have been developed for the recovery of uranium and a transuranic product, as well as the decontamination of these elements from fission-product elements and process materials. The ACL has contributed to this effort by determining elements of interest in samples from the halide-salt electrolyte, cadmium anode, and the cathode product. Special dissolution procedures are followed for each type of sample matrix, and separation schemes based on solvent extraction and ion exchange are used to isolate the desired elements from matrix components and, subsequently, to separate these elements. Uranium, plutonium, and rare earth concentrations in IFR samples are measured with an inductively coupled plasma/atomic emission spectrometer (ICP/AES) configured to analyze radioactive solutions. The mass spectrometric isotope dilution (MSID) technique is used whenever higher precision and accuracy than attainable with ICP/AES are required. An inductively coupled plasma/mass spectrometer (ICP/MS) is used when the concentrations of uranium and rare earths are below the detection limits of the ICP/AES instrument.

Experiments to which the ACL contributed during the past year include tests of salt stripping, U-Zr co-deposition, and the liquid cathode performance. In the salt stripper tests, lithium metal was added to spent salt from an engineering-scale IFR electrorefiner to remove uranium and rare earths, which is necessary prior to salt disposal. Analytical data generated from samples taken during these tests provided insight on the behavior of uranium and rare earths with repeated electrotransport cycles. Zirconium from the spent IFR fuel also builds up in the electrorefiner and has to be removed for recycle. Uranium-zirconium deposition on a solid cathode was demonstrated under different operating conditions in the engineering-scale electrorefiner. Analytical data provided information as to the most favorable conditions for U-Zr transport to the solid cathode. The liquid cathode performance was investigated by varying the U/Pu ratio in the electrorefiner salt. Starting with only plutonium in the salt, the electrorefiner was operated using liquid cadmium as the cathode. Uranium was added in increments to vary the amount of uranium in each test run. Samples were taken from the liquid cathode and analyzed for U and Pu content. These data provided insight on the amount of each actinide transferred to the cathode and the liquid cathode performance under a variety of electrorefiner conditions expected in IFR fuel reprocessing.

2. Analytical Certification of IFR Special Reference Materials

The Analytical Laboratory in the Fuels and Engineering Division at ANL-West is developing methodology and procedures for the analyses that will be required for process control

and materials accountability during the planned demonstration of the IFR fuel cycle. To help in their methods development and to provide a source of quality-control samples for use during the fuel-cycle demonstration, CMT personnel are preparing several sets of "Special Reference Materials," each consisting of specified analytes in a matrix typical of samples that will be generated during electrorefiner operations at the IFR Fuel Cycle Facility of ANL-West. The ACL characterizes each batch of materials by chemical analysis and provides reference values for the concentrations of individual constituents in each matrix.

During 1993, batches of two special reference materials were prepared and poured into nominally one-gram samples by CMT workers. One of these, designated SRM-A, contains enriched uranium in a LiCl-KCl salt matrix, while the other, SRM-B, has the same salt matrix but contains U, Pu, Am, and a mixture of simulated fission-product and process elements such as rare earths, alkali metals, and transition metals. To provide accurate and precise U and Pu assays in this work, we are applying the MSID method with a special internal-standard technique for mass-spectrometric measurements of uranium.

All of the uranium isotopic and compositional analyses on SRM-A have been completed. The results of uranium assays on ten SRM-A samples analyzed in duplicate showed a mean concentration of 2.5058 wt% U, with a standard deviation of 0.0022 wt%. A group of 185 SRM-A "standards" that remained after these ten were analyzed was shipped to ANL-West, where they will be used for testing and validating methodology under development for comparable uranium assays. Plutonium measurements on SRM-B have almost been completed. The remaining plutonium analyses are to be completed in 1994 along with the characterization of uranium and all the other constituents of this more-complicated, multiple-element reference material.

3. Incinerator Monitoring

This project addresses the need mandated by the Clean Air Act of 1990 to monitor toxic compounds in the air emitted from incinerator stacks. The objective is to develop a combination of a Fourier transform infrared (FTIR) spectrometer and a heated long-path cell for use as a continuous emission monitor of organic products of incomplete combustion from incinerators.

An on-stream monitor for stack effluent would provide an update on incinerator status in near real time. On-stream analysis of the incinerator effluent would simultaneously satisfy the requirements of the Clean Air Act of 1990 and address public concern about incinerator safety. Other benefits include elimination of the need for a trial burn and its associated costs. This past year, the first prototype FTIR monitor was constructed and field tested in the Toxic Substances Control Act (TSCA) incinerator at the K-25 site (Oak Ridge, TN). All instrumentation and software were successfully tested. The long-path cell required no alignment, cleaning, or repairs--a key advance in the application of this technology. Tests were completed to determine the number of background samples and calibration standards that are required to comply with the performance specifications required by the EPA.

We also provided input to a protocol for an FTIR continuous emission monitor previously developed by the EPA. This protocol was converted into a standard operating procedure for the field test at the K-25 site. Major advances have been made in validating calibration standards and generating a quantitative spectral library. Effort is now underway to commercialize the monitor developed in this program. Future plans include construction of an improved monitor based upon the test results obtained at the K-25 test.

4. Method Development in Support of the Waste Isolation Pilot Plant

The Waste Isolation Pilot Plant (WIPP) in Carlsbad, NM, has been selected as a possible permanent disposal site for transuranic radioactive wastes resulting from defense-related activities at DOE sites. Over the next five years, DOE plans to evaluate the behavior of wastes designated for burial at the WIPP site. These wastes will be analyzed at Idaho National Engineering Laboratory, Rocky Flats Plant, and ANL.

Defense-generated wastes to be transported to, and stored at, the WIPP site must be characterized and shown to satisfy Resource Conservation and Recovery Act (RCRA) requirements, which limit the presence of hazardous compounds. One of the wastes to be shipped to the site is Type IV organic waste sludge. The sludge results from the "solidification" of organic waste liquids by the addition of calcium silicate absorbent to immobilize the spent liquids. Because polychlorinated biphenyls (PCBs) are suspected of being present in the liquids and, hence, the sludge, analyses for PCBs must be completed on each container of sludge before shipment.

The ACL has developed an analytical method for determining PCBs in the sludge. The starting point for the analytical procedure is EPA Method 8081 (in EPA document SW-846),[1] which uses a solvent extraction step followed by gas chromatographic analysis with an electron capture detector. To test the method, we prepared batches of synthetic sludge from liquids known to be present in existing waste sludges, such as lathe coolant, machining oils, and hydraulic fluids. The selected liquids were spiked with PCBs, and then blended with calcium silicate to form the sludge. During testing, interferences from the waste that tend to obscure the presence of PCBs were identified, and a procedure was developed to eliminate them before the gas chromatographic step. Measurements using the modified EPA Method 8081 have indicated good recovery (70 to 100%) of PCBs from the sludge.

5. Analysis of Waste-Drum Headspace Gas for WIPP

If volatile organic compounds (VOCs) are in the radioactive mixed-waste drums to be buried at the WIPP site, they will appear in the vapor present in the void space surrounding the packaged solid items. The ACL is to serve as one of the participating laboratories in an effort to determine the VOCs, permanent gases, and low-molecular-weight hydrocarbons (methane

---

[1] U.S. Environmental Protection Agency, *Test Methods for Evaluating Solid Waste*, EPA Document SW-846, U.S. EPA Office of Solid Waste and Emergency Response, Washington, DC (November 1986).

through propane) contained in the headspace of waste drums that will be shipped to the WIPP site for burial.

The VOC determinations use gas chromatography/mass spectrometry (GC/MS) methods developed by the ACL for analysis of 29 target compounds that are of particular interest to the WIPP project. Target compounds include aromatic hydrocarbons, chlorinated aliphatic hydrocarbons, diethylether, alcohols, and ketones. The ACL has been participating in the analysis of WIPP Performance Demonstration (PD) samples and has successfully passed six cycles of analysis. We are now in the process of extending the current range of calibration curves. The extended range will allow us to analyze WIPP samples with fewer dilutions than are currently performed, which will lower our analysis costs.

Volume-percent concentrations of each of ten target-analyte gases (H_2, N_2, O_2, Ar, CO, CO_2, NO_x, CH_4, C_2H_6, and C_3H_8) are measured with a magnetic-sector, gas-analysis mass spectrometer having moderate resolution. Instrument stability and sensitivity have been demonstrated to meet WIPP program requirements regarding precision, accuracy, and detection limits for the gases of interest. Reliability of the instrument and procedures was reaffirmed during this past year by passing scores on a PD sample set.

6. Holding Time Study of Volatile Organics in SUMMA Canisters

As part of the WIPP Waste Characterization Program, headspace gas samples from waste containers are analyzed for a set of 29 volatile organic compounds, as described above. The headspace gas samples are collected in passivated SUMMA canisters with an allowable holding time of 28 days from the date of collection to date of analysis. Experiments are underway to determine how long the holding time can be extended without loss of data quality.

The experimental data on holding times are best obtained from "real" headspace samples collected from the WIPP waste containers; two field samples were thus selected for the study. The samples had been analyzed within the 28-day holding time by Idaho National Engineering Laboratory and were later sent to ANL. One of the samples has been analyzed periodically over the last 4 months without addition of any other compounds. The second sample was spiked with eight WIPP analytes that have occurrence frequency of 50% or higher (i.e., typically occur in 50% of field samples) to allow a time-zero measurement. Preliminary results from both samples indicate that the holding time could be extended well beyond the current 28-day limit. Extension to 3 months, for example, would allow batching of larger numbers of samples and, therefore, more efficient and cost-effective analyses.

7. Integrated Performance Evaluation Program

In collaboration with DOE's Radiological and Environmental Sciences Laboratory (RESL) and the Environmental Measurements Laboratory (EML), who serve as lead laboratories, ANL is developing and implementing a comprehensive Integrated Performance Evaluation Program (IPEP) for DOE's Office of Environmental Restoration and Waste Management (EM-563). The program is designed to provide information on the quality of radiological and non-radiological analytical data being produced by all laboratories on which DOE is relying for

analysis of environmental restoration and waste management samples. Argonne is assisting the two lead DOE laboratories in the development of the program requirements and strategies for implementation, especially in the non-radiological portions of the program. Argonne is also developing the strategies for compiling and analyzing the performance evaluation results from the participating laboratories, and for monitoring to assure that needed corrective actions are taken.

The IPEP also supports EM-563 efforts to develop the pilot Mixed Analyte Performance Evaluation Program (MAPEP), which was established because no EPA performance evaluation program currently exists for inorganic and radionuclide analytes in the same samples. During the past year, we developed data entry software that allows participants to electronically enter their results from these samples into the IPEP data base. Results have been received from all participants. Argonne also provided statistical analysis of the data using performance-based assessment tools being developed for the IPEP.

8. Analysis of Environmental and Waste Samples

The ACL provided analytical services to a variety of environmental monitoring, characterization, and remediation projects administered by the Environmental Research (ER) and Energy Systems (ES) Divisions at ANL, the Environment/Waste Management (EWM) programs at ANL, and programs at other DOE facilities (Nevada Test Site and Idaho National Engineering Laboratory). Samples processed during 1993 included waters, soils/sediments, and miscellaneous other materials (vegetation, air, filters, and sludges). These samples were analyzed according to protocols described in the U.S. EPA Contract Laboratory Program (CLP) Statement of Work, the methods described in Ref. 1, or other appropriate procedures. Approximately 200 analyses were completed in 1993, including determination of inorganic constituents (metals, anions, cyanide, sulfide, and total dissolved and suspended solids), organic compounds (volatiles, semivolatiles, PCBs/pesticides, phenolics, and oil and grease), and radionuclides (gamma emitters and actinides).

Under the RCRA, facilities or areas that have been involved in the storage, treatment, or disposal of hazardous wastes must undergo a formal sequence of characterization, remediation, and recharacterization before they are returned to general use. This sequence, designated a "closure" of the affected area, is performed according to a predetermined plan prepared in collaboration with the appropriate regulatory agencies. Through EWM, ANL has initiated closure activities at several locations. During 1993, the ACL provided both laboratory and technical support to some of these activities.

In one of these activities, the ACL analyzed samples of wash and rinse waters generated during the cleanup operations, as well as concrete and paint removed from the facilities. We determined specific contaminants (e.g., sulfide, metals), classes of contaminants (volatile organics), hazardous waste characteristics as defined by RCRA (corrosivity, ignitability, reactivity, and toxicity), and radiological parameters (alpha, beta, and gamma emitters).

The RCRA closure of two other areas at ANL was begun. One of these, the "Shoot-and-Burn Pile," consisted of a large mound of sand on which shock-reactive waste

chemicals had been detonated by rifle shot in past years as a means to render the chemicals safe for disposal. The other area, the "Alkali Metal Passivation Tank," is a concrete structure that had held water for the purpose of neutralizing water-reactive chemicals. Chemical analyses of numerous samples of water, sand, soil, and sludge from these areas will be required to complete their RCRA closures. Most of these analyses involve commonly applied EPA methods. However, for the Shoot-and-Burn Pile, special methods had to be devised to provide data on specific materials known to have been detonated on the sand pile.

Involvement by the ACL in these RCRA closures has typically extended beyond performing laboratory measurements on samples. The ACL also participated in the selection and specification of methods for the analysis of samples, interacted with contractors that performed the sampling and remediation activities or provided third-party oversight of the closure process, and assisted in evaluation or interpretation of analysis results. Input from ACL along with the analytical laboratory during the planning and performance of the closure activities helped to determine how waste generated during the cleanup should be disposed and whether the remediation achieved decontamination standards established in the closure plan.

9. X-ray Diffraction Support

The ACL's X-ray diffraction (XRD) facility has supported research in several ANL programs in 1993, including the high-temperature superconductivity, advanced battery, and fuel cell programs. To optimize fabrication of superconductive tapes (Sec. IX.B.1), a series of experiments was conducted by varying parameters such as temperature, composition, atmosphere, and pressure. Analysis of each sample by XRD, along with metallography and transmission and scanning electron microscopy, produced information with which we determined the region of most favorable conditions for superconductive tape formation. The XRD technique can monitor phase formation, orientation of the phases, and crystallinity, which are important factors in suitable tape formation. The ACL also applied XRD to failure analysis of components in electrochemical cells (Sec. I). Low cell performance can be associated with unwanted migration of materials and consequent change in the character of the electrode separator and interconnect material. The XRD technique was used for examining phase changes before and after cell operation to determine component integrity and extent of cell degradation.

In other work, orphan waste samples (see Sec. X.B.12) are being screened by XRD and X-ray fluorescence before consideration for disposal or further analysis.

10. Studies of TRU•Spec and RE•Spec Chromatography

The Separations Group in the Chemistry Division has developed unique column extraction phases that have applications in environmental and bioassay areas. These materials (designated TRU•Spec and RE•Spec) are now commercially available (Eichrome Industries, Inc.). However, only a limited amount of information has been published on their extraction properties. In 1993, we completed a comprehensive survey of distribution ratios (K_d's) for the TRU•Spec and RE•Spec extraction phases as a function of mobile phase composition for 30 rare earth and actinide elements. Column elution experiments were used to generate a K_d data base for samples containing these elements and dissolved in hydrochloric and nitric acid solutions.

Distribution ratios for the 30 elements were determined from ICP/AES measurements. The results of this study indicate that, by proper choice of the mobile phase, group separations (rare earths, actinides) can be achieved, thus simplifying analytical determinations and facilitating data interpretation. This approach has been applied to determination of selected elements in simulated nuclear fuel standards, nuclear waste glasses, and environmental samples. Availability of the K_d data allowed design of selective separation schemes for application to many different matrix compositions and greatly simplified the task of choosing the best column/mobile-phase combination for each application.

11. Improved Methods to Determine Actinides in Environmental Samples

During the past decade, DOE's environmental restoration and waste management mission has increased in importance and cost. The DOE has budgeted billions of dollars for these efforts and has forecasted that over a million analytical measurements will be required annually. It is only through the development and implementation of new technologies that the anticipated high costs of these measurements can be contained. In an ongoing collaborative effort with the Chemistry Division, efficient and cost-effective methods utilizing extraction chromatography are being developed to determine actinides in soil samples.

During the past year, we demonstrated the feasibility of TRU•Spec and Teva•Spec resins (Eichrome Industries, Inc.) for use in extraction chromatography for environmental samples. However, several limitations were identified. Both the acid concentrations and volumes used in these methods are significantly lower than those required for traditional methods as described in HASL-300.[2] Whereas this reduction is desirable from a waste minimization viewpoint, it is very difficult to maintain many soil samples in solution under these conditions. Additionally, experience at ANL has shown that the sample dissolution technique affects chromatographic column behavior.

A preconcentration step of the actinide and lanthanide elements using diphonix resin (Eichrome Industries) is being investigated to address these problems. Diphonix exhibits excellent selectivity for the actinides and lanthanides in hydrochloric acid. Larger solution volumes may also be practically employed with this resin. To ensure widespread applicability of this preconcentration method, a wide variety of soils are being processed by several dissolution techniques, namely, use of a hot plate, mixed-acid leaching, microwave digestion, and total dissolution fusion. Additionally, we are developing a separation scheme for the actinide elements that uses extraction chromatography resins; this scheme will satisfy the requirements of both radiometric and non-radiometric detection methods.

12. Animal Orphan Waste

The Biological and Medical Research Division has a large collection of rats, mice, and other animals that have been preserved in 5-gal (9-L) stainless steel containers with

---

[2] *Procedures Manual (HASL-300)*, 27th ed., Environmental Measurements Laboratory, U.S. Department of Energy, New York (1990).

formaldehyde and glycol added as preservatives. These containers of "pickled rats," which date back to the late 1940s and early 1950s, resulted from studies investigating the radiation effects on animals and relating it to humans. There was little or no documentation to identify the contents of these ~200 containers, so they qualified as an orphan or unknown waste. The disposal of these wastes required characterization prior to shipment and burial at the Hanford site in Washington.

The ACL prepared a sample and analysis plan for this orphan waste, which included first withdrawing 250 mL of the preservative liquid for radiochemical analysis, as well as 40 mL aliquots for organic analysis, from each of the containers. These aliquots were then analyzed for volatile organic constituents by a method adapted from the EPA CLP Statement of Work. Formaldehyde, ethylene glycol, and propylene glycol were determined by a GC/MS method.

We also analyzed selected orphan liquids for formaldehyde, type of glycol and fixative agents, volatile organic compounds, and radioactive constituents. To quantify the relationship between radioactive isotopes in the preservative solution and the amount of radioactivity in the animal, calcium content was also determined. The published literature indicates that calcium and other bone-seeking elements such as Sr and Ra leach out when stored for long periods of time in formaldehyde. By determining the isotope-to-calcium ratio in the liquid, we could calculate the amount of radioactivity per animal in the container.

The analytical data showed that the majority of the liquids contained ^{226}Ra and/or $^{90}Sr/^{90}Y$. Less common constituents were ^{235}U, ^{223}U, ^{241}Am, and ^{232}Th. We found that 128 containers had measurable β/γ radiation above background levels and suspected that some of the canisters may have up to microcurie quantities of ^{239}Pu. The project was successfully completed when the waste was shipped to Hanford for disposal. This waste, characterized as radioactive and hazardous or mixed, was the first shipment of this type to be sent from ANL-East and the first mixed-waste shipment to be accepted by the Hanford site.

13. Development of High-Temperature Superconductor

The ACL continued providing extensive analytical support to high-temperature superconductivity programs in the Energy Technology and CMT Divisions (Sec. IX.B.1). Much of this work involves analysis of starting materials, process samples, and products related to fabrication and characterization studies on various ceramic compositions, including $YBa_2Cu_3O_{7-x}$ and newer ceramics such as lead-doped bismuth/strontium/calcium/copper oxides ("BSCCO" ceramics). Our measurements include determining elemental composition by ICP/AES or classical methods, anions by ion chromatography, carbon with a LECO analyzer, and phase composition by XRD (see Sec. X.B.9). We also use an iodometric titration method to determine excess valence of the metals in a given ceramic.

The BSCCO ceramics exhibit several superconducting phase compositions that are of interest to researchers at ANL and their collaborators. In one case, ACL was asked to determine the metal content of viscous, organic-acid solutions used as starting material in a new approach to making BSCCO ceramics. Providing the needed data required development of a

special microwave-assisted digestion procedure to destroy the organic phase and produce sample solutions compatible with measurements by ICP/AES. We have also established a closed-vessel acid-dissolution procedure to dissolve virtually any BSCCO material for compositional analysis. Compositional changes can arise from variations in metal stoichiometry, as well as from variations in the valence of Pb, Bi, or Cu. This range of compositional variation in the BSCCO materials makes chemical analysis of individual specimens very important to understanding and comparing results from different specimens. Our experience with these materials suggests that more precise methodology is needed for their compositional analysis, and that new approaches are needed to characterize the metal valences that occur in them. The ACL plans to pursue development of capabilities to satisfy these needs.

14. Methodology for Characterizing Chlorofluorocarbons in Polyurethane Foam

Researchers in the ES Division are collaborating with the U.S. Bureau of Mines and the Appliance Recycling Centers of America in a study to characterize chlorofluorocarbons (CFC) present in the polyurethane foam insulation from discarded appliances, such as refrigerators and freezers. The information from this study is intended to aid development of technology to recover CFC from discarded foam as part of a worldwide effort to reduce CFC emissions to the atmosphere and prevent CFC destruction of the earth's ozone layer. There is more CFC as insulating gas in the polyurethane foam of a typical refrigerated appliance (680 to 1530 g) than is present as refrigerant in the appliance cooling system (170 to 340 g). The ACL was asked to investigate methods for determining the CFC content of representative foams for this research. To determine the total CFC content of a foam sample, we applied a method that involved combustion of the foam sample under high-pressure oxygen (25 atm or 2.5 MPa), followed by ion-chromatographic measurement of the chloride and fluoride products of the CFC combustion. We also devised a method for releasing CFC from the foam cells by cooling the foam to liquid nitrogen temperature in a closed vessel and pulverizing the embrittled foam to destroy the cell structure. Mass spectrometric examination of gas released during pulverization of the foams showed the gas to contain >99% $CFCl_3$ ("CFC-11"), which is a common blowing agent and insulating gas for polyurethane foams. From oxygen-bomb combustion of the pulverized foam residue, we determined that only about 60 to 80% of the chlorine and fluorine in the original foam could be released by breaking up the foam structure. This result might reflect CFC having permeated into the solid foam matrix. This condition would make it difficult to recover CFC by the foam-maceration technologies currently in use by the recycling industry.

15. Analysis of Nuclear Waste Glasses and Slags

The production of stable nuclear waste forms and their long-term storage in nuclear repositories are of great importance to nuclear power production and to DOE's environmental restoration and waste management activities. The CMT Glass Testing Program (Sec. IV.B) has the objective of evaluating factors that are likely to affect glass reactions in an unsaturated environment typical of a candidate repository site, such as Yucca Mountain in Nevada. In support of this and other programs over many years, the ACL has established a variety of dissolution and analysis methods tailored to the challenging task of determining the composition of materials classified as glasses and slags. These methods were put to use during the past year in characterizing Minimum Additive Waste Stabilization (MAWS) samples

(Sec. IV.C), which included synthetic slags containing high levels (up to 22 wt%) of iron and glasses that were high (about 12%) in fluorine content. Closed-vessel decomposition with mixed mineral acids (usually nitric and hydrofluoric acids) is usually most effective for dissolving these materials; we use both Parr bombs and microwave-heated digestion vessels for this application. The solutions obtained are subsequently analyzed by ICP/AES to determine component elements.

Some of ACL's methodology for analyzing glasses was also applied to a Waste Glass Analytical Round Robin (Round Robin 7) administered by the Materials Characterization Center at Pacific Northwest Laboratory. With support from the Glass Testing Program in CMT, the ACL prepared two unknown glasses and a glass standard in duplicate and analyzed each resulting glass by ICP/AES for 20 elements on three days. Ferrous iron in each of the glasses was determined by a modified Pratt titration. All the analytical results compared favorably with the accepted compositional data provided for the Round Robin by Corning, Inc. Both the component concentrations measured by ICP/AES and the ferrous/ferric iron ratios we reported were within measurement uncertainties of the reference values. These results confirmed satisfactory performance of our methods and help corroborate data we provide to ANL programs for similar materials.

16. Calcium Isotopic Determination in Canine Bone and Blood Serum

Biological and Medical Research Division staff are studying the effect of cadmium exposure and ovary removal on metabolic uptake and incorporation of calcium into bone. The protocol for this study involved administering oral and intravenous doses of enriched calcium isotopes to canine subjects; serum and bone samples were withdrawn from the subjects at an appropriate interval after the dose was administered. The relative abundances of the calcium isotopes in the samples indicate the extent of uptake and incorporation.

We are using ICP/MS to measure the extent of isotopic depletion or enrichment in the samples. The samples were ashed and reconstituted in nitric acid such that the total calcium concentration was approximately 10 mg/L, which minimizes spectral interferences inherent at the mass-to-charge ratios of interest. The isotope ratios in the samples were measured relative to a control sample (i.e., a bone or serum sample that was unspiked) in an effort to closely match the sample matrix to a standard of known (natural) isotopic composition. The isotope ratios were typically measured with an internal precision of ±0.2% relative standard deviation.

Isotopic analysis of 24 bone samples indicated no clear departure in bone from the natural calcium isotopic distribution. Agreement between duplicates was generally within one standard deviation. Isotopic analysis of eight serum samples (without duplicates) indicated a significant departure from the natural calcium isotopic abundance. Because bones are an extremely large calcium reservoir, it is unlikely that the expected isotopic perturbations in bone could be detected. Thus, determination of metabolic calcium uptake will be based on our isotopic analysis of the serum samples.

17. Automated, Real-Time Analysis of Chemical Sensor Data

"Instantaneous" detection of target analyte(s) is the ultimate goal of environmental monitoring. It does not matter whether the analyte is a toxic gas or an impurity in a process stream, nor does it matter whether the detection is accomplished by spectroscopic, electrochemical, or chromatographic techniques; rapid data collection, processing, and accurate evaluation are required for real-time detection. In modern instrumentation, computer-controlled data collection generates a plethora of data, which can be quite complex and require further mathematical treatment to be useful. Therefore, data are commonly stored for subsequent expert analysis, which is contrary to the goal of real-time detection.

Real-time analyte measurements must be performed by a sensor that includes the data analysis and evaluation steps. Such sensors must employ a signal processing strategy that is able to (1) extract analyte information from background noise and interferences and (2) make a decision as each scan is taken regarding the presence or absence of analyte information.

The first goal can be accomplished using digital filters. A digital filter is mathematically calculated and is described by a frequency response function defined by the analyst and tailored for a particular target compound. Different compounds of interest require separate digital filters. A digital filter extracts and enhances the analyte signal by suppressing unwanted signal components caused by other sources and, therefore, significantly improves the detection limit and helps to minimize interferences from other compounds. Because filtered data containing analyte information are visually different from filtered data containing no analyte information, standard pattern recognition techniques can be used to make an automated decision regarding the presence or absence of target analyte information.

Current work in the ACL is focused on designing computer software for creating real-time signal processing algorithms for chemical sensors of interest to the Arms Control and Nonproliferation Program. The software integrates digital filtering and pattern recognition techniques and has been implemented on a Silicon Graphics (Mountain View, CA) Indigo workstation. The computational power of a workstation is optimal for manipulating large quantities of data and for performing the extensive calculations required to construct customized digital filters and to develop reliable pattern discriminants. The capabilities and general utility of the software are being evaluated using data collected by a passive FTIR remote sensor.

18. Stand-off Detection

The U.S. Army's Edgewood Research, Development and Engineering Center (ERDEC) has an ongoing program in stand-off detection of chemical plumes. The ACL contributes to this program by determining the sensitivity of instrumentation, such as newly designed passive-remote FTIR spectrometers, and improving the ability of existing spectrometers to detect plumes in the presence of interferences.

Research was first focused on testing the ability of FTIR spectrometry to differentiate a single agent in a complex mixture of components that have interfering spectral absorbances. The results showed that detection can be accomplished in the spectral domain even

on these difficult mixtures. We found that use of partial least squares methods is more appropriate than classical least squares methods for detection under these circumstances. We are currently building an analyte data base consisting of quantitative data at different black-body temperatures. This data base will be used to determine the ability of the FTIR instrumentation to detect analytes under differing background conditions. The black-body emission spectra will be correlated with different field emission data.

19. Characterization of Products and Residues from Automobile Shredder "Fluff" Recycling

About 225 kg (25%) of every junked car that is processed by automobile shredders to recover ferrous-metal scrap is made up of a mixture of plastics, glass, fibers, and foam. This mixture is referred to as "fluff" and represents a substantial waste side stream from the automobile shredder industry. At present, shredder fluff is placed in a landfill. Researchers in the ES Division have developed and are testing technologies to segregate and recover the plastic and foam fluff components for recycling and are exploring alternatives to landfill disposal for residues ("fines") that are collected during segregation of the recyclable materials. The ACL is providing chemical analyses to help characterize the various product streams from these processes, including oils, recovered plastics and foams, and the shredder fines. An FTIR microscope is used to examine plastics recovered by solvent extraction of shredder residues. Here, selectivity of the extraction and purity of the products are assessed by comparing spectra from polyvinylchloride and acrilonitrilebutadienestyrene standards to spectra of reconstituted plastics from the process. Other analysis methods are applied to determine specific contaminants in the foams, oils, and fines. Heavy metals and PCBs are common contaminants in the shredder fluff as a result of their presence in automotive components and fluids (e.g., lead from batteries, mercury from mercury switches, PCB from capacitors or hydraulic fluids). After suitable treatment of samples to bring the metals into solution, they are analyzed by ICP/AES or cold vapor atomic absorption. The PCBs are extracted with an appropriate solvent and measured by gas chromatography. We also determined the total chlorine content of many samples by a procedure that employs oxygen-bomb combustion and ion chromatography to measure the chlorine as chloride.

These and other analysis tools were used during the past year to provide the ES Division with (1) data on the effectiveness of a new process to remove metal and oil contaminants from polyurethane foams from the shredder fluff and (2) a comprehensive characterization of shredder fines to determine their suitability for disposal by incineration in a cement kiln.

20. Radiochemical Method Evaluation and Development

The Department of Energy estimates suggest that 1.4 million radiochemical analyses or more will be required per annum to support environmental restoration and waste management activities. The cost of these analyses could be reduced substantially by streamlining radioanalytical procedures. The ACL in collaboration with the ER Division is examining existing radiochemical procedures and formulating research and/or subcontracting plans to develop new techniques for sample preparation and measurement.

As part of this program, ACL staff reviewed existing radiochemical procedures and recommended areas for improvement; the ACL recommendations were affirmed and strengthened by an expert working group convened by DOE/EM-563. From that point, strategies were developed to facilitate improvements in sample preparation and analysis. As part of that strategy, specifications were developed for subcontract procurement of automated gross alpha/beta emitter determination and automated soil dissolution. In addition, work plans were formulated to develop improved actinide isolation procedures and determine radioisotopes by ICP/MS at ANL. The ACL is now developing improved methods for actinide isolation and suitable ICP/MS procedures for radioisotope determination. Both efforts will continue in 1994 with emphasis on demonstration and automation.

21. Analysis of Soils for Explosives

Soil samples were submitted to the ACL by the ER Division for analysis by liquid chromatography/mass spectrometry (LC/MS) as part of a study to identify two unknown intermediates of trinitrobenzene (TNB) that were detected in previous work using high-pressure liquid chromatography. Identification of these unknowns is required to understand the bioremediation of trinitrotoluene (TNT) from soil in a slurry reactor.

The instrumentation used for the work consisted of a mass spectrometer interfaced with a liquid chromatograph including a photodiode array detector. Analytical data were initially obtained using the LC/MS particle beam for low level concentrations (50 ppm) of TNB, but the identification of corresponding intermediates was inconclusive, since the analyte was typically removed with the solvent mobile phase in the particle beam/generator interface. As larger concentrations of TNB standard (71,000 ppm) were injected into the LC/MS, enough analyte reached the ionization chamber of the mass spectrometer to allow identification. Later work revealed that using a thermospray interface with a softer ionization technique allowed TNB detection at lower concentrations. The spectra obtained using thermospray differ from traditional electron impact; however, the molecular ion is clearly visible in thermospray spectra for qualitative analysis.

22. Treatment of Cesium-Contaminated Milk

In the Ukraine, a million gallons of milk is destroyed each day as a consequence of radioactive cesium and strontium contamination. In 1993, a team led by staff from the ES Division conducted tests with Bradtec Ltd. (Bristol, UK) to demonstrate that its MAG*SEP(TM) process (which uses specially coated magnetic particles to adsorb heavy metals and radioactive contaminants from solution) could be used to reduce the cesium concentration in milk to acceptable levels.

Two separate tests were conducted by ES and ER staff during this demonstration. In a laboratory-scale test, 65 pCi/g of ^{137}Cs and 2 mg/L of natural cesium were added to one liter of milk prior to treatment. After four contacts with MAG*SEP(TM) particles, the ^{137}Cs activity was reduced to 4 pCi/g, which is 2.5 times less than the prescribed intervention level. In a second test, 2 mg/L of natural cesium was added to 60 L milk prior to MAG*SEP(TM) treatment in a

pilot-scale facility. We then determined the cesium content in the pilot-plant feedstock and effluent (i.e., contaminated and treated milk, respectively).

The method of standard additions was selected for these determinations because it is relatively impervious to matrix-related interferences. Cesium (analyte) and indium (internal standard) spikes were added to the sample aliquots before any preparative chemistry was performed to compensate for analyte losses during preparation. Samples were then treated by method 16.047 of the Association of Official Analytical Chemists (AOAC)[3]; this procedure was used solely to remove suspended solids and proteins from the milk prior to instrumental analysis. Once the AOAC method was completed, ICP/MS was used to determine the cesium content in the supernatant liquid.

The cesium detection limit for the AOAC method was found to be 2 ng/mL. The "measured" and "prepared" concentration of cesium in the untreated milk agreed to within 10% (i.e., one standard deviation of the instrumental measurement), and the cesium content of the treated milk indicated that 78% of the cesium was removed by a single contact with MAG*SEP(TM). This result did not agree initially with the laboratory-scale test, where 50% of the cesium had been removed per contact; however, we later found that the milk had been inadvertently diluted by water in the process lines. Dilution reduced the cesium concentration in the process effluent, thereby increasing the apparent decontamination factor. With this correction taken into account, reasonable agreement was obtained between our results and the laboratory-scale test.

---

[3] *Official Methods of Analysis of the Association of Official Analytical Chemists*, Kenneth Helrich, Ed., 15th ed., Association of Official Analytical Chemists, Arlington, VA (1990).

XI. ADDENDUM.

CHEMICAL TECHNOLOGY DIVISION PUBLICATIONS --- 1993

The Division's publications and oral presentations for 1993 were entered into a bibliographic data base. The pages that follow are a printout of this information sorted into six categories: (1) journal articles, books, and book chapters, (2) patents, (3) ANL progress and topical reports, as well as contributions to reports published by organizations other than ANL, (4) abstracts and papers published in proceedings of conferences, symposiums, workshops, etc., (5) oral presentations at scientific meetings and seminars not referenced in the fourth category, and (6) papers accepted for publication but not yet published.

Chemical Technology Division Publications—1993

A. Journal Articles, Books, and Book Chapters

Distribution of Plutonium, Americium, and Several Rare Earth Fission Product Elements Between Liquid Cadmium and LiCl-KCl Eutectic
J. P. Ackerman and J. L. Settle
J. Alloys Comp. **199**, 77–84 (1993)

Protein Monolayer Electrochemistry: Strategy for Probing Biological Electron Transfer Kinetics
E. F. Bowden, R. A. Clark, J. L. Willit, and S. Song
Redox Mechanisms and Interfacial Properties of Molecules of Biological Importance, Eds., F. Schultz and I. Taniguchi, Electrochem. Soc., Pennington, NJ, pp. 34–45 (1993)

Ab Initio Molecular Orbital Cluster Studies of the Zeolite ZSM-5. 1. Proton Affinities
H. V. Brand, L. A. Curtiss, and L. E. Iton
J. Phys. Chem. **97**(49), 12773–12782 (1993)

Stability and Growth of the $(Bi,Pb)_2Sr_2Ca_2Cu_3O_x$ Phase in a Silver Sheath
W. L. Carter, G. N. Riley, J. S. Luo, N. Merchant, and V. A. Maroni
Appl. Supercond. **1**(10–12), 1523–1534 (1993)

Beneficiation of Pu Residues by Ultrafine Grinding and Aqueous Biphasic Extraction
D. J. Chaiko, R. Mensah-Biney, C. J. Mertz, and A. Rollins
Sep. Sci. Tehnol. **28**(1–3), 765–780 (1993)

Measurements of $Al(NO_3)_3$ Activities in Aqueous Nitrate Solutions
D. J. Chaiko, I. R. Tasker, D. R. Fredrickson, A. A. Difilippo, S. M. Smidt, and G. F. Vandegrift
J. Nucl. Mater. **201**, 184–189 (1993)

Low Symmetry in the Crystal Structure of (Octapentylphthalocyaninato) (methyl)rhodium(III)
M. J. Chen, J. W. Rathke, and J. C. Huffman
Organomet. **12**(11), 4673–4677 (1993)

In-Situ Synchrotron X-ray Reflectivity Measurements at the Calcite-Water Interface
R. P. Chiarello, R. A. Wogelius, and N. C. Sturchio
Geochim. Cosmochim. Acta **57**, 4103–4110 (1993)

Molecular Photofragmentation during Nonresonant Multiphoton Ionisation of Sputtered Species
S. R. Coon, W. F. Calaway, M. J. Pellin, J. W. Burnett, and J. M. White
Surf. Interface Analysis **20**, 1007–1010 (1993)

Kinetic Energy Distributions of Sputtered Neutral Aluminum Clusters: Al-Al_6
S. R. Coon, W. F. Calaway, M. J. Pellin, G. A. Curlee, and J. M. White
Nucl. Instrum. Methods B **82**, 329–336 (1993)

New Findings on the Sputtering of Neutral Metal Clusters
S. R. Coon, W. F. Calaway, M. J. Pellin, and J. M. White
Surf. Sci. **298**, 161–172 (1993)

Superexchange Pathway Calculation of Long-Distance Electron Coupling in $H_2C(CH_2)_{m-2}CH_2$ Chains
L. A. Curtiss, C. A. Naleway, and J. R. Miller
Chem. Phys. **176**, 387–405 (1993)

Theoretical Study of Long Distance Electronic Coupling in $H_2C(CH_2)_{n-2}CH_2$, n = 3–16
L. A. Curtiss, C. A. Naleway, and J. R. Miller
J. Phys. Chem. **97**, 4050 (1993)

The Accurate Determination of Enthalpies of Formation
L. A. Curtiss, K. Raghavachari, and J. A. Pople
Chem. Phys. Lett. **214**(2), 183–185 (1993)

Gaussian-2 Theory Using Reduced Møller-Plesset Orders
L. A. Curtiss, K. Raghavachari, and J. A. Pople
J. Chem. Phys. **98**(2), 1293–1298 (1993)

The Vapour Phase Complex HF-AlF_3: A New *Ab Initio* Molecular Orbital Study
L. A. Curtiss and G. Scholz
Chem. Phys. Lett. **205**(6), 550–554 (1993)

The Effects of the Leachate pH and the Ratio of Glass Surface Area to Leachant Volume on Glass Reactions
W. L. Ebert
Phys. Chem. Glasses **34**(2), 58–65 (1993)

A Comparison of Glass Reaction at High and Low Surface Area to Volume
W. L. Ebert and J. K. Bates
Nucl. Technol. **104**(3), 372–384 (1993)

Long-Term Comparison of Dissolution Behavior Between Fully Radioactive and Simulated Nuclear Waste Glasses
X. Feng, J. K. Bates, E. C. Buck, C. R. Bradley, and M. Gong
Nucl. Technol. **104**, 193–206 (1993)

Electromagnetic Modes and Prism-Film Coupling in Anisotropic Planar Waveguides of Epitaxial (101) Rutile Thin Films
C. M. Foster, S.-K. Chan, H. L. M. Chang, R. P. Chiarello, T. J. Zhang, J. Guo, and D. J. Lam
J. Appl. Phys. **73**(11), 7823–7830 (1993)

Cadmium Transport Through Molten Salts in the Reprocessing of Spent Fuel for the Integral Fast Reactor
K. M. Goff, A. Schneider, and J. E. Battles
Nucl. Technol. **102**, 331–340 (June 1993)

Use of Halocarbon Oils as a Matrix for Transmission Spectroscopic Studies of Solid Inorganic Materials in the Near-Infrared and Visible Regions
N. S. Guyot-Sionnest and V. A. Maroni
Appl. Spectrosc. **47**(5), 556–559 (1993)

Thermomechanical Processing of Reactively Sintered Ag-Clad $(Bi,Pb)_2Sr_2Ca_2Cu_3O_x$ Tapes
D. Y. Kaufman, M. T. Lanagan, S. E. Dorris, J. T. Dawley, I. Bloom, M. C. Hash, N. Chen, M. R. DeGuire, and R. B. Poeppel
Appl. Supercond. **1**, 81 (1993)

High Temperature Lithium/Sulfide Batteries
T. D. Kaun, P. A. Nelson, L. Redey, D. R. Vissers, and G. L. Henricksen
Electrochim. Acta **38**(9), 1269–1287 (1993)

Finite-Size Effect on the First-Order Metal-Insulator Transition in VO_2 Films Grown by Metal-Organic Chemical-Vapor Deposition
H. K. Kim, H. You, R. P. Chiarello, H. L. M. Chang, T. J. Zhang, and D. J. Lam
Phys. Rev. B **47**(19), 900–907 (1993)

Distribution of Actinides in Molten Chloride Salt/Cadmium Metal Systems
T. Koyama, T. R. Johnson, and D. F. Fischer
J. Alloys Comp. **189**, 37–44 (1993)

The Centrifugal Contactor as a Concentrator in Solvent Extraction Processes
R. A. Leonard, D. G. Wygmans, M. J. McElwee, M. O. Wasserman, and G. F. Vandegrift
Sep. Sci. Technol. **28**(1–3), 177–200 (1993)

Salt-Occluded Zeolites as an Immobilization Matrix for Chloride Salt Waste
M. A. Lewis
Am. Ceram. Soc. **76**(11), 2826–2832 (1993)

Theoretical Study of the Silicon-Oxygen Hydrides $SiOH_n$(n = 0-4) and $SiOH_n^+$ (n = 0-5): Dissociation Energies, Ionization Energies, Enthalpies of Formation, and Proton Affinities
D. J. Lucas, L. A. Curtiss, and J. A. Pople
J. Chem. Phys. **99**(9), 6697–6703 (1993)

Phase Chemistry and Microstructure Evolution in Silver-Clad $(Bi_{2-x}Pb_x)Sr_2Ca_2Cu_3O_y$ Wires
J. S. Luo, N. Merchant, E. Escorcia-Aparicio, V. A. Maroni, D. M. Gruen, B. S. Tani, G. N. Riley, and W. L. Carter
IEEE Trans. Appl. Superconduc. **3**(1), 972–975 (1993)

Kinetics and Mechanism of the $(Bi,Pb)_2Sr_2Ca_2Cu_3O_{10}$ Formation Reaction in Silver-Sheathed Wires
J. S. Luo, N. Merchant, V. A. Maroni, D. M. Gruen, B. S. Tani, W. L. Carter, and G. N. Riley
Appl. Supercond. **1**(1/2), 101–107 (1993)

Influence of Silver Cladding on the Formation and Alignment of the $(Bi_{2-x}Pb_x)Sr_2Ca_2Cu_3O_{10+\delta}$ Phase
J. S. Luo, N. Merchant, V. A. Maroni, G. N. Riley, and W. L. Carter
Appl. Phys. Lett. **63**(5), 690–692 (1993)

Synthesis of High-Temperature Superconductors by Oxidation of a Precursor Alloy
J. S. Luo, D. Michel, J.-P. Chevalier, N. Merchant, V. A. Maroni, D. M. Gruen, K. H. Sandhage, and C. A. Craven
Mater. Sci. Forum **137–139**, 523–546 (1993)

Synchrotron Infrared Spectroscopy of H_2O Adsorbed on Polycrystalline Gold
C. A. Melendres, B. Beden, G. Bowmaker, C. Liu, and V. A. Maroni
Langmuir **9**(8), 1980–1982 (1993)

DC Electrochemical Techniques for the Measurement of Corrosion Rates

Z. Nagy

Modern Aspects of Electrochemistry, Eds., J. O'M. Bockris et al., Plenum Press, New York, Vol. 25, pp. 135–190 (1993)

Introduction and Synopsis of the TITAN Reversed-field-pinch Fusion-Reactor Study

F. Najmabadi, D. K. Sze, et al.

Fusion Eng. Design **23**, 69–80 (1993)

The TITAN-I Reversed-field-pinch Fusion-power-core Design

F. Najmabadi, D. K. Sze, et al.

Fusion Eng. Design **23**, 81–98 (1993)

Utilisation of Crown Ether Chemistry to Prepare Bimetallic Compounds: Preparation and Structural Characterization of [Ba (15-Crown-5)$_2$][$CuCl_4$]

L. Nunes and R. D. Rogers

J. Coord. Chem. **28**, 347–354 (1993)

Composition and Structure of the Anodic Films on Titanium in Aqueous Solutions

M. Pankuch, R. Bell, and C. A. Melendres

Electrochim. Acta **38**, 2777 (1993)

Thermodynamic Analysis of Phase Equilibria in the Iron-Zirconium System

A. D. Pelton, L. Leibowitz, and R. A. Blomquist

J. Nucl. Mater. **201**, 218–224 (1993)

Chemical and Isotopic Characterisation of the CO_2-Rich Volcanic-Hydrothermal Discharges from the Canarian Volcanoes, Spain

N. M. Peres, N. C. Sturchio, Y. Sano, S. N. Williams, J. C. Carracedo, J. Coello, and H. Wakita

Ann. Geophys., Suppl. 1 **11**, 80 (1993)

Progress in the Pyrochemical Processing of Spent Nuclear Fuels

R. D. Pierce, T. R. Johnson, C. C. McPheeters, and J. J. Laidler

J. Met. **45**(2), 40–44 (1993)

Internal U-Series Systematics in Pumice from the 13-November-1985 Eruption of Nevado del Ruiz, Colombia

S. Schaefer, N. C. Sturchio, M. T. Murrell, and S. N. Williams

Geochim. Cosmochim. Acta **57**, 1215–1220 (1993)

Review of *Uranium-Series Disequilibrium: Applications to Earth, Marine, and Environmental Sciences*, Eds., M. Ivanovich and R. S. Harmon, 2nd ed., Clarendon Press, Oxford (1992)

N. C. Sturchio

Geochim. Cosmochim. Acta **57**, 4327–4328 (1993)

Radium Isotope Geochemistry of Thermal Waters, Yellowstone National Park, Wyoming

N. C. Sturchio, J. K. Bohlke, and F. Markun

Geochim. Cosmochim. Acta **57**, 1203–1214 (1993)

Late Quaternary Geothermal Activity in the Northern Kenya Rift

N. C. Sturchio, P. N. Dunkley, and M. Smith

Nature **362**, 233–234 (1993)

The Hydrothermal System of Puracé Volcano, Columbia
N. C. Sturchio, S. N. Williams, and Y. Sano
Bull. Volcanol. **55**, 289–296 (1993)

Dynamics of Room-Temperature Melts: Nuclear Magnetic Resonance Measurements of Dialkylimidazolium Haloaluminates
S. Takahashi, M.-L. Saboungi, R. J. Klingler, M. J. Chen, and J. W. Rathke
J. Chem. Soc. Faraday Trans. **89**(19), 3591–3595 (1993)

Tritium Transport in Lithium Ceramics Porous Media
S.-W. Tam and V. Ambrose
J. Nucl. Mater. **191–194**, 253–257 (1992)

A Study of Fluidised-Bed Dynamical Behavior—A Chaos Perspective
S.-W. Tam and M. K. Devine
Applied Chaos, Eds., J. Kim and J. Stringer, John Wiley, New York, Chapt. 16, pp. 381–391 (1992)

Solubility of $FeCl_2$ in Molten NaCl-$AlCl_3$
P. J. Tumidajski and M. Blander
Can. Metall. Q. **31**(1), 25–30 (1992)

Theoretical Analysis of a Blocking-Electrode Oxygen Sensor for Combustion-Gas Streams
M. W. Verbrugge and D. W. Dees
J. Electrochem. Soc. **140**(7), 2001 (1993)

Utility Programs Used for EPA Contract Laboratory Program Computations
R. J. Wingender and E. Y. Hwang
Sci. Comput. Auto., 37–44 (1993)

Rotating-Frame NMR Microscopy Using Toroid Cavity Detectors
K. Woelk, J. W. Rathke, and R. J. Klingler
J. Magn. Reson. A **105**, 113–116 (1993)

The TITAN-II Reversed-field-pinch Fusion-power-core Design
C. P. C. Wong, D. K. Sze, et al.
Fusion Eng. Design **23**, 173–200 (1993)

Prediction of the Thermodynamic Properties and Phase Diagrams of Silicate Systems—Evaluation of the FeO-MgO-SiO_2 System
P. Wu, G. Eriksson, A. D. Pelton, and M. Blander
Iron and Steel Institute of Japan Int. **33**(1), 26–35 (1993)

X-ray Reflectivity and Scanning-Tunneling-Microscope Study of Kinetic Roughening of Sputter-Deposited Gold Films during Growth
H. You, R. P. Chiarello, H. K. Kim, and K. G. Vandervoort
Phys. Rev. Lett. **70**(19), 2900–2903 (1993)

Applications of X-ray Scattering Techniques for the Study of Electrochemical Interphases
H. You and Z. Nagy
Current Topics in Electrochemistry, Council of Scientific Research Integration, Trivandrum, India, Vol. 2, pp. 21–43 (1993)

A Theoretical Study of the Oxygen K Absorption Edge in Cluster Models of Sodalite
S. A. Zygmunt, L. A. Curtiss, and L. E. Iton
Chem. Phys. **173**, 357–366 (1993)

B. Patents

Solid-Oxide Fuel Cell Electrolyte
I. Bloom, M. C. Hash, and M. Krumpelt
Patent No. 5,213,911, issued May 25, 1993

Method of Electrode Fabrication and an Electrode for Metal Chloride Battery
I. Bloom, P. A. Nelson, and D. R. Vissers
Patent No. 5,194,343, issued March 16, 1993

Processing Method for Superconducting Ceramics
I. Bloom, R. B. Poeppel, and B. K. Flandermeyer
Statutory Invention Registration No. H1138, issued February 2, 1993

Centrifugal Pyrocontactor
L. S. Chow and R. A. Leonard
Patent No. 5,254,076, issued October 19, 1993

Method of Preparing Corrosion-Resistant Composite Materials
T. D. Kaun
Patent No. 5,194,298, issued March 16, 1993

Ionic Conductors for Solid Oxide Fuel Cells
M. Krumpelt, I. Bloom, J. D. Pullockaran, and K. M. Myles
Patent No. 5,232,794, issued August 3, 1993

Improved Fuel Cell System for Transportation Applications
R. Kumar, S. Ahmed, M. Krumpelt, and K. M. Myles
Patent No. 5,248,566, issued September 28, 1993

Method for Immobilising Mixed Waste Chloride Salts Containing Radionuclides and Other Hazardous Wastes
M. A. Lewis and T. R. Johnson
Statutory Invention Registration No. H1227, issued September 7, 1993

Electrowinning Process with Electrode Compartment to Avoid Contamination of Electrolyte
D. S. Poa, R. D. Pierce, T. P. Mulcahey, and G. K. Johnson
Patent No. 5,225,051, issued July 6, 1993

Cobalt Carbonyl Catalysed Olefin Hydroformylation in Supercritical Carbon Dioxide
J. W. Rathke and R. J. Klingler
Patent No. 5,198,589, issued March 30, 1993

Electrically Conductive Material
J. P. Singh, A. L. Bosak, C. C. McPheeters, and D. W. Dees
Patent No. 5,242,873, issued September 7, 1993

C. Reports

Stability of Low Concentration Calibration Standards for Graphite Furnace Atomic Absorption Spectrophotometry

D. A. Bass and L. B. TenKate

ANL/ACL-93/3 (November 1993)

ANL Technical Support Program for DOE Environmental Restoration and Waste Management Annual Report, October 1991–September 1992

J. K. Bates, W. L. Bourcier, C. R. Bradley, E. C. Buck, J. C. Cunnane, N. L. Dietz, W. L. Ebert, J. W. Emery, R. C. Ewing, X. Feng, T. J. Gerding, M. Gong, J. C. Hoh, H. Li, J. J. Mazer, L. E. Morgan, L. Newton, J. K. Nielsen, B. L. Phillips, M. Tomozawa, L. Wang, and D. J. Wronkiewicz

ANL-93/13 (May 1993)

Chemical Technology Division Annual Technical Report, 1992

J. E. Battles et al.

ANL-93/17 (June 1993)

Lead Exposures and Biological Responses in Military Weapons Systems: Aerosol Characteristics and Acute Lead Effects Among U.S. Army Artillerymen—Final Report

M. H. Bhattacharyya, J. H. Stebbings, D. P. Peterson, S. A. Johnson, R. Kumar, B. D. Goun, I. Janssen, and J. E. Trier

ANL-93/7 (March 1993)

Technical Area Status Report for Chemical/Physical Treatment

C. H. Brown, W. E. Schwinkendorf, D. J. Chaiko, et al.

DOE/MWIP-8 (August 1993)

Waste Treatment and Reduction: A Basic Science Approach, in *Workshop on Innovation in Materials Processing and Manufacture: Exploratory Concepts for Energy Applications*

D. J. Chaiko and A. Galli

Oak Ridge National Laboratory Report ORNL-6760 (September 1993)

Soil Decontamination by Aqueous Biphasic Extraction, Part 4 in *Removal of Uranium from Uranium-Contaminated Soils. Phase I: Bench-Scale Testing*

D. J. Chaiko, R. Mensah-Biney, and E. H. Van Deventer

Oak Ridge National Laboratory Report ORNL-6762 (Sepember 1993)

Test Plan for Reactions Between Spent Fuel and J-13 Well Water under Unsaturated Conditions

P. A. Finn, D. J. Wronkiewicz, J. C. Hoh, J. W. Emery, L. D. Hafenrichter, and J. K. Bates

ANL-92/48 (January 1993)

Nuclear Technology Programs Semiannual Progress Report, April–September 1991

C. E. Johnson, G. F. Vandegrift, J. K. Bates, P. E. Blackburn, R. A. Blomquist, S. Betts, C. R. Bradley, E. C. Buck, D. B. Chamberlain, J. M. Copple, N. L. Dietz, J. A. Dow, W. L. Ebert, J. W. Emery, X. Feng, S. E. Farley, P. A. Finn, A. K. Fischer, D. R. Fredrickson, T. J. Gerding, J. C. Hoh, J. C. Hutter, I. Johnson, J. P. Kopasz, L. Leibowitz, R. A. Leonard, J. J. Mazer, M. J. McElwee, L. Nunez, D. Redfield, M. C. Regalbuto, M. F. Roche, J. Sedlet, S.-W. Tam, E. H. Van Deventer, J. P. Webb, D. J. Wronkiewicz, and D. G. Wygmans

ANL-93/21 (July 1993)

Evaluate FIBROSIC^{TM} Candle Filter for Particulate Control in PFBC

S. H. D. Lee and W. M. Swift

Final Report to Illinois Clean Coal Institute, September 1, 1992 through December 31, 1993 (December 1993)

Evaluate FIBROSIC^{TM} Candle Filter for Particulate Control in PFBC

S. H. D. Lee, W. M. Swift, and F. G. Teats

Interim Final Technical Report to Illinois Clean Coal Institute, September 1, 1992 through August 31, 1993 (August 1993)

A Vibration Model for Centrifugal Contactors

R. A. Leonard, M. O. Wasserman, and D. G. Wygmans

ANL-92/40 (November 1992)

Determination of PCBs in Rocky Flats Type IV Waste Sludge by Gas Chromatography/Electron Capture Detection

K. J. Parish, D. V. Applegate, A. S. Boparai, and G. T. Reedy

ANL/ACL-93/1 (December 1993)

Practical Superconductor Development for Electrical Power Applications, Annual Report for FY 1993

R. B. Poeppel, K. C. Goretta, T. R. Askew, U. Balachandran, Y. S. Cha, J. A. DeLuca, S. E. Dorris, J. T. Dusek, W. A. Ellingson, J. E. Emerson, K. C. Goretta, K. E. Gray, J. D. Hettinger, J. Hu, J. R. Hull, R. T. Kampwirth, D. S. Kupperman, M. T. Lanagan, V. A. Maroni, R. L. McDaniel, D. J. Miller, R. C. Niemann, J. J. Picciolo, J. L. Routbort, J. P. Singh, K. L. Uherka, and C. A. Youngdahl

ANL-93/33 (October 1993)

Solidus and Liquidus Temperatures of Core-Concrete Mixtures

M. F. Roche, L. Leibowits, J. K. Fink, and L. Baker

NUREG/CR-6032, ANL-93/9 (June 1993)

Annual Report for Ion Replacement Program

Z. Tomcsuk, J. L. Willit, and A. K. Fischer

ANL-93/24 (July 1993)

Preliminary Plan for Treating Mixed Waste

G. F. Vandegrift, C. Conner, J. C. Hutter, R. A. Leonard, L. Nunes, J. Sedlet, and D. G. Wygmans

ANL-93/29 (June 1993)

Effects of Radionuclide Decay on Waste Glass Behavior—A Critical Review

D. J. Wronkiewicz

ANL-93/45 (December 1993)

D. Abstracts and Proceedings Papers

New High-Level Waste Management Technology for IFR Pyroprocessing Wastes

J. P. Ackerman and T. R. Johnson

Proc. of the GLOBAL '93 Int. Conf. and Technology Exhibition on Future Nuclear Systems, Seattle, WA, September 12–17, 1993, Vol. 2, pp. 969–973 (1993)

Chemical and Isotopic Composition of Fumaroles, Volcan Galeras, Colombia

G. B. Arehart, N. C. Sturchio, T. Fischer, and S. N. Williams

Abstracts with Programs, Geological Soc. of America Annual Meeting, Boston, MA, October 25–28, 1993, Vol. 25, pp. 326–327 (1993)

Sr Isotopic Heterogeneity in the Milk River Aquifer, Alberta

S. Armstrong, N. C. Sturchio, and M. J. Hendry

Trans. of the Fall Meeting of the Am. Geophys. Union, EOS, San Francisco, CA, December 6–9, 1993, Vol. 74, p. 270 (1993)

Controls on Late Quaternary Landscape Evolution—Red Sea Coast, Egypt

R. E. Arvidson, R. Becker, A. Shanabrook, M. Sultan, W. Luo, and N. C. Sturchio

Trans. of the Fall Meeting of the Am. Geophys. Union, EOS, San Francisco, CA, December 6–9, 1993, Vol. 74, p. 193 (1993)

Validation of Tritium Transport Models in Li_2O

M. C. Billone, J. P. Kopasz, and H. Attaya

Proc. of the Second Int. Workshop on Ceramic Breeder Blanket Interactions, Ed., M. Yamawaki, Tokyo, Japan, October 26–29, 1992, pp. 101–133 (1993)

Modeling SA/V Effects in Borosilicate Glass Dissolution

W. L. Bourcier, W. L. Ebert, and X. Feng

Mater. Res. Soc. Symp. Proc. **294**, 577–582 (1993)

Analytical Electron Microscopy Study of Colloids from Nuclear Waste Glass Reaction

E. C. Buck, J. K. Bates, J. C. Cunnane, W. L. Ebert, X. Feng, and D. J. Wronkiewicz

Mater. Res. Soc. Symp. Proc. **294**, 199–206 (1993)

Analytical Electron Microscopy Examination of Uranium Contamination at the DOE Fernald Operation Site

E. C. Buck, N. L. Dietz, J. K. Bates, and J. C. Cunnane

Proc. of the Waste Management '93 Conf., 19th Annual Nuclear Waste Symp., Tucson, AZ, February 28–March 4, 1993, Vol. 1, pp. 797–801 (1993)

Proliferation Resistance of the Fuel Cycle for the Integral Fast Reactor

L. Burris

Proc. of the GLOBAL '93 Int. Conf. and Technology Exhibition on Future Nuclear Systems, Seattle, WA, September 12–17, 1993, Vol. 1, pp. 328–333 (1993)

Tests of Prototype Salt Stripper System for IFR Fuel Cycle

E. L. Carls, R. J. Blaskovitz, T. Ogata, and T. R. Johnson

Proc. of the GLOBAL '93 Int. Conf. and Technology Exhibition on Future Nuclear Systems, Seattle, WA, September 12–17, 1993, Vol. 2, pp. 974–981 (1993)

In-Situ Synchrotron X-ray Reflectivity Measurements at the Calcite-Water Interface

R. P. Chiarello, N. C. Sturchio, and R. A. Wogelius

Trans. of the Fall Meeting of the Am. Geophys. Union, EOS, San Francisco, CA, December 6–9, 1993, Vol. 74, p. 627 (1993)

Continuous Extraction of Molten Chloride Salts with Liquid Cadmium Alloys

L. S. Chow, J. K. Basco, J. P. Ackerman, and T. R. Johnson

Proc. of the GLOBAL '93 Int. Conf. and Technology Exhibition on Future Nuclear Systems, Seattle, WA, September 12–17, 1993, Vol. 2, pp. 1080–1085 (1993)

High-Level Nuclear Waste Borosilicate Glass: A Compendium of Characteristics

J. C. Cunnane, J. K. Bates, W. L. Ebert, X. Feng, J. J. Maser, D. J. Wronkiewicz, J. Sproull, W. L. Bourcier, and B. P. McGrail

Mater. Res. Soc. Symp. Proc. **294**, 225–232 (1993)

Field Demonstration of Technologies for Characterization of Uranium Contamination in Surface and Subsurface Soils

J. C. Cunnane, S. Y. Lee, D. L. Perry, V. C. Tidwell, J. Schwing, K. R. Nuhfer, and G. Weigand

Proc. of the Waste Management '93 Conf., 19th Annual Nuclear Waste Symp., Tucson, AZ, February 28–March 4, 1993, Vol. 1, pp. 803–809 (1993)

Many-Body Effects in $Cu^{2+}(H_2O)_m$ Clusters

L. A. Curtiss and W. Rodrigues

Proc. of the Symp. on Microscopic Models of Electrode/Electrolyte Interfaces, Toronto, Canada, October 12–16, 1992, Vol. 93–5, pp. 52–61 (1993)

Ab Initio Molecular Orbital Calculations of Molten Salt Vapor Complexes Using Gaussian-2 Theory: $LiAlF_4$ and $NaAlF_4$

L. A. Curtiss and G. Schols

Proc. of the Third Int. Symp. on Molten Salt Chemistry and Technology, 183rd Electrochem. Soc. Meeting, Honolulu, HI, May 16–21, 1993, Vol. 93–3, pp. 31–41 (1993)

Advances in Passive-Remote and Extractive Fourier Transform Infrared Systems

J. Demirgian, C. Hammer, E. Hwang, and Z. Mao

Proc. of the Incineration Conf., 12th Annual Int. Symp. on Thermal Treatment Technologies, Knoxville, TN, May 3–7, 1993, Vol. 12, pp. 761–765 (1993)

Soil Washing as a Potential Remediation Technology for Contaminated DOE Sites

J. S. Devgun, M. E. Natsis, N. J. Beskid, and J. Walker

Proc. of the Waste Management '93 Conf., 19th Annual Nuclear Waste Symp., Tucson, AZ, February 28–March 4, 1993, Vol. 1, pp. 835–843 (1993)

The Reaction of SRL 202 Glass in J-13 and DIW

W. L. Ebert, J. K. Bates, and E. C. Buck

Mater. Res. Soc. Symp. Proc. **294**, 137–144 (1993)

Accelerated Glass Reaction under PCT Conditions

W. L. Ebert, J. K. Bates, E. C. Buck, and C. R. Bradley

Mater. Res. Soc. Symp. Proc. **294**, 569–576 (1993)

Does Fully Radioactive Glass Behave Differently than Simulated Waste Glass?

X. Feng, J. K. Bates, C. R. Bradley, and E. C. Buck

Mater. Res. Soc. Symp. Proc. **294**, 207–214 (1993)

Study on the Colloids Generated from Testing of High-Level Nuclear Waste Glasses

X. Feng, E. C. Buck, C. Mertz, J. K. Bates, and J. C. Cunnane

Proc. of the Waste Management '93 Conf., 19th Annual Nuclear Waste Symp., Tucson, AZ, February 28–March 4, 1993, Vol. 1, pp. 1015–1021 (1993)

Prism-Film Coupling in Anisotropic Planar Waveguides of Epitaxial (101) Rutile Thin Films

C. M. Foster, S.-K. Chan, H. L. M. Chang, R. P. Chiarello, and D. J. Lam

Proc. of the Materials Research Soc. Spring Meeting, San Francisco, CA, April 12–16, 1993, Vol. 313 (1993)

Plant-Scale Anodic Dissolution of Unirradiated IFR Fuel Pins

E. C. Gay and W. E. Miller

Proc. of the GLOBAL '93 Int. Conf. and Technology Exhibition on Future Nuclear Systems, Seattle, WA, September 12–17, 1993, Vol. 2, pp. 1086–1093 (1993)

Jahn Teller Effect of Cations in Water: The Cupric Ion in Water

J. W. Halley, X. R. Wang, and L. A. Curtiss

Proc. of the Symp. on Microscopic Models of Electrode/Electrolyte Interfaces, Toronto, Canada, October 12–16, 1992, Vol. 93–5, pp. 42–51 (1993)

Advanced Batteries for Electric Vehicle Applications—Nontechnical Summary

G. L. Henriksen

Proc. of the Am. Chem. Soc. Meeting, Chicago, IL, August 22–27, 1993, Vol. 38–4 (1993)

Advanced Chemical Separations in Support of the Clean Option Strategy

E. P. Horwitz, M. L. Dietz, H. Diamond, R. D. Rogers, and R. A. Leonard

Proc. of the GLOBAL '93 Int. Conf. and Technology Exposition on Future Nuclear Systems: Emerging Fuel Cycles and Waste Disposal Options, Seattle, WA, September 12–17, 1993, Vol. 1, pp. 39–43 (1993)

Combined TRU-Sr Extraction/Recovery Process

E. P. Horwitz, M. L. Dietz, H. Diamond, R. D. Rogers, and R. A. Leonard

Proc. of the Int. Solvent Extraction Conf. on Solvent Extraction in the Process Industries, York, England, September 9–15, 1993, Elsevier Applied Science, London, pp. 1805–1812 (1993)

Combined TRU-Sr Extraction/Recovery Process

E. P. Horwitz and R. A. Leonard

Proc. of the Information Exchange Meeting on Waste Retrieval, Treatment, and Processing, Houston, TX, March 15–17, 1993, U.S. DOE Environmental Restoration and Waste Management Technology Development Program, CONF-930149, pp. 294–298 (1993)

Thermodynamic Behavior of the Li_2O-H_2O(g) System

C. E. Johnson, I. Johnson, L. A. Curtiss, and P. E. Blackburn

Proc. of the Second Int. Workshop on Ceramic Breeder Interactions, Ed., M. Yamawaki, Tokyo, Japan, October 26–29, 1992, pp. 23–30 (1993)

Reference Electrodes for Solid Polymer Electrolytes

C. S. Johnson, J. Prakash, and D. W. Dees

Extended Abstracts, 184th Electrochem. Soc. Meeting, New Orleans, LA, October 10–15, 1993, Vol. 93–2, p. 66 (1993)

A Shuttle Mechanism for Molten-Electrolyte Lithium Batteries

T. D. Kaun and P. A. Nelson

Extended Abstracts, 184th Electrochem. Soc. Meeting, New Orleans, LA, October 10–15, 1993, Vol. 93–2, p. 19 (1993)

Tritium Transport in Single Crystal $LiAlO_2$

J. P. Kopasz, C. A. Seils, and C. E. Johnson

Proc. of the Second Int. Workshop on Ceramic Breeder Interactions, Ed., M. Yamawaki, Tokyo, Japan, October 26–29, 1992, pp. 88–95 (1993)

Cathode Materials for the Molten Carbonate Fuel Cell

G. H. Kucera, A. P. Brown, M. F. Roche, E. J. Indacochea, M. Krumpelt, and K. M. Myles

Proc. of the Am. Chem. Soc. Meeting, Chicago, IL, August 22–27, 1993, Vol. 38–4 (1993)

Fuel Processing Requirements and Techniques for Fuel Cell Propulsion Power

R. Kumar, S. Ahmed, and M. Yu

Proc. of the Am. Chem. Soc. Meeting, Chicago, IL, August 22–27, 1993, Vol. 38–4, pp. 1471–1476 (1993)

Solid Oxide Fuel Cells for Transportation—A Clean, Efficient Alternative for Propulsion

R. Kumar, M. Krumpelt, and K. M. Myles

Proc. of the Third Int. Symp. on Solid Oxide Fuel Cells, 183rd Electrochem. Soc. Meeting, Honolulu, HI, May 16–21, 1993, Vol. 93–4, pp. 948–956 (1993)

Development of IFR Pyroprocessing Technology

J. J. Laidler, J. E. Battles, W. E. Miller, and E. C. Gay

Proc. of the GLOBAL '93 Int. Conf. and Technology Exhibition on Future Nuclear Systems, Seattle, WA, September 12–17, 1993, Vol. 2, pp. 1061–1065 (1993)

Measurement of Alkali-Vapor Emission from Pressurized Fluidized-Bed Combustion of Illinois Coals

S. H. D. Lee, F. G. Teats, W. M. Swift, and D. D. Banerjee

Proc. of the Int. Conf. on Fluidized-Bed Combustion, San Diego, CA, May 9–13, 1993, Vol. II, pp. 1359–1368 (1993)

Mechano-Chemical Effects of High-Energy Attrition Milling on the $Bi_2Sr_2CaCu_2O_x$ Superconductor

J. S. Luo, H. G. Lee, and S. Sinha

Mater. Res. Soc. Symp. Proc. **286**, 55–59 (1993)

On-Line Monitoring of Incinerator Emissions

Z. Mao, J. C. Demirgian, and E. Hwang

Proc. of the Incineration Conf., 12th Annual Int. Symp. on Thermal Treatment Technologies, Knoxville, TN, May 3–7, 1993, Vol. 12, pp. 755–760 (1993)

Pyrochemical Methods for Actinide Recovery from LWR Spent Fuel

C. C. McPheeters, R. D. Pierce, D. S. Poa, and P. S. Maiya

Proc. of the GLOBAL '93 Int. Conf. and Technology Exhibition on Future Nuclear Systems, Seattle, WA, September 12–17, 1993, Vol. 2, pp. 1094–1101 (1993)

Laser Raman and X-ray Scattering Studies of Corrosion Films on Metals

C. A. Melendres

Proc. of the 12th Int. Corrosion Congress, Houston, TX, September 19–24, 1993, Vol. 5B, pp. 3973–3981 (1993)

Synchrotron Infrared Spectroscopy of H_2O and CO Adsorbed on Polycrystalline Gold

C. A. Melendres, V. A. Maroni, C. Q. Liu, B. Beden, and G. Bowmaker

Extended Abstracts, 183rd Electrochem. Soc. Meeting, Honolulu, HI, May 16–21, 1993, Vol. 93–1, p. 2601 (1993)

Surface Enhanced Raman Spectroelectrochemical Studies of the Corrosion Films on Iron and Chromium in Aqueous Solution Environments

C. A. Melendres, M. Pankuch, Y. S. Li, and R. L. Knight

Extended Abstracts, 183rd Electrochem. Soc. Meeting, Honolulu, HI, May 16–21, 1993, Vol. 93–1, p. 179 (1993)

Chloride Ion Catalysis of the Cu^{2+}/Cu Metal Deposition/Dissolution Reaction

Z. Nagy, N. C. Hung, and D. J. Zurawski

Extended Abstracts, 183rd Electrochem. Soc. Meeting, Honolulu, HI, May 16–21, 1993, Vol. 93–1, pp. 2381–2382 (1993)

Unvented Thermal Process for Treatment of Hazardous and Mixed Wastes

P. A. Nelson and W. M. Swift

Proc. of the Incineration Conf., 12th Annual Int. Symp. on Thermal Treatment Technologies, Knoxville, TN, May 3–7, 1993, pp. 671–678 (1993)

Premonitory Geochemical Evidence of Magmatic Reactivation of Teide Volcano and Relation to the Recent Seismic Activity in the Canary Islands, Spain

N. M. Perez, P. A. Hernandez, F. J. Hernandez, J. C. Carracedo, and N. C. Sturchio

Abstracts with Programs, Geological Soc. of America Annual Meeting, Boston, MA, October 25–28, 1993, Vol. 25, p. 327 (1993)

Isotope Geochemistry of Thermal Waters and Gas Discharges, Pueblo-Alvord Valley, Harney County, Oregon

A. M. St. John, M. L. Cummings, and N. C. Sturchio

Abstracts with Programs, Geological Soc. of America Annual Meeting, Boston, MA, October 25–28, 1993, Vol. 25, p. 151 (1993)

New Isotopic Perspectives of Atmospheric Carbon Monoxide

C. M. Stevens

Trans. of the Fall Meeting of the Am. Geophys. Union, EOS, San Francisco, CA, December 6–9, 1993, Vol. 74, p. 179 (1993)

Chemical and Isotopic Composition of Thermal Waters in Egypt

N. C. Sturchio, G. B. Arehart, M. Sultan, Y. Abo Kamar, and S. M. Ibrahim

Abstracts with Programs, Geological Soc. of America Annual Meeting, Boston, MA, October 25–28, 1993, Vol. 25, p. 323 (1993)

Relation Between Ra Isotopes, Ba, and Salinity in Midcontinent Groundwaters

N. C. Sturchio, J. L. Banner, M. Musgrove, A. M. Stueber, P. Pushkar, and C. M. Binz

Trans. of the Fall Meeting of the Am. Geophys. Union, EOS, San Francisco, CA, December 6–9, 1993, Vol. 74, p. 299 (1993)

Ra Isotopes-Ba-Salinity Relations: Midcontinent Groundwaters

N. C. Sturchio, J. L. Banner, M. L. Musgrove, A. M. Stueber, P. Pushkar, and C. M. Binz

Trans. of the Fall Meeting of the Am. Geophys. Union, EOS, San Francisco, CA, December 6–9, 1993, Vol. 74, p. 299 (1993)

Summary of the Workshop, "How Clean is Clean? Statistical Approaches to Final Release of Cleaned Up Radioactive Sites"

G. Subbasaman and J. S. Devgun

Proc. of the Waste Management '93 Conf., 19th Annual Nuclear Waste Symp., Tucson, AZ, February 28–March 4, 1993, Vol. 2, p. 1879 (1993)

Dialkylimidasolium Chloroaluminates: *Ab Initio* Calculations, Raman and Neutron Scattering Measurements

S. Takahashi, L. A. Curtiss, D. Gosztola, N. Koura, C.-K. Loong, and M. L. Saboungi

Proc. of the Third Int. Symp. on Molten Salt Chemistry and Technology, 183rd Electrochem. Soc. Meeting, Honolulu, HI, May 16–21, 1993, Vol. 93–9, pp. 622–631 (1993)

Development and Demonstration of the TRUEX Solvent Extraction Process

G. F. Vandegrift, D. B. Chamberlain, R. A. Leonard, J. C. Hutter, D. G. Wygmans, C. Conner, J. Sedlet, L. Nunes, J. M. Copple, J. A. Dow, B. Srinivasan, M. C. Regalbuto, S. Weber, and L. Everson

Proc. of the Waste Management '93 Conf., 19th Annual Nuclear Waste Symp., Tucson, AZ, February 28–March 4, 1993, Vol. 2, pp. 1045–1050 (1993)

Advanced Batteries for EV Applications

D. R. Vissers, W. H. DeLuca, and G. L. Henriksen

Proc. of the Am. Chem. Soc. Meeting, Chicago, IL, August 22–27, 1993, Vol. 38–4, p. 23 (1993)

Chemically Bonded Phosphate Ceramics for Radioactive and Mixed Waste Solidification and Stabilization

A. S. Wagh, J. C. Cunnane, D. Singh, D. T. Reed, S. Armstrong, W. Subhan, and N. Chawla

Proc. of the Waste Management '93 Conf., 19th Annual Nuclear Waste Symp., Tucson, AZ, February 28–March 4, 1993, Vol. 2, pp. 1613–1617 (1993)

Galeras Volcano, Colombia: 1988–1993 Progress, Tragic 14 January 1993 Eruption, The Future

S. N. Williams, M. L. Calvache, G. Arles, J. Stix, N. C. Sturchio, and Y. Sano

Abstracts with Programs, Geological Soc. of America Annual Meeting, Boston, MA, October 25–28, 1993, Vol. 25, p. 326 (1993)

Long and Short Period Oscillatory Zonation in Vein Calcite: Evidence for Marine, Hydrothermal, and Meteoric Fluid Sources

R. A. Wogelius, G. Wall, and D. G. Fraser

Abstracts with Programs, Geological Soc. of America Annual Meeting, Boston, MA, October 25–28, 1993, Vol. 25, p. 203 (1993)

A Comparison of Alteration Paragenesis Between High-Level Nuclear Waste Materials and Geologic Analogues

D. J. Wronkiewicz, C. R. Bradley, and J. K. Bates

Abstracts with Programs, Geological Soc. of America Annual Meeting, Boston, MA, October 25–28, 1993, Vol. 25, p. A-185 (1993)

Effects of Radiation Exposure on Glass Alteration in a Steam Environment

D. J. Wronkiewicz, L. M. Wang, J. K. Bates, and B. S. Tani

Mater. Res. Soc. Symp. Proc. **294**, 183–190 (1993)

The Electrochemical Performance of Thin-Electrolyte Solid Oxide Fuel Cells

D. Zurawski and T. Kueper

Extended Abstracts, 184th Electrochem. Soc. Meeting, New Orleans, LA, October 10–15, 1993, Vol. 93–2, pp. 591–592 (1993)

E. Papers Presented at Scientific Meetings

Partition of Actinides and Fission Products Between Metal and Molten Salt Phases—Theory, Measurement, and Application to IFR Pyroprocess Development

J. P. Ackerman and T. R. Johnson

Presented at the Actinides '93 Int. Conf., Santa Fe, NM, September 19–24, 1993

Pyrochemical Extraction for Selective Removal of Transuranium Elements from Molten LiCl-KCl

J. P. Ackerman and T. R. Johnson

Presented at the 205th National Am. Chem. Soc. Symp., Denver, CO, March 28–April 2, 1993

Engineering Scale Demonstration of the Pyrochemical Actinide Recycle Process

B. H. Altenberg and T. P. Mulcahey

Presented at the 13th Annual Pyrochemical Workshop, Albuquerque, NM, October 18–21, 1993

Sediment-Hosted Disseminated Gold Deposits as Product of Mixing of Deeply Circulating Meteoric Waters in Compressional Tectonic Environments

G. B. Arehart

Presented at the Symp. on Gold Deposits for the Geological Soc. of America, Reno, NV, May 17–19, 1993

Possible Origins of Organic Nitrogen in Crude Oils

A. J. Bakel

Presented at the Organic Geochem. Division Annual Symp., Boston, MA, October 25–28, 1993

Carbon Isotopic Composition of n-Alkanes and Isoprenoids in Slightly Biodegraded Crude Oils from the Phillipstown Fields (Illinois Basin)

A. Bakel, R. M. Dyer, T. E. Ruble, and R. Philp

Presented at the Int. Meeting of Organic Geochemistry, Stravanger, Norway, September 1993

Analytical Chemistry at Argonne National Laboratory and the Need for Environmental Analysis

D. A. Bass

Presented at the Illinois Institute of Technology, Chicago, IL, March 31, 1993

Environmental Analytical Chemistry at Argonne National Laboratory

D. A. Bass

Presented at the University of Northern Iowa, Cedar Falls, IA, April 22, 1993

A Comparison of Extraction of Soils Using the Toxicity Characteristic Leaching Procedure and Total Metal Digestion

D. A. Bass and J. D. Taylor

Presented at the 34th ORNL-DOE Conf. on Analytical Chemistry in Energy Technology, Gatlinburg, TN, October 5–7, 1993

Overview of Nuclear Waste Programs

J. K. Bates

Presented at the U.S. NRC Site Visit, Argonne National Laboratory, October 27–28, 1993

Testing of Spent Fuel Under Unsaturated Conditions

J. K. Bates

Presented at the Spent Nuclear Fuel Workshop '93 Symp., Santa Fe, NM, September 26–29, 1993

Waste Glass Weathering

J. K. Bates and E. C. Buck

Presented at the Fall Meeting of the Materials Research Soc., Boston, MA, November 29–December 3, 1993

Pyrochemical Fundamentals and Analytical Chemistry Requirements for the Fuel Cycle Demonstration

R. W. Benedict and J. P. Ackerman

Presented at the First Workshop on Analytical Chemistry of the IFR Pyroprocess, Argonne National Laboratory–West, Idaho Falls, ID, March 1–3, 1993

Minimum Additive Waste Stabilisation (MAWS)

N. J. Beskid

Presented at the Second Semiannual OTD Information Meeting on Waste Retrieval, Treatment, and Processing, HAZWRAP, Houston, TX, January 26–28, 1993

Analyses and Predictions of the Thermodynamic Properties of Molten Silicates

M. Blander

Presented at the Institute of Inorganic Chemistry, Slovak Academy of Sciences, Bratislava, Slovakia, April 2, 1993

Ordered Ionic Liquids

M. Blander

Presented at the Gordon Conf. on Molten Salts and Metals, Wolfeboro, NH, August 16–20, 1993

Predictions of Silicate Phase Diagrams

M. Blander

Presented at Laboratorie Thermodynamique et de Physico Chemie Metallurgique, Domaine Universitaire, St. Martin d'Heres, France, April 12, 1993

Sealant Research for Solid Oxide Fuel Cells

I. Bloom, M. Krumpelt, K. L. Ley, S. E. Dorris, and A. S. Wagh

Presented at the Contractors' Review Meeting, DOE Morgantown Energy Technology Center, Morgantown, WV, August 3–5, 1993

Analysis of Samples from Integral Fast Reactor (IFR) Program at ANL–East

D. L. Bowers and C. S. Sabau

Presented at the First Workshop on Analytical Chemistry of the IFR Pyroprocess, Argonne National Laboratory–West, Idaho Falls, ID, March 1–3, 1993

Effect of Gamma-Ray Radiation on the Separation Efficiencies of Coated Magnetic Micro-particles

B. A. Buchholz, L. Nunes, G. F. Vandegrift, and M. Dunn

Presented at the Winter Meeting of the Am. Nucl. Soc., San Francisco, CA, November 14–19, 1993

Colloid Formation during Nuclear Waste Form Reactions: Analytical Electron Microscopy Observations

E. C. Buck

Presented at Argonne National Laboratory, May 27, 1993

Uranium Contaminated Soils at Fernald: Electron Beam Analysis

E. C. Buck

Presented at Argonne National Laboratory, June 24, 1993

Identification of Uranium-Bearing Colloidal Phases during the Dissolution of Spent Fuel and UO_2

E. C. Buck and J. K. Bates

Presented at the Great Lakes Electron Microscopy Conf., Indianapolis, IN, October 21–23, 1993

Characterisation of Uranium Phases to Support Soil Decontamination

E. C. Buck, J. K. Bates, and J. C. Cunnane

Presented at the Soil Decontamination Workshop, Gatlinburg, TN, June 16–17, 1993

Distribution of Uranium-Bearing Phases in Soils from Fernald

E. C. Buck, N. R. Brown, and N. L. Dietz

Presented at the Fall Meeting of the Materials Research Soc., Boston, MA, November 29–December 3, 1993

Analytical Electron Microscopy Examination of Solid Reaction Products in Long-Term Tests of SRL 200 Waste Glasses

E. C. Buck, J. A. Fortner, J. K. Bates, X. Feng, N. L. Dietz, C. R. Bradley, and B. S. Tani

Presented at the Fall Meeting of the Materials Research Soc., Boston, MA, November 29–December 3, 1993

Neutral Cluster Emission during Ion Bombardment: New Insights into the Sputtering Process

W. F. Calaway

Presented at the Department of Physics, Northern Illinois University, Dekalb, IL, October 8, 1993

Observation and Characterisation of Clusters Sputtered from Polycrystalline Cu and Al

W. F. Calaway, S. R. Coon, Z. Ma, M. J. Pellin, and D. M. Gruen

Presented at the 18th Department of Energy Surface Science Conf. and the 29th Annual Symp. of the Am. Vacuum Soc., New Mexico Chapter, Santa Fe, NM, April 27–30, 1993

Characterisation of Si Wafers by Resonance Ionisation of Sputtered Neutrals

W. F. Calaway, S. R. Coon, M. J. Pellin, D. M. Gruen, M. Gordon, A. C. Diebold, P. Maillot, R. C. Wiens, and D. S. Burnett

Presented at the 12th Annual Symp. on Electronic Materials, Processing and Characterisation, Austin, TX, June 7–9, 1993

Positionisation Surface Analysis at Argonne National Laboratory: Present and Future

W. F. Calaway and M. J. Pellin

Presented at the SEMATECH SIMS Workshop, Austin, TX, September 14–15, 1993

Actinide Recovery Using Aqueous Biphasic Extraction

D. J. Chaiko

Presented at the Actinide Separations Conf., Pasco, WA, May 17–21, 1993

Biphasic Separation of Ultra-Fine Particles

D. J. Chaiko, R. Mensah-Biney, and E. Van Deventer

Presented at the Engineering Foundation Conf., New Directions in Separation Technology, Noordwijkerhout, Holland, June 27–July 2, 1993

Extraction of Technetium from Simulated Hanford Tank Wastes

D. J. Chaiko, Y. Vojta, and M. Takeuchi

Presented at the Eighth Symp. on Separation Science and Technology for Energy Applications, Gatlinburg, TN, October 24–28, 1993

TRUEX Processing of Wastes for Waste Minimization and Reagent Recycle

D. B. Chamberlain, C. J. Conner, J. C. Hutter, D. G. Wygmans, R. A. Leonard, and G. F. Vandegrift

Presented at the Winter Meeting of the Am. Nucl. Soc., San Francisco, CA, November 14–19, 1993

Volatile Organic Analysis of Mixed Waste Samples

L. L. Chromisky

Presented at the 18th Analytical Chemistry Laboratory Technical Meeting, Argonne National Laboratory, February 25, 1993

Implementation of Thermal Desorption Fourier Transform Infrared Spectroscopy in the Direct Analysis of Soil Samples for Semivolatile and Volatile Organics

M. Clapper-Gowdy, J. C. Demirgian, and J. W. Tang

Presented at the 44th Pittsburgh Conf. and Exposition on Analytical Chemistry and Applied Spectroscopy, Atlanta, GA, March 8–12, 1993

Treatment of Davies-Gray and Other Mixed Wastes at Argonne National Laboratory

C. Conner, D. B. Chamberlain, J. C. Hutter, R. A. Leonard, H. No, L. Nunez, J. Sedlet, B. Srinivasan, D. G. Wygmans, and G. F. Vandegrift

Presented at the Plutonium/Uranium Recovery Operations Conf., Augusta, GA, October 18–21, 1993

Sputtering and Photoionization of Neutral Metal Clusters

S. R. Coon, W. F. Calaway, M. Ma, M. J. Pellin, and D. M. Gruen

Presented at the Spring Meeting of the Am. Vacuum Soc., Illinois Chapter, April 30, 1993

Determination of $^{44}Ca/^{42}Ca$ in Blood Serum and Bone Using Inductively Coupled Plasma-Mass Spectrometry

J. S. Crain, M. H. Bhattacharyya, and A. Wilson

Presented at the Second National Conf. on Inductively Coupled Plasma-Mass Spectrometry, Detroit, MI, October 16-17, 1993

Direct Determination of Impurities in Actinide Matrices by Inductively Coupled Plasma-Mass Spectrometry

J. S. Crain, D. L. Gallimore, and K. P. Coffelt

Presented at the First Workshop on the Analytical Chemistry of the IFR Pyroprocess, Argonne National Laboratory–West, Idaho Falls, ID, March 1–3, 1993

Enhanced Detection of Long-Lived Actinides by Inductively Coupled Plasma-Mass Spectrometry

J. S. Crain and L. L. Smith

Presented at the 20th Annual Meeting of the Federation of Analytical Chemistry and Spectroscopy Societies, Detroit, MI, October 17–22, 1993

High-Level Waste Borosilicate Glass: A Compendium of Corrosion Characteristics

J. C. Cunnane and J. Allison

Presented at the Fall Meeting of the Materials Research Soc., Boston, MA, November 29–December 3, 1993

High-Level Waste Glass Compendium: What It Tells Us Concerning the Durability of Borosilicate Waste Glass

J. C. Cunnane and J. Allison

Presented at the Fall Meeting of the Materials Research Soc., Boston, MA, November 29–December 3, 1993

Battery Testing at Argonne National Laboratory

W. H. DeLuca, K. R. Gillie, J. E. Kulaga, J. A. Smaga, A. F. Tummillo, and C. E. Webster

Presented at the DOE Interagency Advanced Power Group Meeting, March 25, 1993

Continuous Emission Monitoring of Incinerators Using Extractive and Passive-Remote Fourier Transform Infrared Spectroscopy

J. C. Demirgian

Presented at the Air and Waste Management Association Int. Specialty Conf., Atlanta, GA, October 11–14, 1993

Standoff Detection of Chemical Plumes Using Passive-Remote Fourier Transform Infrared Spectroscopy

J. C. Demirgian

Presented at the DOE Expo '93 Conf. and Exhibit, Oak Ridge National Laboratory, Oak Ridge, TN, May 3–7, 1993

Standoff Detection of Simulated Illicit Drug Laboratories

J. C. Demirgian and J. Fortuna

Presented at the Tactical Technologies and Wide Area Surveillance Int. Symp., Chicago, IL, October 19–22, 1993

Field Identification and Quantitation of Volatile Organics in Soils Utilising Fourier Transform Infrared Spectroscopy

J. C. Demirgian, M. Clapper-Gowdy, and G. Robittaille

Presented at the National Symp. on Measuring and Interpreting VOCs in Soils: State of the Art and Research Needs, Las Vegas, NV, January 12–14, 1993

Advances in Passive-Remote and Extractive Fourier Transform Infrared Spectroscopic Systems

J. C. Demirgian, C. Hammer, and E. Y. Hwang

Presented at the Air and Waste Management Association Int. Specialty Conf., Atlanta, GA, October 11–14, 1993

Detection of Chemical Plumes Utilising Passive-Remote Fourier Transform Infrared Spectroscopy

J. C. Demirgian, C. L. Hammer, and W. Killian

Presented at the 44th Pittsburgh Conf. and Exposition on Analytical Chemistry and Applied Spectroscopy, Atlanta, GA, March 8–12, 1993

Characterisation of Solution Derived High-T_c Bismuth Cuprate Superconducting Tapes

L. P. deRochemont, M. Misra, V. A. Maroni, J. H. Johnson, C. C. Frits, D. F. Ryder, R. J. Andrews, M. J. Suscavage, and M. R. Squillante

Presented at the Spring Meeting of the Materials Research Soc., San Francisco, CA, April 11–16, 1993

Cleanup Standards and Pathways Analysis Methods

J. S. Devgun

Presented at the Int. Conf. on Nuclear Waste Management and Environmental Remediation, Prague, Csech Republic, September 5–11, 1993

Main Principles of Radiation Protection and Their Applications in Waste Management

J. S. Devgun

Presented at the Int. Atomic Energy Agency Interregional Training Course on Management of Radioactive Waste from Nuclear Power Plants, Argonne National Laboratory and Whiteshell Laboratories (Canada), August 23–September 17, 1993

Radiation Principles

J. S. Devgun

Presented at Illinois Institute of Technology, March 31–April 2, 1993 and October 27–29, 1993

Review of ICRP-60 Implications for Radioactive Waste Management

J. S. Devgun

Presented at the Int. Atomic Energy Agency Interregional Training Course on Management of Radioactive Waste from Nuclear Power Plants, Argonne National Laboratory and Whiteshell Laboratories (Canada), August 23–September 17, 1993

Role of Risk Assessment in Public Acceptance of Waste Disposal

J. S. Devgun

Presented at the Int. Atomic Energy Agency Interregional Training Course on Management of Radioactive Waste from Nuclear Power Plants, Argonne National Laboratory and Whiteshell Laboratories (Canada), August 23–September 17, 1993

Long-Term Alteration of Borosilicate Waste Glasses

W. L. Ebert and J. K. Bates

Presented at the 95th Annual Meeting and Exposition of the Am. Ceram. Soc., Cincinnati, OH, April 18–22, 1993

The Long-Term Alteration of Borosilicate Waste Glasses

W. L. Ebert, J. K. Bates, C. R. Bradley, E. C. Buck, N. L. Dietz, and N. R. Brown

Presented at the 95th Annual Meeting and Exposition of the Am. Ceram. Soc., Cincinnati, OH, April 18–22, 1993

Laboratory Testing of Waste Glass Aqueous Corrosion, Effects of Experimental Parameters

W. L. Ebert and J. J. Maser

Presented at the Fall Meeting of the Materials Research Soc., Boston, MA, November 29–December 3, 1993

Procurement and Execution of PCB Analyses: Customer-Analyst Interactions

M. D. Erickson

Presented at the Fifth Int. Conf. for the Remediation of PCB Contamination, Houston, TX, March 16–17, 1993

Characterisation of HEPA Filters for Disposal

A. M. Essling, I. M. Fox, F. P. Smith, and D. G. Gracsyk

Presented at the 34th ORNL-DOE Conf. on Analytical Chemistry in Energy Technology, Gatlinburg, TN, October 5–7, 1993

Surface Layer Effects on Waste Glass Corrosion

X. Feng

Presented at the Fall Meeting of the Materials Research Soc., Boston, MA, November 29–December 3, 1993

Factors Influencing Chemical Durability of Nuclear Waste Glasses

X. Feng and J. K. Bates

Presented at the Ninth Int. Conf. on Advanced Science and Technology, Schaumburg, IL, March 27, 1993

Chemical Durabilities of Tailored Slags Versus High-Level Waste Glasses

X. Feng, J. K. Bates, D. J. Wronkiewics, N. R. Brown, E. C. Buck, M. Gong, and W. L. Ebert

Presented at the 185th Electrochem. Soc. Meeting, San Francisco, CA, May 22–27, 1993

Characteristics of Colloids Generated during the Corrosion of Nuclear Waste Glasses in Groundwater

X. Feng, E. C. Buck, C. Mertz, J. K. Bates, J. C. Cunnane, and D. J. Chaiko

Presented at the Fourth Int. Conf. on the Chemistry and Migration Behavior of the Actinides and Fission Products in the Geosphere, MIGRATION '93, Charleston, SC, December 12–17, 1993

A Literature Review of Surface Alteration Layer Effects on Waste Glass Behavior

X. Feng, J. C. Cunnane, and J. K. Bates

Presented at the 95th Annual Meeting and Exposition of the Am. Ceram. Soc., Cincinnati, OH, April 18–22, 1993

Effect of Radiation on Solution Chemistry for Unsaturated Spent Fuel Tests

P. A. Finn

Presented at the Spent Nuclear Fuel Workshop '93 Conf., Santa Fe, NM, September 26–29, 1993

Elements Present in Leach Solutions from Unsaturated Spent Fuel Tests

P. A. Finn, J. K. Bates, J. Hoh, J. W. Emery, L. Hafenrichter, E. C. Buck, and M. Gong

Presented at the Fall Meeting of the Materials Research Soc., Boston, MA, November 29–December 3, 1993

Colloidal Products and Actinide Species in Leachate from Spent Nuclear Fuel

P. A. Finn, E. C. Buck, M. Gong, J. C. Hoh, J. W. Emery, L. Hafenrichter, and J. K. Bates

Presented at the Fourth Int. Conf. on the Chemistry and Migration Behavior of the Actinides and Fission Products in the Geosphere, MIGRATION '93, Charleston, SC, December 12–17, 1993

The Use of Design-for-Manufacturability Techniques to Ensure the Quality of Large Gloveboxes

A. A. Frigo, R. F. Malecha, and E. F. Lewandowski

Presented at the Seventh Annual Conf. and Equipment Exhibit of the Am. Glovebox Soc., Seattle, WA, August 16–19, 1993

Analytical Chemistry Needs of the Fuel Cycle Facility Electrorefiner

E. C. Gay, D. L. Bowers, and W. E. Miller

Presented at the First Workshop on Analytical Chemistry of the IFR Pyroprocess, Argonne National Laboratory–West, Idaho Falls, ID. March 1–3, 1993

Mass Spectrometric Measurement of Uranium and Plutonium Isotope Ratios for Determining Isotopic Composition and for Precise Assays by Isotope Dilution

D. G. Gracsyk

Presented at the First Workshop on Analytical Chemistry of the IFR Pyroprocess, Argonne National Laboratory–West, Idaho Falls, ID, March 1–3, 1993

Sample Transportation

D. W. Green

Presented at the 11th DOE Analytical Laboratory Managers' Meeting, Boulder, CO, October 25, 1993

Innovative Environmental Restoration and Waste Management Technologies at Argonne National Laboratory

J. E. Helt

Presented at the CONEC '93 Conf. on Environmental Commerce, Chattanooga, TN, October 17–20, 1993

The Stability of Calibration Standards for ICP/AES Analysis

D. R. Huff and E. A. Huff

Presented at the 18th Analytical Chemistry Laboratory Technical Meeting, Argonne National Laboratory, February 25, 1993

Analyses of IFR Matrices—Problems and Solutions

E. A. Huff and D. R. Huff

Presented at the First Workshop on the Analytical Chemistry of the IFR Pyroprocess, Argonne National Laboratory–West, Idaho Falls, ID, March 1–3, 1993

TRU· Spec and RE· Spec Chromatography—Basic Studies and Applications

E. A. Huff and D. R. Huff

Presented at the 34th ORNL-DOE Conf. on Analytical Chemistry in Energy Technology, Gatlinburg, TN, October 5–7, 1993

Treatment of Aqueous Mixed Wastes Containing RCRA Metals

J. C. Hutter, D. G. Wygmans, D. B. Chamberlain, C. Conner, H. No, C. Srinivasan, R. A. Leonard, L. Nunes, J. Sedlet, and G. F. Vandegrift

Presented at the Second Int. Mixed Waste Symp., Baltimore, MD, August 16–20, 1993

Tritium Release from Beryilium Discs and Lithium Ceramics Irradiated in the SIBELIUS Experiment

C. E. Johnson, D. L. Baldwin, and J. P. Kopass

Presented at the Second Int. Workshop on Ceramic Breeder Blanket Interactions, Paris, France, September 22–24, 1993

Treatment of High-Level Radioactive Wastes in the Fuel Cycle of the Integral Fast Reactor

T. R. Johnson, J. P. Ackerman, L. S. H. Chow, and E. L. Carls

Presented at the AIChE Meeting, St. Louis, MO, November 12–17, 1993

Cation Composition and Reactive Sintering of Ag-Clad (Ei,Pb)-Sr-Ca-Cu-O (2223) Tapes

D. Y. Kaufman, M. T. Lanagan, S. E. Dorris, T. A. Ballen, I. Bloom, S. C. Hatchcox, R. A. Olson, J. T. Dawley, E. M. Galves, R. B. Poeppel, and M. R. DeGuire

Presented at the 95th Annual Meeting and Exposition of the Am. Ceram. Soc., Cincinnati, OH, April 18–22, 1993

Bipolar Li/FeS_2 Component Development

T. D. Kaun

Presented at the *Ad Hoc* Workshop on Ceramics for Li/FeS_2 Batteries, Oak Brook, IL, September 29–30, 1993

Particle Beam Liquid Chromatography/Mass Spectrometry

S. D. Kent

Presented at the 18th Analytical Chemistry Laboratory Technical Meeting, Argonne National Laboratory, February 25, 1993

High-Pressure NMR Studies of the OXO Catalyst in Supercritical Media

R. J. Klingler and J. W. Rathke

Presented at the Gordon Research Conf. on Organometallic Chemistry, Newport, RI, July 12–16, 1993

Tritium Release from Lithium Titanate, a Low Activation Tritium Breeding Material

J. P. Kopasz, J. M. Miller, and C. E. Johnson

Presented at the Second Int. Workshop on Ceramic Breeder Blanket Interactions, Paris, France, September 22–24, 1993

Spatial Tritium Transport in Single Crystal Lithium Aluminate

J. P. Kopasz, C. A. Seils, and C. E. Johnson

Presented at the Sixth Int. Conf. on Fusion Reactor Materials, Ispra, Italy, September 26–October 1, 1993

Microwave Plasma Destruction of Volatile Organic Compounds

T. R. Krause

Presented at the Second Semiannual OTD Information Meeting on Waste Retrieval, Treatment, and Processing, HAZWRAP, Houston, TX, January 26–28, 1993

Thermal Effects in Electrokinetics Processing

T. R. Krause

Presented at the Symp. on Air-Water-Soil Transport of Fine Particles in the Envionment, 24th Annual Meeting of the Fine Particle Soc., Chicago, IL, August 24–28, 1993

Thermal Effects on Electrokinetics Soil Processing

T. R. Krause

Presented at the Second Semiannual OTD Information Meeting on Waste Retrieval, Treatment, and Processing, HAZWRAP, Houston, TX, January 26–28, 1993

Applications of Microwave Radiation in Environmental Remediation Technology

T. R. Krause and J. E. Helt

Presented at the 95th Annual Meeting and Exposition of the Am. Ceram. Soc., Cincinnati, OH, April 18–22, 1993

Preliminary Results from the Investigation of Thermal Effects in Electrokinetics Soil Remediation

T. R. Krause and B. Tarman

Presented at the Meeting on Emerging Technologies in Hazardous Waste Management V, Am. Chem. Soc., Industrial and Engineering Chemistry, Atlanta, GA, September 27–29, 1993

Will Fuel Cells Replace Heat Engines in the 21st Century?

M. Krumpelt

Presented at the Massachusetts Institute of Technology, Cambridge, MA, October 15, 1993

Research and Development of Alternative Components at Argonne National Laboratory for Molten Carbonate Fuel Cells

M. Krumpelt, G. H. Kucera, M. F. Roche, and E. Indacochea

Presented at the Contractors' Review Meeting, DOE Morgantown Energy Technology Center, Morgantown, WV, August 3–5, 1993

Fundamentals of System Integration

M. Krumpelt, R. Kumar, and K. M. Myles

Presented at the Third Grove Fuel Cell Symp., London, England, September 28–October 1, 1993

The U.S. Fuel Cell Transportation Program

M. Krumpelt and K. M. Myles

Presented at the Fuel Cell Workshop on Fuel Cell Technology R&D, New Orleans, LA, April 13–14, 1993

Development and Testing of Alternative Components for the Molten Carbonate Fuel Cell

G. H. Kucera, A. P. Brown, M. F. Roche, and E. J. Indacochea

Presented at the Third Int. Symp. on Molten Salt Chemistry and Technology, 183rd Electrochem. Soc. Meeting, Honolulu, HI, May 16–21, 1993

Modeling of Polymer Electrolyte Fuel Cell Systems

R. Kumar, R. Ahluwalia, H. K. Geyer, and M. Krumpelt

Presented at the Automotive Technology Development Contractors' Coordination Meeting, Dearborn, MI, October 18–21, 1993

IFR Pyroprocessing for High-Level Waste Minimisation

J. J. Laidler

Presented at the Am. Nucl. Soc. Annual Meeting, San Diego, CA, June 1993

Pyrochemical Recovery of Actinides

J. J. Laidler

Presented at the Am. Power Conf., Chicago, IL, April 1993

Pyroprocessing of IFR Metal Fuel

J. J. Laidler

Presented at the 205th National Am. Chem. Soc. Symp., Denver, CO, March 28–April 2, 1993

Molten Salt Electrorefining of Spent Nuclear Fuel

J. J. Laidler and J. E. Battles

Presented at the Third Int. Symp. on Molten Salt Chemistry and Technology, 183rd Electrochem. Soc. Meeting, Honolulu, HI, May 16–21, 1993

Evaluate FIBROSIC^{TM} Candle Filter for Particulate Control in PFBC

S. H. D. Lee, W. M. Swift, F. G. Teats, and F. I. Honea

Presented at the 11th Annual Contractors' Technical Meeting, Illinois Clean Coal Institute, Champaign-Urbana, IL, August 3–5, 1993

Solvent Characterization Using the Dispersion Number

R. A. Leonard

Presented at the Eighth Symp. on Separation Science and Technology for Energy Applications, Gatlinburg, TN, October 24–28, 1993

Densification of Salt-Occluded Zeolite A Powders to a Leach Resistant Solid Monolith

M. A. Lewis, D. F. Fischer, and C. D. Murphy

Presented at the Fall Meeting of the Materials Research Soc., Boston, MA, November 29–December 3, 1993

Sealant Development for Solid Oxide Fuel Cells

K. L. Ley, I. Bloom, and M. Krumpelt

Presented at the Fuel Cell Workshop on Fuel Cell Technology R&D, New Orleans, LA, April 13–14, 1993

Performance Evaluation Programs—Alternatives Based on User Needs

P. C. Lindahl, W. E. Streets, R. Newberry, D. Bottrell, C. Klusek, S. Morton, and S. Hedayat

Presented at the 34th ORNL-DOE Conf. on Analytical Chemistry in Energy Technology, Gatlinburg, TN, October 5–7, 1993

A Study of the Chemistry and Development of Non-Superconducting Secondary Phases in Silver-Sheathed $(Bi,Pb)_2Sr_2Ca_2Cu_3O_{10+\delta}$ (Bi-2223)

J. S. Luo, N. Merchant, E. J. Escorcia-Aparicio, M. C. Morr, V. A. Maroni, G. N. Riley, Jr., and W. L. Carter

Presented at the Fall Meeting of the Materials Research Soc., Boston, MA, November 29–December 3, 1993

Phase Formation of $(Bi_{1-x}Pb_x)_2Sr_2Ca_2Cu_3O_y$ in Silver-Clad Wires

J. S. Luo, N. Merchant, V. A. Maroni, D. M. Gruen, B. S. Tani, G. N. Riley, and W. L. Carter

Presented at the Annual Meeting of the Minerals, Metals, and Materials Soc. Symp., Denver, CO, February 21–25, 1993

Oxygen Nonstoichiometry and Superconducting Transition Temperatures of the $(Bi,Pb)_2Sr_2Ca_2Cu_3O_{10+\delta}$ Phase Clad in a Silver Sheath

J. S. Luo, N. Merchant, V. A. Maroni, M. Tetenbaum, D. Kaufman, M. T. Lanagan, and S. E. Dorris

Presented at the Fall Meeting of the Materials Research Soc., Boston, MA, November 29–December 3, 1993

Sputtering Yield Measurements of Neutral and Ionic Indium Clusters

Z. Ma, W. F. Calaway, S. R. Coon, M. J. Pellin, D. M. Gruen, and E. I. von Nagy-Felsobuki

Presented at the Fall Meeting of the Illinois Chapter of the Am. Vacuum Soc., Chicago, IL, September 17, 1993

Installing a Very Large Glovebox in a Very Small Laboratory

R. F. Malecha, A. A. Frigo, E. F. Lewandowski, and S. Wiedmeyer

Presented at the Seventh Annual Conf. and Equipment Exhibit of the Am. Glovebox Soc., Seattle, WA, August 16–19, 1993

Factors that Influence the Kinetics and Mechanism of the Bi-2223 Formation Reaction in Ag-Sheathed Wires

V. A. Maroni, J. S. Luo, and N. Merchant

Presented at the Spring Meeting of the Materials Research Soc., San Francisco, CA, April 11–16, 1993

The Role of Natural Glasses as Analogues in Projecting the Long-Term Alteration of High-Level Nuclear Waste Glasses

J. J. Mazer

Presented at the Fall Meeting of the Materials Research Soc., Boston, MA, November 29–December 3, 1993

ANL Pyrochemical Processes for LWR Spent Fuel

C. C. McPheeters

Presented at the 13th Annual Pyrochemical Workshop, Albuquerque, NM, October 18–21, 1993

Recovery of Actinides from LWR Spent Fuel by Pyrochemistry

C. C. McPheeters, R. D. Pierce, G. K. Johnson, and D. S. Poa

Presented at the 205th National Am. Chem. Soc. Symp., Denver, CO, March 28–April 2, 1993

Studies of the Chemical and Structural Properties of Interfaces Using Synchrotron Radiation

C. A. Melendres, Z. Nagy, H. You, and V. A. Maroni

Presented at the Spring Meeting of the Materials Research Soc., San Francisco, CA, April 11–16, 1993

Effect of Oxygen Partial Pressure on Phase Evolution and Microstructure Development in Silver-Clad $(Bi,Pb)_2Sr_2Ca_2Cu_3O_{10+\delta}$

N. Merchant, J. S. Luo, V. A. Maroni, S. Sinha, G. N. Riley, and W. L. Carter

Presented at the Fall Meeting of the Materials Research Soc., Boston, MA, November 29–December 3, 1993

Characterization of Solvent Extraction Systems by Dynamic Light Scattering

C. J. Mertz

Presented at Argonne National Laboratory, July 22, 1993

Dynamic Light Scattering Characterization of Aerosol OT and CMPO Microemulsions used for Colloidal Plutonium Separation

C. J. Mertz and D. J. Chaiko

Presented at the AIChE Meeting, St. Louis, MO, November 12–17, 1993

Activities of the Advisory Committee on Nuclear Waste

D. W. Moeller, M. J. Steindler, W. J. Hinze, and P. W. Pomeroy

Presented at the 38th Annual Meeting of the Health Physics Soc., Atlanta, GA, July 11–15, 1993

Tritium Recovery from Liquid Metals

H. Moriyama and D, K. Sze

Presented at the ISFNT-3 Meeting, Los Angeles, CA, June 22–July 1, 1993

Chloride Ion Catalysis of the Cu^{2+}/Cu Metal Deposition/Dissolution Reaction

Z. Nagy, N. C. Hung, and D. J. Zurawski

Presented at the Gordon Research Conf. on Electrochemistry, Ventura, CA, January 18–22, 1993

Batteries for Range-Extender Hybrid Vehicles

P. A. Nelson and G. L. Henriksen

Presented at the 28th Intersoc. Energy Conversion Eng. Conf., Atlanta, GA, August 8–13, 1993

Treatment of Radioactive Liquid Waste at Argonne National Laboratory

H. No, D. G. Wygmans, D. B. Chamberlain, C. Conner, J. C. Hutter, R. A. Leonard, L. Nunez, J. Sedlet, and G. F. Vandegrift

Presented at the Second Int. Mixed Waste Symp., Baltimore, MD, August 16–20, 1993

Waste Remediation Using *In Situ* Magnetically Assisted Chemical Separation

L. Nunez, B. A. Buchholz, and G. F. Vandegrift

Presented at the Eighth Symp. on Separation Science and Technology for Energy Applications, Gatlinburg, TN, October 24–28, 1993

In Situ Magnetically Assisted Chemical Separation

L. Nunez, G. F. Vandegrift, R. D. Roger, and M. J. Dunn

Presented at the Eighth Symp. on Separation Science and Technology for Energy Applications, Gatlinburg, TN, October 24–28, 1993

Reduction of Actinide Oxides with Li/LiCl Systems

R. D. Pierce, G. K. Johnson, D. S. Poa, D. W. Warren, and E. J. Wesolowski

Presented at the 13th Annual Pyrochemical Workshop, Albuquerque, NM, October 18–21, 1993

High Temperature Molten Salt Batteries

J. Prakash

Presented at the Gordon Conf. on Molten Salts and Liquid Metals, Wolfeboro, NH, August 16–20, 1993

Resistivity Measurements of Separators

L. Redey

Presented at the *Ad Hoc* Workshop on Ceramics for Li/FeS_2 Batteries, Oak Brook, IL, September 29–30, 1993

Electric Vehicle Battery Performance Projections from Research Cell Measurements

L. Redey, T. Rauworth, J. Prakash, and D. R. Vissers

Presented at the 184th Electrochem. Soc. Meeting, New Orleans, LA, October 10–15, 1993

Radiolytic Generation of Chloro-Organic Compounds in Transuranic and Low-Level Radioactive Waste

D. T. Reed, S. C. Armstrong, and T. R. Krause

Presented at the National Groundwater Association Annual Convention, Special Session on Chlorinated Volatile Organic Compounds in Groundwater, Kansas City, MO, October 17–20, 1993

VOC Generation and Remediation Studies at Argonne National Laboratory

D. T. Reed, T. R. Krause, and S. Armstrong

Presented at the National Groundwater Association Annual Convention, Special Session on Chlorinated Volatile Organic Compounds in Groundwater, Kansas City, MO, October 17–20, 1993

Generation of Volatile Organic Carbon Compounds by Alpha Particle Degradation of WIPP Plastic

D. T. Reed and M. A. Molecke

Presented at the Fall Meeting of the Materials Research Soc., Boston, MA, November 29–December 3, 1993

Stability and Speciation of Plutonium(VI) in WIPP Brine

D. T. Reed and S. Okajima

Presented at the Fourth Int. Conf. on the Chemistry and Migration Behavior of the Actinides and Fission Products in the Geosphere, MIGRATION '93, Charleston, SC, December 12–17, 1993

Research on Components of the Molten Carbonate Fuel Cell

M. F. Roche, A. P. Brown, G. H. Kucera, M. Krumpelt, and K. M. Myles

Presented at the EPRI/GRI Fuel Cell Workshop on Fuel Cell Technology Research and Development, New Orleans, LA, April 13–14, 1993

Design Requirements for Bipolar Plates

J. A. Smaga

Presented at the *Ad Hoc* Workshop on Ceramics for Li/FeS_2 Batteries, Oak Brook, IL, September 29–30, 1993

Analysis of Paint Samples—A Comparative Study Using FTIR Microspectroscopy and SEM-EDX

C. T. Snyder

Presented at the 18th Analytical Chemistry Laboratory Technical Meeting, Argonne National Laboratory, February 25, 1993

Fourier Transform Infrared (FTIR) Microspectroscopy: A Cost Effective Approach to Characterizing Unknown Liquid Waste Samples

C. T. Snyder

Presented at the 44th Pittsburgh Conf. and Exposition on Analytical Chemistry and Applied Spectroscopy, Atlanta, GA, March 8–12, 1993

Potential to Cofire High-Sulfur Coal and MSW/RDF in Illinois Boilers: A Survey and Analysis

D. W. South, W. F. Podolski, O. O. Ohlsson, and F. Stodolsky

Presented at the Tenth Annual Int. Pittsburgh Coal Conf., Pittsburgh, PA, September 20–24, 1993

Development of an Integrated Performance Evaluation Program (IPEP) for the Department of Energy's Office of Environmental Restoration and Waste Management

W. E. Streets, D. Bottrell, R. Newberry, C. Klusek, S. Morton, K. Karp, and P. C. Lindahl

Presented at the 20th Annual National Energy and Environmental Quality Division Conf. for the American Soc. for Quality Control (ASQC), Indian Wells, CA, September 19–24, 1993

Heat and Seed Recovery Technology Project

W. Swift, M. Petrick, and K. Natesan

Presented at the Contractors' Review Meeting, Pittsburgh, PA, February 2–4, 1993

Engineering Design of ARIES-III

D. K. Sze

Presented at the Second Wisconsin Symp. on Helium-3 and Fusion Power, Madison, WI, July 19–21, 1993

Recent Designs for Advanced Fusion Reactor Blankets

D. K. Sze

Presented at the 11th Topical Meeting on the Technology of Fusion Energy, New Orleans, LA, June 20–24, 1993

Design Windows for a He Cooled Fusion Reactor

D. K. Sze and A. Hassanein

Presented at the Symp. on Fusion Enginering, Hyannis, MA, October 11–15, 1993

Assessment of Different Methods for Tritium Recovery from Lithium

D. K. Sze et al.

Presented at the ISFNT-3 Meeting, Los Angeles, CA, June 27–July 1, 1993

Tritium Recovery from Lithium Based on Gas Purging/Isotope Swapping Concept

D. K. Sze et al.

Presented at the ISFNT-3 Meeting, Los Angeles, CA, June 27–July 1, 1993

Thermodynamic and Nonstoichiometric Behavior of the Rare Earth and Bismuth Based Superconductors

M. Tetenbaum

Presented at the Workshop on High Temperature Superconductor Phase Diagrams, Santa Fe, NM, June 2–4, 1993

Oxygen Stoichiometry, Structural Transitions, and Thermodynamic Behavior of the $(Bi,Pb)_2Sr_2Ca_2Cu_3O_x$ System

M. Tetenbaum, M. C. Hash, and V. A. Maroni

Presented at the Spring Meeting of the Materials Research Soc., San Francisco, CA, April 11–16, 1993

TRUEX Technology-Base Development Program

G. F. Vandegrift

Presented at the Second Semiannual OTD Information Meeting, HAZWRAP, Houston, TX, January 26–28, 1993

Recent Upgrades to the Generic TRUEX Model

G. F. Vandegrift, J. M. Copple, R. A. Leonard, M. C. Regalbuto, R. J. Jaskot, J. Sedlet, L. Nunez, and D. B. Chamberlain

Presented at the Plutonium/Uranium Recovery Operations Conf., Augusta, GA, October 18–21, 1993

Decontamination of Groundwater by Membrane-Assisted Solvent Extraction

G. F. Vandegrift and J. C. Hutter

Presented at the Second Semiannual OTD Information Meeting, HAZWRAP, Houston, TX, January 26–28, 1993

Development of LEU Targets for ^{99}Mo Production and Their Chemical Processing

G. F. Vandegrift, J. C. Hutter, B. Srinivasan, J. E. Matos, and J. L. Snelgrove

Presented at the 16th Int. Meeting on Reduced Enrichment for Research and Test Reactors, RERTR '93, Oarai, Ibaraki, Japan, October 3–7, 1993

Demonstration of the TRUEX Solvent Extraction Process on Highly Irradiated PuO_2 Targets

G. F. Vandegrift, R. A. Leonard, L. Kefelker, D. Benker, and R. M. Wham

Presented at the Eighth Symp. on Separation Science and Technology for Energy Applications, Gatlinburg, TN, October 24–28, 1993

Separator Design Requirements

D. R. Vissers

Presented at the *Ad Hoc* Workshop on Ceramics for Li/FeS_2 Batteries, Oak Brook, IL, September 29–30, 1993

Solubility of Plutonium(VI) in Phosphate Solutions

H. Weger and D. T. Reed

Presented at the Fourth Int. Conf. on the Chemistry and Migration Behavior of the Actinides and Fission Products in the Geosphere, MIGRATION '93, Charleston, SC, December 12–17, 1993

Solubility and Speciation of Pu(VI) with Phosphate

H. T. Weger, D. T. Reed, S. Okajima, and J. C. Cunnane

Presented at the Fourth Int. Conf. on the Chemistry and Migration Behavior of the Actinides and Fission Products in the Geosphere, MIGRATION '93, Charleston, SC, December 12–17, 1993

Experimental Studies of the Role of Photodesorption in the Formation of Planetary Na Atmospheres

R. C. Wiens, D. S. Burnett, W. F. Calaway, and M. J. Pellin

Presented at the AAS Division of Planetary Sciences Meeting, Boulder, CO, October 18–22, 1993

Ion-Sputtering Products of Sodium Sulfate, and Implications for the Surface and Atmosphere of Io

R. C. Wiens, D. S. Burnett, W. F. Calaway, and M. J. Pellin

Presented at the AAS Division of Planetary Sciences Meeting, Boulder, CO, October 18–22, 1993

Optimization of the IFR Liquid Cadmium Cathode

J. L. Willit, Z. Tomczuk, J. J. Heiberger, and W. E. Miller

Presented at the 13th Annual Pyrochemical Workshop, Albuquerque, NM, October 18–21, 1993

Development of a Zirconium-Based Reference Electrode for Molten Chloride Applications

J. L. Willit, Z. Tomczuk, and W. E. Miller

Presented at the First Workshop on Analytical Chemistry of the IFR Pyroprocess, Argonne National Laboratory–West, Idaho Falls, ID, March 1–3, 1993

Ion Replacement Electrorefining

J. L. Willit, Z. Tomczuk, W. E. Miller, and J. J. Laidler

Presented at the 13th Annual Pyrochemical Workshop, Albuquerque, NM, October 18–21, 1993

High Pressure NMR Investigations Using Toroid Detectors

K. Woelk, J. W. Rathke, and R. J. Klingler

Presented at the University of Bonn, Germany, June 28–July 9, 1993

Rotating Frame NMR Microscopy

K. Woelk, J. W. Rathke, and R. J. Klingler

Presented at the Int. Conf. on Magnetic Resonance Microscopy, Heidelberg, Germany, September 6–9, 1993

Rotating Frame NMR Microscopy

K. Woelk, J. W. Rathke, and R. J. Klingler

Presented at the University of Bonn, Germany, June 28–July 9, 1993

Nuclear Waste-Form Alteration Research at ANL

D. J. Wronkiewicz

Presented at the New Mexico Bureau of Mines and Mineral Resources Seminar, Socorro, NM, October 1, 1993

Radionuclide Decay Effects on Waste Glass Corrosion and Weathering

D. J. Wronkiewicz

Presented at the Fall Meeting of the Materials Research Soc., Boston, MA, November 29–December 3, 1993

Effects of Radiation Exposure on SRL 131 Composition Glass in a Steam Environment

D. J. Wronkiewicz, C. R. Bradley, L. M. Wang, and J. K. Bates

Presented at the Fall Meeting of the Materials Research Soc., Boston, MA, November 29–December 3, 1993

Eight-Year Results from Unsaturated Drip Tests with UO_2

D. J. Wronkiewicz

Presented at the Spent Nuclear Fuel Workshop '93 Conf., Santa Fe, NM, September 26–29, 1993

TRUEX Processing of Plutonium Analytical Solutions at Argonne National Laboratory

D. G. Wygmans, D. B. Chamberlain, C. Conner, J. C. Hutter, R. A. Leonard, and G. F. Vandegrift

Presented at the Plutonium/Uranium Recovery Operations Conf., Augusta, GA, October 18–21, 1993

X-ray Reflectivity and STM Study of Kinetic Roughening of Sputter-Deposited Gold Films during Growth

H. You, R. P. Chiarello, and H. K. Kim

Presented at the Spring Meeting of the Materials Research Soc., San Francisco, CA, April 12–16, 1993

Applications of X-ray Scattering Techniques for the Study of Electrochemical Interfaces

H. You, Z. Nagy, and D. J. Zurawski

Presented at the 16th Int. Congress on Crystallography, Beijing, China, August 21–29, 1993

In-Situ X-ray Scattering Study of Incipient Oxidation of Pt(111) Single Crystal Surface

H. You, Z. Nagy, and D. J. Zurawski

Presented at the Third Int. Conf. on Surface X-ray and Neutron Scattering, Dubna, Russia, June 24–29, 1993

Partial Oxidation Reforming and Steam Reforming of Methanol

M. Yu, S. Ahmed, and R. Kumar

Presented at the 13th North American Meeting of the Catalysis Soc., Pittsburgh, PA, May 2–7, 1993

X-ray Studies of Electrochmical Interfaces

D. Zurawski

Presented at the Illinois Institute of Technology, Chicago, IL, January 20, 1993

F. Papers Accepted for Publication

Structure and Dynamics of Molten Aluminum and Gallium Trihalides II: Raman Spectroscopy and *Ab Initio* Calculations

A. D. Alvarenga, M.-L. Saboungi, L. A. Curtiss, M. Grimsditch, and L. E. McNeil

To be published in Mol. Phys.

Climatic, Eustatic, and Tectonic Controls on Quaternary Deposits and Landforms, Red Sea Coast, Egypt

R. Arvidson, R. Becker, A. Shanabrook, W. Luo, N. C. Sturchio, M. Sultan, Z. Lotfy, A. M. Mahmood, and A. El Alfy

To be published in J. Geophys. Res.

Carbon Isotopic Analysis of Individual n-Alkanes: Evaluation of Accuracy and Application to Marine Particulate Organic Material

A. J. Bakel, H. Ostrom, and N. Ostrom

To be published in *Compound Specific Isotope Analysis in Biogeochemistry and Petroleum Research*

Theoretical and Inelastic Neutron-Scattering Studies of Tetraethylammonium Cation as a Molecular Sieve Template

H. V. Brand, L. A. Curtiss, L. E. Iton, F. R. Trouw, and T. O. Brun

To be published in J. Phys. Chem.

Characterisation of Ni on Si Wafers: Comparison of Surface Analysis Techniques

W. F. Calaway, S. R. Coon, M. J. Pellin, D. M. Gruen, M. Gordon, A. C. Diebold, P. Maillot, J. C. Banks, and J. A. Knapp

To be published in Surf. Interface Analysis

Quartz Crystal Microbalance and Synchrotron X-ray Reflectivity Study of Water and Liquid Xenon Adsorbed on Gold and Quartz

R. P. Chiarello

To be published in Surf. Sci.

Neutral Copper Cluster Sputtering Yields: Ne^+, Ar^+, and Xe^+ Bombardment

S. R. Coon, W. F. Calaway, and M. J. Pellin

To be published in Nucl. Instrum. Methods

Calculation of Accurate Bond Energies, Electron Affinities, and Ionization Energies

L. A. Curtiss and K. Raghavachari

To be published in *Quantum Mechanical Electronic Structure Calculations with Chemical Accuracy: Understanding Chemical Reactivity*

An Evaluation of Vitrification Technology Application to Mixed Waste at Argonne National Laboratory

J. S. Devgun, J. J. Maser, and N. J. Beskid

To be published in Waste Management '94

Asymptotic Power Spectrum Analysis of Chaotic Behavior in Fluidized Beds

J. Ding and S.-W. Tam

To be published in the Int. J. Bifurcation and Chaos

Effects of Glass Surface Area-to-Surface Volume Ratio (S/V) on Glass Dissolution: Relationship Between S/V and Leachate pH

X. Feng and I. L. Pegg

To be published in J. Non-Cryst. Solids

Effects of Salt Solutions on Glass Dissolution

X. Feng and I. L. Pegg

To be published in Phys. Chem. Glasses

Removal of VOCs from Groundwater Using Membrane-Assisted Solvent Extraction

J. C. Hutter, G. F. Vandegrift, L. Nunez, and D. H. Redfield,

To be published in AIChE J.

Method for Encapsulating and Immobilising IFR Waste Salt and Other Salts Containing Radionuclides

M. A. Lewis and T. R. Johnson

DOE Case No. 71128 (Patent applied for)

Sputtering of Neutral and Ionic Indium Clusters

Z. Ma, S. R. Coon, W. F. Calaway, M. J. Pellin, and D. M. Gruen

To be published in J. Vac. Sci. Technol. A

Dissolution Kinetics of Silica Glass as a Function of pH Between 40 and 85°C

J. J. Mazer and J. V. Walther

To be published in J. Non-Cryst. Solids

Tritium Recovery from Liquid Metals

H. Moriyama and D. K. Sze

To be published in Fusion Eng. Design

Evaluation of Bond Energies to Chemical Accuracy by Quantum Chemical Techniques

K. Ragavachari and L. A. Curtiss

To be published in *Modern Electronic Structure Theory*, Ed., D. Yarkony

Uranium-Series Ages of Travertines and Timing of the Last Glaciation in the Northern Yellowstone Area, Wyoming-Montana, U.S.A.

N. C. Sturchio, K. L. Pierce, M. T. Murrell, and M. L. Sorey

To be published in Quat. Res.

Recent Designs for Advanced Fusion Reactor Blankets

D. K. Sze

To be published in Fusion Technol.

Assessment of Different Methods for Tritium Recovery from Lithium

D. K. Sze et al.

To be published in Fusion Eng. Design

Tritium Recovery from Lithium Based on Gas Purging/Isotope Swapping Concept

D. K. Sze et al.

To be published in Fusion Eng. Design

Development of LEU Targets for ^{99}Mo Production and Their Chemical Processing

G. F. Vandegrift, J. C. Hutter, B. Srinivasan, J. E. Matos, and J. L. Snelgrove

To be published in Proc. of the 16th Int. Meeting on Reduced Enrichment for Research and Test Reactors, RERTR '93

Yields of Sputtered Metal Clusters: The Influence of Surface Structure

A. Wucher, Z. Ma, W. F. Calaway, and M. J. Pellin

To be published in Surf. Sci. Lett.

Oxidation-Reduction Induced Roughening of Platinum(111) Surface

H. You and Z. Nagy

To be published in Phys. B

In-Situ X-ray Reflectivity Study of Incipient Oxidation of Pt(111) Surface in Electrolyte Solutions

H. You, D. J. Zurawski, Z. Nagy, and R. M. Yonco

To be published in J. Chem. Phys.

Distribution for ANL-94/15

Internal:

J. P. Ackerman
J. G. Asbury
J. K. Bates
J. E. Battles (75)
N. J. Beskid
P. R. Betten (5)
M. Blander
I. D. Bloom
A. S. Boparai
D. L. Bowers
E. C. Buck
F. A. Cafasso
E. L. Carls
D. J. Chaiko
D. B. Chamberlain
Y. I. Chang
L. D. Chipman
C. C. Christianson
J. C. Cunnane
D. W. Dees
L. W. Deitrich
W. H. DeLuca
H. Drucker
B. D. Dunlap
W. L. Ebert
A. Ellison
X. Feng
P. A. Finn
J. Fortner
F. Y. Fradin
S. D. Gabelnick
E. C. Gay
D. G. Graczyk
D. W. Green
D. M. Gruen
J. E. Harmon (2)
J. E. Helt
G. L. Henriksen
C. E. Johnson
T. R. Johnson
T. D. Kaun
T. R. Krause
M. Krumpelt
G. H. Kucera
R. Kumar
J. J. Laidler
K. K. Larsen
S. H. D. Lee
L. Leibowitz
R. A. Leonard
L. G. LeSage
M. A. Lewis
P. C. Lindahl
M. J. Lineberry
R. F. Malecha
V. A. Maroni
C. C. McPheeters
J. F. Miller
W. E. Miller
K. M. Myles
P. A. Nelson
W. H. Perry
R. D. Pierce
W. F. Podolski
R. B. Poeppel
J. W. Rathke
L. Redey
D. T. Reed
D. K. Schmalzer
A. Schriesheim
W. B. Seefeldt
M. A. Slawecki
J. A. Smaga
D. L. Smith
M. Steindler
L. M. Stock
N. C. Sturchio
T. G. Surles
W. M. Swift
S.-W. Tam
M. Thackeray
C. E. Till
Z. Tomczuk
G. F. Vandegrift
D. R. Vissers
D. C. Wade
L. C. Walters
R. W. Weeks
C. L. Wilkinson
J. L. Willit
R. D. Wolson
TIS Files

External:

DOE-OSTI, per distribution per UC-400 and -500 (98)
ANL-E Library (2)
ANL-W Library
Manager, Chicago Operations Office, DOE
R. C. Baker, DOE-CH
A. Bindokas, DOE-CH
J. Haugen, DOE-CH
J. O. Hunze, DOE-CH

J. Neff, DOE-CH
A. L. Taboas, DOE-CH/AAO
J. R. LaFevers, DOE-UC
Chemical Technology Division Review Committee Members:
E. R. Beaver , Monsanto Company, St. Louis, MO
D. L. Douglas, Consultant, Bloomington, MN
R. K. Genung, Oak Ridge National Laboratory, Oak Ridge, TN
J. G. Kay, Drexel University, Philadelphia, PA
G. R. St. Pierre, Ohio State University, Columbus, OH
J. Stringer, Electric Power Research Institute, Palo Alto, CA
J. B. Wagner, Arizona State University, Tempe, AZ
R. D. Alkire, University of Illinois, Urbana, IL
J. Allison, USDOE, Office of Waste Operations, Germantown, MD
K. F. Barber, USDOE, Office of Transportation Technologies, Washington, DC
S. Barker, Westinghouse Hanford Company, Richland, WA
J. Batchelor, USDOE, Office of Fossil Energy, Germantown, MD
D. Battleson, Mountain States Energy, Inc., Butte, MT
T. F. Bechtel, USDOE, Morgantown Energy Technology Center, Morgantown, WV
C. L. Bendixsen, Westinghouse Idaho Nuclear Company, Idaho Falls, ID
S. E. Berk, USDOE, Office of Fusion Energy, Germantown, MD
E. Beyma, USDOE, Office of Fossil Energy, Germantown, MD
J. R. Birk, Electric Power Research Institute, Palo Alto, CA
A. L. Boldt, Westinghouse Hanford Company, Richland, WA
D. F. Bowersox, Los Alamos National Laboratory, Los Alamos, NM
E. Bramlitt, Defense Nuclear Agency, Kirtland Air Force Base, Kirtland, NM
J. Braunstein, Oak Ridge National Laboratory, Oak Ridge, TN
J. J. Brogan, USDOE, Div. of Energy Utilization Research, Washington, DC
S. A. Butter, USDOE, Office of Basic Energy Sciences, Washington, DC
E. J. Cairns, Lawrence Berkeley Laboratory, Berkeley, CA
M. H. Campbell, Westinghouse Hanford Company. Richland, WA
K. A. Chacey, USDOE, Office of Waste Management, Germantown, MD
S. Chalk, USDOE, Office of Transportation Technologies, Washington, DC
S. W. Chun, USDOE, Pittsburgh Energy Technology Center, Pittsburgh, PA
R. P. Clark, Sandia National Laboratories, Albuquerque, NM
S. P. Cowan, USDOE, Office of Waste Operations, Germantown, MD
E. Dowgiallo, USDOE, Office of Transportation Technologies, Washington, DC
R. E. Erickson, USDOE, Office of Waste Operations, Germantown, MD
G. Escobar, LATO Office, Rocky Flats Plant, Golden, CO
R. C. Ewing, Department of Geology, University of New Mexico, Albuquerque, NM
H. Feibus, USDOE, Office of Fossil Energy, Germantown, MD
C. W. Frank, USDOE, Office of Technology Development, Washington, DC
D. Geiser, USDOE, Office of Technology Development, Washington, DC
M. R. Ghate, USDOE, Morgantown Energy Technology Center, Morgantown, WV
R. Gilchrist, Westinghouse Hanford Company, Richland, WA
Government Documents Department, University of California, Berkeley, CA
T. Gross, USDOE, Office of Energy Efficiency, Washington, DC
T. Grumbly, USDOE, Office of Environmental Management, Washington, DC

R. A. Guidotti, Sandia National Laboratories, Albuquerque, NM
K. L. Heitner, USDOE, Office of Transportation Technologies, Washington, DC
R. J. Herbst, Los Alamos National Laboratory, Los Alamos, NM
T. M. Hohl, Westinghouse Hanford Company, Richland, WA
N. Holcombe, USDOE, Morgantown Energy Technology Center, Morgantown, WV
D. Hooie, USDOE, Morgantown Energy Technology Center, Morgantown, WV
W. Huber, USDOE, Morgantown Energy Technology Center, Morgantown, WV
G. L. Hunt, EG&G Idaho, Inc., Idaho Falls, ID
G. Jansen, Westinghouse Hanford Company, Richland, WA
L. J. Jardine, Lawrence Livermore National Laboratory, Livermore, CA
E. F. Johnson, Princeton University, Princeton, NJ
E. Jones, Pacific Northwest Laboratory, Richland, WA
F. Kane, University of Idaho, Moscow, ID
R. D. Kelley, USDOE, Office of Basic Energy Sciences, Germantown, MD
J. J. Kelly, Electrodex Laboratories, Inc., Willingboro, NJ
B. Knutson, Westinghouse Hanford Company, Richland, WA
R. A. Kost, USDOE, Office of Conservation & Renewable Energy, Washington, DC
A. R. Landgrebe, USDOE, Office of Transportation Technologies, Washington, DC
B. Lee, Institute of Gas Technology, Chicago, IL
S. C. T. Lien, USDOE, Office of Technology Development, Washington, DC
L. Little, USDOE, Nevada Operations Office, Las Vegas, NV
G. J. Lumetta, Pacific Northwest Laboratory, Richland, WA
J. E. Lytle, USDOE, Office of Waste Management, Washington, DC
M. J. Mayfield, USDOE, Morgantown Energy Technology Center, Morgantown, WV
F. R. McLarnon, Lawrence Berkeley Laboratory, Berkeley, CA
J. R. Morrey, USDOE, Office of Technology Development, Washington, DC
A. C. Muscatello, LATO Office, Rocky Flats Plant, Golden, CO
W. E. O'Grady, Naval Research Laboratory, Washington, DC
J. O'Sullivan, Electric Power Research Institute, Palo Alto, CA
A. L. Olson, Westinghouse Idaho Nuclear Co., Inc., Idaho Falls, ID
G. Ordaz, USDOE, Office of Technology Development, Washington, DC
R. A. Osteryoung, North Carolina State University, Raleigh, NC
P. G. Patil, USDOE, Div. of Electric and Hybrid Propulsion, Washington, DC
C. E. Pax, USDOE, Office of Fossil Energy, Germantown, MD
L. Petrakis, Brookhaven National Laboratory, Upton, NY
S. T. Picraux, Sandia National Laboratories, Albuquerque, NM
W. M. Polansky, USDOE, Office of Basic Energy Sciences, Germantown, MD
R. Price, USDOE, Office of Fusion Energy, Germantown, MD
G. Reddick, Westinghouse Hanford Company, Richland, WA
E. Riddel, Electric Power Research Institute, Palo Alto, CA
G. Rudins, USDOE, Office of Fossil Energy, Germantown, MD
A. J. Salkind, Rutgers University, Piscataway, NJ
L. A. Salvador, USDOE, Morgantown Energy Technology Center, Morgantown, WV
R. L. San Martin, USDOE, Renewable Energy, Washington, DC
P. S. Schaus, Westinghouse Hanford Company, Richland, WA
W. C. Schutte, USDOE, Office of Technology Development, Washington, DC
L. H. Schwartz, National Institute of Standards and Technology, Gaithersburg, MD

A. W. Searcy, Lawrence Berkeley Laboratory, Berkeley, CA
R. Sehgal, Electric Power Research Institute, Palo Alto, CA
R. W. Shivers, USDOE, Div. of Energy Utilization Research, Washington, DC
R. R. Shockley, Illinois Clean Coal Institute, Carterville, IL
J. S. Siegel, USDOE, Office of Fossil Energy, Germantown, MD
W. A. Siegel, USDOE, Office of Transportation Technologies, Washington, DC
A. Simmons, USDOE, Las Vegas, NV
M. I. Singer, USDOE, Office of Fossil Energy, Germantown, MD
S. N. Sinha, University of Illinois--Chicago, Chicago, IL
E. Slaathug, Westinghouse Hanford Company, Richland, WA
F. D. Stevenson, USDOE, Office of Basic Energy Sciences, Germantown, MD
R. B. Stout, Lawrence Livermore National Laboratory, Livermore, CA
J. P. Strakey, USDOE, Pittsburgh Energy Technology Center, Pittsburgh, PA
R. A. Sutula, USDOE, Office of Transportation Technologies, Washington, DC
R. Swaroop, Electric Power Research Institute, Palo Alto, CA
J. C. Tseng, USDOE, Office of Waste Operations, Germantown, MD
G. P. Turi, USDOE, Office of Environmental Restoration, Germantown, MD
J. A. Turi, USDOE, Office of Environmental Restoration, Germantown, MD
G. E. Voelker, USDOE, Office of Technology Development, Washington, DC
M. P. Whelan, Gas Research Institute, Chicago, IL
R. P. Whitfield, USDOE, Office of Environmental Restoration, Washington, DC
K. Yeager, Electric Power Research Institute, Palo Alto, CA
R. J. Harrison, Atomic Energy of Canada, Ltd., Chalk River, Ontario, CANADA
M. Tokiwai, CRIEPI FBR Division, Komae-shi Tokyo, JAPAN